# Synthesis, Characterization and Application of Selected Heterogeneous Catalysts in Widely Useful Organic Transformations

A Thesis submitted in

Partial Fulfilment of the Requirements for the Degree of

Doctor of Philosophy

KALYANI RAJKUMARI

(17-3-23-101)

Under Supervision of

Dr. Lalthazuala Rokhum



## DEPARTMENT OF CHEMISTRY

## NATIONAL INSTITUTE OF TECHNOLOGY SILCHAR

(2020)

# DECLARATION

Thesis Title:   **Synthesis, characterization and application of selected heterogeneous catalysts in widely useful organic transformations**

Degree for which the Thesis is submitted: Doctor of Philosophy

I declare that the presented thesis represents largely my own ideas and work in my own words. Where others ideas or works have been included, I have adequately cited and listed in reference materials. The thesis has been prepared without resorting to plagiarism. I have adhered to all principles of academic honesty and integrity. No falsified or fabricated data have been presented in the thesis. I understand that any violation of the above will cause for disciplinary action by the institute, including revoking the conferred degree, if conferred, and can also evoke penal action from the sources which have not been properly cited or from whom proper permission has not been taken.

*Kalyani Rajkumari*

Kalyani Rajkumari

Registration No: 17-3-23-101

Date: 7/10/2020

# CERTIFICATE

It is certified that the work contained in this thesis entitled "**Synthesis, characterization and application of selected heterogeneous catalysts in widely useful organic transformations**" submitted by **Kalyani Rajkumari**, Registration no 17-3-23-101 for the award of PhD is absolutely based on her own work carried out under my supervision and this thesis has not been submitted elsewhere for any degree.

Dr. Lalthazuala Rokhum
Supervisor
Designation: Assistant Professor
Department of Chemistry
National Institute of Technology, Silchar

Date: 7/10/2020

iii

# ABSTRACT

The thesis is based on the synthesis and characterization of a few chosen heterogeneous catalysts which find catalytic applications in some valuable organic transformations. The catalysts explored in this research work include magnetic nanocatalysts, polymer, simple metal oxide and some novel biowaste-based compounds. The catalytic compounds are analyzed by various characterization techniques which not only validate their formation but also provide knowledge about their properties, functionalities, structure and morphology. The acid/base solid compounds are then tested for their probable catalytic activities in number of chemical reactions that include tetrahydropyranylation/depyranylation, Henry reaction, Wittig reaction, transesterification of triglycerides and acetalization reaction of glycerol. The aspects of green chemistry are specially kept in mind while designing the catalytic protocols. In most of the cases, the use of additional solvents in reaction systems is avoided promoting solvent-free conditions. Apart from room-temperature procedures, ultrasonic-assisted and microwave-assisted reactions are also performed in some transformations in order to afford time and energy-efficient methods.

At the preface, Chapter 1 sheds light on the historical background of catalysis followed by chronology of heterogeneous catalysis and its mechanistic working principle and advantages over homogeneous catalysis. Different categories of heterogeneous catalysts are discussed with their individual plusses and other important aspects. All these lead to the motivation, scope and objectives of the present research work. In Chapter 2, systematic literature survey on heterogeneous catalysis in the field of chemical reactions mentioned in this research work are discussed. The survey validates that application of heterogeneous catalysts in these organic transformations is in recent trend and fabricating efficient and recyclable heterogeneous green catalytic systems for these reactions can be a worthwhile practice.

Chapter 3 presents a magnetite nanoparticle based core-shell magnetic nanocatalyst which effectively catalyzes protection/deprotection of alcohols with dihydropyranes under solvent-free, room temperature condition. In addition, tetrahydropyranyl ethers could also be deprotected to the parent alcoholic compounds in the presence of MeOH using the same catalyst. After completion of the reactions, the catalyst is easily separated from the reaction medium using an external magnet, which ameliorated the overall synthetic process.
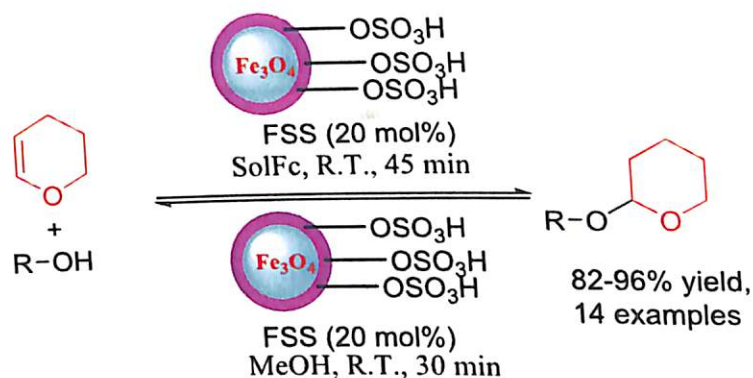
The same catalyst is also found to be efficient in acetalization of glycerol to form industrially important compound solketal. The ultrasonic-assisted reaction affords the desired product within 15 minutes with 100% selectivity.



**Glycerol**     **Acetone**

**Sol-ketal**

**(4-hydroxymethyl-2,2-dimethyl-1,3-dioxolane)**
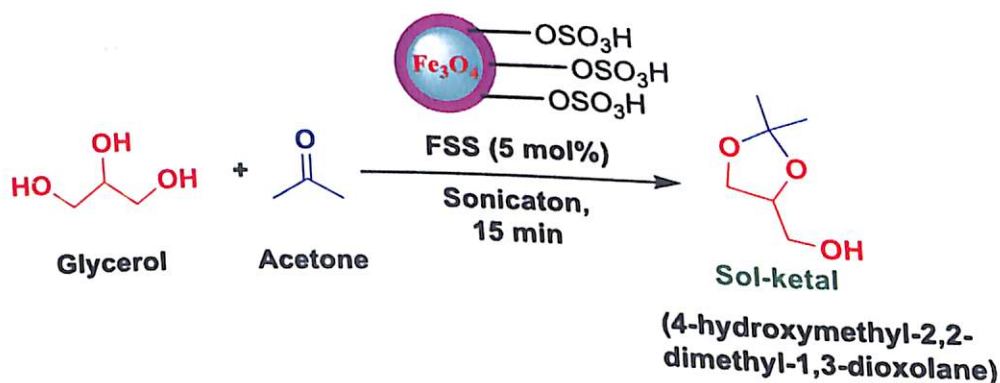
In Chapter 4, tetrahydropyranylation/depyranylation reactions for both alcohol and phenols are demonstrated using a polymer catalyst. The ion-exchange resin based catalyst was synthesized in laboratory and characterized with various analytical techniques to investigate its properties. Recyclability up to 10 catalytic cycles are achieved for the catalyst without any further chemical treatment.



**3,4-dihydro-2H-pyran (DHP)**

R-OH

PAFR (O.25 g), SolFc, RT

PAFR (O.25 g), MeOH, RT

R= Alkyl, Phenyl

**THP ether**

Yield 87-98%
18 examples

Chapter 5 reveals a novel biowaste solid base catalyst, prepared from *M acuminata* banana peel ash, which finds application in Henry reaction and effect produces nitroalcohol products in excellent yield under solvent- free condition.

biowaste-derived catalyst is thoroughly investigated by various characterization techniques which finally presents a low-cost, eco-friendly, highly efficient green catalytic method for the synthesis of nitroalcohols with excellent atom-economy and E-factor.



84-98% Yield
24 examples
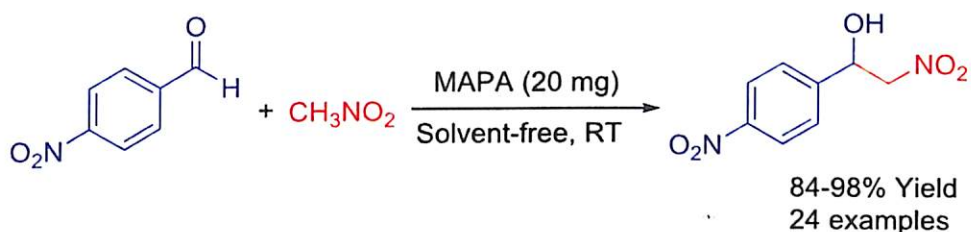
Another similar novel biowaste-derived catalyst *M. acuminata* banana trunk ash was demonstrated in Chapter 6 which was used for transesterification reaction to synthesize biodiesel product from soybean oil. A high yield of biodiesel (98.95 %) was achieved and the catalyst was recoverable up to 4 times without much depreciation in its catalytic activity.



Biodiesel, 98.39% yield
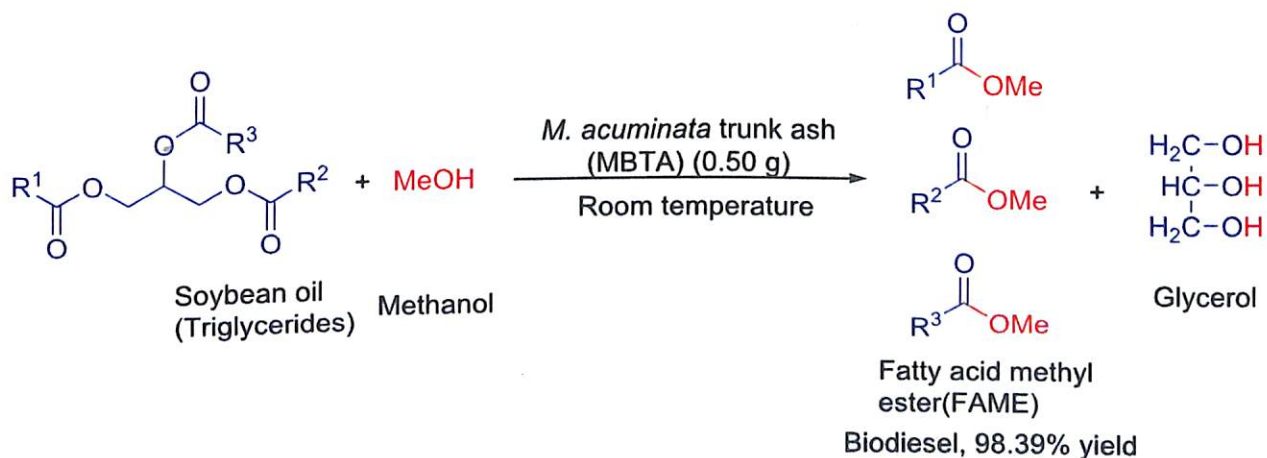
Chapter 7, on the other hand, accounts for a microwave-assisted one-pot Wittig reaction method using basic alumina as catalyst-support. The protocol is generalized for both stabilized and semi-stabilized ylides and prominent *E*-selectivity is noticed during olefination. In addition, owing to the solid state nature of the reactions, the procedure prevented the need for tedious aqueous extraction at the end of the reaction
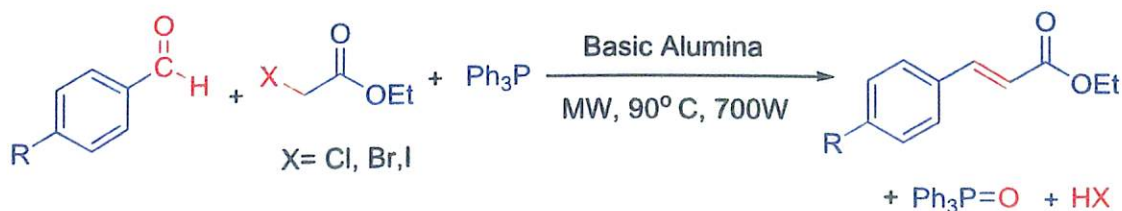


In conclusion, synthetic utility of a few selected heterogeneous catalysts are established in this thesis for some useful organic reactions. The catalytic paths are

optimized to be effective as well as environment-friendly in nature. The presented catalysts can be immensely useful for forthcoming research and can be investigated for wide range of organic synthetic processes in near future.

# ACKNOWLEDGEMENT

# TABLE OF CONTENTS

xiii

# LIST OF FIGURES

# LIST OF SCHEMES

# LIST OF TABLES

# LIST OF SYMBOLS/ABBREVIATIONS

| Symbol/ Abbreviations | Brief Description/Definition |
|---|---|
| ° | Degree |
| δ | Chemical shift, ppm (parts per million) |
| Å | Angstrom |
| λ | Lambda |
| eV | Electron volt |
| BET | Brunauer–Emmett–Teller |
| $cm^{-1}$ | Wave number |
| CHNS | Carbon Hydrogen Nitrogen Sulphur analyzer |
| $ClSO_3H$ | Chlorosulfonic acid |
| d | Doublet |
| DCM | Dichloromethane |
| dd | Doublet of doublet |
| DHP | 3,4-dihydro-2H-pyran |
| DMAP | 4-Dimethylamino pyridine |
| DMF | *N,N*-dimethylformamide |
| DMSO | Dimethyl sulfoxide |
| DPRN | Depyranylation |
| DSC | Differential scanning calorimetry |
| F | $Fe_3O_4$ |
| FAME | Fatty acid methyl esters |
| FS | $Fe_3O_4@SiO_2$ |
| FSS | $Fe_3O_4@$silica sulfonic acid |
| ECA | Ethyl chloroacetate |
| EDX | Energy-dispersive X-ray spectroscopy |
| FTIR | Fourier-transform infrared spectroscopy |
| GC-MS | Gas chromatography–mass spectrometry |
| h | Hour |
| *H_* | Hammett indicator value |
| HPLC | High-performance liquid chromatography |
| IR | Infrared |
| ICP-OES | Inductively coupled plasma atomic emission spectroscopy |
| J | Coupling constant |
| KHz | Kilo hertz |
| m | Multiplet |
| mmol | Millimole |
| MAPA | *Musa acuminata* peel ash |
| MBTA | *Musa acuminata* banana trunk ash |
| MeOH | Methanol |
| Min | Minutes |
| MHz | Mega Hertz |
| MW | Microwave |
| $NH_3$-TPD | Ammonia- temperature programmed desorption |
| nm | Nanometer |

| | |
|---|---|
| NMR | Nuclear magnetic resonance spectroscopy |
| PB | Polymer-bound |
| PB-PPh$_3$ | Polymer-bound triphenylphosphine |
| PAFR | Phenolsulfonic acid formaldehyde resins |
| RT | Room temperature |
| s | Singlet |
| SAED | Selected Area Electron Diffraction |
| SEM | Scanning Electron Microscopy |
| SolFc | Solvent-free condition |
| SPOS | Solid Phase Organic Synthesis |
| SSA | Silica Sulfuric acid |
| t | Triplet |
| TBS | *tert*-Butydimethylsillyl |
| TEM | Transmission electron microscopy |
| TEOS | Tetraethyl orthosilicate |
| TGA | Thermogravimetric analysis |
| THP | Tetrahydropyran |
| THPRN | Tetrahydropyranylation |
| THF | Tetrahydrofuran |
| TLC | Thin layer chromatography |
| TMS | Tetramethylsilane |
| TPP | Triphenylphosphine |
| UV | Ultra violet |
| VSM | Vibrating sample magnetometer |
| XPS | X-ray photoelectron spectroscopy |
| XRD | X-ray powder diffraction |
| XRF | X-ray fluorescence |

# CHAPTER
# 1

# Introduction

*"Chemistry without catalysis would be a sword without a handle, a light without brilliance, a bell without sound."*[1] – Alwin Mittasch

Catalysis is an inevitable part of chemistry. History of catalysis dates back to the onset of civilization, when mankind inculcated the art of fermentation to produce alcohol from sugar.[2,3] It was then in the alchemic period, in 1552, first report of using sulfuric acid as catalyst in transformation of alcohol to ether by Valerius Cordus was documented.[3] In "Alchemia", the first known textbook of chemistry, Libavius mentioned the phenomenon of catalysis mostly as the conversion of base metals into noble metals.[2,4]

However, studies in catalysis was first systematically investigated and categorized by noted Swedish scientist Jöns Jacob Berzelius in 1836.[2,5] He is also credited for first coining the term 'Catalysis' and forward the basic idea of catalysts as- "Several simple or compound bodies, soluble and insoluble, have the property of exercising on other bodies an action very different from chemical affinity. By means of this action they produce, in these bodies, decompositions of their elements and different recombinations of these same elements to which they remain indifferent"[6,7].

Once it was established that catalysis is pertinent in almost all kind of chemical reactions, investigation of catalytic applications in various reactions became an indispensable practice in research in chemistry. Along with that, their translation into industrial implementation also started vigorously. Today millions of catalytic processes have surrounded both academia, industry and even daily life- starting from iron catalyzed large-scale industrial production of ammonia by Haber-Bosch[2,3,8] process to development of exhaust gas catalyst systems[9] (for converting toxic $CO$ to $CO_2$) in vehicles, production of biofuel, drug and polymer synthesis etc. Note worthily, all the biological processes in living world are also governed by catalytic action of some proteins, called enzymes. At present, above 85% of chemicals are produced via catalytic processes, while 15% to 20% of economic activities in developed countries are directly dependent upon catalysis.[10,11] In 2016, the global market value of catalysts is around USD 23.08 billion which is projected to reach USD 34.06 billion by the year 2025. The economic background of catalysis in present

world can be estimated by these above statistics. The industrial usage of catalysts is predominantly distributed among four major sectors- energy sector, polymer industry, synthesis of fine and bulk chemicals and environmental abatement processes.[11]

In the first definition itself, by using the terms "soluble and insoluble compound bodies" Berzelius distinctly categorized catalysts into two major classes; which soon popularized as homogeneous and heterogeneous catalysts. Homogeneous catalysts partake the same phase as of the reactants and products while heterogeneous catalysts are of different phases from reactant and product phase.

## 1.1 Heterogeneous catalysts

Mostly, heterogeneous catalysts are solid materials which are not miscible in liquid or gases, but it may include liquid catalyst in gaseous reaction mixture and even immiscible liquid catalysts in liquid reaction mixture too.[12] The solid surfaces of solid heterogeneous catalysts have the fascinating property of making and breaking bonds, which is the ground behind the interesting phenomenon of heterogeneous catalysis. Both homogeneous and heterogeneous catalysts have their own distinct advantages. Since heterogeneity offers catalysts to facilitate easy separation from the product mixture, so the catalysts can be recovered and reused after each cycle and that makes them superior than the homogeneous catalysts in both industrial and environmental approach.[13]

The century-long journey of heterogeneous catalysis began as an 'empirical discipline'. Though the actual mechanism and thermodynamics behind the process were known to world much later, but many illustrious chemical conversions were achieved during the end of nineteenth century which led to large-scale industrial catalytic production.[14] Some classic achievements include Haber's process for production of ammonia using iron powder as catalyst, Ostwald's process for oxidation of ammonia to nitric acid using Pt/Rd as catalyst, Zeiglar- Natta catalyst for polymerization of alkenes etc. Currently heterogeneous catalysts are being exploited in numerous industrial chemical processes owing to its easy preparation, handling and separation. Particularly, the energy sector is highly reliant on heterogeneous catalysis.[15-17]

Conventionally solubility is considered to be the only criterion to categorize homogeneous and heterogeneous catalysts, however, Schwartz's modern definition throw light on a different approach too. According to his concept, heterogeneous catalysts can have multiple types of active sites unlike homogeneous catalysts which have single type of active sites.[18,19]

### 1.1.1 Mechanistic aspect of heterogeneous catalysis

The fundamental of heterogeneous catalysis lies in the extraordinary property of solid surfaces which are capable of making and breaking bonds to molecules from the surroundings. There are large variations in activity of surface to surface and understanding of this variations require detailed knowledge of the mechanistic route of the catalysis. The phenomenon of heterogeneous catalysis is an amalgamation of several closely related catalytic steps take place on the solid surface of the catalyst. Following steps describes the mechanism involved in the catalytic process[10,20]:

- Diffusion of the substrate molecules to the surface of the catalyst. This also involves two stages- first external diffusion of the molecules to the bulk surface followed by their internal diffusion towards the pores of surface to grasp the active sites.
- Physisorption of the reactant particles over the catalyst surface via van der Waals forces.
- Chemisorption of the reactant molecules. This takes place by formation of chemical bonds of the molecules to the catalyst surface.
- Chemical reaction between the reactant molecules leading to result the conversion into product molecules via formation of intermediates.
- Desorption of the product molecules from active sites.
- Diffusion of the product particles from the pores of catalyst surface back to the surrounding.

Each mechanistic step plays their own role in the whole process of catalytic route. It is therefore difficult to opine which factors decide whether a surface will act as good catalyst or not. Sabatier's principle suggests that "a good catalyst provides an optimum strength of bonding between the reactants and the catalyst surface".[10,21] To understand the magic behind the catalytic activity of a solid surface, it is crucial to understand the adsorption bond of the surface and substrate molecules.
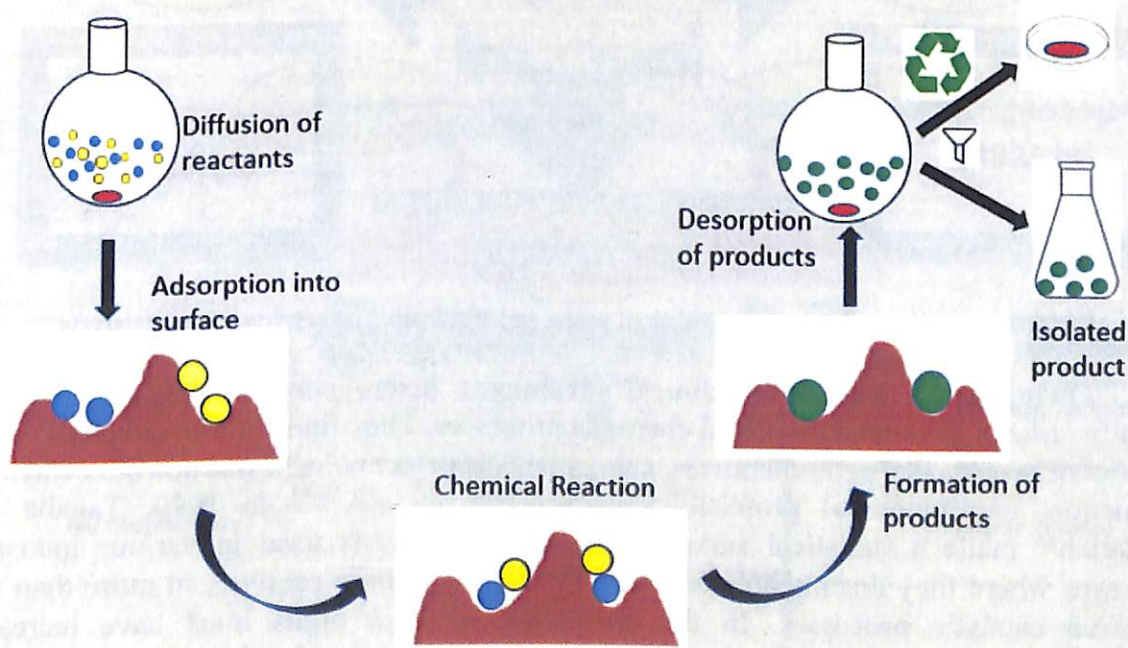


FIGURE 1.1 Catalytic mechanism of heterogeneous catalysis.

## 1.1.2. Advantages and scope of heterogeneous catalysis

Both the homogeneous and heterogeneous catalytic systems have their own series of pros and cons. Homogeneous catalysts due to their better interaction with reacting particles can show high activity and selectivity and that is why they are still being used in some fine

chemical synthetic processes.[22] But in spite of their high catalytic activity, industrial application of these catalysts is not much relevant due to the tedious separation and purification methods like chromatography. Also since the catalysts once used cannot be recovered and reused, it leads to accumulation of waste, thereby, depreciating the environmental as well as economic viability of the synthetic protocols. To the contrary, heterogeneous catalysts offer very simple and easy separation of catalysts from product mixture. The catalysts can be recovered by filtration and reused further for several catalytic cycles.[23-25] Due to this reason the latter is considered as green catalyst which fits into most of the 12 principles of green chemistry. Heterogeneous catalysts can be potentially incorporated for continuous reactors and micro-reactors which make major technical benefit over homogeneous catalysts.[26] Another remarkable advantage of these catalysts is the wide operating conditions due to their high temperature resistance in most cases.[27,28] However due to the limiting surface area, the reactivity of such catalytic reaction might be restrained which comes out as the major challenge of modern catalytic advancement researchers.[22]
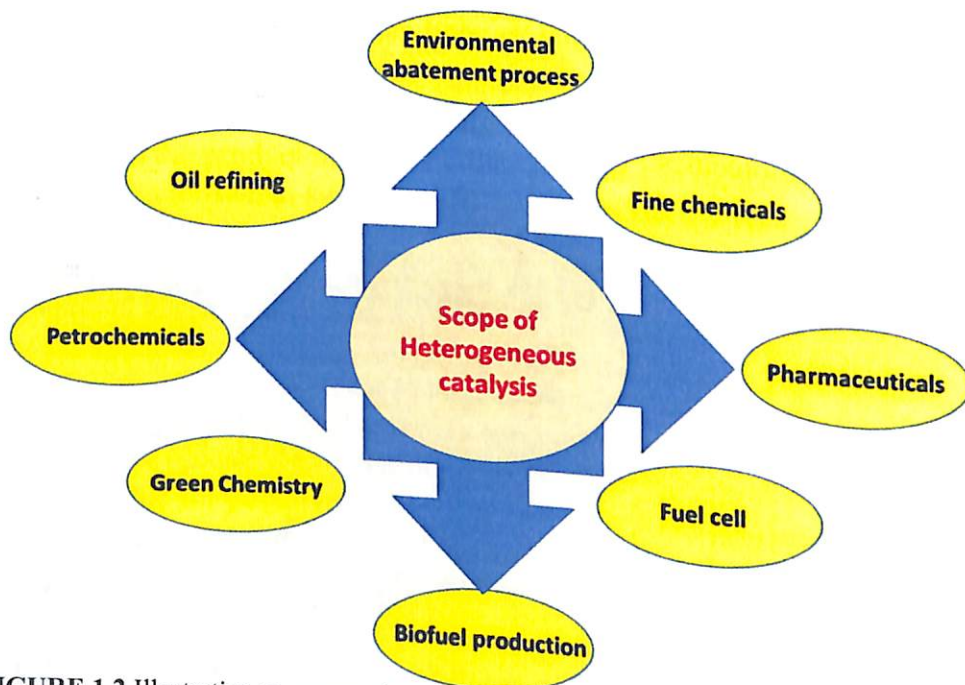


FIGURE 1.2 Illustrative representation of scope and application of heterogeneous catalysis.

Owing to the attractive technical advantages, heterogeneous catalysts have been robustly utilized in various industrial chemical processes. They find widespread applications in various domains like petrochemicals, energy and clean technology, fine and bulk chemical production, environmental protection, pharmaceuticals etc.[29-32] In 1999, Tanabe and Hölderich[33] made a statistical survey on types of catalysts used in various industrial processes where they documented around 180 solid acid-base catalysts in more than 120 industrial catalytic processes. In the last decades, these digits must have increased exponentially looking at the world-wide enormously growing industrialization. One of the prominent field reliant on heterogeneous catalysis is the energy sector. For an instance, gasoline, in its refining process through refinery to fuel station, has to confront almost ten catalysts.[14] Apart from this, there are many chemical products and pharmaceuticals that require solid catalysts for their economic and environment-friendly synthesis. Exhaust gas cleaning system in automobiles for environmental abatement process is another important field which essentially require heterogeneous catalysts. It is therefore a major challenge for modern catalytic science to design more efficient and green heterogeneous catalysts to mitigate the growing demand in near future.

4

## 1.2 Nano particles as heterogeneous catalysts

In the present era, nanotechnology has brought revolutionary hurricane of changes to diverse domains like medicine, electronics, catalysis, food industry, communication, fine chemicals, energy, environmental science etc.[34-36] Harnessing nanotechnology to catalytic processes is one of the most explored key areas in contemporary research.[37] Due to the tiny nano-sized particles, the exposed surface area of catalysts increase massively which turn out to be the reason behind the excellent activity of nanocatalysts. **This eventually marks them as 'bridge between homogeneous and heterogeneous catalysts'.**[38] Homogeneous catalysts although have several major drawbacks regarding catalyst separation, but their superb catalytic activity and selectivity can never be overlooked.[39,40] This activity arises due to the high degree of interaction between reactant and catalyst molecules while activity of heterogeneous catalysts is, to some extent, restricted due to limited number of active sites on catalyst surface. But dramatic rise in activity can be observed when nanoparticles are used as heterogeneous catalysts. Owing to their tiny size, nanocatalysts have very large surface area which leads to better exposure of catalytic active sites and enables better contact between reactant and catalyst mimicking homogeneous catalysts.[41-43] The insoluble nature of the catalysts in reactant phase makes them easily separable and isolable incorporating all the goodness of heterogeneous counterpart too. Another major benefit of using nanocatalysts is that the physical and chemical properties of these catalysts like size, shape, morphology, functionality etc. can be tuned to manipulate the activity and selectivity of a catalyst.[44,45] All these advantageous properties of nanocatalysts is therefore fascinating the scientific community in recent times leading flurry of research practices in heterogeneous nanocatalysis.
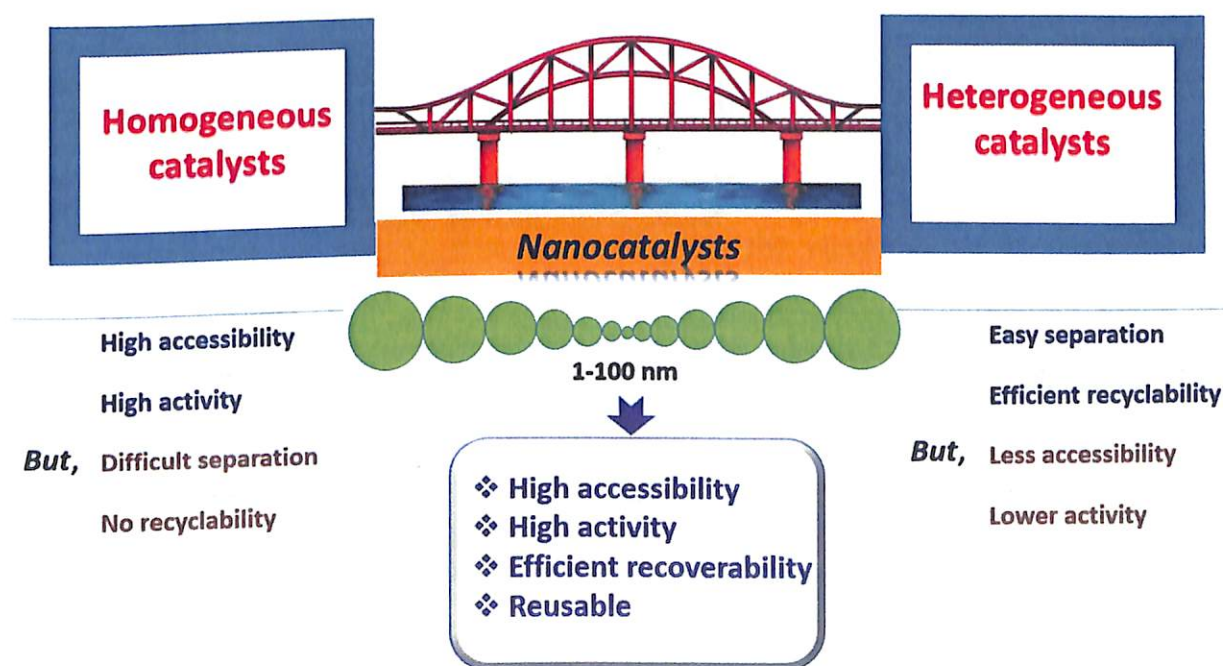


**FIGURE 1.3** Schematic diagram of advantages of nanocatalysis over homogeneous and heterogeneous catalysis

Metallic nanoparticles has been finding prominent significance in both industry and academia over several decades due to their widespread role in various fields like catalysis,[46] biomedical applications,[47-49] engineering[50] etc. Varying some simple physical properties like size, shape, they can be tailored to show different physical and chemical properties. These

tailored nanomaterials are extensively utilized as catalysts[51], semiconductors[52,53], antimicrobial agents[54], sensors[55,56], drug delivery agents[57,58] etc.

## 1.2.1. Techniques for synthesis of nanoparticles

In the last decades, numerous efforts have been made to develop effective methodologies for the synthesis of nanoparticles in laboratory scale as well as industrial scale. Depending on the physical and chemical properties required in the NPs and also considering their application-wise requirements, different synthetic techniques can be adopted. All these techniques however fall under two classes: top-down and bottom-up technologies.[59-61] In top-down method, bulk materials are miniaturized to atomic levels by external tools leading to the formation of nano-sized particles of desired physical, structural or mechanical properties. On contrary to this, in bottom-up approach smaller building blocks are assembled to form a controlled, more complex nano-structure.[62-68]
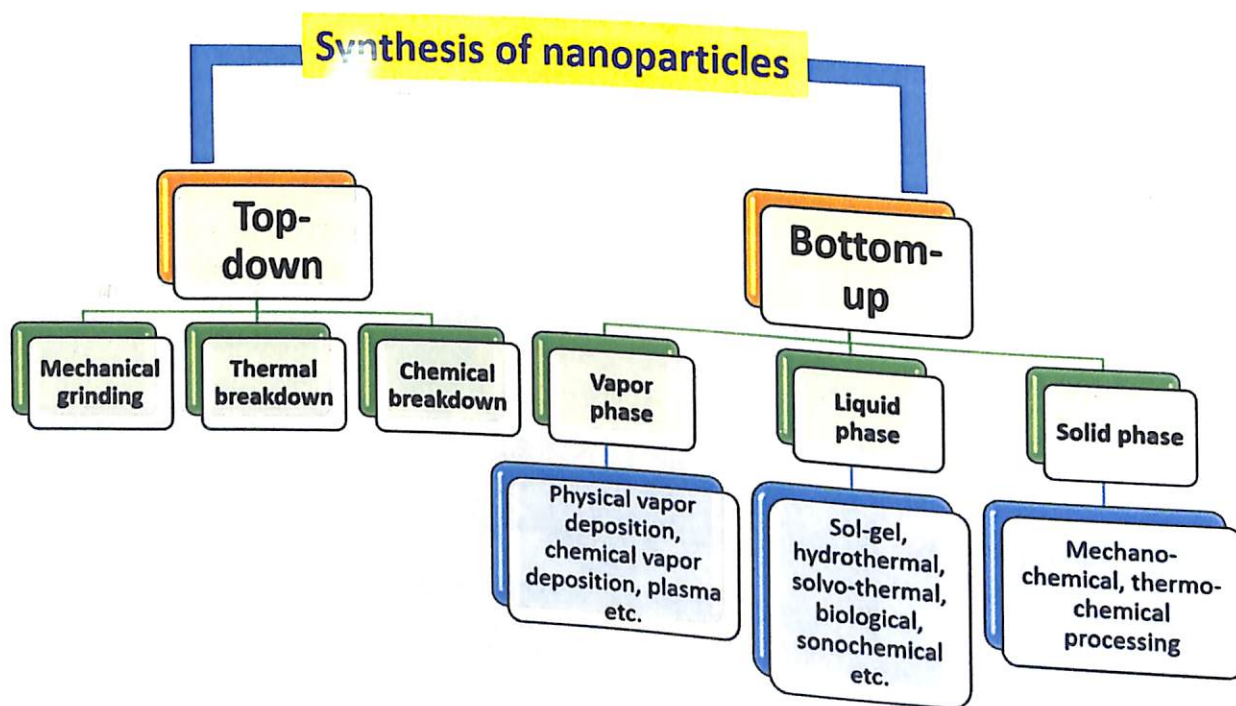


FIGURE 1.4 Various techniques used for synthesis of nanoparticles.

Categorization of different synthetic techniques used for the production of nanomaterials can be viewed in Fig. 1.4. Top-down approach is a traditional method to produce bulk amount of fine nano-powders mostly by high energy dry/wet mechanical grinding. Although this method is simple and easily operative but ensuring uniform particle-size distribution is very difficult during milling process which play as major disadvantage of the method.[69-72]

Vapor-phase nano-synthetic technique of bottom-up approach involves solidification of liquid or gas in gaseous medium where the metal precursor is vaporized by resistance, electron beam, laser etc. This method is extensively used for the synthesis of metal oxide NPs with high purity and crystalinity.[73-74]

One of the most economic and hence commonly utilized method for nano-synthesis is liquid-phase technique that involves varied processes like sol-gel, co-precipitation, hydrothermal, ultra sonication, microwave irradiation, micro emulsion, biological and many more new techniques as well. The ability to control particle-size, shape and flexibility in

6

reaction pathway makes this a universal technique for production of nanoparticles in laboratory-scale.[75,76] Liquid-phase technique is best way to tailor size, shape, morphology and composition of NPs by tuning synthetic pathway, reaction conditions, pH etc. Since size of particle plays a very crucial part for activity of nanocatalysts, different stabilizing agents or capping agents can be used for well-controlled synthesis of NPs. On the other hand, template-mediated synthesis allows production of nanoparticles of specific shapes as required.[77-80]

In the bottom-up mechanochemical processing technology, high energy dry milling process is used to induce chemical reaction between precursor materials that leads to formation of nanoscale composite structure of desired phase within the solid milieu. This solid-phase technology is advantageous in terms of operational simplicity, agglomeration-free and uniform sized nanoparticle synthesis but removal of solid matrix sometimes leads to additional cost to the processing.[81,82]

Currently more than twenty synthetic methods can be listed that are known to laboratory scale production of nanoparticles while for commercial production, most of the industry use vapor-phase (43%) or liquid-phase (41%) synthetic techniques.[69]

## 1.2.2 Magnetic Nanocatalysts

Although the extraordinary surface area-to-volume ratio brings tremendous accessibility and activity to nanocatalysts, but sometimes isolation of these nanosized particles from the reaction system is not a piece of cake.[83] As metal NPs form high stabilized solution, so conventional techniques like filtration are not effective to separate the tiny particles. Whereas introduction of sophisticated techniques like cross-flow filtration, high-speed centrifugation etc. for catalyst recovery hampers the sustainability and economy of the catalytic protocol.[84,85] Magnetic nanocatalysts have emerged as a viable solution to overcome this shortcomings. The magnetic nature of these materials are exploited to retrieve the catalyst from reaction mixture using an external magnet with utmost ease and simple manner. Thus magnetically retrievable nanocatalysts not only offers attractive scope for great accessibility and activity but also mitigates the challenge of recoverability of nanocatalysts.[86-88]

Various magnetic nanomaterials of metals like Fe, Co, Ni etc. have been reported in literature till date. Iron oxide, especially ferrite ($Fe_3O_4$) nanoparticles are the most prominently investigated class of magnetic nanocatalyst due to their attractive magnetic property, easy synthetic methods, wide scope of chemical modification and functionalization and biocompatibility of such NPs.[84,86,89] Functionalized $Fe_3O_4$ NPs shows wide range of applications in plethora of organic transformations like hydrogenation[90], oxidation[91], multicomponent reactions[92,93] etc.

# 1.3 Organic polymers as heterogeneous catalysts

Polymers have been flag-bearer of heterogeneous catalysts for a very long time. They have been extensively used as catalyst in their own right or as supports to other homogeneous catalytic species, stoichiometric reagents, protecting groups, substrate carriers etc.[94-96]

The application of polymers as heterogeneous catalysts in organic synthetic procedure dates back to its use as ion-exchange resin catalysts in 1911.[97,98] I. G.

Farbenindustrie first translated this application for commercial purpose in 1940 by developing an esterification and ester-hydrolysis process over Wofatit phenol-formaldehyde resin where it was employed as a substitute for mineral acids and bases.[97] However until mid of 1960, synthetic polymers were of substantial technological attention mainly as material, but not preferably studied as organic molecules in their own right.[96]
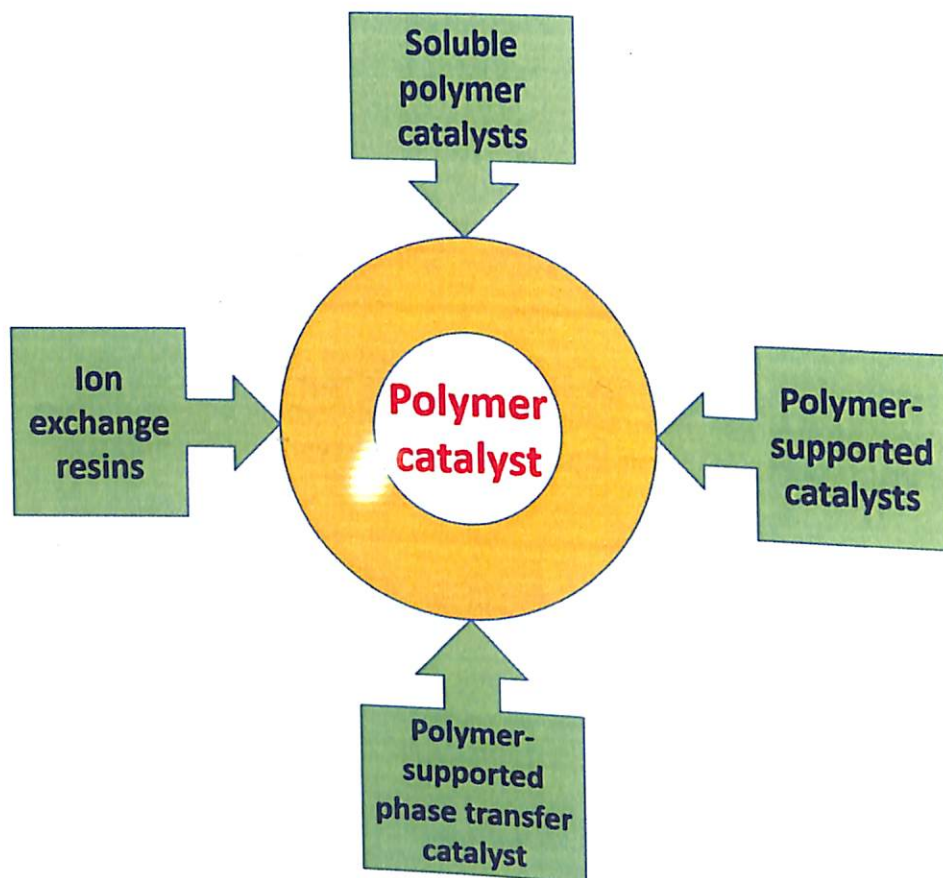


FIGURE 1.5 Types of various polymer catalysts

In 1963, Merrifield[99] first introduced the revolutionary concept of 'solid-phase technique' of peptide synthesis using an insoluble cross-linked polystyrene-based polymer. This innovatory idea paved the way for polymer-assisted synthesis where heterogeneous polymers found application in solid-phase synthesis as support, reagent and also in catalyst immobilization.[96,100]

Owing to their applications, polymer catalysis can be divided into following primary categories[94]-1) Soluble polymer catalysis, 2) Ion-exchange resin catalysis, 3) Catalysis by polymer- supported metal complexes, and 4) Catalysis by polymer-supported phase-transfer catalysts.

The first category of polymer catalysts consist of polymeric backbones tailed with organic catalytic pendent groups like pyridine, imidazole, phenolate ion etc. While in ion-exchange resins, there is a cross-linked polymer network to which an ion is electrostatically bound. The ion, when comes in contact with solution having ions of same charge, an exchange of ions can happen without affecting the polymeric backbone and that derives the name of the class of these materials. Owing to this property, both cation and anion ion-exchange resins have been explored in various applications like softening of water, waste-water treatment, metal-purification, chromatographic processes, bio-molecular separation in

pharmaceuticals, decolorizing agents in food industry etc. apart from being used in catalytic procedures.[101-103] The attractive distinction of these polymers with the former category is that the cross-linked resins are highly insoluble in solvents or said as 'macroscopically insoluble' and even during swelling in particular solvents, cannot form molecular solution.[94,101] The third category of catalysts assimilates the catalytic properties of homogeneous transition metal complexes with the technically advantageous heterogeneous polymeric framework. Due to the tremendous combination, these materials are appealing researchers in various domains.[104] Polymer supported phase-transfer catalysis is another interesting field of catalysis which utilizes insoluble polymers containing active functional groups viz. quaternary ammonium or phosphonium ions, cryptands, crown ethers etc. The active functional groups assist the transfer of ionic nucleophile present in aqueous phase into organic phase of the second reactant.[105]

With respect to the content of this thesis and brevity purpose, a glimpse of ion-exchange catalysts will only be outlined in this chapter.

## 1.3.1. Ion exchange resins as heterogeneous catalysts

There has always been a hunt for greener and safer chemicals throughout the expedition of research in chemistry. The innovative idea of utilizing ion exchange resin materials as heterogeneous catalysts in organic reaction was brought as a substitute for corrosive mineral acid catalysts in the early 20th century. The mineral acids $H_2SO_4$, toluene sulfonic acid are known for their highly corrosive action which creates hurdle in maintaining safety and hazard control during industrial applications. A further complication arises due to the need for neutralization of catalyst prior to catalyst separation where alkali metal oxides are added to neutralize the acid. Higher the amount of acid catalysts used, higher is the amount of alkali metal oxides needed for the process which finally results upsurge in the production cost as well as large outflow of waste to the environment.[106,107] All together these technical hitches worked as a strong driver to use acid-functionalized ion exchange resin materials as catalysts in important acid-catalyzed organic reactions. Due to the insoluble organic polymer matrix, ion-exchange resin catalysts can be easily separated out by simple filtration providing a corrosion-free atmosphere. Also polymer catalysts allows reactions to be carried out in wide range of conditions comprising aqueous/non-aqueous, polar/non-polar media.[107,108] It may be worth to mention that although the use of ion exchange resins as catalyst is a century-old concept and it was implemented commercially more than hundred years ago, but in its early age, the chemical properties of these resins were not preferably studied as organic molecules, rather they were scrutinized in material point-of-view. Lack of proper analytical techniques and instruments are also responsible for the very few structural and chemical knowledge available for these compounds. In recent times, various acid-functionalized, base-functionalized and even acid-base bi-functionalized (ampholytic) ion-exchange resin catalysts are available in literature and a good number of them avails commercial production of them.

A functionalized resin/polymer is a synthetic polymer having catalytically active functional group chemically bonded to it. There are two possible way for anchoring the active functional group- 1) direct polymerization or copolymerization of monomers having the required functionality; 2) post-functionalization of synthesized polymer; 3) Self polymerization of functional organic groups.[96] The first technique is often easier to carry out although the crucial point is to obtain the optimized condition of synthetic procedure to maintain the physical form of the resinous material. While the later one generally provides uniformly functionalized surface of material but it is rarely possible to achieve

functionalization of each repeating monomer of the resin by this technique.[96,101] In fact, different methods of preparation leads to different distribution of functionalized monomers and that turns out to show variation in their activities. Therefore this remains as an area demanding detailed investigations and more experiments in near future. Majority of the commercial ion exchange resins involves post-functionalization during production. But looking at the enormously evolving synthetic technologies and instrumentation and characterization facilities, copolymerization method of functionalized monomers forwards a good scope for further studies.



| Strong acid cation resin | Strong base Type I anion resin | Strong base Type II anion resin | Weak base anion resin |
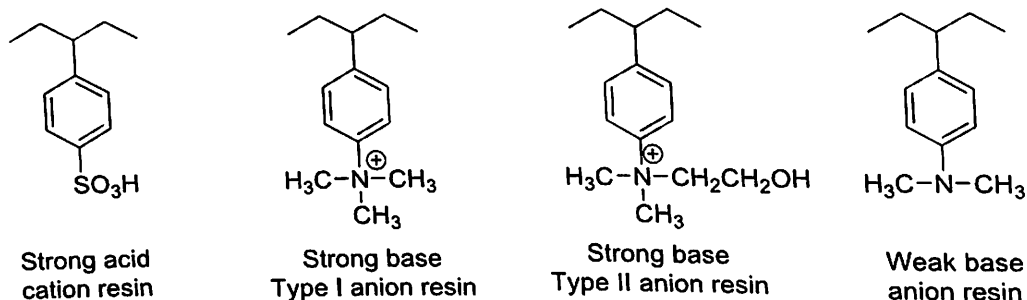
FIGURE 1.6 Some Styrene-DVB based ion exchange resins with different functionalities.

Most of the ion exchange resins manufactured worldwide are based on polymerization of styrene, cross-linked with divinylbenzene (DVB). Followed by the formation of polymer, different functional groups viz. sulfonic acid group, tertiary amine, quaternary amine group etc. are anchored to the polymer. Some important styrene-DVB based ion exchange resins with their structures are mentioned in Fig. 1.6. Another important class of ion exchange resins is phenol formaldehyde resins. In Fig.1.7, some interesting members of this category are displayed. The non-functionalized phenol formaldehyde resins prepared in basic condition are known as Bakelite while the same polymers synthesized in acidic conditions are known as Novolak.[101] Resins prepared from polyphenol, polyamine groups cross-linked with different monomers also offers important applications in extended fields. Some commercially available ion exchange resins include Dowex-50, Amberlyst-15, Amberlite IR-120 etc. which have been widely exploited in various chemical reactions.[108,109]
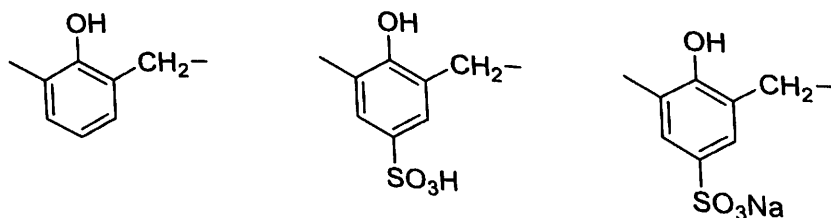


FIGURE 1.7 Some phenol-formaldehyde ion exchange resins.

## 1.3.2. Porosity of polymers

An important feature of ion exchange resins is the porous framework present in the internal structure of most of the resins. Just after the unveiling of excellent applicability of zeolites, porous materials are explosively experimented for wide range of applications. In the field of catalysis too, porosity of catalysts can take part a wonderful role for better activity. This is due to the fact that in porous catalysts, the ability to interact with reactant species does not get confined to the catalyst surface only but its scope extends up to the bulk of the material through the pore channels. This higher accessibility definitely helps to increase the surface area and thereby accelerate the catalyst activity.[110] After metal- organic framework (MOF)

or crystalline covalent-organic framework (COF), porous organic polymers (POP) are therefore gaining enormous attention as heterogeneous catalysts.

The pores of polymer catalysts (or for any porous material) can be ordered as micropores (< 2 nm), mesopores (2-50 nm) and macropores (> 50 nm) as recommended by IUPAC. The selectivity and activity of a porous polymer highly depends upon the pore-size, pore-volume or distribution of pores in its structure. Presence of micropores in organic polymers is very advantageous in terms of catalyst selectivity, however it renders the diffusion of reaction molecules resulting lower activity. Mesoporous resins can, therefore, be a sensible solution to this problem maintaining good balance between the catalyst activity and selectivity.[110,111]

The synthesis of POPs or generation of pores can be carried out by two ways- either by templating or without templating. Meanwhile templates in synthesis of polymers are very costly, and more than that, removal of templates after completion of the synthetic reaction is an energy-consuming and waste-generating process.[110] Hence template-free, simple protocols with controlled porosity are always desirable for synthesis of porous resin materials. The synthetic approach also influences the possible structure of a polymer. Post-modification, although, is a widely acceptable method for polymer synthesis but it always offers chance of pore-blocking. Copolymerization and self-polymerization processes are therefore advantageous for porous polymer synthesis in both perspectives- functional group concentration and porosity.

Stability of porous materials is another essential criterion for suitable applications. The strong covalent chemical bonding imparts stability to porous organic polymers which is sometimes difficult to maintain in the MOF and COF counterparts due to the reversible chemical bond forming reactions between their molecular units.[113,114] Thus porous organic polymers are much advantageous as heterogeneous catalysts due to their stability which facilitate the excellent recovery and reuse of the catalysts.

## 1.4 Waste biomass-based heterogeneous catalysts

Our planet is currently struggling with the dilemma between technological advancement of human life standard and the deterioration caused to the environment by those efforts. While natural non-renewable resources are being used up open-handedly, but the replenishment is continuously ignored; wastes are generated exceeding the product and hazardous chemicals are thrown into the atmosphere ruthlessly.[115] Owing to the eve-rising concern regarding harmful impact of chemicals, demand for cleaner technologies and safer chemicals is a need of the hour. Green chemistry aims to address this problem with 'responsible care' of chemical industries.[116] Since the evolving of the concept of green chemistry, waste-minimization and waste valorization in processing technology are getting solemn attention. To curtail the amount of waste generated in a chemical process, it is needful that the raw material or feedstock are always renewable or recyclable, the synthetic route limits the consumption of auxiliary substances like solvents and avoids the use of any toxic or hazardous substances in the reaction pathway.[116,117]

Since catalysts play a key role in synthetic procedures and contributes majorly to the cost of the protocol, it is necessary to check out the sustainability of catalytic substances. A large portion of traditional catalysts are based on metals that are toxic and precious. Apparently, application of such scarce metals makes the reaction protocols highly expensive

and also hazardous towards environment.[118] Recently, exploiting waste biomass for sustainable conversion to catalytic material has emerged as a burgeoning field of research. Utilizing bio-based waste for catalysts production can make the catalysts extremely ecofriendly, easy handling, biocompatible and most importantly economic due to their abundant nature compared to traditional metal catalysts. They eliminate the problem of disposal due to the biodegradable nature. Designing of biomass-based catalysts can be a fruitful solution to the hazards caused by chemical process as they present non-toxic, non-corrosive green catalyst.[119] On the other hand, such effort leads to valorization of waste material giving a breakthrough to the traditional thinking. Especially in agricultural sector, it is impossible to nullify waste generation. **During the process 'from farm to fork', each** year billion tons of food supply chain waste (FSCW) are generated worldwide. So there is a serious need to valorize those wastes to valuable materials in a profitable way.[120-122]
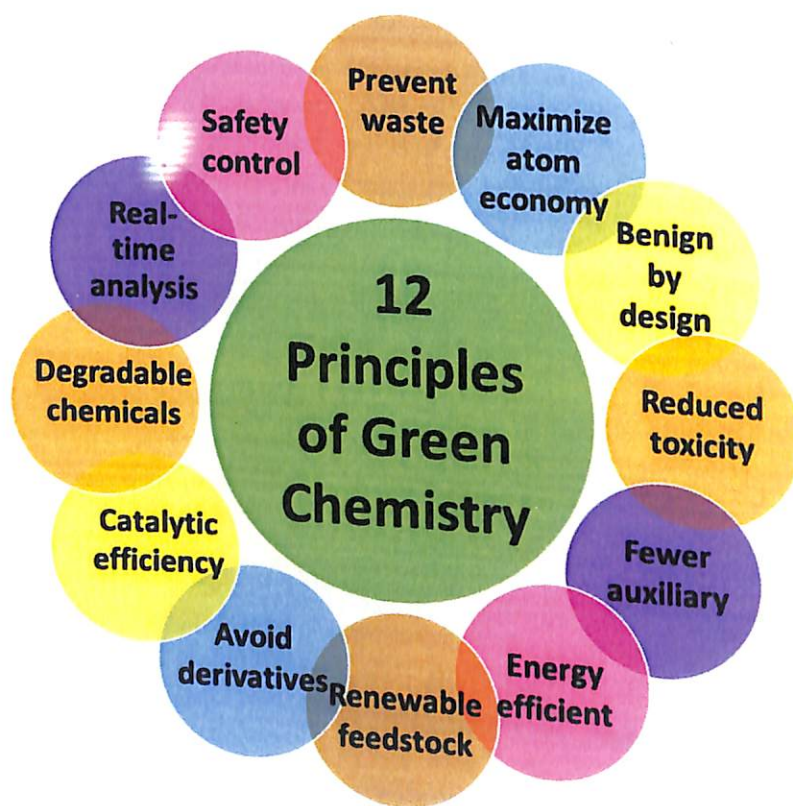


**FIGURE 1.8** Principles of green chemistry.

Owing to the concern regarding limiting resources and exponentially increasing waste materials worldwide, plethora of research have been carried on in different part of the world which are committed for transformation of agro-waste or biogenic waste materials to significant products. Quality research can be noticed in literature that involves valorization of waste into heterogeneous catalysts. However, this approach is still limited compared to the extensive research done involving utilization of wastes as feedstock to fuels and chemicals.

## 1.4.1. Sulfonated bio-derived carbon-based solid acid catalysts

Currently, there is considerable focus in exploring natural resources for designing carbon-based solid catalysts. The carbon-value of the food chain supply waste is very high and most importantly it is a renewable source. So they have been explored as heterogeneous catalysts after undergoing some chemical modification and functionalization.[121,123]

In a trending practice of preparing solid acid catalysts, carbon material is obtained by incomplete carbonization of natural organic materials which results in a rigid solid. The resultant solid material is then functionalized with –SO$_3$H group giving rise to a robust solid acid heterogeneous catalyst. Different biomass waste have been explored for carbonization which includes rice husk[124], bamboo[125], coffee residue[126], oil palm trunk[127], sugar cane bagasse[128], peanut shell[129], coconut shell[130], fungi resdue[131], olive cake[132], sweet potato[133], orange peel[134] etc.

Hara et al.[135] pioneered the synthetic strategy of these sulfonated carbonaceous catalysts using incomplete carbonization of sulfoaromatic compounds.[136] This was followed by introduction of carbonized and sulfonated solid acids derived from natural products like sugar, starch, cellulose etc. by Toda et al.[137] which showed potential stability and catalytic performance towards esterification reactions. Soon the carbon-source starting materials in the technique were replaced by biomass wastes resulting possible upsurge in their economic as well as sustainable viability. These partially carbonized solid acid carbon catalysts are hugely recognized due to their high acid density over the hydrophobic carbon surface. Porous structures of such materials are another significant factor which contribute to their interesting catalytic efficiency. More important to that, the biomass-derived sulfonated carbon catalysts are highly stable and insoluble in a wide range of solvents. Thus they carry the potential to the temperature-limitations of ion exchange resin catalysts.[123,124,138] Also due to the hydrophobicity of carbonous surface, the in-water reactions are driven smoothly towards forward direction.[139,140]

Studies have shown that the catalytic performance of these class of catalysts are largely dependent on the type of starting material used for the carbonization[128] and therefore keen research in this field is highly desirable as important as their application in industry-level production.

## 1.4.2. Biomass-derived solid base catalysts

Recently, a good number of solid base catalysts derived from biomass waste materials have emerged as potential candidates for heterogeneous catalyst. These catalysts find applications mainly in transesterification reactions for biodiesel production. As homogeneous alkali catalysts leads to saponification as a side reaction in transesterification, heterogeneous catalysts have found to be very advantageous in this context. Use of naturally abundant resources as feedstock for catalyst preparation potentially decreases the catalyst price and presents a green version of solid base catalyst.

The biomass-derived solid base catalysts are synthesized by using two types of sources- waste shells and biomass ashes.[119,141,142] Since waste shells of egg[143], shrimp[144], snail[145], oyster[146], mollusk[147] etc. are very rich in calcium (mainly as CaCO$_3$), so heating or calcination of these shells to certain higher temperature leads to the formation of CaO from CaCO$_3$. This biowaste-derived oxide material is then utilized as heterogeneous base catalysts in reactions. In general, CaO is obtained from limestone ore through a long synthetic route. Therefore the method of preparing bio-derived CaO based catalyst utilizing waste shells can be a potential substitution to the non-renewable source of limestone, also providing a step-efficient and inexpensive route to produce CaO.[148] Owing to the basicity of CaO, calcined waste shell derived heterogeneous catalysts show robust catalytic activity. Boro et al.[149] have reported that the catalytic performance of these catalysts are largely dependent on the calcination temperature used during its preparation. To explore better results, the calcined

waste shell derived catalyst powders are sometimes further modified, doped or impregnated with other molecules to offer synergic effect to their catalytic properties.[150-152]

Biomass ashes are another important class of waste-derived solid base catalysts which are prepared by burning or calcining biomass waste residues. During calcination process, substantial amount of mass loss happens with reduction of the carbonaceous matter.[119] Consequently, this results some highly active ash particles enriched with various metal oxides which can directly be used in reactions as catalyst. In order to enhance their performance, the ash are sometimes treated with potassium or calcium containing compounds.[153] Owing to their simple and easy preparation method and biowaste feedstock, biomass ash heterogeneous catalysts are prompting researchers for further effective investigations. Different types of ashes originated from biological waste feedstock have been exploited for preparing these solid base catalysts which includes coconut husk[153], cocoa husk[154], *Musa balbisiana* Colla peel[155], wood[156], torrey[157], palm fruit empty brunch[158], tucuma peel[159] etc. In addition to this, rice husk, camphor tree ash etc. have been explored as effective catalyst support or precursor in several synthetic methodologies.[160-162] The intrinsic composition, morphology, surface porosity and functionality of ash catalysts play significant role in determining their efficiency in catalytic reactions. Utilization of sophisticated analytical techniques can help to explore the behavior of the catalysts.

### 1.4.3. Other biomass-derived modified heterogeneous catalysts

Apart from the above mentioned categories, several attempts have been made to design bio-inspired catalytic systems which comprises metal complexes, nanoparticles immobilized onto biomass based compounds.[163,164] Recently, a number of metal impregnated biomass-derived catalysts have appeared in literature showing tailored advantages of both metal-based catalysts and biogenic catalysts.[165-167] Biochar is another important class of biomass-based heterogeneous catalysts which is a carbonous material obtained as a by-product in pyrolysis process of converting biomass to oil.[168] Owing to the porous structure and carbon-rich nature, biochar have been utilized in diverse range of applications like amending soil fertility[169], adsorbent of water contaminant[170], carbon storage[171] etc. and recently as heterogeneous catalysts or catalyst supports.[172] Different modification, fabrication or impregnation techniques have been employed to enhance the applicability of the catalysts.

However it can be clearly observed that almost all the efforts to design biomass based catalysts are centralized in the field of biofuel production, while the utilization of these catalysts can be rarely observed in fine chemical synthesis. So there is a vast scope to widen the domain of biomass-derived catalysts in other important organic synthetic schemes.

## 1.5 Other important heterogeneous catalysts

Apart from the categories mentioned above, diverse range of other heterogeneous catalysts are there in literature and in laboratory or industrial use. Zeolites are one of the most renowned and investigated class of heterogeneous catalysts that have been used from decades. Mesoporous silica or alumina are being used both as solid catalysts or catalyst-supports. Another very much studied and popular category of heterogeneous catalysts includes layered double hydroxides (LDH). Recently, metal organic framework (MOF) as heterogeneous catalysts have stimulated interests in the persistently growing field of catalytic research.

## Motivation and scope of present work

A brief assessment of literature and current scenario of catalytic research suggested the massive significance of using green catalysts in modern synthetic pathways. In order to meet the sustainability goal for future world, designing efficient, economic, recyclable and corrosion-free catalysts are 'need of the hour' in research and requires further attention. Heterogeneous catalysis has proven to be much advantageous in terms of step efficiency in product separation, purification and recyclability of the catalyst. However the biggest challenge of modern catalytic research is to cope up with the high catalytic performance and selectivity of homogeneous catalysis using the heterogeneous counterpart. There are several categories of heterogeneous catalysts, each of which has their öwn merits.

The background of most of the class of heterogeneous catalysts are discussed in this chapter which suggest that it is highly needful to design efficient catalysts that can take care of the shortcomings of homogeneous catalysts and also limitations of some heterogeneous catalysts available in previous literature. The present work was intended to carry out synthesis of some efficient heterogeneous catalysts that can be employed to useful organic synthetic processes. Characterization of the synthesized catalysts using various analytical and spectroscopic techniques facilitates the thorough investigation and assessment of the structure, property and behavior of the catalysts. The recovery and reusability of the catalysts are another interesting dimension of study of the catalytic protocols.

## Objective of the present work

After systematic assessment of the current status of utilization of various types of heterogeneous catalysts, the research problem and objectives were proposed as projected below-

- ➤ To synthesize a facile magnetic nanocatalyst, its characterization and application of the catalyst in some valuable organic transformation.
- ➤ To develop a polymer-based heterogeneous catalyst, study its functionality and morphology and investigate its catalytic activity in some useful organic reaction.
- ➤ To develop novel biowaste material-based solid catalyst, investigate its composition, structure and morphology and to discover its catalytic applicability in some known organic reaction.
- ➤ To explore green solvent-free methodologies for synthetically important organic transformations.

## References

1. R. E. Oesper, *J. Chem. Educ.* 1948, **25**, 531.
2. B. Lindström and L. J. Pettersson, *Cattech* 2003, **7**, 130-139.
3. S. J. Green, Industrial Catalysis, Macmillan Company, New York, 1928.
4. A. Libavius, Alchemia, Johannes Sautrius, Frankfurt, 1597.
5. H. Hartley, Studies in the history of chemistry, Clarendon press, Oxford, 1971.
6. A. J. B. Robertson, *Platinum Metals Rev.* 1975, **19**, 64-69.
7. J. J. Berzelius, *Annls. Chim. Phys.* 1836, **61**, 146.
8. F. Haber and G. van Oordt, *Z. Anorg. Chem.* 1905, **44**, 341.
9. G. Cohn, *Environ. Health Prospect* 1975, **10**, 159.
10. J. Heveling, *J. Chem. Educ.* 2012, **89**, 1530-1536.
11. A. Behr and P. Neubert, Applied Homogeneous Catalysis, Wiley-VCH, Weinheim, 2012.

12. V. Polshettiwar, R. Luque, A. Fihri, H. Zhu, M. Bouhrara and J. M. Basset, *Chem. Rev.* 2011, **111**, 3036-3075.
13. I. W. Davies, L. Matty, D. L. Hughes and Paul J. Reider, *J. Am. Chem. Soc.* 2001, **123**, 10139-10140.
14. T. Bligaard and J. K. Nørskov, Chemical Bonding at Surfaces and Interfaces, Elsevier, Amsterdam 2008.
15. N. R. Shiju and V. V. Guliants, *Appl. Catal. A Gen.* 2009, **356**, 1-17.
16. M. K. Sabbe, M. Reyniers and K. Reuter, *Catal. Sci. Technol.* 2012, **2**, 2010-2024.
17. I. Chorkendorff and J.W. Niemantsverdriet, Concepts of Modern Catalysis and Kinetics, Wiley-VCH, Weinheim, 2003.
18. Jason A. Widegren and Richard G. Finke, *J. Mol. Cat. A: Chem.* 2003, **198**, 317-341.
19. J. Schwartz, *Acc. Chem. Res.* 1985, **18**, 302-304.
20. N. Mizuno and M. Misono, *Chem. Rev.* 1998, **98**, 199-218.
21. P. Sabatier, J. B. C. R. Senderens and J. B. C. R. *Acad. Sci.* 1902, **134**, 514-516.
22. J. Chen, *Edu. Ped. Sci.* 2014, **4**, 3923-3926.
23. S. W. Kim, M. Kim, W. Y. Lee and T. Hyeon, *J. Am. Chem. Soc.* 2002, **124**, 7642-7643.
24. K. Yamaguch, K. Mori, T. Mizugaki, K. Ebitani, and K. Kaneda, *J. Am. Chem. Soc.* 2000, **122**, 7144-7145.
25. C. Copéret, M. Chabanas, R. Petroff Saint-Arroman and J.-M. Basset, *Angew. Chem. Int. Ed. Engl.* 2003, **42**, 156-181.
26. P. T. Anastas, M. M. Kirchhoff and T. C. Williamson, *Appl. Catal., A: Gen.* 2001, **221**, 3.
27. E. Amayuelas, A. Fidalgo-Marijuán, B. Bazán, M. K. Urtiaga, G. Barandika and M. I. Arriortua, *Cryst. Eng. Comm.* 2017, **19**, 7244-7252.
28. N. Diamantopoulos, D. Panagiotaras and D. Nikolopoulos, *J. Thermodyn. Catal.* 2015, **6**, 1-8.
29. M. K. Sabbe, M. Reyniers and K. Reuter, *Catal. Sci. Technol.* 2012, **2**, 2010-2024.
30. J. N. Armor, *Appl. Catal. A: Gen.* 2001, **222**, 407–426.
31. D. Macquarrie, *Appl. Organomet. Chem.* 2005, **19**, 696–696.
32. M. D. Serio, R. Tesser, L.Pengmei and E. Santacesaria, *Chem. Rev.* 2003, **103**, 4307-4365.
33. K. Tanabea and W. F. Hölderich, *Appl. Catal., A: Gen.*1999, **181**, 399-434.
34. S. B. Kalidindi and B. R. Jagirdar, *ChemSusChem.* 2012, **5**, 65–75.
35. R. P. Goodman, I. A. T. Schaap, C. F. Tardin, C. M. Erben, R. M. Berry, C. F. Schmidt and A. J. Turberfield, *Science*, 2005, **310**, 1661–1665.
36. Y. Jiang, P. Wang, X. Zang, Y. Yang, A. Kozinda and L. Lin, *Nano Lett.* 2013, **13**, 3524–3530.
37. J. Grunes, J. Zhu and G. A. Somorjai, *Chem. Commun.* 2003, **8**, 2257– 2260.
38. V. Polshettiwar and R. S. Varma, *Green Chem.* 2010, **12**, 743–754.
39. D. J. Cole-Hamilton, *Science* 2003, **299**, 1702.
40. R. T. Baker and W. Tumas, *Science* 1999, **284**, 1477.
41. D. Astruc, F. Lu and J. R. Aranzaes, *Angew. Chem. Int. Ed.* 2005, **44**, 7852 – 7872.
42. M.-C. Daniel and D. Astruc, *Chem. Rev.* 2004, **104**, 293.
43. D. I. Gittins and F. Caruso, *Angew. Chem.* 2001, **113**, 3089.
44. R. Schlgl and S. B. A. Hamid, *Angew. Chem. Int. Ed.* 2004, **43**, 1628 –1637.
45. M. C. Moulton, L. K. Braydich-Stolle, M. N. Nadagouda, S. Kunzelman, S. M. Hussain and R. S. Varma, *Nanoscale* 2010, **2**, 763-770.
46. R. J. White, R. Luque, V. L. Budarin, J. H. Clark and D. J. Macquarrie, *Chem. Soc. Rev.* 2009, **38**, 481-494 .
47. N. T. K. Thanh and L. A. W., *Green, Nano Today* 2010, **5**, 213–230.
48. K. McNamara and S. A. M., Tofail, *Adv. Phys. X*, 2017, **2**, 54–88.
49. L. Dykman and N. Khlebtsov, *Chem. Soc. Rev.* 2012, **41**, 2256–2282.
50. X. Li, F. Zhang and D. Zhao, *Chem. Soc. Rev.* 2015, **44**, 1346–1378.
51. J. M. Campelo, D. Luna, R. Luque, J. M. Marinas and A. A. Romero, *ChemSusChem* 2009, **2**, 18–45.
52. K. Zdansky, P. Kacerovsky, J. Zavadil, J. Lorincik and A. Fojtik, *Nanoscale Res. Lett.*, 2007, **2**, 450–454.
53. W. Kim, J. Zide, A. Gossard, D. Klenov, S. Stemmer, A. Shakouri and A. Majumdar, *Phys. Rev. Lett.* 2006, **96**, 1–4.
54. X. Li, S. M. Robinson, A. Gupta, K. Saha, Z. Jiang, D. F. Moyano, A. Sahar, M. A. Riley and V. M. Rotello, *ACS Nano* 2014, **8**, 10682–10686.
55. M. Segev-Bar and H. Haick, *ACS Nano* 2013, **7**, 8366–8378.
56. X. Luo, A. Morrin, A. J. Killard and M. R. Smyth, *Electroanalysis* 2006, **18**, 319–326.
57. R. Singh and J. W. Lillard, *Exp. Mol. Pathol.* 2009, **86**, 215–223.
58. O. Veiseh, J. W. Gunn and M. Zhang, *Adv. Drug Deliv. Rev.* 2010, **62**, 284–304.

59. U. P. M. Ashik, S. Kudo and J. Hayashi, An Overview of Metal Oxide Nanostructures, Elsevier Ltd., 2018.

60. A. Biswas, I. S. Bayer, A. S. Biris, T. Wang, E. Dervishi and F. Faupel, *Adv. Colloid Interface Sci.* 2012, **170**, 2–27.

61. Z. H. Low, S. K. Chen, I. Ismail, K. S. Tan and J. Y. C. Liew, *J. Magn. Magn. Mater.* 2017, **429**, 192–202.

62. A. Biswas, I. S. Bayer, A. S. Biris, T. Wang, E. Dervishi and F. Faupel, *Adv. Colloid Interface Sci.* 2012, **220**, 2-27.

63. K. Sakakibara, J. P. Hill and K. Ariga, *Small* 2008, **7**, 1288.

64. K. Ariga, M. V. Lee, T. Mori, X. Y. Yu and J. P. Hill, *Adv Colloid Interface Sci.* 2008, **154**, 20-29.

65. K. Ariga, M. Li, G. J. Richards and J. P. Hill, *J. Nanoscl. Nanotechno.* 2008, 11, 1-9.

66. S. Acharya, J. P. Hill and K. Ariga, *Adv Mater.* 2008, **21**, 2959-2989.

67. K. Ariga K, J. P. Hill and Q. Ji, *Phys Chem Chem Phys.* 2008, **9**, 2319-2340.

68. B. D. Gates, X. Qiaobing, M. Stewart, D. Ryan, C. G. Willson, G. M. Whitesides *Chem Rev.* 2005, **105**, 1171-1196.

69. T. Tsuzuki, *Int. J. Nanotechnol.* 2009, **6**, 567-.

70. D. L. Zhang, *Prog. Mater. Sci.* 2004, **49**, 537–560.

71. C. C. Koch, *Rev. Adv. Mater. Sci.* 2003, **5**, 91–99.

72. C. Suranarayana, *Prog. Mater. Sci.* 2001, **46**, 1–184.

73. C. g. Granqvist, L. B. Kish and W. H. Marlow, Gas Phase Nanoparticle Synthesis, Springer, Dordrecht, 2004.

74. F. E. Kruis, H. Fissan, H. and A. Peled, *J. Aerosol Sci.* 1998, **29**, 511–535.

75. J. Park, J. Joo, S. G. Kwon, Y. Jang, and T. Hyeon, *Angew. Chem. Int. Ed.* 2007, **46**, 4630–4660.

76. J. Eastoe, M. J. Hollamby and L. Hudson, L., *Adv. Colloid Interface Sci.* 2006, **128**, 5–15.

77. R. K. Sharma, S. Dutta, S. Sharma, R. Zboril, R. S. Varma and M. B. Gawande, *Green Chem.* 2016, **18**, 3184-3209.

78. P. Hu, L. Yu, A. Zuo, C. Guo and F. Yuan, *J. Phys. Chem. C.* 2008, **113**, 900–906.

79. N. Dong, F. He, J. Xin, Q. Wang, Z. Lei and B. Su, *Mater. Lett.* 2015, **141**, 238–241.

80. F. N. Sayed and V. Polshettiwar, *Sci. Rep.* 2015, **5**, 9733.

81. M. Senna, *Int. J. Inorg. Mater.* 2001, **3**, 509–514.

82. Boldyrev, V.V., *Mater. Sci. Forum.* 1996, 225, 511–520.

83. V. Polshettiwar, R. Luque, A. Fihri, H. Zhu, M. Bouhrara, and J. M. Basset, *Chem. Rev.* 2011, 111, 3036–3075.

84. Y. Zhu, L. P. Stubbs, F. Ho, R. Liu, C. P. Ship, J. A. Maguire and N. S. Hosmane, *ChemCatChem* 2010, **2**, 365 – 374.

85. S. Ko and J. Jang, Angew. Chem. 2006, 118, 7726 –7729; *Angew. Chem. Int. Ed.* 2006, **45**, 7564 – 7567.

86. L. M. Rossi, N. J. S. Costa, F. P. Silva and R. V. Gonçalves, *Nanotechnol Rev.* 2013, **2**, 597–614.

87. V. Polshettiwar, R. S. Varma, *Green Chem.* 2010, **12**, 743-754.

88. S. Shylesh, V. Schünemann, W. R. Thiel, *Angew. Chem. Int. Ed.* 2010, **49**, 3428.

89. W. Wu, Q. He and C. Jiang, *Nanoscale Res. Lett.* 2008, **3**, 397–415.

90. D. K. Yi, S. S. Lee and J. Y. Ying, *Chem. Mater.* 2006, **18**, 2459 –2461.

91. S. M. El-Sheikh, F. A. Harraz and K. S. Abdel-Halim, *J. Alloys Compd.* 2009, **487**, 716–723.

92. B. Dam, A. Kumar Pal and A. Gupta, *Synth. Commun.* 2016, **46**, 275–286.

93. J. Safari and Z. Zarnegar, *J. of Mol. Cat. A: Chem.*, 2013, **379**, 269– 276.

94. D. C. Sherrington, *Polym. Int.* 1980, **12**, 70-74.

95. M. Benaglia, A. Puglisi, and F. Cozzi, *Chem. Rev.* 2003, **103**, 3401-3429.

96. A. Akelah, *Chem. Rev.* 1981, **81**, 557-587.

97. A. Chakrabarti and M.M. Sharma, *React. Polym.* 1993, **20**, 1-45.

98. B. Tacke and H. Sfichting, *Landwirtsch. Jahrb.* 1911, **41**, 717-719.

99. R. B. Merrifield, *J. Am. Chem. Soc.* 1963, **85**, 2149-2154.

100. J. Lu and P. H. Toy, *Chem. Rev.* 2009, **109**, 815–838.

101. S. D. Alexandratos, *Ind. Eng. Chem. Res.* 2009, **48**, 388–398.

102. P. Barbaro and F. Liguori, *Chem. Rev.* 2009, **109**, 515–529.

103. J. M. Montgomery, Water Treatment Principals and Design; John Wiley & Sons, New York, 1985.

104. Y. Chauvin, D. Commereuc and I. Dawans, *Progress in Polymer Sci.* 1977, **5**, 95-98.

105. Y. Zhou, Z. Guo, W. Hou, Q. Wang and J. Wang, *Catal. Sci. Technol.*, 2015, **5**, 4324-4335.

106. A. L. Cardoso, S. C. G. Neves and M. J. da Silva, *Energies* 2008, **1**, 79-92.

107. M. A. Harmer, Q. Sun, *Appl. Catal. A.* 2001, **221**, 45-62.

108. M. M. Sharma, *React Funct Polym.*, 1995, **26**, 3-23.

109. S. H. Ali, A. Tarakmah, S. Q. Merchant, T. Al-Sahhaf, *Chem. Eng. Sci.* 2007, **62**, 3197-3217.
110. Q. Sun, Z. Dai, X. Meng and F. S. Xiao, *Chem. Soc. Rev.* 2015, **44**, 6018-6034.
111. B. L. Su, C. Sanchez and X. Y. Yang, Hierarchically Structured Porous Materials from Nanoscience to Catalysis, Separation, Optics, Energy, and Life Science, Wiley-VCH, Weinheim, Germany, 2012.
112. Y. Zhang and S. N. Riduan, *Chem. Soc. Rev.* 2012, **41**, 2083.
113. W.-Y. Gao, M. Chrzanowski and S. Ma, *Chem. Soc. Rev.* 2014, **43**, 5841-.
114. H. M. El-Kaderi, J. R. Hunt, J. L. Mendoza-Cortes, A. P. Cote, R. E. Taylor, M. O'Keeffe and O. M. Yaghi, *Science*, 2007, **316**, 268.
115. M. M. Kirchhoff, *Resour. Conserv. Recycl.* 2005, **44**, 237-243.
116. M. Poliakoff, J. M. Fitzpatrick, T. R. Farren and P. T. Anastas, *Science*, 2002, **297**, 807-810.
117. P. T. Anastas and J. C. Warner, *Green Chem. Theory Pract.* 1998, 30.
118. M. Poliakoff and P. Licence, *Nature* 2007, **450**, 810-813.
119. S. H. Y. S. Abdullah, N. H. M. Hanapi, A. Azid, R. Umar, H. Juahira, H. Khatoon and A. Enduta, *Renewable Sustainable Energy Rev.* 2017, **70**, 1040-1051.
120. R. A. Sheldon, *J. of Mol. Cat. A: Chem.* 2016, **422** -12.
121. R. Luque and J. H. Clark, *Sustainable Chem. Processes* 2013, **1**, 1-3.
122. C. O. Tuck, E. Pérez, I. T. Horváth, R. A. Sheldon and M. Poliakoff, *Science* 2012, **337**, 695-699.
123. X. Qi, H. Guo, L. Li, and R. L. Smith, *ChemSusChem* 2012, **5**, 2215-2220.
124. D. Zeng, Q. Zhang, S. Chen, S. Liu and G. Wang, *Microporous Mesoporous Mater.* 2016, **219**, 54-58.
125. Y. Zhou, S. Niu and J. Li, *Energy Convers.Manage.* 2016, **144**, 188-196.
126. K. Ngaosuwan, J. G. Goodwin and P. Prasertdham, *Renewable Energy* 2016, **86**, 262–269.
127. F. Ezebor, M. Khairuddean, A. Z. Abdullah and P. L. Boey, *Energy* 2014, **70**, 493-503.
128. W. Y. Lou, Q. Guo, W. J. Chen, M. H. Zong, H. Wu and T. J. Smith, *ChemSusChem* 2012, **5**, 1533-1541.
129. D. Zeng, S. Liu, W. Gong, G. Wang, J. Qiu and H. Chen, *Appl. Catal., A: Gen.* 2014, **469**, 284–289.
130. A. Endut, S. H. Y. S. Abdullah, N. H. M. Hanapi, S H. A. Hamid, F. Lananan, M. K. A. Kamarudin, R. Umar, H. Juahir and H. Khatoon, *Int. Biodeterior. Biodegrad.* 2017, **124**, 250-257.
131. M. Wang, W.W. Wu, S.S. Wang, X.Y. Shi, F.A. Wu and J. Wang, *BioResources* 2015, **10**, 5691-5708.
132. A. Sandouqa, Z. Al-Hamamre and J. Asfar, *Renewable Energy* 2019, **132**, 667-682.
133. H. Y. Chen and Z. W. Cui, *Catalysts* 2016, **6**, 211- 224.
134. D. R. Lathiya, D. V. Bhatt and K. C. Maheria, *Bioresour. Technol. Rep.* 2018, **2**, 69-76.
135. M. Hara, T. Yoshida, A. Takagaki, T. Takata, J. N. Kondo, S. Hayashi and K. Domen, *Angew. Chem. Int. Ed.* 2004, **43**, 2955 –2958.
136. H. Yu, S. Niu, C. Lu, J. Li and Y. Yang, *Fuel* 2017, **208**, 101–110.
137. M Toda, A. Takagaki, M. Okamura, J. N. Kondo, S. Hayashi, K. Domen, M. Hara, *Nature* 2005, **438**, 178.
138. T. Liu, Z. Li, W. Li, C. Shi and Y. Wanga, *Bioresour. Technol.* 2013, **133**, 618-621.
139. B. B. Hu, K. Wang, L. Wu, S. H. Yu, M. Antonietti and M. M. Titirici, *Adv. Mater.* 2010, **22**, 1–16.
140. R. Luque and J. H. Clark, *ChemCatChem* 2011, **3**, 594 – 597.
141. J. Boroa, D. Dekaa and A. J. Thakur, *Renewable Sustainable Energy Rev.* 2012, **16**, 904– 910.
142. R. Chakraborty, S. Chatterjee, P. Mukhopadhyay and S. Barman, *Procedia Environ. Sci.* 2016, **35**, 546-554.
143. Z. Wei, C. Xu and B. Li, *Bioresour. Technol.* 2009, **100**, 2883–2885.
144. L. Yang, A. Zhang and X. Zheng, *Energy Fuels* 2009, **23**, 3859–3865.
145. W. Roschat, T. Siritanon, T. Kaewpuang, B. Yoosuk and V. Promarak, *Bioresour. Technol.* 2016, **209**, 343-350.
146. N. Nakatani, H. Takamori, K. Takeda and H. Sakugawa, *Bioresour. Technol.* 2009, **100**, 1510-1513.
147. N. Viriya-empikul, P. Krasae, B. Puttasawat, B. Yoosuk, N. Chollacoop and K. Faungnawakij, *Bioresour. Technol.* 2010, **101**, 3765-3767.
148. L. M. Correia, R. M. A. Saboya, N. d. S. Campelo, J. A. Cecilia, E. Rodriguez-Castellon, C. L. Cavalcante and R. S. Vieira, *Bioresour Technol.* 2014, **151**, 207-213.
149. J. Boro, A. J. Thakur and D. Deka, *Fuel Process. Technol.* 2011, **92**, 2061-2067.
150. S. Jairam, P. Kolar, R. Sharma-Shivappa, J. A. Osborne and J. P. Davis, *Bioresour Technol.* 2012, **104**, 329-335.
151. H. Liu, H. S. Guo, X. J. Wang, J. Z. Jiang, H. Lin, S. Han and S. P. Pei, *Renewable Energy* 2016, **93**, 648-657.
152. N. S. Lani, N. Ngadi, N. Y. Yahya and R. A. Rahman, *J. Cleaner Prod.* 2017, **146**, 116-124.

153. V. Vadery, B. N. Narayanan, R. M. Ramakrishnan, S. K. Cherikkallinmel, S. Sugunan, D. P. Narayanan and S. Sasidharan, *Energy* 2014, **70**, 588-594.
154. V. O. Odude, A. J. Adesina, O. O. Oyetunde, O. O. Adeyemi, N. B. Ishola, A. O. Etim and E. Betiku, *Waste and Biomass Valorization* 2019, **10**, 877–888.
155. D. C, Deka and S. Basumatary, *Biomass Bioenergy* 2011, **35**, 1797–1803.
156. M. Sharma, A. A. Khan, S. K. Puri and D. K. Tuli, *Biomass and Bioenergy* 2012, **41**, 94-106.
157. A. P. S. Chouhan and A. K. Sarma, *Biomass and Bioenergy* 2013, 55, 386-39.
158. Z. Yaakob, I. S. B. Sukarman, B. Narayanan, S. R. S. Abdullah and M. Ismail, *Bioresour Technol.* 2012, **104**, 695-700.
159. I. M. Mendonça, O. A. R. L. Paes, P. J. S. Maia, M. P. Souza, R. A. Almeida, C. C. Silva, S. Duvoisin and F. A. de Freitas, *Renewable Energy* 2019, **130**, 103-110.
160. K. T. Chen, J. X. Wang, Y. M. Dai, P. H.Wanga, C. Y. Liou, C. W. Nien , J. S. Wua and C. C. Chen, *J. Taiwan Inst. Chem. Eng.* 2013, **44**, 622-629.
161. G. Y. Chen, R. Shana, J. Fu. Shi and B. B.Yan, *Fuel Process. Technol.* 2015, **133**, 8–13.
162. C. Li, X. Hu, W. Feng, B. Wu and K. Wu, *Energy Sources Part A.* 2018, **40**, 142-147.
163. B. Sahoo, D. Formenti, C. Topf, S. Bachmann, M. Scalone, K. Junge and M. Beller, *ChemSusChem* 2017, **10**, 3035-3039.
164. Y. Morioka, A. Matsuoka, K. Binder, B. R. Knappett, A. E. H. Wheatley, H. Naka, *Catal. Sci. Technol.* 2016, **6**, 5801-5805.
165. Q. Yan, C. Wan, J. Liu, J. Gao, F. Yu, J. Zhangc and Z. Cai, *Green Chem.* 2013, **15**, 1631-1640.
166. S. Eibner, F. Broust, J. Blin and A. Julbe, *J. Anal. Appl. Pyrolysis* 2015, **113**, 143-152.
167. L. Hu, X. Tang, Z. Wua, L. Linc, J. Xu, N. Xu and B. Dai, *Chem. Eng. J.* 2015, **263**, 299-308.
168. J. Lee, K. H. Kim and E. E. Kwon, *Renewable and Sustainable Energy Rev.* 2017, **77**, 70-79.
169. M. Inyang and E. Dickenson, *Chemosphere* 2015, 134, 232–240.
170. M. Uchimiya M, S. Hiradate and M. J. Antal, *ACS Sustain. Chem. Eng.* 2015, **3**, 1642-1649.
171. D. Woolf, J. E. Amonette, F. A. Street-Perrott, J. Lehmann and S. Joseph, *Nat Commun.* 2010, **1**, 6.
172. X. Xiong, I. K. M. Yu, L. Cao, D. C. W. Tsang, S. Zhang and Y. S. Ok, *Bioresour Technol.* 2017, **246**, 254-270.

# CHAPTER

# 2

# Literature Review

## 2.1 Applications of heterogeneous catalysts in tetrahydropyranylation/ depyranylation reaction of organic hydroxyl compounds

### 2.1.1 Introduction to tetrahydropyranylation/ depyranylation reactions

Protection/deprotection of a reactive functional group is a frequently dealt with operation in synthetic organic chemistry involving multifunctional organic compounds. Such synthetic manipulation is used to attack selective functionalities of a molecule by blocking another reactive group. Therefore synthesis of fine chemicals which are some complex and polyfunctional molecules involves protection/deprotection as additional tactics to selectively prevent side-reactions of particular functional groups.[1-4] Some commonly encountered functional groups which are often targeted for protection during any multistep synthetic route are hydroxyl, amino, carboxylic acid, carbonyl and thiol groups. In particular, hydroxy compounds are of massive significance in both biological and synthetic interests which constitute a major compartment of organic compounds including alcohols, phenols, carbohydrates, steroids etc. A large number of compounds having alcoholic and phenolic functionality find remarkable use in pharmaceutical and industrial purpose. Since –OH functionality is prone to oxidation and assessable to many reagents, most of the multi-step synthetic protocols require blocking of this group for further conversions. Protection of hydroxyl group, therefore, plays an important role during the synthesis and chemical reactions of these polyfunctional hydroxy compounds.[5,6]

Tremendous efforts have been made to design ideal hydroxy protection methodologies which led to the development of various protecting reagents over the years. Most of the strategies include ester formation by acylation[7] or tosylation[8] of alcohols and etherification using silyl ethers[9], alkoxyalyl ethers[10] and allyl ethers[11]. Among range of protecting groups, 3,4-dihydro-2H-pyran (DHP) is the most extensively used protecting group which converts alcohol to tetrahydropyranyl (THP) ether. This is because THP ethers

remain stable under wide range of reaction conditions and chemical reagents. They can withstand strongly acidic or basic conditions as well as oxidizing and reducing agents during various synthetic steps.[12-14] Moreover, THP ethers can be converted to multiplicity of functional groups according to the demand of the protocol.[15,16] The cleavage of the blocking group can easily be carried out under mild conditions with utmost selectivity which is an essential criteria for an ideal protecting group as mentioned by Schelhaas et al.[1,13,17,18]



R-OH + (3,4-dihydro-2H-pyran) DHP $\underset{DPRN}{\overset{THPRN}{\rightleftharpoons}}$ THP ether

Alcohol
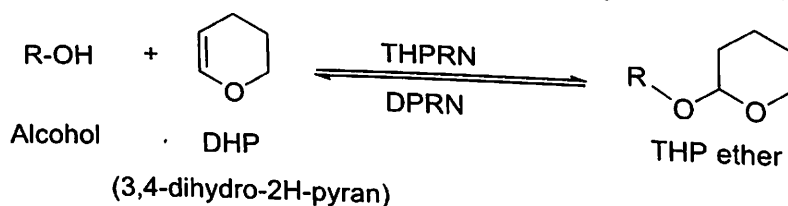
**SCHEME 2.1** Schematic representa'·n of tetrahydropyranylation (THPRN)/depyranylation (DPRN)

Despite the widespread use of protecting groups, it is has to be mentioned that use of protecting reagents along with unrecoverable, moisture-sensitive homogeneous catalysts makes a synthetic plan very complex and leads to a laborious and lengthy maneuver to carry out.[6,18,19] This is due to the additional (minimum of two) steps of protection/deprotection reactions coupled with tedious product purification processes associated to each step which creates extra hurdles and generates more wastes to the environment. Apparently, the yield of the final product of a synthetic process falls down in an observable manner. Therefore, for an ideal green synthesis to carry out, T. Anastas[20] in his famous twelve green chemistry principles recommended to minimize the use of protecting groups and to encourage the application of recoverable catalysts. To address these issues and considering the inevitable role of protection strategy, scientists have adopted heterogeneous catalytic techniques as an easily operable way to conduct the protection/deprotection reactions. Heterogeneous catalysis helps to minimize the laborious steps of product purification practice by introducing simple catalyst separation methods like filtration, centrifugation etc. Therefore use of such catalysts not only curtail the operational steps and time taken for a multistep synthesis but also contribute to enhance the final isolated yield of desired product and minimizing waste.[21-23]

A good amount of literature can be found engrossed in the application of heterogeneous catalysts for tetrahydropyranylation (THPRN) and depyranylation (DPRN) of hydroxy groups. The heterogeneous catalysts used for this organic transformation includes mainly polymer-based catalysts,[24,25] zeolites,[26,27] clays,[28] silica-based supported catalysts[29,30] and metal based catalysts.[12,31] Most recently functionalized nanoparticles[32,33] have also appeared as a powerful alternative to homogeneous catalysts.[13,34-36] In 2004, Sartori et al.[6] in their review article based on use of heterogeneous catalysis in various protection/deprotection techniques, mentioned the application of a number of heterogeneous catalysts in THPRN. A recent review of Kumar et al.[37] published in 2014 includes both homogeneous and heterogeneous catalysts used for THP ether formation and their conversion reactions. However, careful assessment of literature solely devoted to heterogeneous catalysis in tetrahydropyranylation/ depyranylation processes is yet not noticed to the best of our knowledge.

## 2.1.2 Polymer-based heterogeneous catalysts in the synthesis of THP ethers

Both ion-exchange resins and polymer-supported catalysts were found to be utilized in the synthesis of THP ethers from corresponding alcohols in literature. The commercially available resin Dowex 50WX4–100 efficiently catalyzed protection/deprotection reactions of alcohols in dichloromethane (DCM) under room temperature.[38] The protocol smoothly converted primary, secondary and cyclic alcohols to THP ethers resulting good yield.

(Scheme 2.2) Apart from that, resins like amberlyst[39], nafion[40] etc. are also utilized in THPRN reaction.

$$R\text{-OH} \quad + \quad \text{DHP} \quad \xrightarrow[\text{CH}_2\text{Cl}_2,\ \text{RT}]{\text{Dowex 50WX4-100}} \quad \text{THP ether}$$

Alcohol      DHP
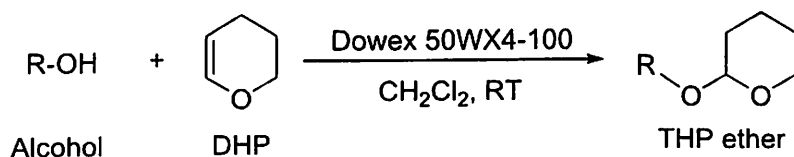
**SCHEME 2.2** THPRN reaction with Dowex 50WX4–100 resin as catalyst

A. Rahmatpour[41] in 2012 designed a polystyrene-supported gallium trichloride catalyst (PS-GaCl₃) as a reusable heterogeneous Lewis acid catalyst for successful THPRN/DPRN of alcohols and phenols (Scheme 2.3). The reaction was carried out using DCM as solvent under room temperature and a wide range of corresponding THP ethers were obtained in short reaction time with good yield. Also the procedure offered chemoselectivity towards monoetherification of symmetric diols.

$$R\text{-OH} \quad + \quad \text{DHP} \quad \xrightarrow[\text{CH}_2\text{Cl}_2,\ \text{RT}]{\text{PS-GaCl}_3} \quad \text{THP ether}$$

DHP      THP ether
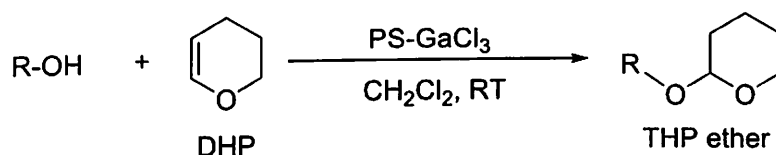
**SCHEME 2.3** THPRN reaction with polystyrene-supported gallium trichloride catalyst

Moghadam *et al.*[42], on the other hand, developed a metalloporphyrine tetrakis(p-aminophenyl)porphyrinatotin(IV) trifluoromethanesulfonate, [Sn$^{IV}$(TNH₂PP)(OTf)₂] which was heterogenized on chloromethylated polystyrene support and established the Lewis acid as an efficient catalyst for the synthesis of THP ethers from corresponding alcohols and phenols (Scheme 2.4). The catalyst was recycled for six catalytic runs without any loss of activity.

$$R\text{-OH} \quad + \quad \text{DHP} \quad \xrightarrow[\text{CH}_2\text{Cl}_2,\ \text{RT}]{[\text{Sn}^{IV}(\text{TNH}_2\text{PP})(\text{OTf})_2@\text{CMP}]} \quad \text{THP ether}$$

DHP      THP ether
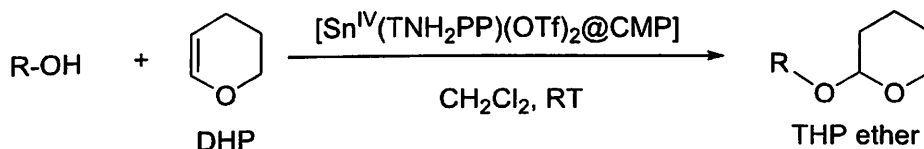
**SCHEME 2.4** THPRN reaction with polystyrene-bound tin(IV) porphyrin catalyst

## 2.1.3 Clay and zeolites as heterogeneous catalysts in THPRN/DPRN reactions

A vast range of naturally abundant clays have been exploited as heterogeneous catalysts for the THPRN/DPRN process. Hoyer *et al.*[28] in 1986 pioneered the use of K-10 clay, which is an acidic montmorillonite type phyllosilicate, in the THP etherification of alcohols and phenols (Scheme 2.5). The procedure gave an efficient yet inexpensive way to convert primary, secondary, tertiary, allylic, polyfunctional alcohols as well as phenols to respective THP ethers.

$$R\text{-OH} \quad + \quad \text{DHP} \quad \xrightarrow[\text{Dry CH}_2\text{Cl}_2,\ \text{RT}]{\text{K-10 Montmorillonite clay}} \quad \text{THP ether}$$

DHP      THP ether
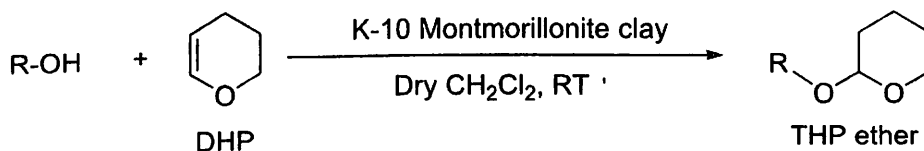
**SCHEME 2.5** THPRN reaction with K-10 Montmorillonite clay

Recently, Shirini *et al.*[43] in 2014 have developed a Sulfonic acid-functionalized ordered nanoporous Na$^+$-montmorillonite (SANM) clay-based heterogeneous catalyst and found its application in protection/deprotection of alcohols and phenols via THPRN/DPRN reactions using dry DCM solvent (Scheme 2.6). The protocol showed wide scope for

23

tetrahydropyranylation of primary/secondary alkyl, benzylic and phenols. Also the synthesized THP ethers were successfully deprotected using the same catalyst in methanol as solvent.

R-OH $\underset{\underset{\text{MeOH, RT}}{\text{SANM catalyst}}}{\overset{\overset{\text{DHP, SANM catalyst}}{\text{Dry CH}_2\text{Cl}_2\text{, RT}}}{\rightleftharpoons}}$ THP ether
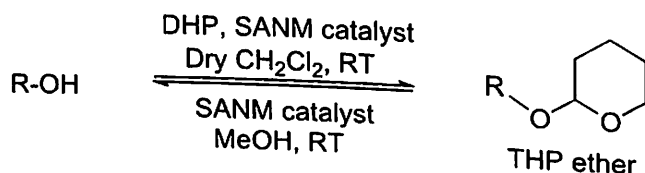
**SCHEME 2.6** THPRN/DPRN reaction using sodium montmorillonite clay catalyst

Some other clays that have been exploited in THPRN reaction are sepiolite clay[44], natural kaolinitic clay[45] etc. Many zeolites such as HY zeolite[46], HSZ zeolite[47], ITQ-2[48] are also established as effective heterogeneous catalysts in THPRN/DPRN reactions.

R-OH + DHP $\xrightarrow[\text{Dry CH}_2\text{Cl}_2\text{, RT}]{\text{Ersorb-4}}$ THP ether

Ar-OH + DHP $\xrightarrow[\text{Dry CH}_2\text{Cl}_2\text{, RT}]{\text{Ersorb-4}}$ THP ether

THP ether $\xrightarrow[\text{MeOH, RT}]{\text{Ersorb-4 catalyst}}$ R-OH + Byproduct
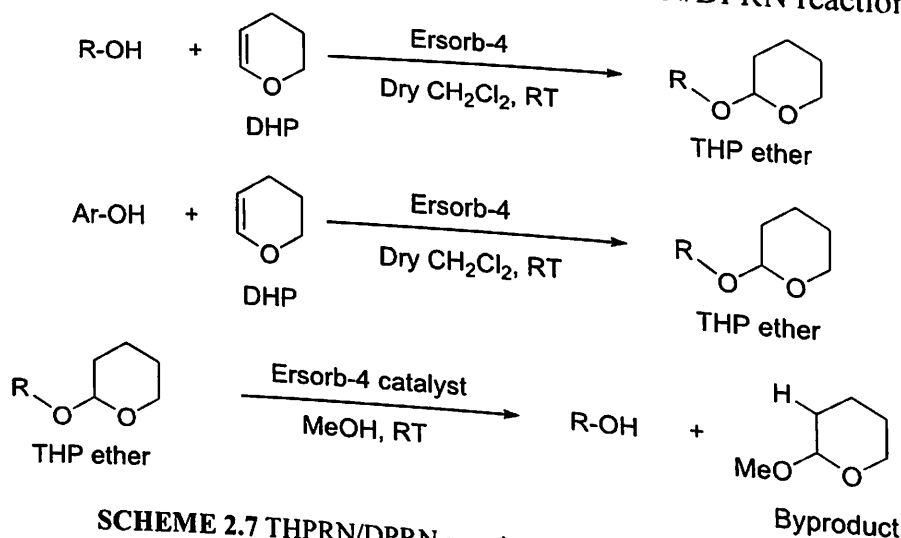
**SCHEME 2.7** THPRN/DPRN reaction using Ersorb-4 catalyst

As a recent example, Hegedüs et al.[27] have reported Ersorb-4 (E4) zeolite as an environment-friendly, inexpensive catalyst for the conversion of THP ethers from alcohols and phenols. The etherification of alcohols were carried out in dry DCM solvent while that of phenols were accomplished in toluene as solvent. The THP ethers synthesized were successfully deprotected using the same catalytic system but changing the solvent to methanol (Scheme 2.7).

## 2.1.4 Silica based heterogeneous catalysts in THPRN/DPRN reactions

Heterogenization of traditional homogeneous acid catalysts by impregnating the acid group onto a silica chain is a common practice seen in catalytic research. A number of silica-based catalysts have been developed to utilize in THP etherification reaction of hydroxy groups.[49,50] Shimizu et al.[28] first experimented SO$_3$H-functionalized amorphous silica as a heterogeneous catalyst for protection/deprotection of hydroxy group via acetalization and tetrahydropyranylation. The centrifugally separated catalyst after drying was recycled further for three another catalytic cycles without any reactivation needed. The deprotection of the THP ethers were conducted using the same catalyst with protonated solvent (Scheme 2.8).

R-OH $\underset{\underset{\text{MeOH, 25°C}}{\text{SiO}_2\text{-SO}_3\text{H}}}{\overset{\overset{\text{DHP, SiO}_2\text{-SO}_3\text{H}}{\text{Dry CH}_2\text{Cl}_2\text{, 25°C}}}{\rightleftharpoons}}$ THP ether
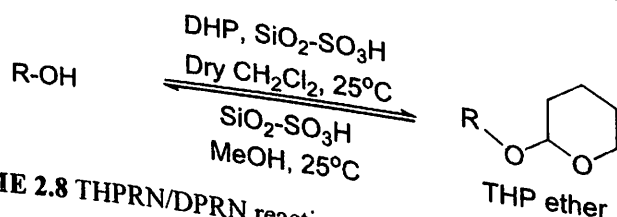
**SCHEME 2.8** THPRN/DPRN reaction using silica sulfuric acid catalyst

24

Karimi *et al.*[18] synthesized a sulfonated 3-mercaptopropylsilica (MPS) catalyst which successfully catalyzed THPRN reaction of alcohols and phenols using $CHCl_3$ solvent (Scheme 2.9). The catalyst showed high thermal stability up to 300°C, excellent heterogeneity and reusability up to at least 8th reaction cycles. Particularly, the procedure successfully protected allyllic alcohols without any dehydration product and isomerization of C=C bond.

R-OH + DHP — Sulfonated MPS / $CHCl_3$, RT → THP ether
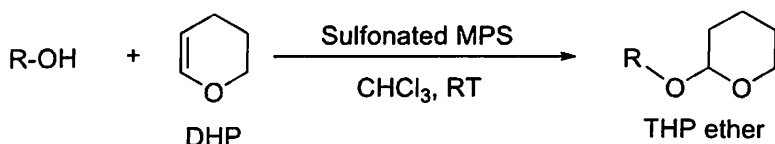
**SCHEME 2.9** THPRN reaction using sulfonated MPS catalyst

Recently, Azzena *et al.*[15] in 2018 have performed protection of alcohols by THPRN reaction using $NH_4HSO_4$ supported on silica as a recyclable solid acid catalyst and cyclopentyl methyl ether (CPME) or 2-methyltetrahydrofuran (2-MeTHF) as solvents (Scheme 2.10). The easy recovery of the catalyst and versatility of solvents were the key points of the protocol.

R-OH + DHP — $NH_4HSO_4@SiO_2$ / CPME or 2-MeTHF → THP ether
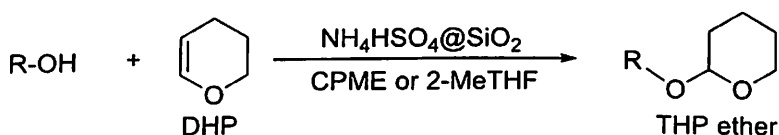
**SCHEME 2.10** THPRN reaction using $NH_4HSO_4$ supported silica catalyst.

## 2.1.5 Metal based heterogeneous catalysts in THPRN/DPRN reactions

Metal based heterogeneous catalysts comprise significant role in the catalysis of tetrahydropyranylation of hydroxy groups.[51,52,12]

Recently in 2016, Yadegari *et al.*[53] reported titanium salophen, a Schiff base metal complex, as efficient heterogeneous catalyst in THPRN reaction (Scheme 2.11). The catalyst resulted up to 100% yield of THP ethers from corresponding alcohols and phenols within very short time (minimum 2 minutes).

R-OH + DHP — $[Ti^{IV}(salophen)(OSO_2CF_3)_2]$ / $CH_2Cl_2$ → THP ether
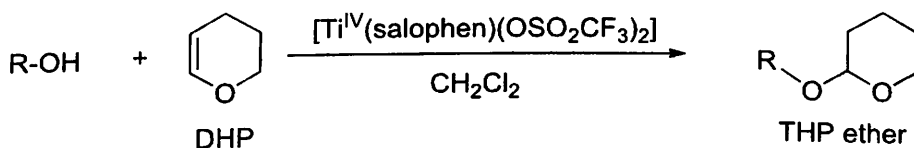
**SCHEME 2.11** THPRN reaction using titanium salophen as heterogeneous catalyst

Ziconium dioxide or zirconia based catalysts are another promising class of catalysts in organic transformations. Reddy *et al.*[54] employed sulfated zirconia in the successful protection of alcohols and phenols by THPRN (Scheme 2.12). The easy operation and simplified work-up procedure is the major advantage of the solvent-free protocol.

R-OH + DHP — $SO_4^{2-}/ZrO_2$ / Solvent-free → THP ether
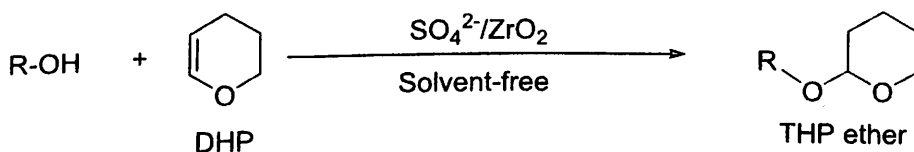
**SCHEME 2.12** THPRN reaction using sulfated zirconia

Taghavi *et al.*[12] introduced a porphyrine based Vanadium(IV) complex, which is high-valent tetraphenylporphyrinatovanadium(IV) trifluoromethanesulfonate, $[V^{IV}(TPP)(OTf)_2]$, as an effective heterogeneous catalyst for chemoselective

25

tetrahydropyranylation of primary alcohols over secondary, tertiary alcohols and phenols (Scheme 2.13).

R-OH  +  [DHP structure]  →  [V$^{IV}$(TPP)(OTf)$_2$] / Solvent-free, RT  →  [THP ether structure]

DHP                                                                    THP ether
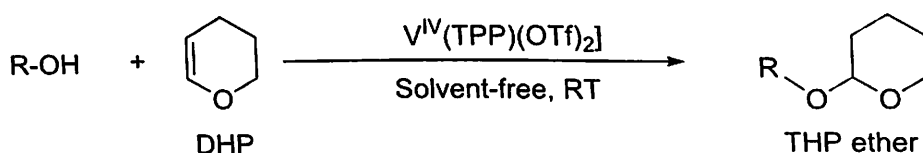
**SCHEME 2.13** THPRN reaction using [V$^{IV}$(TPP)(OTf)$_2$] catalyst

## 2.1.6 Nanomaterials as heterogeneous catalysts in THPRN/DPRN reactions

As a very recent practice, nanocatalysts have arisen as promising heterogeneous catalysts for the synthesis of THP ethers. In 2017, A. Rostami et al.[32] have designed a functionalized core-shell structure of magnetic nanocatalyst which finds application in the THPRN/DPRN of hydroxyl groups of wide range of alcohols and phenols (Scheme 2.14). The novel heterogeneous catalyst 1,4-Diazabicyclo[2.2.2]octane tribromide supported on magnetic Fe$_3$O$_4$ nanoparticles (MNPs-DABCO tribromide) is easily separable with external magnet which minimizes loss of catalyst during separation and provides simple operability to the reaction route.

DHP

R-OH  ⇌  MNP-DABCO tribromide / Dry CH$_2$Cl$_2$, RT  //  MNP-DABCO tribromide / MeOH, RT  ⇌  [THP ether structure]

THP ether
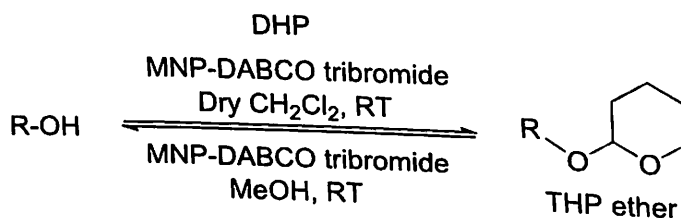
**SCHEME 2.14** THPRN/DPRN reaction using MNPs-DABCO tribromide catalyst

In 2016, the same author and his group[33] synthesized N-propylsulfamic acid supported Fe$_3$O$_4$ magnetic nanoparticles (MNPs-PSA), another magnetite based novel magnetic nano catalyst, and conducted THPRN/DPRN catalyst-reactions using that catalyst (Scheme 2.15). The magnetically retrievable catalyst can be reused up to ten times without any reactivation operation.

R-OH  ⇌  MNP-PSA / Dry CH$_2$Cl$_2$, RT  //  MNP-psa / MeOH, RT  ⇌  [THP ether structure]

THP ether
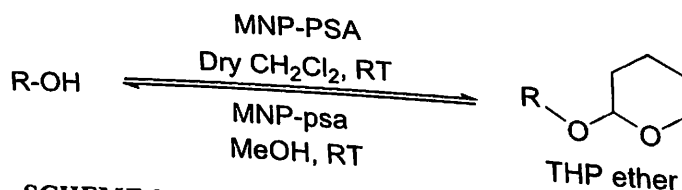
**SCHEME 2.15** THPRN/DPRN reaction using MNP-PSA

## 2.2 Heterogeneous catalysis in Henry reaction

### 2.2.1 Introduction to Henry reaction

The formation of C-C bond between two molecular entities is of paramount significance for the elaboration of a carbon framework and synthesis of newer organic compounds. Out of numerous examples, Henry reaction is an illustrious C-C bond forming reaction since its discovery in 1895.[55] The classical Henry reaction involves coupling of a carbonyl compound and a nucleophile (nitronate anion) generated by nitroalkane bearing α-hydrogen which leads to the concomitant generation of a bifunctional molecule called nitroalcohol.[56] Due to the similarity with Aldol reaction, this transformation is also known as Nitroaldol reaction. In the domain of synthetic organic chemistry, Henry or Nitroaldol reaction occupies a

26

distinctive place owing to the synthetically important nitroalcohol product.[57] Nitroalcohols are versatile synthetic precursor to form multiplicity of valuable organic compounds. Manipulation of the nitro and hydroxy group of nitroalcohol to rather complex functionalities results many pharmaceutically important molecules like β-aminoalcohol, 2-nitroketone, α-hydroxycarboxylic acid etc.[58-60]

The major challenge of Henry reaction procedure is the multiple number of possible side-reactions which sometimes results in less selectivity of the protocol. The nitroalcohol products, specially the products generated from aromatic aldehydes, are prone to undergo dehydration often giving β-nitrostyrene as side-product. In addition to that, the starting aldehyde compounds may follow Aldol, Cannizaro or Michael reaction routes to give respective products.[61,62] Diverse catalytic systems, both homogeneous and heterogeneous, have been reported till date to tackle with this challenge and deliver an efficient as well as selective protocol to synthesize nitroalcohols. Sharma et al.[63] recently reviewed in an article that the selectivity of Henry product is catalyst and substiuent-dependent for heterogeneous base-catalyzed reaction. Whereas Choudhury et al.[64] noticed that the basicity of the catalyst system and reaction system is crucial to achieve maximum yield of Henry product. Therefore designing a suitable, efficient, selective and environmentally benign heterogeneous catalyst for the above organic transformation is of utmost concern. The environment-friendly and green nature of the prospective catalysts will be of utmost significance because Henry reaction is itself a vital example of best atom economy.

## 2.2.2 Application of polymer-based catalysts in Henry reaction

Various ion-exchange resins and polymer-supported catalysts have been proved to be successfully catalyze Henry reaction to form nitroalcohols. Balini et al.[65] pioneered the use of Amberlyst-21 as a superior heterogeneous catalyst during the synthesis of nitroalcohols with or without solvent. Later in 2015, Lodh et al.[59] showed that the anion exchange resin Ambersep® 900 OH can be useful as a heterogeneous catalyst in Henry reaction (Scheme 2.16). The protocol resulted average to good yield (72-91%) of respective nitroalcohols. After the reaction the catalyst could be reused upto 3 times.
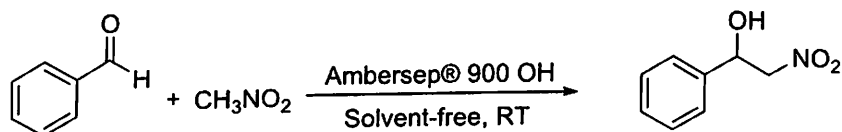


**SCHEME 2.16** Ambersep® 900 catalyzed Henry reaction

Recently in 2017, Gupta et al.[66] have synthesized a robust two dimensional Zn(II)-coordination polymer having 5-(benzylamino)isophthalic acid (H₂L) as linker which finds application in catalytic Henry reaction (Scheme 2.17). They checked different solvent-system for the reaction but solvent-free condition gave best result at optimized temperature 70°C.
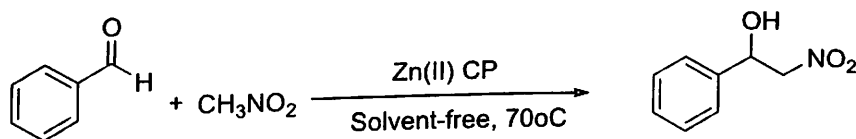


**SCHEME 2.17** 2-D Zn(II)-coordination polymer catalyzed Henry reaction

Das et al.[58] and Rokhum et al.[61] reported several polymer-supported catalyst which were found to efficiently catalyze Henry reaction for selective synthesis of nitroalcohols. In the report by Rokhum et al.[61] in 2012, an in situ generated ethyl acrylate conjugated polystyryldiphenylphosphine (PDPP–EA) polymer generated from the reaction of ethyl acrylate and polystyryl-diphenylphosphine was utilized for the synthesis of Henry reaction.

The reaction was conducted under solvent-free condition at room temperature and catalyst was successfully separated by washing with $CH_2Cl_2$ and ethyl acetate solvent. In 2013, Das et al.[58] they stated another protocol for Henry reaction[58] catalyzed by polymer based catalyst using commercially available polymer-bound DMAP (Scheme 2.18). The relatively greener method delivered moisture- insensitivity as well as tolerance towards various protecting groups due to polymeric backbone present in it.
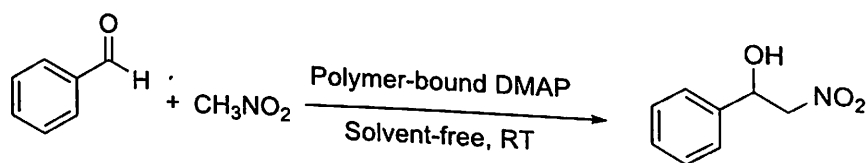


**SCHEME 2.18** Polymer-bound DMAP catalyzed Henry reaction

## 2.2.3 Application of metal oxide and carbonate based catalysts in Henry reaction

Basic alumina was the first solid base catalyst introduced by Ballini et al.[67] to replace the traditional homogeneous aqueous alkali solution catalysts in Henry reaction. Three years after that in 1986, Mélc· et al.[68] modified the catalyst as $KF/Al_2O_3$ which shortened the reaction time (5 hours) ·r the same yield (50% to 79%) of nitroalcohol (Scheme 2.19). The procedure was extended for aromatic aldehyde too without being dehydrated to styrene products.
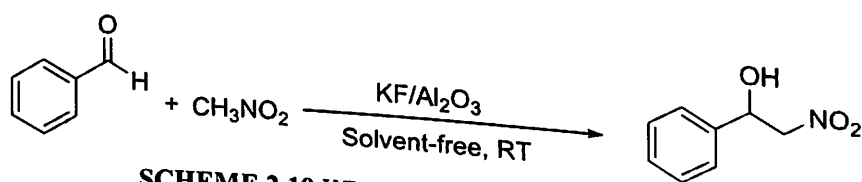


**SCHEME 2.19** $KF/Al_2O_3$ catalyzed Henry reaction

Akutu et al.[69] examined several metal oxides, hydroxides and carbonates that comprised of CaO, MgO, ZnO, SrO, BaO, $ZrO_2$, $Sr(OH)_2$, $Ba(OH)_2$, $KOH/Al_2O_3$, $MgO/Al_2O_3$, $MgCO_3$ etc. as probable solid base catalysts for Henry reaction. The catalytic activities of the solid bases in accordance with their output are tabularized in Table 2.1. Surprisingly, the order of the catalytic activities of alkaline earth metal oxide was opposite the order of basic strength but in accordance with their surface area.

**Table 2.1**: Activity of various metal oxide, hydroxide and carbonates as solid base catalysts in Henry reaction[69]

| Catalysts with good activity | Catalysts with moderate activity | |
|---|---|---|
| MgO, CaO, $Ba(OH)_2$, $Sr(OH)_2$, $MgCO_3$, KOH/alumina, KF/alumina and MgO-alumina | $Mg(OH)_2$, $Ca(OH)_2$, SrO, $SrCO_3$, BaO, $BaCO_3$, and $La_2O_3$ | Catalysts with no activity |
| | | $CaCO_3$, $ZrO_2$, and ZnO |

Recently, Bosica et al.[70] in 2017, reported $K_2CO_3$ as a versatile heterogeneous catalyst for solvent-free Henry and Michael reactions (Scheme 2.20). The method can be considered as an inexpensive yet neat synthesis procedure for nitroalcohols.
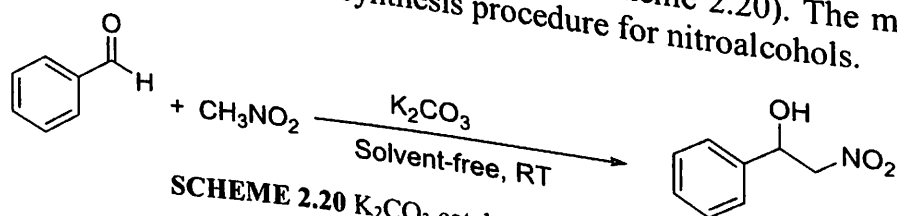


**SCHEME 2.20** $K_2CO_3$ catalyzed Henry reaction

## 2.2.4 Nanocatalysts in Henry reaction

A good variety of nanocatalysts have been developed as effective catalysts for nitroaldol reaction. Pradhan et al.[71] developed a $Ba^+$ modified zirconia ($Ba/ZrO_2$) nanoparticles which efficiently catalyzed Henry reaction (Scheme 2.21).
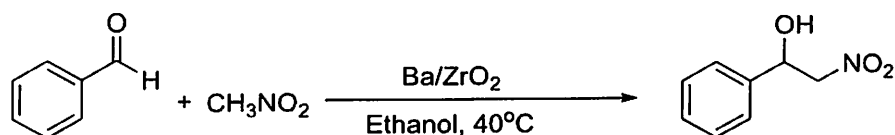
**SCHEME 2.21** Ba/ZrO₂ catalyzed Henry reaction

Sachdev *et al.*[72], on the other hand, presented a silica–polymer nanocomposites functionalized with piperazine SBA-Piperazine Catalyst or (SBA/PP) which was used to conduct nitroalcohol synthesis. The reaction procedure resulted best yield when conducted under solvent-free condition at 65°C (Scheme 2.22).
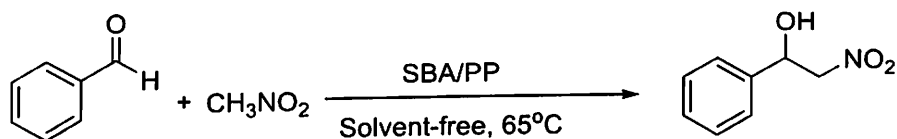


**SCHEME 2.22** SBA/PP catalyzed Henry reaction

Neelakandeswari *et al.*[73] studied the application of a nickel hydroxyapatite nanocomposite (Ni-HAp) in microwave-assisted Henry reaction. However unlike other protocols, the major product in this reaction appeared as nitrostyrenes with good yield (47.2%- 97.1%). Assessing the utility of nitrostyrene, this reaction can be a green synthetic route to synthesize nitrostyrene compounds (Scheme 2.23).
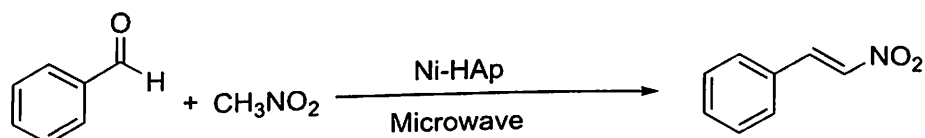


**SCHEME 2.23** Ni-HAp catalyzed Henry reaction

Kiasat *et al.*[74] in 2015 designed a Fe₃O₄ based magnetic nanoparticle which worked as a phase- transfer catalyst in water when employed to Henry reaction (Scheme 2.24). The catalyst was Fe₃O₄-copoly[(styrene/acrylic acid)/grafted ethylene oxide (nano-Fe₃O₄-PS-Co-[PAA-g-PEG]). After completion of the reaction the catalyst was separated using external magnet and reused up to 5$^{th}$ catalytic run without much depression in its activity.
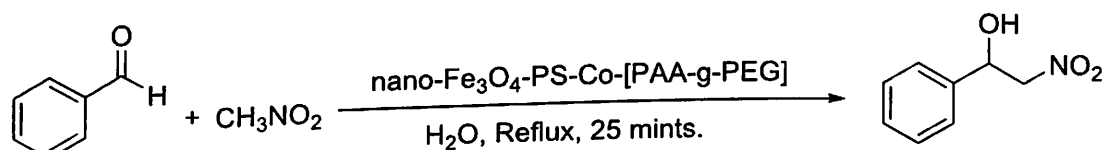


**SCHEME 2.24** Fe₃O₄-PS-Co-[PAA-g-PEG] catalyzed Henry reaction

## 2.2.5 Metal-Organic Framework catalyst in Henry reaction

Lately, a new class of heterogeneous catalysts has appeared as a promising material namely metal-organic framework which find tremendous applications in variety of fields. Recent reports of catalytic Henry reactions involve number of MOF catalysts to give selective nitroalcohol products.

Karmakar *et al.*[75] developed three Zn(II) based MOF by reacting with different functional groups including 2-acetamidoterephthalic acid (Framework 1), 2-propionamidoterephthalic acid (Framework 2) and 2-benzamidoterephthalic acid (Framework 3). Out of the all three novel compounds, framework 1 showed highest efficiency in catalyzing Henry reaction producing β-nitroalcohols in high yields (up to 95%) (Scheme 2.25).
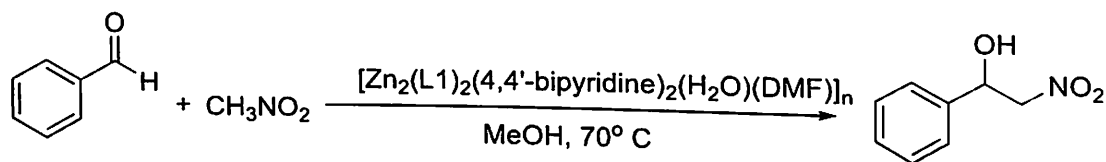
**SCHEME 2.25** Zn(II) based MOF catalyzed Henry reaction

A novel three dimensional nanoporous metal organic framework was designed by Shi *et al.*[76] from Cu(II) nodes and two kinds of pyridine carboxylate ligands. In the 3-D framework $[Cu_3(pdtc)L_2(H_2O)_3]$.2DMF.10H$_2$O, each one of the three Cu sites contains 1-D nanoscale opening channel and out of the five coordination sites of Cu, three are occupied by labile water molecules that can be easily replaced by other molecules making suitable for chemical reaction to happen. This MOF motif apparently shown good catalytic activity towards Henry reaction (Scheme 2.26). The catalyst was tested for heterogeneity and was successfully recovered by simple filtration.
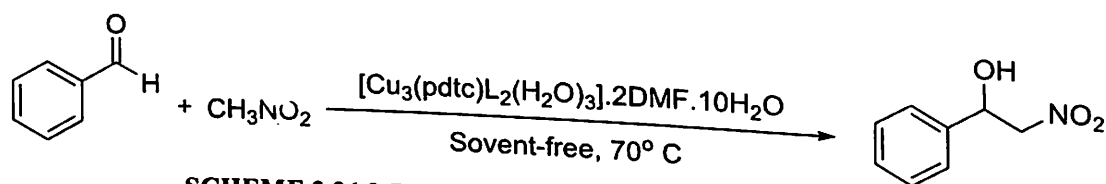


**SCHEME 2.26** 3-D Cu(II) based MOF catalyzed Henry reaction

In 2017, Gupta *et al.*[77] synthesized a novel porous 3-D NbO type framework in single crystal form containing piperazine-derived ligands and secondary building units of paddle wheel dinuclear $Cu_2(COO)_4$ as active centre. The framework worked as heterogeneous catalyst to synthesize β-nitroalcohols via Henry reaction of substituted benzaldehydes (Scheme 2.27).
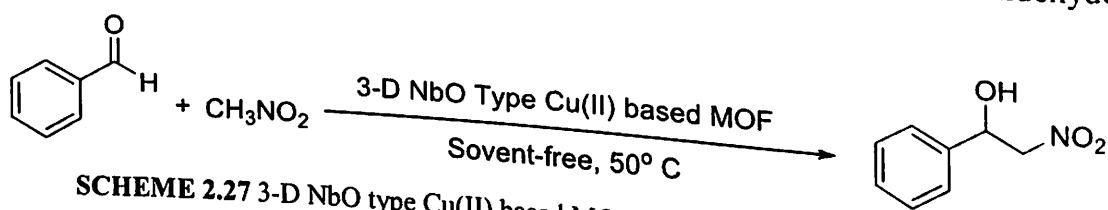


**SCHEME 2.27** 3-D NbO type Cu(II) based MOF catalyzed Henry reaction

Similarly an H-bond donating UiO-67 framework containing biphenyl-4,40-dicarboxylate struts and dicarboxylate functionalized by urea, was studied by Siu *et al.*[78]. Due to the porous structure, this MOF was also evidenced as a powerful heterogeneous catalyst for Henry reaction.

## 2.2.6 Other miscellaneous heterogeneous catalyst in Henry reaction

In addition to the classification mentioned above, diverse amount of other heterogeneous catalysts were being used for Henry reaction as can be noticed in literature. A common example is silica-based catalysts which offer wide scope for modification and functionalization as per requirement in reaction. The porous structure of silica surface adds extra perk to its potential catalytic activity for which many researchers opted them as catalyst support. N,N-diethylpropylamine-functionalized KG-60 silica was found to be efficient catalyst in Henry reaction in 2002[62], while in 2015 Borah *et al.*[79] presented a novel periodic mesoporous organosilica containing urea-pyridine moiety as a heterogeneous catalyst. Lately in 2018, Shokouhimehr *et al.*[80] synthesized a mesoporous silica with tuned pore and surface area, functionalized by amine groups which produced a solid base catalyst for Henry reaction.
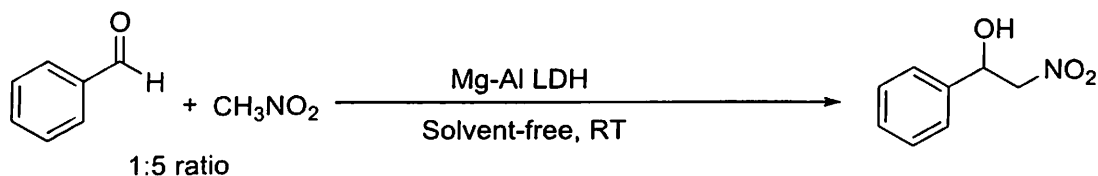
**SCHEME 2.28** Mg-Al HT LDH catalyzed Henry reaction

Another important category of heterogeneous catalysts popular in modern catalysis reactions are layered double hydroxides (LDH). Assessing the environmental threats and need for eco-friendly synthetic catalysts, Choudhury et al.[64] group designed a modified Mg-Al hydrotalcite material as an LDH catalyst to conduct Henry reaction (Scheme 2.28). Recently Abdellattif[81] and his co-authors synthesized three different types of LDH catalysts based on Cu, Mg and Al by varying their proportion. Cu:Mg:Al hydrotalcite (HT) shown advantageous effects on catalysis of Henry reaction compared to Cu:Al HT materials under microwave irradiation.

Some important metal complexes have also been studied extensively as heterogeneous catalysts for the useful transformation of aldehyde to nitroalcohols. In this context, copper complexes are the most studied and effective catalysts in Henry reaction to produce β-nitroalcohols.[82,83]

# 2.3 Efforts towards a greener Wittig reaction

## 2.3.1 General introduction to Wittig reaction

Synthesis of olefins by the formation of C=C has always been a corner stone in synthetic organic chemistry. The 'essential and ubiquitous' nature of C-C double bond makes olefin products targeted compound or precursor for many synthetic procedures. But it was indeed a challenging task to perform olefination of carbonyl group until 1953, when George Wittig and Geissler[84], the German chemists, first published a unique methodology for that valuable transformation. The reaction, known as Wittig reaction, involves formation of an alkene by the addition of alkylidinephosphorane/phosphonium ylide (or Wittig reagent) and an aldehyde or ketone by the consequent elimination of triphenylphosphine oxide (Scheme 2.29). Due to the generality and efficacy, the chemical reaction sooner got wide popularity as a regioselective and chemoselective procedure to prepare olefins, and was even employed in industrial scale.[85-87]
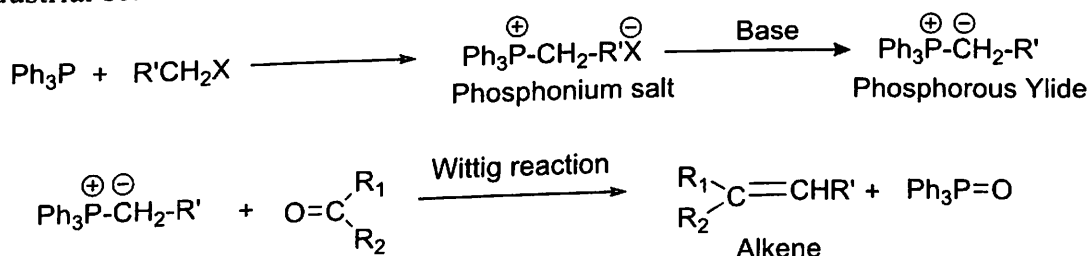


**SCHEME 2.29** Wittig reaction

However, the classical protocol has several shortcomings in view of the environmental and economic concern which forbids it to be used extensively in industrial scale. The major limitations includes its tedious multistep protocol[88] along with the less stereo-control of the products.[89,90] Another serious challenge is the low atom economy of the reaction protocol due to the formation of triphenylphosphine oxide as waste product, often difficult to separate.[91] Also, use of solution phase reactions of multistep procedure creates

31

hurdles due to the long, tiresome separation process associated with each step.[92] Therefore over the ensuing years, a number of efforts for modifications of the classical procedure have been attempted to enhance the green aspect of the reaction. Introduction of one-pot synthetic protocol[93], microwave-assisted reaction[91], Ball-milling[94] etc. are a few examples of the kind of modifications carried out to improve the protocol.

## 2.3.2 One-pot Wittig reaction

Conventionally, Wittig reaction involves three steps- first, formation of the phosphonium salt by reacting triphenylphosphine (Ph₃P) with a halide followed by base catalytic treatment of the salt to give Phosphorous ylide. The synthesized ylide is then allowed to react with carbonyl compounds (aldehyde or ketone) to afford the required olefin product. This three-step procedure is undoubtedly a tiresome practice and takes long operational time which prompted researchers to hunt for replacement of the multistep process.[95] In 1968, Buddrus[92] first introduced the one-pot version of Wittig reaction protocol, where coupling of three substrate components were conducted in a single efficient operation. This attempt not only reduced the operational time of the reaction but most significantly it minimized the energy and raw-material (like solvent) consumption in the overall procedure.[92,95]

In 2006, B. M. Choudary et al.[92] investigated a one-pot synthesis of alkene via Wittig reaction by the application of nanocrystalline magnesium oxide as a powerful catalyst (Scheme 2.30). The method successfully afforded the excellent yield of α,β-unsaturated esters and nitriles with high E-selectivity.

$$R-CHO + \underset{R'}{\overset{X}{<}} \xrightarrow[\text{DMF, RT}]{\text{NAP-MgO, PPh}_3} R\overset{R'}{=\!\!=} + Ph_3P=O$$
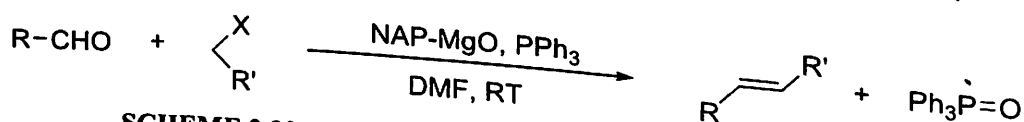
SCHEME 2.30 One-pot Wittig reaction using nanocrystalline MgO

M. L. Kantam et al.[96] performed one-pot Wittig reaction of aldehyde, α-halo esters and PPh₃ to synthesize α,β-unsaturated esters (Scheme 2.31). They used Mg/La mixed oxide as a highly basic heterogeneous catalyst for the transformation.

$$R-CHO + \underset{R'}{\overset{X}{<}} \xrightarrow[\text{DMF, RT}]{\text{Mg/La mixed oxide, PPh}_3} R\overset{R'}{=\!\!=} + Ph_3P=O$$
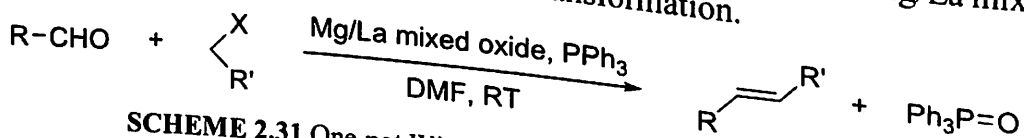
SCHEME 2.31 One-pot Wittig reaction using Mg/La mixed oxide

Other contribution to the field of one-pot Wittig protocols include the synthesis of macrolides by Liu and Tian[97], aqueous Wittig reaction for α,β-unsaturated esters by Wu and Yue[98] and many more methods still evolving.

## 2.3.3 Microwave-assisted Wittig reaction

The revolutionary idea of employing microwave heating in lieu of conventional heating for conducting organic synthetic reactions is credited to Giguere and Gedye[99]. Starting from the pioneering work of Gedye in 1986, numerous reports have emerged in the domain of microwave-assisted synthetic organic chemistry which gave a breakthrough to the difficulties associated with conventional heating viz. slow and time-consuming process, overheating of substrate, decomposition, high energy consumption etc. by reducing time hours to minute and enhancing yield and selectivity.[100,101] Wittig reaction conducted in conventional heating also suffers from these drawbacks and therefore it can be ameliorated by employing microwave heating. As per our survey, Xu et al.[102] first performed a microwave-assisted Wittig reaction in the year 1995 where reaction of aldehyde with the stable ylide triphenylcarbethoxymethylene phosphorane gave enhanced yield (82-96%) of ethyl cinnamate product (Scheme 2.32).

$$\text{Ar}-\text{CHOH} + \text{Ph}_3\text{P}=\text{CHCOOCH}_2\text{CH}_3 \xrightarrow[\text{Silica gel}]{\text{Microwave, 5-6 min}} \text{Ar}-\underset{\text{H}}{\text{C}}=\text{CHCOOCH}_2\text{CH}_2 + \text{Ph}_3\text{P}=\text{O}$$

Stable ylide
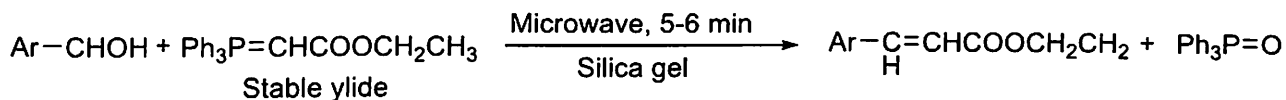
**SCHEME 2.32** First Microwave- assisted Wittig reaction

In the year 2001, Westman et al.[88] investigated a one-pot Wittig reaction using polymer-bound triphenylphosphine under microwave irradiation (Scheme 2.33). Production of olefins were obtained by using variety of aldehyde and organic halides and *in-situ* formation of solid-supported ylide.
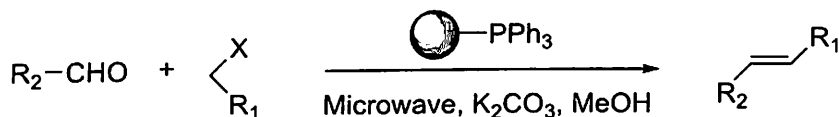


**SCHEME 2.33** Microwave- assisted one-pot Wittig reaction

Recently Werner et al.[91] in 2014 forwarded for the first time a microwave-assisted catalytic Wittig reaction using commercially available tributylphosphane oxide as a pre-catalyst. On the other hand, Frattini et al.[103] investigated a kinetic study of Microwave-assisted Wittig reaction carried out using aromatic aldehydes and stabilized ylides.

## 2.3.4 Oxidative Wittig reaction and heterogeneous catalysis

Lately, a number of publications emerged in literature reporting heterogeneous catalysis engrossed in Oxidation-Wittig reaction where starting product is alcohol and *in-situ* oxidation of alcohols to aldehyde takes place.

In 2008, Lee et al.[104] developed a metal nanocatalyst where Ru nanoparticles are entrapped in the porous structure of oxyhydroxides and utilized this catalyst for the production of olefins by Oxidation-Wittig reactions of alcohols via *in-situ* aerobic oxidation of alcohols to aldehyde (Scheme 2.34). Both aliphatic and benzylic alcohols are applicable to the procedure and apart from oxygen, no other additives are required.
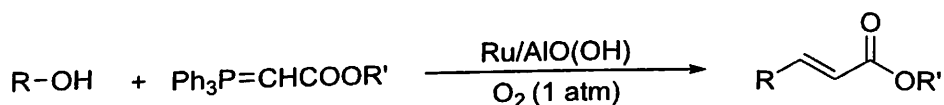


**SCHEME 2.34** Ru/AlO(OH) catalyzed Oxidation-Wittig reaction

Alonso et al.[105] demonstrated Oxidation-Wittig reactions of primary alcohols using Ni nanoparticles (Scheme 2.35). The reaction was particularly effective in case of benzyl alcohol and semi-stabilized benzyl ylides whereas limited scope was observed for aliphatic alcohol and non-stabilized alcohols.



**SCHEME 2.35** NiNPs catalyzed Oxidation-Wittig reaction

Carillo et al.[106] in 2014 synthesized mesoporous silica supported Ru nanoparticles which finds application in oxidative Wittig reaction of alcohols as heterogeneous catalysts (Scheme 2.36).
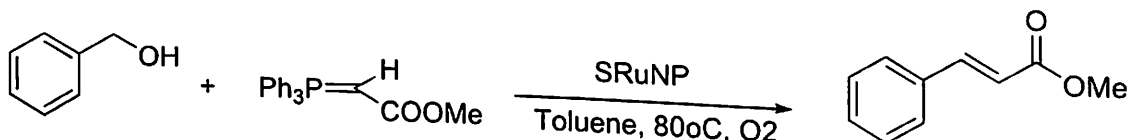
**SCHEME 2.36** Ru@SiO$_2$ catalyzed Oxidation-Wittig Olefination

Apart from these, many significant modifications to the classical protocol are still going on. One noteworthy replacement is Catalytic Wittig reaction where specially designed phosphines are used in catalytic amount that are regenerated by *in-situ* reduction of phosphine oxides. However the reaction still uses stoichiometric amount of reductant for the conversion.[91,107]

### 2.3.5 Substitutes for traditional solution phase Wittig reaction

In the year 2002, Balema *et al.*[94], reported solid state preparation of phosphorous ylides (stabilized, semi-stabilized and non-stabilized) by ballmilling the corresponding phosphonium salts with excess of K$_2$CO$_3$. More advantageously, they showed that mechanochemical generation of phosphorous ylides and the Wittig reaction of this with carbonyl compound can be carried out as a 'one pot' synthesis without undergoing time and solvent-consuming multistep protocol under a solvent-free manner. This investigation enlightened a new path for solvent-free, one-pot Wittig reaction relieving from conventional solution-phase reaction.

To get rid of the harmful effects and disposal problems of organic solvents, researchers came forward with aqueous Wittig reaction protocol and it has been effectively applied in case of stabilized[108] and semi-stabilized ylides[109].

# 2.4 Heterogeneous catalysis in transesterification reaction

## 2.4.1 Transesterification: Synthesis of biodiesel

As the world entered into a technology-reliant modern civilization, the demand for energy sources are ascending towards higher and higher altitude. The sharp decline in petroleum resources and the detrimental effects of the fossil fuels are constantly alarming to hunt for newer and cleaner sources of energy.[110-112] Biodiesel has emerged as a promising alternative to fossil fuels owing to its renewable resources, less CO$_2$ emissions, no sulfur content, non-toxicity and ecofriendly nature.[113-115] Synthesis of biodiesel is based on the chemical reaction of triglyceride molecules of vegetable oil with small alcohols, mostly methanol, using appropriate catalyst to afford a mixture of fatty acid methyl esters (FAME) and glycerol as by-product. The reaction is known as transesterification in which the viscosity of the vegetable oil gets reduced and it becomes suitable to be used in conventional engines.[116]
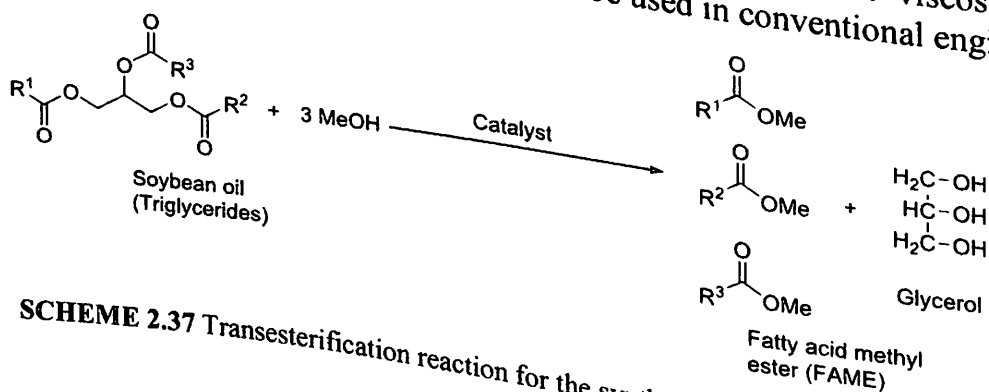


**SCHEME 2.37** Transesterification reaction for the synthesis of FAME or biodiesel

Earlier homogeneous alkali solutions, NaOH or KOH solutions were used as catalysts for this conversion due to their miscibility and high activity. But these aqueous alkali solutions when react with the triglyceride molecules often leads to saponification reaction as side-reaction. The soap formed in the reaction not only decreases the FAME yield but also inhibits the separation of glycerol from product mixture.[117-119] In view of this, heterogeneous catalysts have been a preferred catalyst for biodiesel production from recent past decades and have also been applied in industrial level.[120] Since catalysts take part a significant role in the processing of biodiesel and also substantially contribute to the production cost, thesaurus of heterogeneous catalysts are being investigated for an efficient, economic and environment-friendly transesterification reaction. Both acid and base catalysts have found effective in catalyzing transesterification reaction, although base catalysts are far more active (4000 times!) than the acid catalysts.[121] Diverse range of heterogeneous catalysts including metal oxides, carbonates, zeolites, polymers, double layered halides (LDH) etc. have found application in the biodiesel production reaction.[122-125] As a special mention, biowaste derived catalysts are of stimulating interest due to their abundance and green nature. So here, transesterification reaction catalyzed by biowaste-derived catalysts will only be discussed for brevity purpose.

### 2.4.2 Waste-shell derived biowaste catalysts in transesterification

Shells of eggs, snails, mollusks etc. are very rich in calcium, due to which calcination or combustion of these shells leads to the formation of calcium oxide (CaO). The basicity of calcium oxide makes these calcined shells as efficient and low-cost heterogeneous catalysts in transesterification reaction of vegetables oils.[126,127]

Nakatani et al.[128] performed the synthesis of FAME by transesterification of soybean oil at 65°C using combusted oyster shells (25 wt%) (Scheme 2.38). It was optimized that oyster shells combusted above the temperature of 700°C, are converted to CaO and thereby attain catalytic ability for biodiesel synthesis. Since in east Asian countries like Japan and Korea, oyster farming is a common practice so a large amount of shells are thrown as garbage. Valorization of these oyster shell as catalyst in biodiesel industries can not only lower the cost of catalyst production but also eliminate the problem of shell-waste disposal problem.
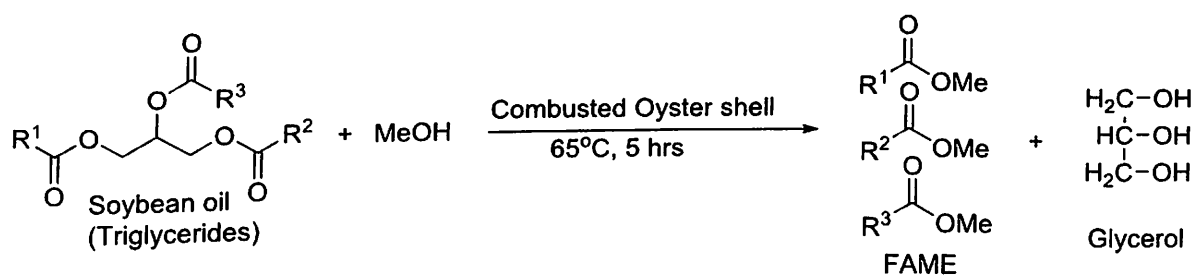


SCHEME 2.38 Transesterification reaction using combusted oyster shells as catalyst

Wei et al.[129] utilized calcined egg shells for biodiesel production from soybean oil (Scheme 2.39). The yield of FAME was obtained as maximum when the egg shells were calcined above 800°C. The optimized condition for the reaction was achieved with oil: methanol ratio as 1:9, 3% egg shell calcined at 1000°C and reaction temperature as 65°C which resulted 95% yield of biodiesel product after 3 hours of stirring.

35
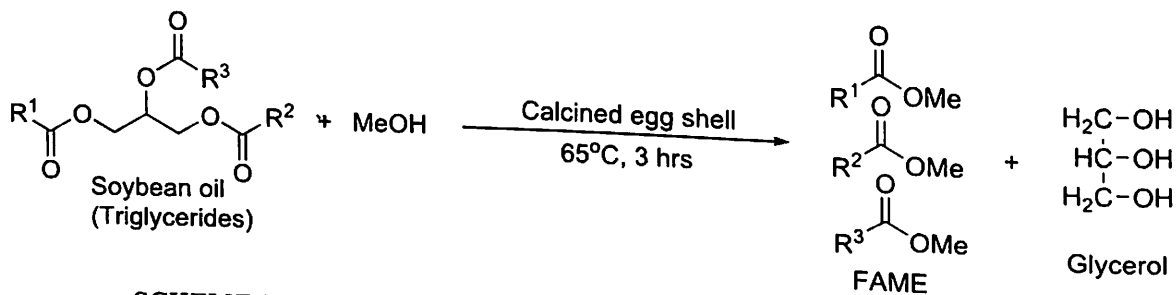
**SCHEME 2.39** Transesterification reaction using calcined egg shells as catalyst

Recently in 2018, Laskar *et al.*[130] reported 98% isolated yield of biodiesel from soybean oil using 3 wt% of waste snail shell calcined at 900°C as heterogeneous catalyst. The synthesis was performed using 1:6 oil to methanol ratio at an ambient temperature of 28°C for 7 hours reaction time. (Scheme 2.40).
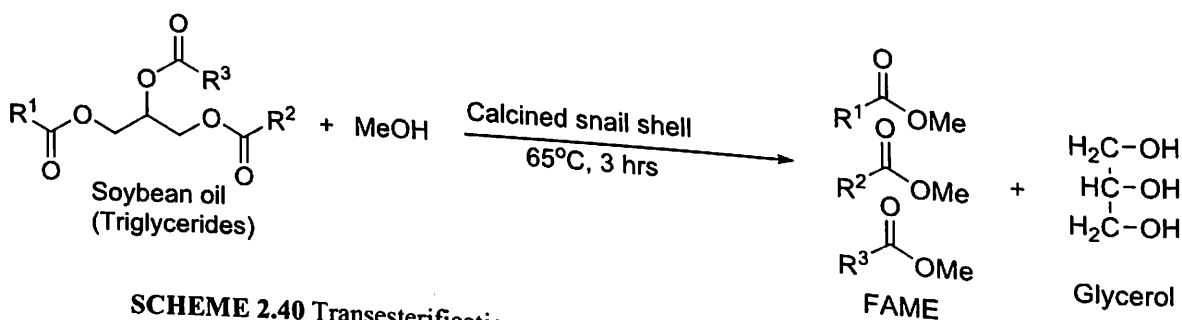


**SCHEME 2.40** Transesterification reaction using calcined snail shells as catalyst

Apart from these, calcined or combusted shrimp shell[131], mollusk shells[132] are also being utilized as heterogeneous catalysts for biodiesel synthesis.

Liu *et al.*[133], on the other hand, carried out some modification to snail shell in order to design it as an efficient heterogeneous catalyst for transesterification. They tried impregnation of the snail shell with KBr by immersing the precursor in KBr solution and subsequent activation at 500°C for 3 hours. The catalysis method resulted up to 98.5% yield of FAME. Similarly, Lani *et al.*[134] designed a silica-impregnated CaO catalyst for transesterification reaction where the precursor used for CaO and Silica were egg shell and rice husk respectively. The catalyst efficiently catalyzed biodiesel synthesis from both virgin and waste cooking oil.

## 2.4.3 Biomass ash based heterogeneous catalysts in transesterification reaction

In addition to this, various other biological sources, especially parts of plants like fruit shell, stem, peel etc., if combusted or calcined, the carbonaceous portion is reduced resulting a good amount of metal oxides and carbonates in it. Due to the enriched proportion of metal oxides together with the intrinsic properties of such ashes- like porous structure, basicity etc., the ash sample can attain the catalytic property. Multiple number of reports can be found in literature utilizing biomass ash as heterogeneous catalysts in recent time.

Mendonça *et al.*[135] in 2019 presented tucumã peel (*Astrocaryum aculeatum Meyer*) ash as heterogeneous catalysts in transesterification reaction (Scheme 2.41). The experimental procedure used 1% w/w amount of calcined peel ash (calcination temperature 800°C), oil to methanol ratio as 1:15 at temperature 80°C to afford 97.3% yield.
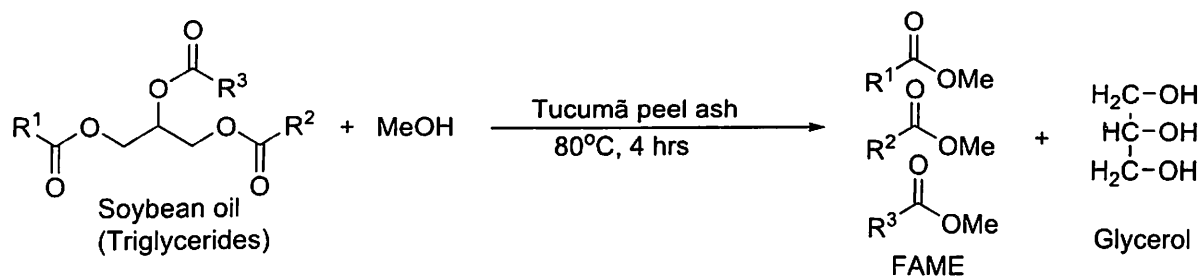
**SCHEME 2.41** Transesterification reaction using tucumã peel ash as catalyst

In the year 2018, Pathak *et al.*[136] recently reported an efficient and environment-friendly method of biodiesel synthesis from soybean oil using *Musa acuminata* banana peel ash as a heterogeneous catalyst (Scheme 2.42). Interestingly, the reaction was conducted at room temperature using 0.7 wt% of combusted banana peel ash and 1:6 oil to methanol ratio. After 4 hours of reaction it resulted maximum yield of 98.95%.
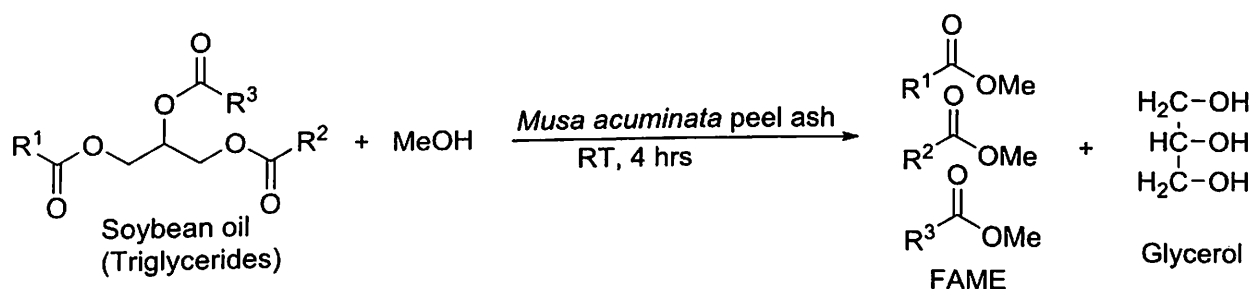


**SCHEME 2.42** Transesterification reaction using *Musa acuminata* banana peel ash catalyst

Chen *et al.*[137] synthesized a Li-modified biomass based catalyst using rice husk ash activated by LiCO$_3$ which act as a powerful catalyst in transesterification reaction. While Li *et al.*[138] used a K$_2$CO$_3$ impregnated camphor tree ash as catalyst for FAME synthesis.

## 2.4.4 Biochar based heterogeneous catalysts in transesterification reaction

Biochar is a carbon-rich material produced as a result of pyrolysis of biomass which find wide range of applications in various fields. The inherent properties of this low-cost substances *viz.* large surface area, porous morphology, large pore volume, stability, intrinsic surface functionality etc. makes biochar an attractive class of heterogeneous catalyst or catalyst precursor.[139] A number of biochar products have been investigated as heterogeneous catalysts or catalyst support in biodiesel synthesis.

Mckay *et al.*[140] reported a palm kernel-shell derived biochar as solid ash heterogeneous catalyst in the synthesis of biodiesel from sunflower oil. A yield of 99% FAME was achieved by the transesterification reaction using 3% catalyst loading and 1:9 oil to methanol ratio at 65°C. Li *et al.*[141] performed simultaneous transesterification of triglycerides and esterification of free fatty acids of cooking oil using sulfonated rice husk biochar.

# 2.5 Heterogeneous catalysis in solketal synthesis

## 2.5.1 Glycerol acetalization and synthesis of solketal

In recent decades, biodiesel industries all over the world have witnessed revolutionary growth owing to the diminishing fossil fuel reserves.[142,143] Since glycerol is a major by-product in biodiesel synthesis transesterification reaction, so there is a large out flux of

glycerol waste-stream which is far beyond its market demand. As a result of this, not only the commercial value of glycerol (or glycerin) is constantly subsiding, but also it is affecting the sustainable growth of the biodiesel industries. So the practice of transformation of glycerol to valuable products has become an eye-catching research in present scenario.[144-146]

Glycerol can be profitably converted to many derivatization processes such as esterification, etherification, oxidation and most importantly acetalization. Acetalization of glycerol with acetone leads to the formation of 2,2-dimethyl-1,3-dioxolane-4-methanol, a five-membered ring with one unprotected hydroxy group. This compound is commonly known as solketal and have been extensively used as fuel-additive, suspending agent, surfactant, plasticizer and flavoring agent.[147,148] It has been evidenced that applying solketal as vehicle fuel-additive results substantial improvement in the octane number and cold flow properties of fuel as well as potential reduction of particulate emission during fuel combustion.[143,149]

Heterogeneous catalysis finds significant applications in solketal synthesis which comprise of ion exchange resins, zeolites, mixed oxides, nanocatalysts etc.

## 2.5.2 Ion-exchange resins in the synthesis of solketal

Nanda et al.[145] reported Amberlyst-35 catalyzed solketal synthesis and its kinetic study where acetalization reaction was performed with glycerol and acetone using ethanol as solvent (Scheme 2.43). Silva et al.[150] used Amberlyst-36 for the same conversion.
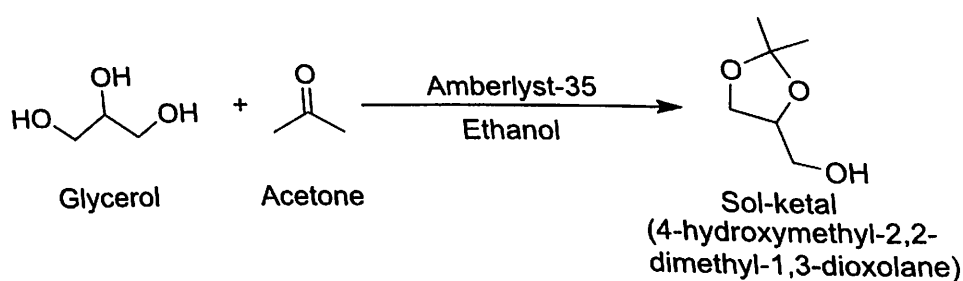


**SCHEME 2.43** Solketal synthesis using Amberlyst-35 as catalyst

Shirani et al.[151] reported acetalization reaction of glycerol with acetone on continuous reactor using Purolite® PD206 as heterogeneous catalyst (Scheme 2.44). The reaction was conducted at temperature 20°C, pressure 120 bar, glycerol to acetone ratio 1:5, feed flow rate 0.1 mL·min⁻¹ and catalyst amount 0.77 g to afford 95% yield of solketal.
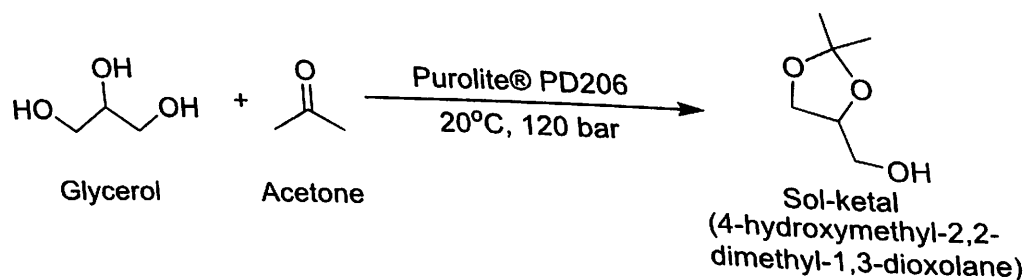


**SCHEME 2.44** Solketal synthesis using Purolite® PD206 as catalyst

Recently in 2018, Laskar et al.[152] synthesized a mesoporous Phenolsulfonic acid formaldehyde resin and forwarded an efficient method of solketal synthesis using that catalyst (Scheme 2.45). The protocol took 4 hours to attain 97% conversion and 100% selectivity at 60°C and using 1:5 glycerol to acetone ratio. The catalyst was reused up to 4th cycle without any reactivation needed before reuse.
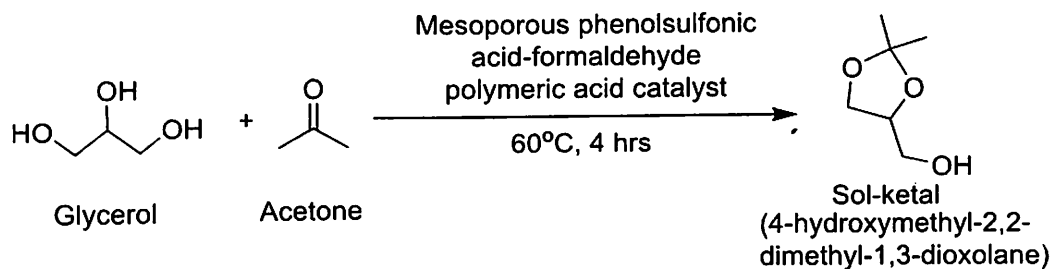
**SCHEME 2.45** Solketal synthesis using mesoporous Phenolsulfonic acid- formaldehyde resin as catalyst

## 2.5.3 Zeolites in the synthesis of solketal

Multiple number of zeolites have been used in glycerol acetalization reaction. Manjunathan et al.[142] investigated several zeolite type solid acid catalysts where H-Beta (with lower crystalline size) catalyzed synthesis of solketal by glycerol acetalization gave best result with 86% conversion and 98% selectivity (Scheme 2.46).
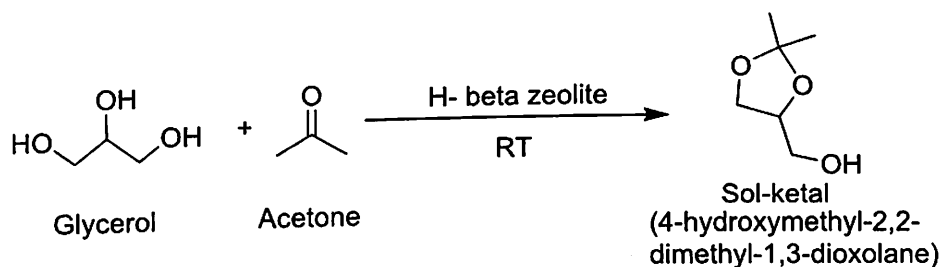


**SCHEME 2.46** Solketal synthesis using H-beta zeolite as catalyst.

In 2017, Priya et al.[153] demonstrated the use of various transition metal promoted mordenite zeolite based catalysts in acetalization reaction of glycerol (Scheme 2.47). The Cu-Mordenite catalyst resulted maximum conversion of 95% with 98% selectivity under microwave-assisted reacton.
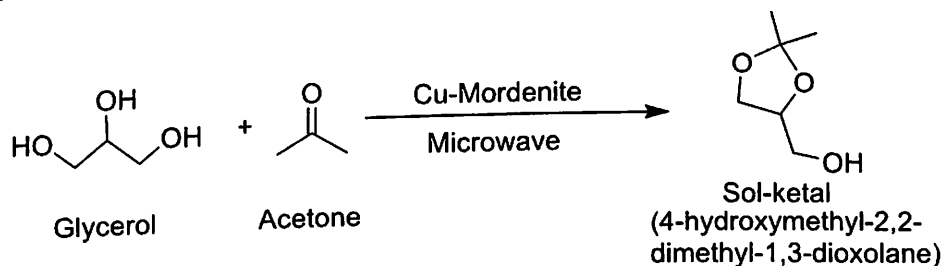


**SCHEME 2.47** Solketal synthesis using Cu-Mordenite zeolite as catalyst.

## 2.5.4 Metal oxides in the synthesis of solketal

Mallesham et al.[154] various $SnO_2$ based catalyst for utilization in glycerol acetalization reaction and reported $SO_4^{2-}/SnO_2$ as the most effective catalyst for the conversion compared to $WO_3/SnO_2$ and $MoO_3/SnO_2$ (Scheme 2.48). They anticipated that the higher activity of the former attributed to the increased acidic and ample superacidic sites.
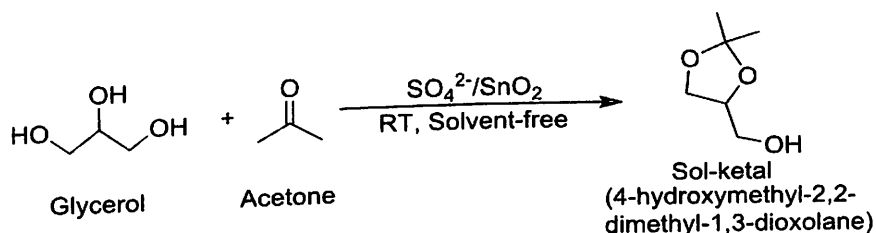


**SCHEME 2.48** Solketal synthesis using $SO_4^{2-}/SnO_2$ as catalyst.

Nair *et al.*[155] have performed solketal synthesis using Niobia (Nb$_2$O$_5$-573) catalyst at 70°C (Scheme 2.49). The method gave up to 70% yield and they observed that yield increases with increase in calcintion temperature of the catalyst
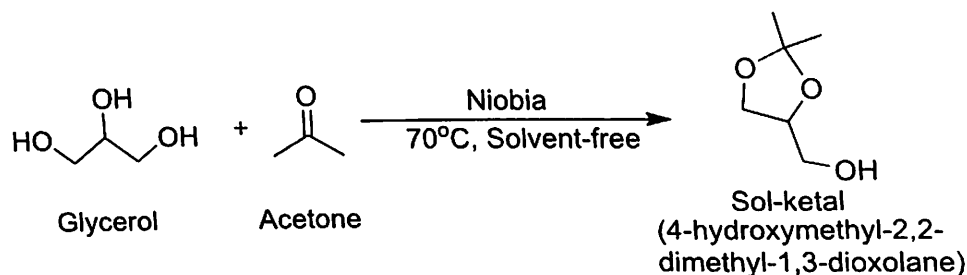


**SCHEME 2.49** Solketal synthesis using Niobia as catalyst.

## 2.6 Conclusion

After the brief assessmen. of literature on the application of various heterogeneous catalysts in several important organic transformations, it can be anticipated that heterogeneous catalysis is a leading catalytic technique in present era of catalytic research. While this technique being already used in industrial level in some special domains like biodiesel synthesis, several fields are yet to implement in large-scale production. Therefore this is need of the hour to design some efficient and environment-friendly heterogeneous catalytic pathway to perform significant chemical reactions like C-C bond forming reactions, protection deprotection strategies and industrially relevant biodiesel synthesis and glycerol valorization etc. For this, needful characterization of catalysts is utmost necessary to elucidate the properties of the catalytic compounds. Reusability is another important criteria which must be examined to learn the green character of a catalyst under investigation.

In consideration of the survey, the experimental studies of synthesis, characterization and applications of a few selected heterogeneous catalysts have been presented in this thesis. We believe that, in context of the present catalytic research, the findings of this thesis can be helpful in laboratory or industrial applications.

## References

1. M. Schelhaas and H. Waldmann, *Angew. Chem. Int. Ed. Engl.* 1996, **35**, 2056-2083.
2. T. W. Greene and P. G. M. Wuts, Protective Groups in Organic Synthesis, John Wiley, New York, 1999.
3. K. Jarowicki and P. J. Kociénski, *J. Chem. Soc., Perkin Trans.* 2001, **1**, 2109-2135.
4. B. Kumar, M. A. Aga, D. Mukherjee, S. S. Chimni and S. C. Taneja, *Tetrahedron Lett.* 2009, **50**, 6236-6240.
5. M. Sefkow and H. Kaatz, *Tetrahedron Lett.* 1999, **40**, 6561-6562.
6. G. Sartori, R. Ballini, F. Bigi, G. Bosica, R. Maggi and P. Righi, *Chem. Rev.* 2004, **104**, 199-250.
7. D. Orain, J. Ellard and M. Bradley, *Comb. Chem.* 2002, **4**, 1-6.
8. B. Das, V. S. Reddy and M. R. Reddy, *Tetrahedron Lett.* 2004, **45**, 6717.
9. B. E. Blass, C. L. Harris, D. E. Portlock, *Tetrahedron Lett.* 2001, **42**, 1611.
10. J. P. Yardley and H. Fletcher, *Synthesis* 1976, 244.
11. F. Guibe and Y. Saint M'Leux, *Tetrahedron Lett.* 1981, **26**, 5048.
12. S. A. Taghavi, M. Moghadam, I. M. Baltork, S. Tangestaninejad, V. Mirkhani and A. R. Khosropour, *C. R. Chimie* 2011, **14**, 1095-1102.
13. M. M. Heravi, F. K. Behbahani, H. A. Oskooie, R. H. Shoar, *Tetrahedron Lett.* 2005, **46**, 2543-2545.
14. Y. Fukase, K. Fukase and S. Kusumoto, *Tetrahedron Lett.* 1999, **40**, 1169-1175.

15. U. Azzena, M. Carraro, G. Modugno, L. Pisano and L. Urtis, *Beilstein J. Org. Chem.* 2018, **14**, 1655–1659.
16. B. L. A. P. Devi, K.N. Gangadhar, K.L.N. S. Kumar, K. S. Shanker, R.B.N. Prasad and P. S. Prasad, *J. Mol. Cat. A: Chem.* 2011, **345**, 96-100.
17. G. P. Ramanelli, C. Baronetti, H. J. Thomas and J. C. Autino, *Tetrahedron Lett.* 2002, **43**, 7589-7596.
18. M. H. Habibi, S. Tangestaninejad, I. Mohammadpoor-Baltrok, V. Mirkhani and B. Yadollahi, *Tetrahedron Lett.* 2001, **57**, 2851-2858.
19. B. Karimi and M. Khalkhali, *J. Mol. Catal. A: Chem.* 2005, **232**, 113–117.
20. P. T. Anastas and J. C. Warner, 12 Principles of Green Chemistry, J. C. Green Chemistry: Theory and Practice, 1998, 30.
21. S. W. Kim, M. Kim, W. Y. Lee and T. Hyeon, *J. Am. Chem. Soc.* 2002, **124**, 7642–7643.
22. K. Yamaguchi, K. Mori, T. Mizugaki, K. Ebitani, and K. Kaneda, *J. Am. Chem. Soc.* 2000, **122**, 7144-7145.
23. C. Copéret, M. Chabanas, R. Petroff Saint-Arroman and J.-M. Basset, *Angew. Chem. Int. Ed. Engl.* 2003, **42**, 156–181.
24. F. M. Menger and C. H. Chu, *J. Org. Chem.* 1981, **46**, 5044-5045.
25. B. Tamami and K. P. Borujeny, *Tetrahedron Lett.* 2004, **45**, 715-718.
26. I. Rodriguez, M. J. Climent, S. Iborra, V .Forne's and A. J. Corma, *Catal.* 2000, **192**, 441.
27. A. Hegedüs, I. Vígh and Z. Hell, *Synth. Com.* 2004, **34**, 4145–4152.
28. S. Hoyer, P. Laszlo, M. Orlovic and E. Polla, *Synthesis* 1986, 655-657.
29. K. I. Shimizu, E. T. Hayashi, T. Hatamachi, T. Kodamab and Y. Kitayama, *Tetrahedron Lett.* 2004, **45**, 5135–5138.
30. K. R. Kumar, P. V. V. Satyanarayana and B. S. Reddy, *Chin. J. Chem.* 2012, **30**, 1189-1191.
31. B. C. Ranu and M. Saha, *J. Org. Chem.* 1994, **59**, 8269-8270.
32. A. Rostami, O. Pourshiani, Y. Navasi, N. Darvishi and Shaghayegh Saadati, *New J. Chem.* 2017, **41**, 9033-9040.
33. A. Rostami, B. Tahmasbi, F. Abedi, *Res. Chem. Intermed.* 2016, **42**, 3689–3701.
34. M. Miyashita, A. Yoshikoshi, P.A. Grieco, *J. Org. Chem.* 1977, **42**, 3772-3779.
35. M.H. Habibi, S. Tangestaninejad, I. Mohammadpoor-Baltork, V. Mirkhani, B. Yadollahi, *Tetrahedron Lett.* 2001, **42**, 2851-2859.
36. J. H. V. Boom, J. D. M. Herscheid, *Synthesis* 1973, **3**, 169-170.
37. B. Kumar, M. A. Aga, A. Rouf, B. A. Shah, S. C. Taneja, *RSC Adv.* 2014, **4**, 21121-21130.
38. P. S. Poon, A. K. Banerjee, L. Bedoya, M. S. Laya, E. V. Cabrera and K. M. Albornoz, Synth. Com. 2009, 39, 3369-3377.
39. A. Bongini, G. Cardillo, M. Orena, S. Sandri, *Synthesis* 1979, 618–620.
40. G. A. Olah, A. Husain, B. P. Sing, *Synthesis* 1983, 892–895.
41. A. Rahmatpour, *Polyhedron* 2012, **44**, 66–71.
42. M. Moghadam, S. Tangestaninejad, V. Mirkhani, I. Mohammadpoor-Baltork, S. Gharaati, *J. Mol. Catal. A: Chem.* 2011, **371**, 95-101.
43. F. Shirini, M. Abedini, A. N. Abkenar, B. Baghernejad, *J. Nanostruct. Chem.* 2014, **4**, 1-6.
44. J. M. Campelo, A. Garcia, F. Lafont, D. Luna and J. M. Marinas, *Synth. Commun.* 1994, **24**, 1345-1352.
45. A. Cornelis and P. Laszlo, *Synlett* 1994, 155-158.
46. P. Kumar, C. U. Dinesh, R. S. Reddy and B. Pandey, *Synthesis* 1993, **11**, 1069-1074.
47. R. Ballini, F. Bigi, S. Carloni, R. Maggi and G. Sartori, *Tetrahedron Lett.* 1997, **38**, 4169-4177.
48. I. Rodriguez, M. J. Climent, S. Iborra, V. Fornés and A. Corma, *J. Catal.* 2000, **192**, 441-452.
49. D. Nedumaran and A. Pandurangan, *Microporous Mesoporous Mater.* 2013, **169**, 25–34.
50. S. Chandrasekhar, M. Takhi, Y. R. Reddy, S. Mohapatra, C. R. Rao and K. V. Reddy, *Tetrahedron* 1997, **53**, 14997.
51. B. C. Ranu and M. Saha, *J. Org. Chem.* 1994, **59**, 8269-8270.
52. F. Shirini, M. Ali Zolfigol and M. Abedini, *Bull. Chem. Soc. Jpn.* 2005, **78**, 1982–1985.
53. M. Yadegari and M. Moghadam, *Appl. Organometal. Chem.* 2016, **30**, 872-875.
54. B. M. Reddy and P. M. Sreekanth, *Synth. Commun.* 2002, **32**, 3561-3564.
55. L. C. R. Henry, *Hebd. Seances. Acad. Sci* 1895, **120**, 1265-1268.
56. F. A. Luzzio, *Tetrahedron*, 2001, **57**, 915–945.
57. J. Boruwa, N. Gogoi, P. P. Saikia and N. C. Barua, *Tetrahedron: Asym.* 2006, **17**, 3315-3326.
58. D. Das, G. Pathak and L. Rokhum, *RSC Adv.* 2016, **6**, 104154-104163.
59. R. Lodh, M. J. Sarma, *Monatsh Chem.* 2015, **146**, 969-972.

41

60. D. Uraguchi, S. Sakaki and T. Ooi, *J. Am. Chem. Soc.* 2007, **129**, 12392-12393.
61. L. Rokhum and G. Bez, *Can. J. Chem.* 2013, **91**, 300-306.
62. R. Ballini, G. Bosica, D. Livi, A. Palmieri, R. Maggib and G. Sartori, *Tetrahedron Lett.* 2003, **44**, 2271-2273.
63. K. K. Sharma, A. V. Biradar and T. Asefa, *ChemCatChem* 2010, **2**, 61-66.
64. B. M. Choudary, M. L. Kantam, C. V. Reddy, K. K. Rao and F. Figueras, *Green Chem.* 1999, **1**, 187-189.
65. R. Ballini, G. Bosica, and P. Forconi, *Tetrahedron* 1996, **52**, 1677-1684.
66. M Gupta, D. De, S. Pal, T. K. Pal and K. Tomar, *Dalton Trans.* 2017, **46**, 7619-7627.
67. G. Rosini, R. Ballini and P. Sorrenti, *Synthesis* 1983, 1014-1017.
68. J. M. Mélot, F. T. Boullet and A. Foucaud, *Tetrahedron Lett.* 1986, **27**, 493-496.
69. K. Akutu, H. Kabashima, T. Seki and H. Hattori, *Appl. Catal. A Gen.*, 2003, **247**, 65–74.
70. G. Bosica and K. Polidano, *J. Chem.* 2017, **2017**, 6267036-6267045.
71. S. Pradhan, K. Swarnima and B G Mishra, *J. Chem. Sci.*, 2016, **128**, 1119–1130.
72. D. Sachdev A. Dubey, *Catal Lett.* 2011, 141, 1548–1556.
73. N. Neelakandeswari, G. Sangami, P. Em  avaramban, R. Karvembu, N. Dharmaraj, H. Y. Kim, *Tetrahedron Lett.* 2012, **55003**, 2980–2ч o4.
74. A. R. Kiasat, M. Daei, S. J. Saghanezhad, *Res Chem Intermed* 2016, **42**, 581–594.
75. A. Karmakar, S. Hazra, M. F. C. Guedes da Silva, A. Paul and A. J. L. Pombeiro, *CrystEngComm.* 2016, **18**, 1337–1349.
76. L. X. Shi and C. D. Wu, *Chem. Commun.* 2011, **47**, 2928–2930.
77. A. K. Gupta, D. De and P. K. Bharadwaj, *Dalton Trans.*, 2017, **46**, 7782-7790.
78. P. W. Siu, Z. J. Brown, O. K. Farha, J. T. Hupp and K. A. Scheidt, *Chem. Commun.*, 2013, **49**, 10920-10922.
79. P. Borah, J. Mondal and Y. Zhao, *J. Catal.* 2015, 330, 129-134.
80. M. Shokouhimehr, M. S. Asl and B. Mazinani, *Res Chem Intermed* 2018, 44, 1617-1626.
81. M. H. Abdellattif and H. M. Mohamed, *Green Sustainable Chem.*, 2018, **8**, 139-155.
82. G. Murugavel, P. Sadhu and T. Punniyamurthy, *Chem. Rec.* 2016, **16**, 1906-1917.
83. V. J. Mayani, S. H. R. Abdi, R. I. Kureshy, N. H. Khan, A. Das and Hari C. Bajaj, *J. Org. Chem.* 2010, **75**, 6191-6195.
84. G. Wittig, G. Geissler, *Liebigs, Ann. Chem.* 1953, **580**, 44-57.
85. B. E. Maryanoff and A. B. Reitz, *Chem. Rev.* 1989, **89**, 863-927.
86. M. L. Schirmer, S. Adomeit and T. Werner, *Org. Lett.* 2015, **17**, 3078-81.
87. H. Ernst, *Pure Appl. Chem.* 2002, **74**, 2213–2226.
88. J. Westman, *Org. Lett.* 2001, **23**, 3745-3747.
89. D. Habrant, B. Stengel, S. Meunier, C. Mioskowski, *Chem. Eur. J.* 2007, **13**, 5433-5440.
90. E. Vedejs, H. W. Fang, *J. Org. Chem.* 1984, **49**, 211-213.
91. T. Werner, M. Hoffmann, S. Deshmukh, *Eur. J. Org. Chem.* 2014, 6873-6876.
92. B. M. Choudary, K. Mahendar, M. L. Kantam, K. V. S. Ranganath and T. Atharb, *Adv. Synth. Catal.* 2006, **348**, 1977-1985.
93. V. J. Buddrus, *Angew. Chem.* 1968, **80**, 535-536.
94. V. P. Balema, J. W. Wiench, M. Pruski and V. K. Pecharsky, *J. Am. Chem. Soc.* 2002, **124**, 6244-6245.
95. L. A. Morsch, L. Deak, D. Tiburzi, H. Schuster. B. J. Meyer, *Chem. Educ.* 2014, **91**, 611-614.
96. M. L. Kantam, K.B. S. Kumar, V. Balasubramanyam, G.T. Venkanna and F. Figueras, *J. Mol. Catal. A: Chem.* 2010, **321**, 10-14.
97. D. N. Liu and S. K. Tian, *Chem. Eur. J.* 2009, **15**, 4538-4542.
98. J. Wu and C. Yue, *Synth. Commun.* 2006, **36**, 2939-2948.
99. R. Gedye, F. Smith, K. Westaway, H. Ali, L. Baldisera, L. Laberge and J. Rousell, *Tetrahedron Lett.* 1986, **27**, 279-281.
100. P. Lidström, J. Tierney, B. Wathey and J. Westman, *Tetrahedron* 2001, **57**, 9225-9231.
101. J. McNulty, P. Das and D. McLeod, *Chem. Eur. J.* 2010, **16**, 6756-6760.
102. C. Xu, G. Chen, C. Fu and X. Huang, *Synth. Commun.* 1995, **25**, 2229-2233.
103. S. Frattini, M. Quai and E. Cereda, *Tetrahedron Lett.* 2001, **42**, 6827–6829.
104. E. Y. Lee, Y. Kim, J. S. Lee and J. Park, *Eur. J. Org. Chem.* 2009, **2009**, 2943-2946.
105. F. Alonso, P. Riente and M. Yus, *Eur. J. Org. Chem.* 2009, **2009**, 6034-6042.

106. A. I. Carrillo, L. C. Schmidt, M. L. Marinab and J. C. Scaiano, *Catal. Sci. Technol.* 2014, **4**, 435-440.

107. C. J. O'Brien, J. L. Tellez, Z. S. Nixon, L. J. Kang, A. L. Carter, S. R. Kunkel, K. C. Przeworski and G. A. Chass, *Angew. Chem. Int. Ed.* 2009, **48**, 6836 –6839.

108. J. Dambacher, W. Zhao, A. E. Batta, R. Anness, C. Jiang and Mikael Bergdahl, *Tetrahedron Lett.* 2005, **46**, 4473-4477.

109. J. McNulty and P. Das, *Tetrahedron Lett.* 2009, **50**, 5737-5740.

110. S. H. Y. S. Abdullah, N. H. M. Hanapia, A. Azida, R. Umara, H. Juahira, H. Khatoon, and A. Endut, *Renewable Sustainable Energy Rev.* 2017, **70**, 1041-1051.

111. D. Y. C. Leung, X. Wu and M. K. H. Leung, *Appl. Energy*, 2010, **87**, 1083-1095.

112. B. Singh, A. Gulde, I. Rawat, F. Bux, *Renew Sustain Energy Rev.* 2014, **29**, 216-245.

113. F. Ezebor, M. Khairuddean, A. Z. Abdullah and P. L. Boey, *Bioresour. Technol.* 2014, **157**, 252-262.

114. A. M. Dekhoda, A. H. West and N. Ellis, *Appl. Catal. A. Gen.* 2014, **382**, 157-204.

115. F. Ma and M. A. Hanna, *Bioresour. Technol.* 1999, **70**, 1–15.

116. A. L. Ahmad, N. H. M. Yasin, C. J. C. Derek and J. K. Lim, *Renew Sustain Energy Rev.* 2011, **15**, 584-593.

117. G. E. G. Muciño, R. Romero, I. G. Orozco, A. R. Serrano, R. B. Jiménez, R. Natividad, *Catal. Today* 2016, **271**, 220-226.

118. A. T. Kiakalaieh, N. A. S. Amin, H. Mazaheri, *Appl. Energy*, 2013, **104**, 683-710.

119. K. Wilson, C. Hardacre, A. F. Lee, J. M. Monteroa and L. Shellard, *Green Chem.* 2008, **10**, 654–659.

120. M. D Serio, M. Ledda, M. Cozzolino, G. Minutillo, R. Tesser and E. Santacesaria, *Ind. Eng. Chem. Res.* 2006, **45**, 3009-3014.

121. L. J. Konwar, J. Boro, D. Deka, *Renew. Sustain. Energy Rev.*, 2014, **29**, 546–564.

122. A. Refaat, *Int. J. Environ. Sci. Technol.* 2011, **8**, 203-221.

123. W. Xie and M. Fan, *Chem. Eng. J.* 2014, **239**, 60–67.

124. Z. Wen, X. Yu, S. Tu, J. Yan, E. Dahlquist, *Appl. Energy* 2010, **87**, 743-748.

125. A. Navajas, I. Campo, G. Arzamendi, W. Y. Hernández, L. F. Bobadilla and M. A. Centeno, *App. Catal. B: Env.* 2010, **100**, 299–309.

126. J. Boro, D. Deka and A. J. Thakur, *Renewable Sustainable Energy Rev.*, 2012, 16, 904– 910.

127. L. M. Correia, R. M. A. Saboya, N. d. S. Campelo, J. A. Cecilia, E. Rodriguez-Castellon, C. L. Cavalcante and R. S. Vieira, *Bioresour Technol.*, 2014, **151**, 207-213.

128. N. Nakatani, H. Takamori, K. Takeda and H. Sakugawa, *Bioresour. Technol.*, 2009, **100**, 1510-1513.

129. Z. Wei, C. Xu and B. Li, *Bioresour. Technol.*, 2009, **100**, 2883–2885.

130. I. B. Laskar, K. Rajkumari, R. Gupta, S. Chatterjee S, B. Paul and L. Rokhum, *RSC Adv.* 2018, **8**, 20131- 20143.

131. L. Yang, A. Zhang and X. Zheng, *Energy Fuels*, 2009, **23**, 3859–3865.

132. N. Viriya-empikul, P. Krasae, B. Puttasawat, B. Yoosuk, N. Chollacoop and K. Faungnawakij, *Bioresour. Technol.* 2010, **101**, 3765-3767.

133. H. Liu, H. S. Guo, X. J. Wang, J. Z. Jiang, H. Lin, S. Han and S. P. Pei, *Renewable Energy* 2016, **93**, 648-657.

134. N. S. Lani, N. Ngadi, N. Y. Yahya and R. A. Rahman, *J. Cleaner Prod.* 2017, **146**, 116-124.

135. I. M. Mendonça, O. A. R. L. Paes, P. J. S. Maia, M. P. Souza, R. A. Almeida, C. C. Silva, S. Duvoisin, F. A. de Freitas, *Renewable Energy* 2019, **130**, 103-110.

136. G. Pathak, D. Das, K. Rajkumari and L. Rokhum, *Green Chem.* 2018, **20**, 2365-2373.

137. K. T. Chen, J. X. Wang, Y. M. Dai, P. H.Wanga, C. Y. Liou, C. W. Nien , J. S. Wua, C. C. Chen, *J. Taiwan Inst. Chem. Eng.* 2013, 44, 622-629.

138. C. Li, X. Hu, W. Feng, B. Wu and K. Wu, *Energy Sources Part A.,* 2018, **40**, 142-147.

139. X. Xiong, I. K. M. Yu, L. Cao, D. C. W. Tsang, S. Zhang and Y. S. Ok, *Bioresour Technol.* 2017, **246**, 254-270.

140. M. Li, Y. Zheng, Y. Chen and X. Zhu, *Bioresource Technol.* 2014, **154**, 345-348.

141. M. D. Kostic, A. Bazargan, O. S. Stamenkovic, V. B. Veljkovic and G. McKay, *Fuel* 2016, **163**, 304-313.

142. P. Manjunathan, S. P. Maradur, A.B. Halgeri and G. V. Shanbhag, *J. Mol. Catal. A: Chem.*, 2015, **396**, 47-54.

143. A. R. Trifoi, P. Ş. Agachi and T. Pap, *Renewable Sustainable Energy Rev.*, 2016, **62**, 804-814.

144. B. Mallesham, P. Sudarsanam, and B. M. Reddy, *Ind. Eng. Chem. Res.*, 2014, **53**, 18775-18785.

145. M. R. Nanda, Z. Yuan, W. Qin, H. S. Ghaziaskar, M. A. Poirier and C. C. Xu, *Fuel*, 2014, **117**, 470-477.

146.N. Suriyaprapadiloka and B. Kitiyanan, *Energy Procedia*, 2011, **9**, 63-69.

147.J. S. Clarkson, A. J. Walker and M. A. Wood, *Org. Process Res. Dev.*, 2001, **5**, 630-635.

148.M. J. Climent, A. Corma and A. Velty, *Appl. Catal., A*, 2004, **263**, 155–161.

149.C. J. A. Mota, C. X. A. Silva, N. Rosenbach, J. Costa and F. Silva, *Energy Fuels*, 2010, **24**, 2733-2736.

150.C. X. A. Da Silva and C. J. A. Mota, *Biomass Bioenergy*, 2011, **35**, 3547-3551.

151.M. Shirani, H. S. Ghaziaskar and C. C. Xu, *Fuel Process. Technol.*, 2014, **124**, 206-211.

152.I. B. Laskar, K. Rajkumari, R. Gupta and Lalthazuala Rokhum, *Energy Fuels* 2018, **32**, 12567-12576.

153.S. S. Priya, P. R. Selvakannana, K. V. R. Chary, M. L. Kantam, S. K. Bhargav, *Mol. Catal.* 2017, **434**, 184-193.

154.B. Mallesham, P. Sudarsanam and B. M. Reddy, *Catal. Sci. Technol.* 2014, **4**, 803-813.

155.G. S. Nair, E. Adrijanto, A. Alsalme, I. V. Kozhevnikov, D. J. Cooke, D. R. Brown and N. R. Shiju, *Catal. Sci. Technol.* 2012, **2**, 1173-1179.

# CHAPTER

# 3

# Magnetic Fe₃O₄@silica sulfuric acid nanoparticles promoted tetrahydropyranylation/depyranylation of alcohols and acetalization of glycerol under solvent -free conditions

## 3.1 Introduction

### 3.1.1 Functionalized silica-coated magnetite nanoparticles as catalysts

Taking into account the advantages of heterogeneous catalysts over homogeneous catalysts in terms of separation and recoverability, plethora of effective heterogeneous catalysts have been reported in recent years. However the serious disadvantage of heterogeneous catalyst is that the efficiency of the catalyst gets restricted due to limited surface area.[1] This drawback can be overcome by nanocatalyst support due to its "plenty of room at the bottom" nature. Owing to the tiny size, the exposed surface area of nanoparticles are very high which leads to dramatic rise in their catalytic activity. The high accessibility of nanocatalysts with reactant molecules is the reason behind they are considered as the 'bridge between heterogeneous and homogenous catalysts'.[2-5]

In recent decades magnetic nanoparticles (MNPs) are gaining enormous attention due to the technical simplicity of catalyst separation process. These catalysts can be easily separated from reaction medium by external magnet preventing the use of sophisticated techniques like chromatography or high-speed centrifugation, reducing the amount of product-loss, enhancing recyclability and thereby ameliorating the overall synthetic process.[6-9] Magnetic Fe₃O₄ has been investigated the most due to its potential magnetic saturation value, simple synthetic procedure and their biocompatible nature. However, bare

iron oxide nanoparticles have several limitations which includes high chemical reactivity leading to immediate aggregation into large clusters, rapid exothermic reaction with oxygen and thereby reduction of magnetic saturation and dispersibility.[10-12] Surface modification by forming a silica coating over the MNP surface can make it stable, inert, non- toxic, resistant under catalytic condition as well as improve the surface functionality due to the availability of abundant silanol groups (-SiOH) which act as a support for immobilization of different functional groups.[13-15]

A bird-eye-view of literature comprising silica-coated functionalized $Fe_3O_4$ MNPs suggests that a good number of catalysts have been developed by anchoring different functional species like $-SO_3H$, $-NH_2$, Schiff base, polymers etc. onto the surface silanol groups of $Fe_3O_4@SiO_2$ particles.[13] These core shell magnetite nanocatalysts are used in variety of organic reactions as an easily retrievable magnetic catalysts. For instance, sulfuric acid functionalized silica coated magnetite nanoparticles can be found in multiple number of synthetic applications. Sulfuric acid is one of the most industrially important catalyst, though lack of recoverability leads to annual consumption of about 15 million tons of the homogeneous acid 'as an unrecyclable catalyst'.[16] Heterogenization of sulfuric acid over magnetic nanocatalyst-surface not only makes possible easy recovery and reuse of catalysts by magnetic separation but also minimizes product isolation process.

Dam and his group[17] have reported the use of the $Fe_3O_4@SiO_2@SO_3H$ catalyst in one-pot Biginelli-type reaction which involves multicomponent coupling reaction (MCR) to synthesize dihydropyrimidine derivatives. The reaction was performed under solvent-free condition at 60 °C.
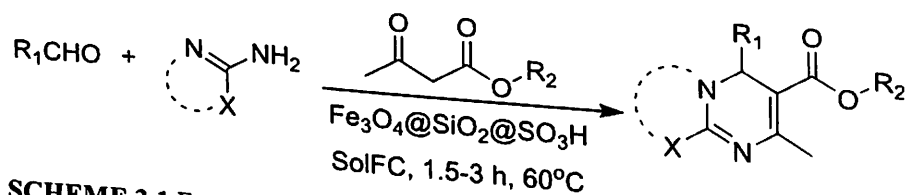


**SCHEME 3.1** $Fe_3O_4@SiO_2@SO_3H$ catalyzed one-pot Biginelli-type reaction.

While Kiasat et al.[18] investigated the application of the same catalyst for one-pot solvent-free synthesis of phthalazine derivatives. Solvent-free MCR pathway was followed for synthesis of products.
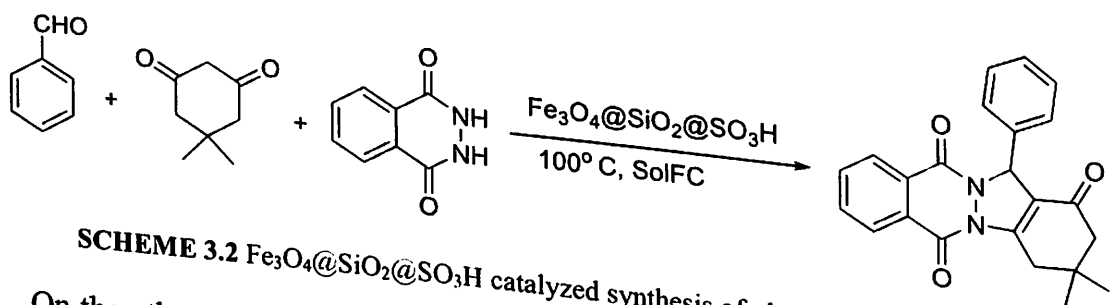


**SCHEME 3.2** $Fe_3O_4@SiO_2@SO_3H$ catalyzed synthesis of phthalazine derivatives.

On the other hand, Ghasemzadeh et al.[19] has functionalized the silica-coated $Fe_3O_4$ MNPs with (3-aminopropyl)triethoxysilane (APTES) to design a base catalyst. This was applied in the synthesis of chromeno[2,3-b]pyridine derivatives via three-component reactions among salicylaldehydes, thiols, and malononitrile.



46
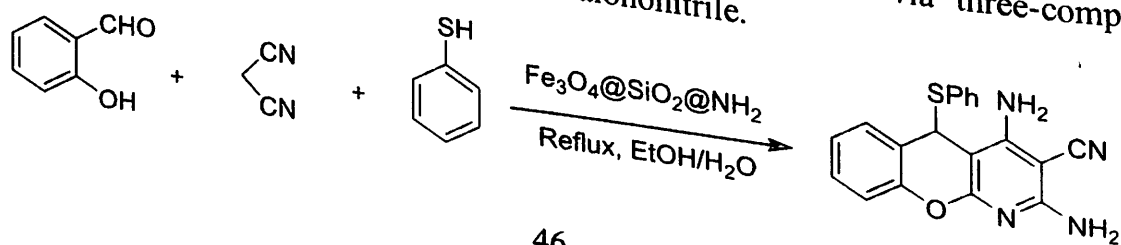
## 3.1.2 Tetrahydropyranylation and depyranylation of hydroxyl group

During the synthesis of an organic compound, the protection (and deprotection) of the free hydroxyl group in a multifunctional alcohol substrate or intermediate is one of the most frequently used strategies.[20,21] For this type of functional manipulation, etherification of the hydroxyl group using 3,4-dihydro-2H-pyran (DHP) is recognized as the most popular and easy protocol. This is because of its several attractive advantages over other protecting reagents, which include ease of its preparation, stability of the corresponding tetrahydropyranyl ethers towards various reaction conditions and use of reagents such as strong bases, hydrides, Grignard reagents and other organometallic reagents.[22-24] Moreover, THP ethers can easily be converted to various derivatives, such as sulfides, halides[25], esters[26], cyanides and carbonyl compounds[27] employing specific methods, which makes them ideal protecting reagents for tetrahydropyranylation. Enumerable catalysts including both homogeneous and heterogeneous catalysts have been reported to date, which have been proposed to catalyze tetrahydropyranylation of free hydroxyl groups.

In this chapter, we report application of core–shell structured $Fe_3O_4$@silica sulfonic acid ($Fe_3O_4@SiO_2@SO_3H$ or FSS) catalyst for tetrahydropyranylation/depyranylation of alcohols under solvent-free conditions. The solvent-free protocol makes it free from the hazardous effects of organic toxic solvents, offering a green and eco-friendly approach. Also due to the magnetic retrievability of the catalysts, the protected alcohol can be easily isolated to be used for further synthetic step.

## 3.1.3 Sol-ketal synthesis by glycerol acetalization

Owing to the alarming situation regarding diminishing fossil fuels and their environmental impacts, biodiesel industry has been witnessing a rapid development.[28-30] Consequently, there is a huge surplus outflow of glycerol which is obtained as an unavoidable by-product of transesterification process of biodiesel synthesis.[31,32] Approximately, one tenth of glycerol is produced from every gallon of biodiesel produced while industrial worth of glycerol (after refining) is far limited compared to its growing production.[33-35] The large waste stream of glycerol is contributing to significant drop in its market-value and thereby putting question mark to the sustainability of biodiesel industry. In this context, innovative practices for valorization of glycerol into useful products seeks utmost concern.[34,36,37]

A lot of pathways are devoted to the conversion of glycerol involving oxidation, hydrogenation, esterification, etherification etc.[38-42] Acetalization of glycerol with acetone can be a lucrative way for utilization of surplus glycerol, giving a five-membered ring molecule with one hydroxyl group unprotected, which is commonly known as solketal (2,2-dimethyl-1,3-dioxolane-4-methanol). Sol-ketal is a commercially valuable product used extensively as fuel additive because it can potentially improve octane number and cold flow properties of transportation fuels and also serve to reduce the particulate emission during fuel combustion and gum formation.[29,43,44] Apart from these benefits, solketals finds applications as versatile solvent, surfactant, plasticizer, suspending agents in pharmaceutical industry and also as flavoring agents.[45-48] So it can be speculated that synthesis of solketal can be a profitable valorization of glycerol generated as by-product from biodiesel synthesis and boost the turnover of biodiesel industries.

Traditionally homogeneous mineral acid catalysts viz. $H_2SO_4$, HCl and *p*-toluenesulfonic acid are employed for acetalization of glycerol. However the fundamental difficulties associated with homogeneous catalysts during separation and purification processes restrict their widespread use. Therefore several heterogeneous catalysts are

introduced to mitigate those problems that include zeolites[49], ion exchange resins[34], mixed oxides[50], heteropolyacids[51] and nanocatalysts.[52] Assessing the outstanding properties of magnetic nanocatalysts, we aimed to find application of $Fe_3O_4@SiO_2@SO_3H$ (FSS) MNPs in the catalytic acetalization of glycerol with acetone to synthesize sol-ketal. As per our knowledge and survey, this the first report of utilizing magnetic nanocatalysts for sol-ketal synthesis.

The reaction of glycerol acetalization was carried out under ultrasonic irradiation, which provides a sustainable route to synthesize solketal. Ultrasonication is a cornerstone among all green synthetic techniques where sound energy propagates throughout the reaction media, resulting in agitation of reactant molecule. When the reaction system is irradiated with ultrasound wave, the alternate rarefication and compression phenomena of sound wave leads to the formation of micro-bubbles in the liquid followed by their violent collapse (cavitation) during compression. This results in localized high temperature and pressure region inside the reaction media and helps to overcome the activation energy of the reaction.[53,54] The micro-scale cavitation combined with the intensified mixing of reactants are known to be the reason behind the accelerated reaction rate of ultrasound-assisted synthetic processes. Citing the advantages allied with ultrasonicated reactions, such as accelerated kinetics (energy saving), improved selectivity (minimized waste), better yield (high efficiency), little instrumental requirement (economic), etc., Jean-Louis Luche[55] linked sonochemistry with green chemistry in 1999 ("green chemistry: the sonochemical approach") just after Anastas and Warner[56] postulated the 12 green chemistry principles (1998).[57]

The advantages of magnetic nano-catalyzed reactions, followed by our interest in sonochemistry encouraged us to design a facile, ultrasound-promoted catalytic pathway for solketal synthesis using magnetic silica supported acid functionalized iron oxide nanoparticles. While magnetic catalyst promotes hurdle-free catalyst separation, on the other way, application of ultrasonication technology to the reaction protocol boosts the reaction rate by means of improved mixing of glycerol and acetone and preventing rapid accumulation of by-product water molecules on the catalyst surface through constant agitation of molecules, hence preventing catalyst deactivation. Therefore, the reaction finds several attractive features, like mild reaction conditions (short reaction time), easy magnetic separation of catalysts, 100% selectivity, efficient product isolation, and good catalyst recyclability.

## 3.2 Experimental

In this section, the details of chemicals and reagents, synthetic procedure of catalyst, reaction methodologies of products, information of various analytical and spectroscopic techniques used during characterization process are discussed briefly.

### 3.2.1 Materials and methods

Ferric chloride, ferric sulfate, all alcohols, DHP (3,4-dihydro-2H-pyran), glycerol, silica gel for TLC (Thin Layer Chromatography) and column chromatography were of analytical grade and purchased from SpectroChem. TEOS (tetraethyl orthosilicate) was purchased from Sigma Aldrich, India. The chemicals were used without further purification. The solvent used were of extra pure grade, purchased from Merck India. Double distilled deionized water was used for the synthesis of magnetic nanoparticles.

For the characterization of catalyst, high resolution transmission electron microscopy (HRTEM) was conducted using an electron microscope JEM-2100, 200 kV, JEOL. The samples were dispersed in ethanol and then treated ultrasonically in order to disperse

48

individual particles over a copper grid. Powder X-ray diffraction (XRD) patterns were obtained on an X'Pert Pro PANalytical diffractometer under the following conditions: K-Alpha 1 wavelength ($\lambda$= 1.54056 Å), K-Alpha 2 wavelength ($\lambda$= 1.54439 Å), generator voltage of 40 kV, a tube current of 35 mA and the count time of 0.5 s per 0.02° in the range of 5°–90° with a copper anode. FT-IR spectra were recorded on a Nicolet 6700, Nicolet Continuum FTIR Microscope. NMR spectra were recorded on Bruker Avance II, 400 MHz. Magnetic measurement was carried out on a Lakeshore VSM 7410 magnetometer. The sonochemical reactions were carried out in a PCi Analytics (3.5L100H/9TC) ultrasonic bath (sonicator) of operating frequency 33±3 KHz. GC of the synthesized product was recorded on an Agilent 7890 gas chromatograph which is fitted with head space injector mode, a CPSIL 8CB capillary column (30 m × 0.25 mm × 0.25 µm) and GC FID detector. The initial oven temperature was 55 °C and it was increased up to a final temperature of 230 °C with a rate of 10 °C min-1. The temperature of the detector and the injector were 300 °C and 250 °C, respectively. For quantitative analysis of the products, biphenyl was used as an internal standard. GC-MS analysis of the isolated product was taken on Jeol AccuTOF GCV mass-spectrometer which is coupled with the Gas chomatogrph instrument. NMR spectra were recorded on Bruker Avance II, 400 MHz.

## 3.2.2 Preparation of the catalyst

**Preparation of iron oxide magnetic nanoparticles $Fe_3O_4$ (F) MNPs:** Magnetic nanoparticles were synthesized according to reported procedure.[18,57,58] Co-precipitation of Fe(II) and Fe(III) was carried out by dissolving first $FeSO_4.7H_2O$ (1 mmol) and $FeCl_3.6H_2O$ (2 mmol) in deionized water under nitrogen atmosphere at 90°C. Ammonium hydroxide solution was added to the solution with vigorous mechanical stirring. The reaction was carried out for 60 min in $N_2$ atmosphere until the color of the bulk solution turned to black. External magnet was used to separate out the resulting black MNPs, washed that 3 times with deionized water and then dried under vacuum at 60°C for 12h.

**Preparation of silica coating of iron oxide magnetic nanoparticles, $Fe_3O_4@SiO_2$ (FS):** The silica coating of $Fe_3O_4$ MNPs was carried out by using a sol-gel method (Stober method) that involves hydrolysis of TEOS on the surface of iron oxide nanospheres. For this, $Fe_3O_4$ particles were dispersed in a mixture of ethanol, deionized water and TEOS followed by the addition of 10% NaOH solution. The solution was stirred in a magnetic stirrer for about 1 hr at room temperature. Then the product was isolated by an external magnet and was washed several times with deionized water and ethanol and dried at 80°C for 10 hr. Thickness of the coated silica can be controlled by tuning experimental parameters.

**Preparation of $SO_3H$ functionalized silica-coated iron oxide magnetic nanoparticles; $Fe_3O_4@SiO_2@SO_3H$ (FSS)**

To immobilize the $SO_3H$ functional group onto the surface of $Fe_3O_4@SiO_2$ nanoparticles, a suction flask was equipped with a constant pressure dropping funnel. The gas outlet was connected to a vacuum system through an absorbing solution of alkali trap for conducting HCl gas. $Fe_3O_4@SiO_2$ was dispersed into the flask containing dry DCM. Chlorosulfonic acid ($ClSO_3H$) was then added drop wise to the mixture of $Fe_3O_4@SiO_2$ and DCM in a cooled ice-bath over a period of 30 minutes at room temperature. HCl gas was evolved from the reaction vessel immediately. After completion of the addition, the mixture was kept for stirring and occasionally shaking for 3 hrs while the residual HCl was eliminated by suction. Then the $Fe_3O_4@$silica sulfonic acid (FSS MNPs) were separated from the reaction mixture by an external magnet and washed several times with DCM. Finally $Fe_3O_4@$silica sulfonic acid was dried under vacuum at 60°C for 24 hr.
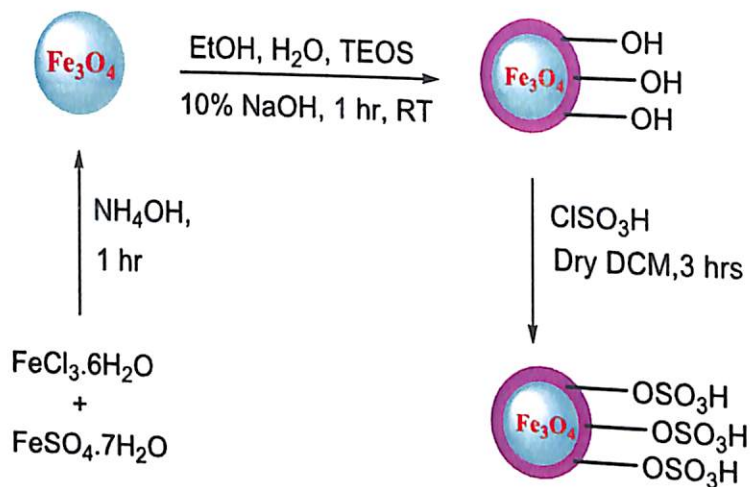
**SCHEME 3.4** Schematic diagram for synthesis of FSS MNP catalyst.

## 3.2.3 General procedure for the tetrahydropyranylation of alcohols using FSS catalyst

A mixture of alcohol (1 mmol), DHP (1.2 mmol) and FSS catalyst (20 mol% of substrate) was stirred in a small reaction vessel at room temperature. The reaction progress was monitored by Thin Layer Chromatography. After completion of the reaction, Ethyl acetate (10 ml) was added to the solution and the catalyst was separated by an external magnet. The solution was concentrated under reduced pressure and the product was passed through a column of silica gel eluting with hexane/ethyl acetate (9:1) to obtain pure THP ether with high purity. The catalyst was washed several times with ethyl acetate and dried under vacuum at 60°C for 24 hrs.

## 3.2.4 General procedure for the deprotection of alcohols using FSS catalyst

THP ether (1 mmol) and $Fe_3O_4$@silica sulfonic acid catalyst (20 mol% of substrate) were stirred in methanol (0.5 ml) at room temperature for 30 min. The cleavage of THP ethers was monitored by TLC. After completion of reaction, the catalyst was taken out with the help of an external magnet and washed with ethyl acetate. The solution was concentrated under reduced pressure to obtain the corresponding pure hydroxyl compound in quantitative yield.

## 3.2.5 General procedure for acetalization of glycerol using FSS catalyst

For the synthesis of solketal, 1 mmol of glycerol (0.092g) and 5 mmol of acetone (0.29g) were taken in a 10 mL round bottom (Rb) flask and added 5 mol% of FSS catalyst to the reaction mixture, followed by ultra-sonication for 15 minutes. No additional solvent was used and thus reaction was performed under solvent-free condition (SolFc),The progress of the reaction was regularly monitored by TLC checking. Once the reaction was completed, the catalyst is removed by magnetic separation, followed by centrifugation (at 3000 rpm for 5 minutes) and removal of excess acetone by rotary evaporation to isolate the desired product. To confirm the synthesis of solketal and its purity, the product was characterized by $^1$H-NMR and GC-MS analysis. The conversion of glycerol and selectivity of solketal was obtained by GC using the following equations-

$$\text{Glycerol conversion} = \frac{\text{mol of glycerol converted}}{\text{initial mol of glycerol}} \times 100\%$$

50

$$\text{Solketal Selectivity} = \frac{\text{mol of solketal formed}}{\text{mol of glycerol converted}} \times 100\%$$

## 3.3 Results and discussion

This chapter depicts the detailed characterization of the FSS catalyst using variety of analytical techniques viz. FT-IR, XRD, TEM-EDX, VSM etc. We demonstrate here the application of the FSS catalyst for protection (and deprotection) of hydroxyl groups via tetrahydropyranylation/depyranylation under solvent-free room temperature conditions. Use of magnetically retrievable nanocatalyst makes the synthetic process operationally simple and time-efficient.

Also we tried acetalization of glycerol to synthesize industrially important Sol-ketal (4-hydroxymethyl-2,2-dimethyl-1,3-dioxolane) by ultra-sonication using the same catalyst. As per our knowledge, magnetic nanocatalysts are used for the first time in the synthesis of sol-ketal.

### 3.3.1 Characterization of FSS catalyst

**Fourier Transform Infrared (FT-IR) Spectroscopy:** In order to identify and ascertain the functionalization of the FSS catalyst, FT-IR analysis of pure $Fe_3O_4$, $Fe_3O_4@SiO_2$ core-shell, $Fe_3O_4@$silica sulfonic acid (FSS) and that of recovered catalysts were carried out and respective spectra are shown in Fig. 3.1(a), Fig. 3.1(b) and Fig. 3.1(c).
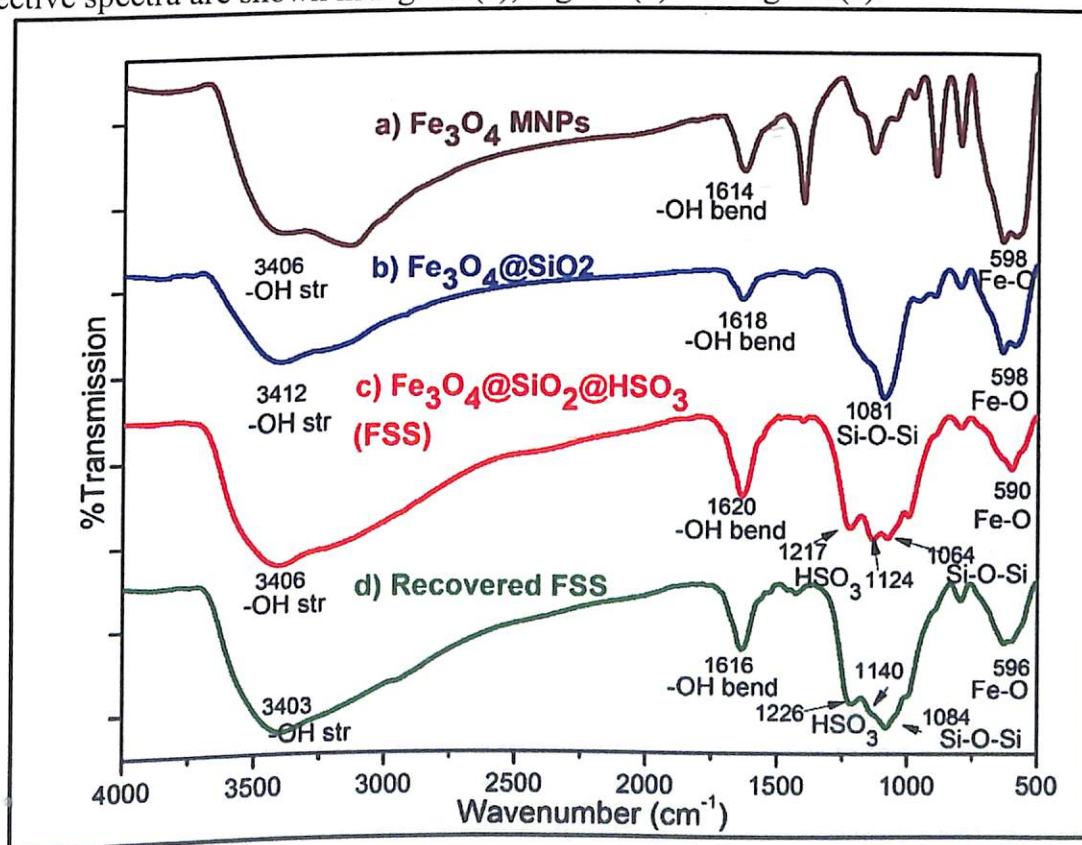


**FIGURE 3.1**: FT-IR spectra of a) $Fe_3O_4$ MNPs, (b) $Fe_3O_4@SiO_2$, (c) FSS, (d) Recovered FSS

In each spectra of Fig. 3.1, the appearance of absorption peak at around 590-598 cm⁻¹ corresponds to the Fe-O stretching vibration of the $Fe_3O_4$ MNPs. In Fig. 3.1(b), the prominent band near 1081 cm⁻¹ can be assigned to the stretching vibration of Si–O bond which clearly indicates the occurrence of silica coating over the nanoparticle surface. The successful anchoring of sulfonic acid (-SO₃H) moiety is evidenced by the introduction of

two additional peaks in the spectra of FSS in Fig. 3.1(c) at 1124 cm$^{-1}$ and 1217 cm$^{-1}$ which are assigned to the vibration bands of symmetric and asymmetric O=S=O bond. The peaks around the ranges 1614-1620 cm$^{-1}$ and 3406-3412 cm$^{-1}$ suggests the bending and stretching vibration bands of –OH groups present on the surface of the nanoparticles respectively. The gradual increase in the intensities of bands due to –OH functionality indicates an increase in the acid sites of catalyst surface after funcionalization.[59, 60]

**X-ray diffraction analysis:** The crystalline structure of $Fe_3O_4$ and $Fe_3O_4@SiO_2$ were analyzed by XRD technique (Fig. 3.2). The diffractogram of bare $Fe_3O_4$ NPs shows diffraction peaks at $2\theta$ values 30.2°, 35.6°, 43.4°, 53.9°, 57.3° and 63.1° that corresponds to (2 2 0), (3 1 1), (4 0 0), (4 2 2), (5 1 1) and (4 4 0) planes respectively. These information complemented well with the library patterns (JCPDS No. 19-0629) suggesting an inverse spinel structure of the magnetic crystalline particles. Interestingly, diffractogram of $Fe_3O_4@SiO_2$ also referred to peaks in the same range which indicated retention of the crystalline structure after silica-coating process. A very broad peak before $2\theta= 30°$ value, evidenced the presence of amorphous silica over the surface of $Fe_3O_4$ MNPs.
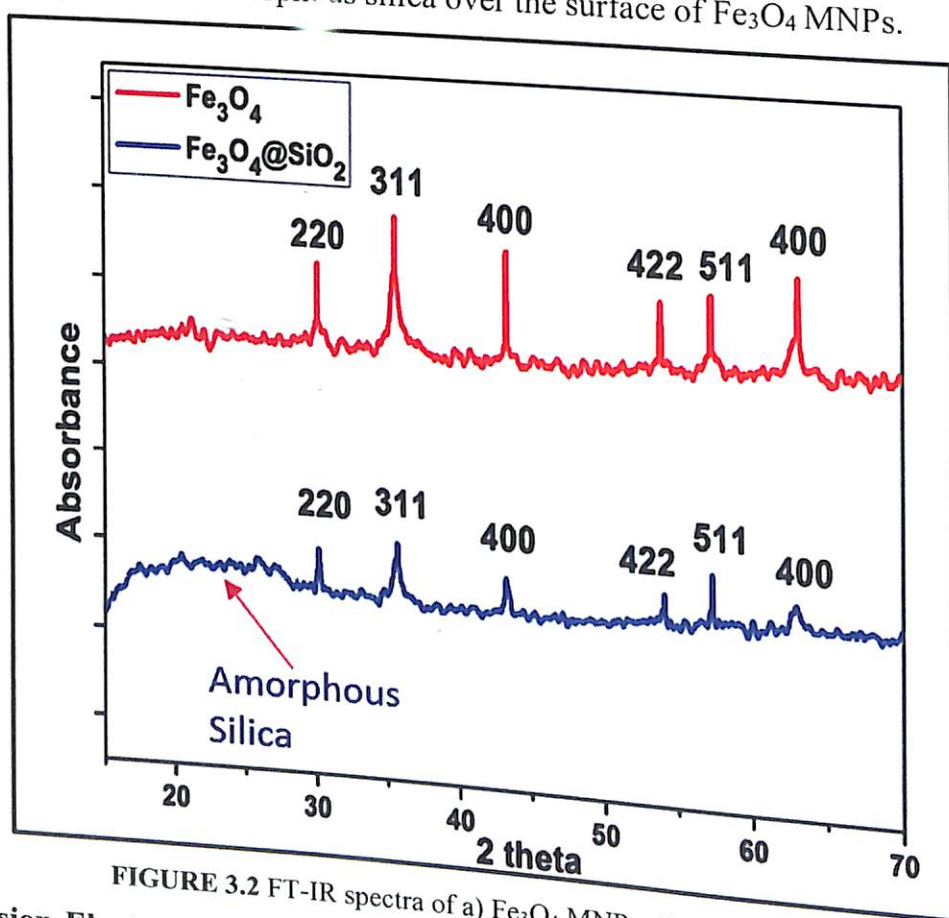


FIGURE 3.2 FT-IR spectra of a) $Fe_3O_4$ MNPs, (b) $Fe_3O_4@SiO_2$

**Transmission Electron Microscopy (TEM):** The size and shape of $Fe_3O_4$, $Fe_3O_4@SiO_2$ nanoparticles and the prepared catalyst FSS were examined by TEM and the corresponding images were displayed in Figure 3.3(a), (b) and (c), respectively. Formation of 'quasi-spherical' shaped $Fe_3O_4$ nanoparticles can be observed in Figure 3.3(a). The fine coating of silica over the $Fe_3O_4$ nanoparticles can be observed in Figure 3.3(b) as well as in Figure 3.3(c), which indicates the retention of the silica coating even after the sulfonic acid functionalization on the silica surface. The SAED (Selected Area Electron Diffraction) pattern of FSS MNPs in Figure 3.3(d) that comprise of small bright spots making up rings, confirms the polycrystalline nature of the sample.

The successful coating and functionalization was further verified by particle-size distribution histogram diagrams of $Fe_3O_4$ and FSS MNPs in Fig. 3.4 (a) and (b) respectively.

The average diameter of bare magnetite nanoparticles were found to be 19.66 nm from the histogram, whereas for FSS particles the average diameter was calculated to be 27.34 nm. The increase in the diameter of FSS can be clearly attributed to the silica shell over the magnetite nanoparticle surface.
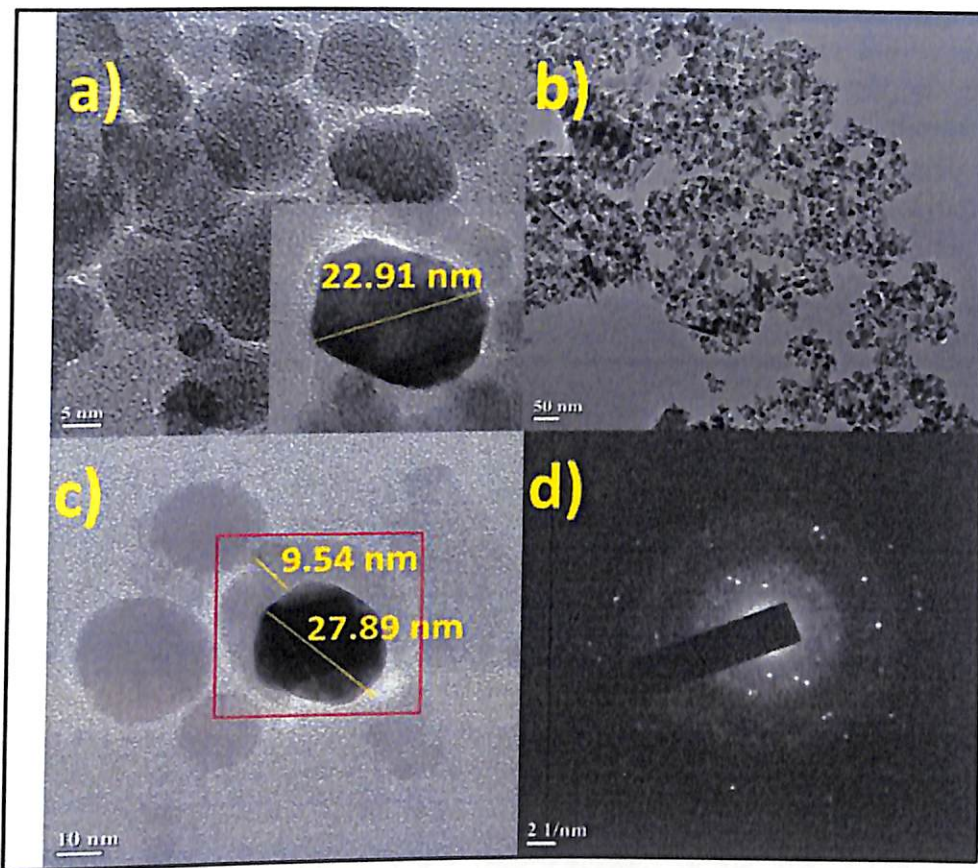


**FIGURE 3.3** HRTEM images of a) $Fe_3O_4$ MNPs, (b) $Fe_3O_4@SiO_2$, (c) FSS and (d) SAED pattern of FSS
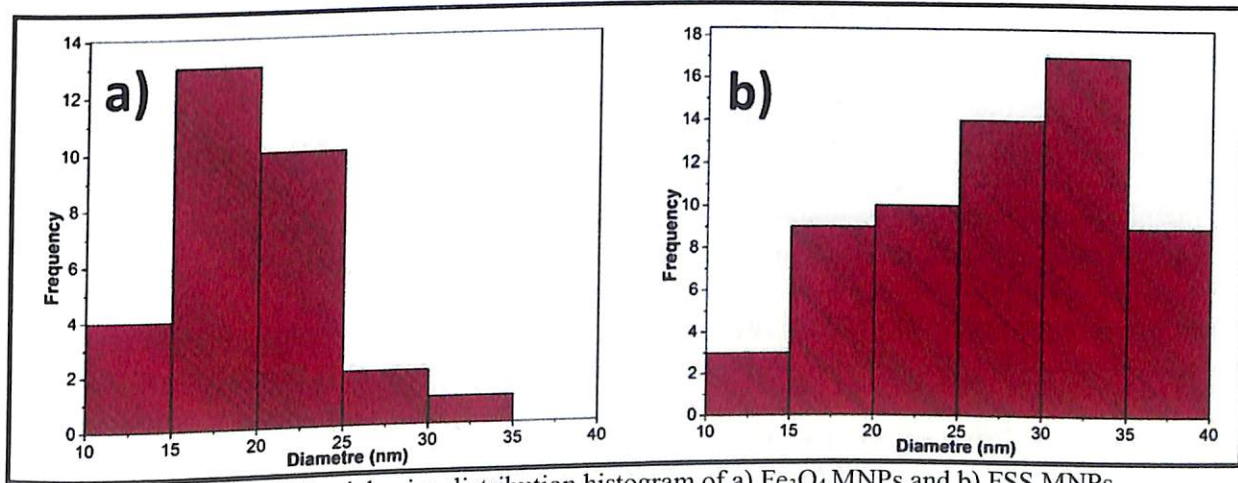


**FIGURE 3.4**: Particle-size distribution histogram of a) $Fe_3O_4$ MNPs and b) FSS MNPs.

**Energy-dispersive X-ray (EDX) spectroscopy:** The EDX spectroscopic technique is an important elemental analysis technique for chemical characterization of an unknown sample. The elemental composition of bare, silica-coated and functionalized $Fe_3O_4$ nanoparticles were investigated by TEM-EDX analysis and results are displayed in Fig. 3.5 (a)-(c). The anchoring of $HSO_3$ group in FSS catalyst was supported by the presence of S element in the EDX spectra and wt% of S was found to be 1.38% in the fresh catalyst FSS.

**Magnetic measurement:** To study the magnetic properties of the nanoparticles, saturation magnetization values of iron oxide MNPs were carried out in a vibrating sample

magnetometer (VSM). Magnetization curves of bare, silica-coated and functionalized $Fe_3O_4$ MNPs were recorded at room temperature (Fig. 3.6 (a)-(c)). The saturation magnetization value of $Fe_3O_4$ particles was obtained as 47.3 emu $g^{-1}$ and after formation of silica shell the value becomes 33.29 emu $g^{-1}$ for $Fe_3O_4@SiO_2$ particles. The saturation magnetization value of FSS catalyst on the other hand was obtained as 16.91 emu $g^{-1}$. The gradual decrease in the magnetization values of $Fe_3O_4$ NPs after silica coating and functionalization can be ascribed to the fact that formation of silica shell and anchoring of $SO_3H$ group, which are non-magnetic in nature, partially covers up the magnetic iron oxide core leading to slight reduction of their magnetic property. However this value is sufficient enough for magnetic separation of catalyst. Also, the negligible remanence and coercivity value in the closed M-H hysteresis loop suggests super magnetic nature of the synthesized FSS catalyst.
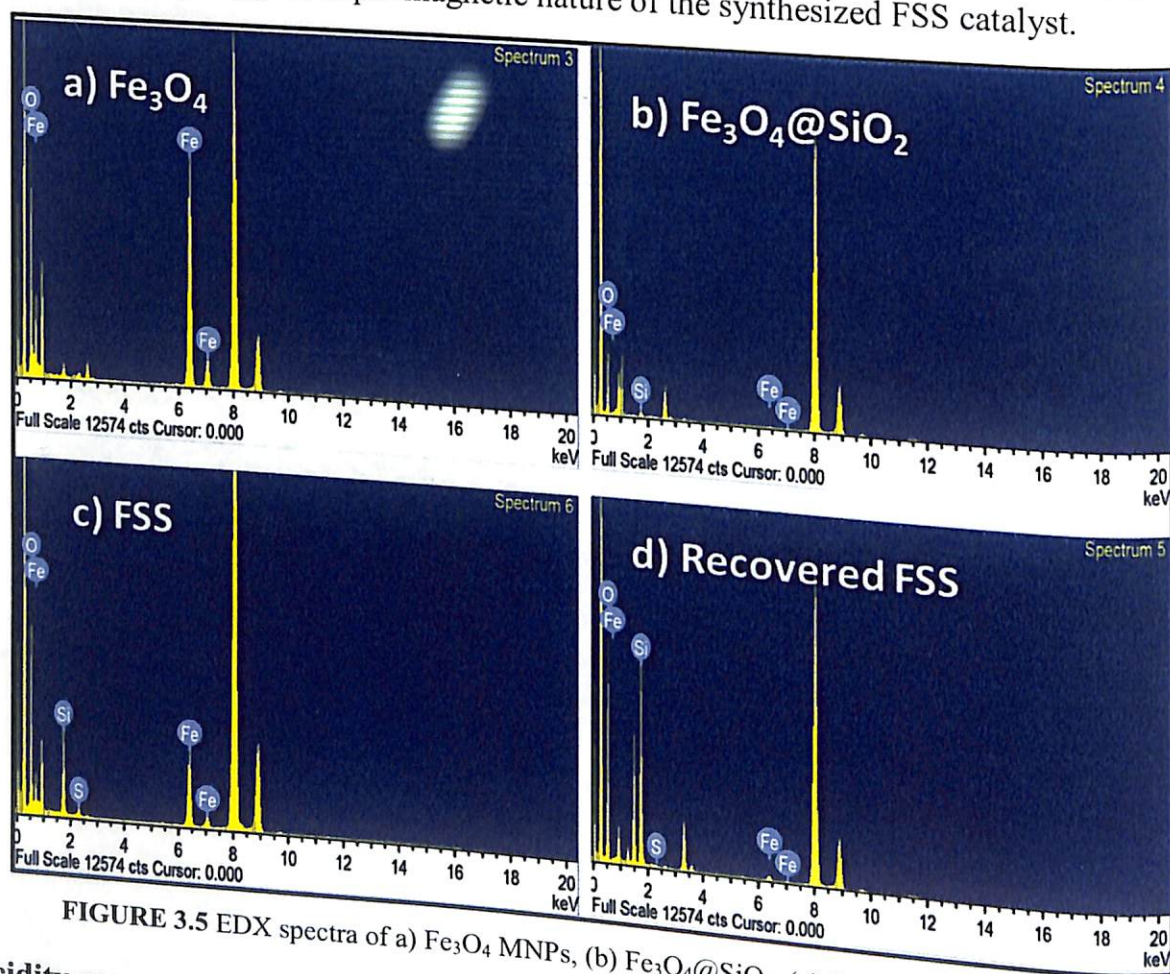


FIGURE 3.5 EDX spectra of a) $Fe_3O_4$ MNPs, (b) $Fe_3O_4@SiO_2$, (c) FSS, (d) Recovered FSS

**Acidity measurement by titration:** The acid loading of the FSS catalyst was determined by neutralization titration where about 50 mg of the acid catalyst was vigorously stirred with 10 mL saturated aqueous NaCl solution. The catalyst was then separated using external magnet and the brine solution was decanted. The process was repeated to collect 30 mL of proton-exchanged brine solution and finally titrated to neutrality with 0.1 M NaOH solution using phenol red indicator. The loading of acid sites in the FSS catalyst was calculated as 1.82 mmol/g.
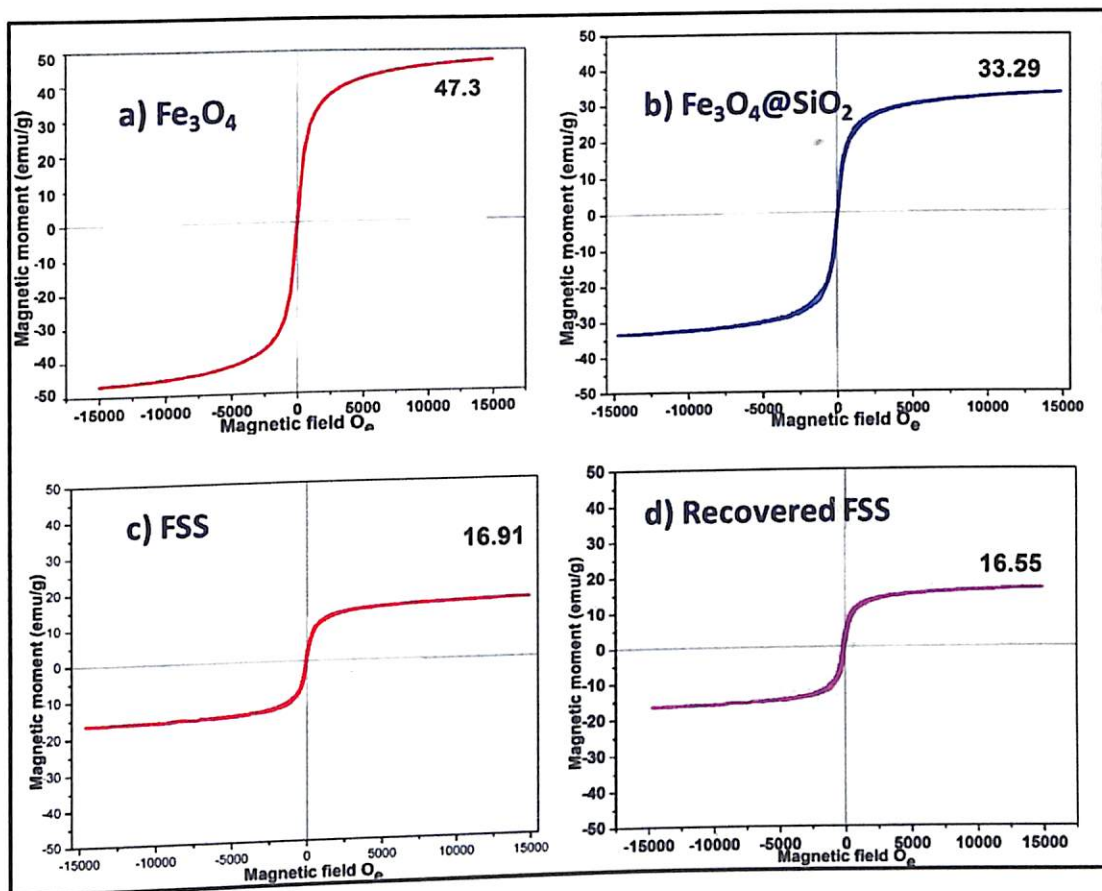
**FIGURE 3.6** Room temperature magnetization curve of a) $Fe_3O_4$ MNPs, (b) $Fe_3O_4@SiO_2$, (c) FSS, (d) Recovered FSS

## 3.3.2 Protection and Deprotection of alcohols

**Tetrahydropyranylation of alcohols:**
In continuation of our ongoing research interest, we applied the synthesized catalyst in tetrahydropyranylation of various alcohol substituents. Initially we tried it with benzyl alcohol and, to our delight; protection of alcohol was successful under solvent-free condition within a very short time of 1 hour only. First, we took equimolar mixture of benzyl alcohol (1 mmol) and DHP (1 mmol) and 10 mol % of the nanocatalyst and stirred the mixture for 1 hr. After stirring for 1 hr, we observed only slight formation of the product as indicated by TLC. Surprisingly, this did not increase even after stirring for another 1 hr. Then we added additional DHP (0.2 mmol) and found that the reaction was completed within the next 1 hr. Inspired by this findings, our next obvious target was to optimize the amount of catalyst. To our satisfaction we found that 20 mol% of the catalyst was optimum for the protection of alcohols. (Table 3.1, Entry 4).

**TABLE 3.1:** Optimization of the catalyst[a]

| Entry | Catalyst amount (mol %) | Time (min) | Yield (%) |
|-------|-------------------------|------------|-----------|
| 1 | 5 | 150 | 65 |
| 2 | 10 | 120 | 85 |
| 3 | 15 | 55 | 90 |
| 4 | 20 | 45 | 95 |
| 5 | 25 | 45 | 95 |

[a]Reaction conditions: Benzyl alcohol (1 mmol), DHP (1.2 mmol), room temperature, SolFc

55

Encouraged by the result and the advantage of using magnetic nanocatalyst over soluble homogeneous catalyst, we carried out the conversion of various alcohols into its protected products as described in Scheme 3.5.
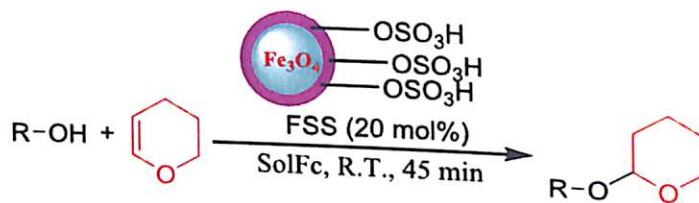


**SCHEME 3.5** Tetrahydropyranylation of alcohols using FSS MNP catalyst.
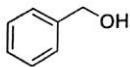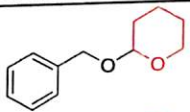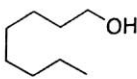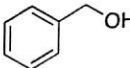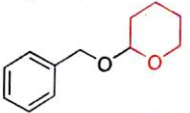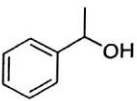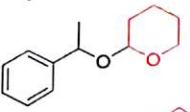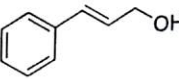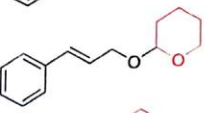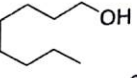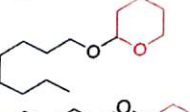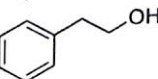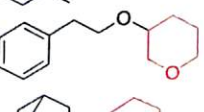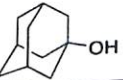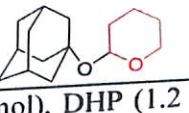
**TABLE 3.2:** Tetrahydropyranylation of alcohols[a]

| Entry | Alcohols | Product | Time (min) | Yield (%)[b] |
|---|---|---|---|---|
| 1 | | | 45 | 95 |
| 2 | | | 40 | 95 |
| 3 | | | 35 | 96 |
| 4 | | | 50 | 92 |
| 5 | | | 55 | 90 |
| 6 | | | 45 | 88 |
| 7 | | | 45 | 87 |
| 8 | | | 50 | 85 |
| 9 | | | 55 | 83 |
| 10 | | | 65 | 84 |
| 11 | | | 75 | 82 |
| 12 | | | 90 | 80 |
| 13 | | | 50 | 84 |
| 14 | | | 50 | 86 |

[a]Reaction condition: Alcohol (1 mmol), DHP (1.2 mmol), catalyst (20 mol%), room temperature, SolFc

With the optimum reaction condition in our hand we carried out the tetrahydropyranylation of variety of primary, secondary, tertiary, benzylic and allylic alcohols which were smoothly converted to the corresponding desired products in good to excellent yields at room temperature. The results are tabularized in Table 3.2. It was observed that benzylic alcohols substituted with electron-donating groups are highly reactive under our reaction condition giving the corresponding protected alcohols in excellent yields (Table 3.2, Entries 2, 3). However, reactions of benzyl alcohols substituted with electron-withdrawing groups were to some extent slower as compared to their electron-donating counterparts (Table 3.2, Entry 5). Although the reaction rates of aliphatic alcohols were lower as compared to benzylic ones, they were easily converted into their corresponding products in high yields. It was observed that aliphatic alcohols with longer chain length take more time for completion than that with smaller chain length (Table 3.2, entries 7, 8, 9). However, secondary and tertiary ones took longer time for complete conversion (Table 3.2, entries 11, 12). Allyl alcohols (Table 3.2, entry 13 and 14) were converted into the corresponding protected alcohols leaving the olefinic bonds intact.

**TABLE 3.3** Competitive reactions of different binary mixtures[a]

| Entry | Alcohols | Products | Time (min) | % Conversion |
|---|---|---|---|---|
| 1 | | | 45 | 95 |
| | | | | 5 |
| 2 | | | 45 | 100 |
| | | | | 0 |
| 3 | | | 60 | 94 |
| | | | | 6 |
| 4 | | | 60 | 100 |
| | | | | 0 |

[a]Reaction condition: Alcohol (1 mmol), DHP (1.2 mmol), Catalyst (20 mol%), Room temperature, SolFc.

In order to have more insight into the selectivity of our method, we studied various competitive reactions between structurally different alcohols in binary mixtures as shown in Table 3.3. This study reveals that benzylic alcohol can be converted into its protected products with excellent selectivity in the presence of aliphatic ones (Table 3.3, Entry 1). Interestingly, benzylic alcohols were converted quantitatively to its protected alcohols, while the secondary alcohol remained intact (Table 3.3, Entry 2). An allyl alcohol also reacted faster as compared to their aliphatic counterpart giving the allyl product in high yield (Table 3.3, entry 3). Similarly, primary alcohol can also

be converted to their corresponding iodide in the presence of tertiary ones with complete selectivity (Table 3.3, entry 6).
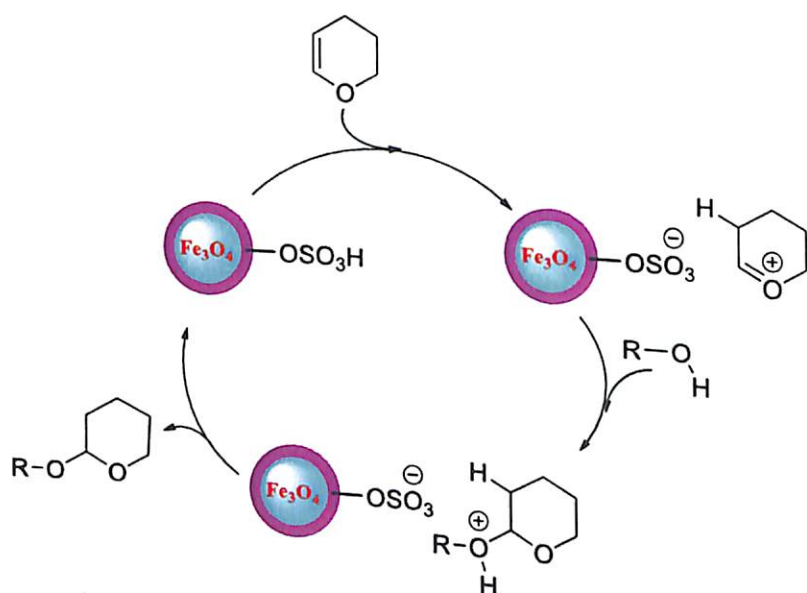


**SCHEME 3.6** Proposed mechanism for the tetrahydropyranylation of alcohols using FSS MNP catalyst.

Mechanism proposed for the tetrahydropyranylation of alcohols catalyzed by $Fe_3O_4@SiO_2@SO_3H$ is shown in Scheme 3.6. It is anticipated to involve first the abstraction of one proton from the catalyst by the double bond of DHP and thus formation of an oxonium ion intermediate. The intermediate then abstracts one electron from the nucleophile alcohol to produce THP ethers. The mechanism well-established the regeneration of the FSS catalyst after successful etherification of alcohol.

**Deprotection/depyranylation of THP ether:**

**TABLE 3.4 Deprotection of THP ethers**

| Entry | Alcohols | Product | Time (min) | Yield (%)[a] |
|-------|----------|---------|------------|--------------|
| 1. |  |  | 25 | 95 |
| 2. |  |  | 30 | 92 |
| 3. |  |  | 25 | 95 |
| 4. |  |  | 20 | 90 |
| 5. |  |  | 30 | 90 |

[a]Reaction condition: THP ether (1 mmol), methanol (0.5 ml), catalyst (20 mol%), room temperature

The deprotection of THP ethers was investigated by changing the solvent system. We found that the addition of methanol served as an efficient deprotecting reagent for THP ethers in presence of FSS as catalyst at room temperature to provide the corresponding free alcohols in excellent yield of 90-95% as shown in Table 3.4, irrespective of structural variations. It is interesting to note that the deprotection of all the compounds reported in the present study was completed within 30 min.

SCHEME 3.7 Depyranylation of alcohols using FSS MNP catalyst

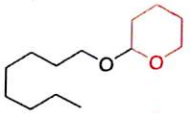Proposed mechanism for the deprotection or depyranylation of THP ether using FSS catalyst is shown in Scheme 3.7.
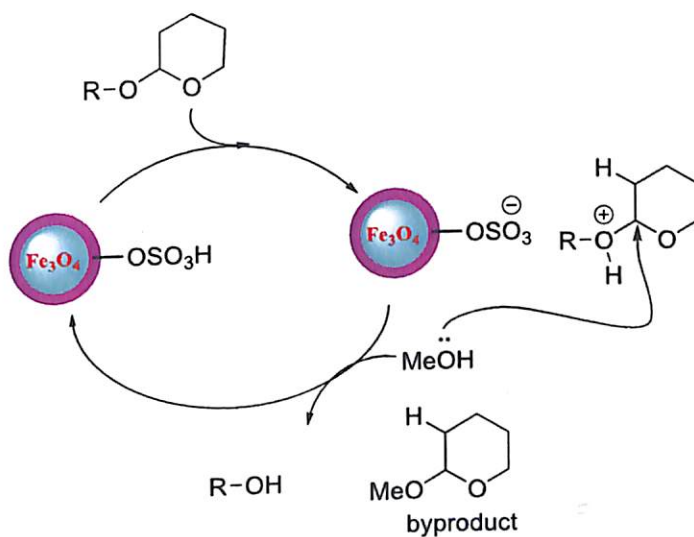


SCHEME 3.8 Proposed mechanism for the deprotection of THP ethers using FSS MNP catalyst.

**Recycling of the catalyst**
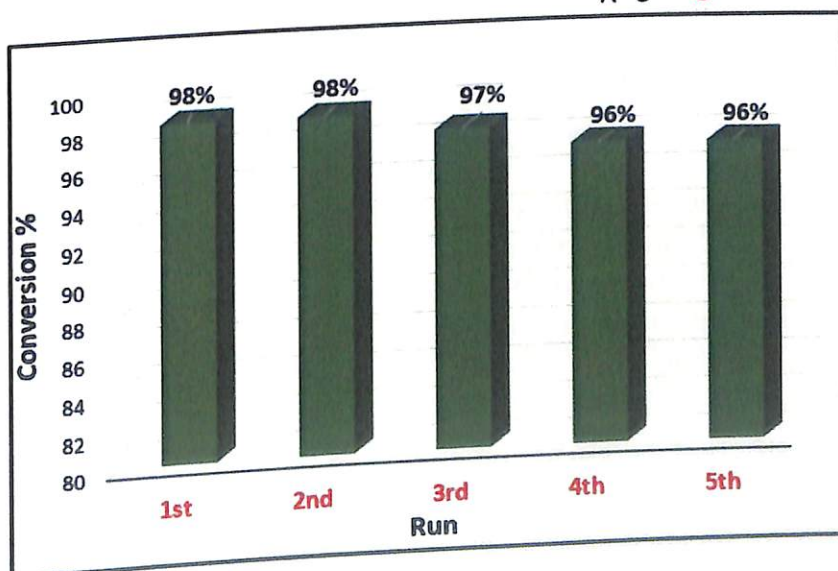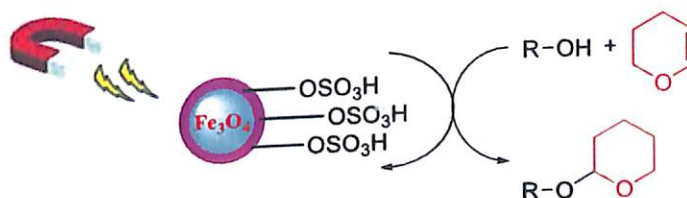


FIGURE 3.7 Recyclability test of FSS catalyst

59

The recyclability of magnetic nanocatalyst was investigated with consecutive tetrahydropyranylation reaction using different substrates.

## Spectroscopic data of synthesized compounds

### 2-((4-Methylbenzyl)oxy)-tetrahydro-2H-pyran (Table 3.2, entry 2)

$^1$H-NMR (400 MHz, CDCl$_3$, TMS): δ 7.26 (d, J= 10 Hz, 2H), 7.17 (d, J= 8Hz, 2H), 4.79-4.71 (m, 2H), 4.48 (d, J= 15 Hz, 1H), 3.93 (t, J=5 Hz, 1H), 3.57 (t, J=5 Hz,1H), 2.36 (s, 3H), 1.91-1.54 (m, 6H); $^{13}$C-NMR (100 MHz, CDCl$_3$, TMS): δ 137.29, 135.34, 129.16, 128.09, 97.64, 68.77, 62.17, 30.71, 25.64, 21.29, 19.49.

### 2-(4-Methoxybenzyloxy)-tetrahydro-2H-pyran (Table 3.2, entry 3)

$^1$H-NMR (400 MHz, CDCl$_3$, TMS): δ 7.27(d, J=10 Hz, 2H),6.85(d, J=10 Hz, 2H), 4.66-4.71(m, 2H), 4.42 (d, J=15Hz, 1H), 3.89(t, J=5Hz, 1H), 3.74(s, 3H), 3.52(t, J=5Hz, 1H), 1.83-1.49(m, 6H); $^{13}$C-NMR (100 MHz, CDCl$_3$, TMS): δ 159.24, 13: 37, 129.56, 113.81, , 68.53, 62.11, 55.21, 30.70, 25.59, 19.50.

### Tetrahydro-2-(phenethyloxy)-2H-pyran (Table 3.2, entry 6)

$^1$H-NMR (400 MHz, CDCl$_3$, TMS): δ 7.26-7.15(m, 5H), 4.56 (t, J=2 Hz, 1H), 3.95-3.89 (m,1H), 3.78-3.68(m,1H), 3.60-3.54(m, 1H), 3.43-3.39(m,1H), 2.88(t, J=9Hz, 2H), 1.79-1.42 (m, 7H); $^{13}$C-NMR (100 MHz, CDCl$_3$, TMS): δ 139.15, 129.03,128.48, 128.29, , 126.17, 98.61, 68.29, 62.01, 36.45, 30.71, 25.55, 19.63.

### 2-(2-Ethylhexyloxy)-tetrahydro-2H-pyran (Table 3.2, entry 7)

$^1$H-NMR (400 MHz, CDCl$_3$, TMS): δ 4.51 (t, J=5 Hz, 1H), 3.81-3.56( m, 2H), 3.21-3.18(m, 2H),1.77-1.24(m, 15H), 0.86-0.82 (m, 6H); $^{13}$C-NMR (100 MHz, CDCl$_3$, TMS): δ 98.99, 70.47, 62.06, 39.69, 30.70, 29.15, 25.62, 23.94, 23.14, 19.57, 14.13, 11.12.

### 2-(8-Methylnonyloxy)-tetrahydro-2H-pyran (Table 3.2, entry 8)

$^1$H-NMR (400 MHz, CDCl$_3$, TMS): δ 4.572 (s, 1H), 3.88-3.72 (m, 2H), 3.49 (d, J=10.4 Hz, 2H),1.84-1.40 (m, 19H), 1.33-1.07 (m, 10H); $^{13}$C-NMR (100 MHz, CDCl$_3$, TMS): δ98.47, 67.38, 61.84, 37.08, 30.62, 29.93, 29.24, 29.81, 27.80, 27.14, 26.68, 25.26, 22.74, 19.45.

### 2-(Octyloxy)-tetrahydro-2H-pyran (Table 3.2, entry 9)

$^1$H-NMR (400 MHz, CDCl$_3$, TMS): δ 4.54 (t, J=4 Hz, 1H), 3.83-3.70 (m, 1H), 3.69-3.66 (m, 1H), 3.51-3.47 (m, 1H), 3.35-3.32 ( m, 1H), 1.78-1.23 (m, 16H), 0.85 (t, J=8 Hz, 3H); $^{13}$C-NMR (100 MHz, CDCl$_3$, TMS): δ 98.87, 67.74, 62.34, 31.91, 30.84, 29.82, 29.53, 26.32, 25.58, 22.73, 19.74, 14.16.

## 3.3.3 Acetalization of glycerol using FSS catalyst to synthesize sol-ketal

After successful preparation and characterization of FSS catalyst, the catalyst was investigated for acetalization reaction of glycerol with acetone to synthesize solketal. In a typical procedure, initially 1 mmol of glycerol was mixed with 2 mmol of acetone in a small (10 mL) round bottom flask, to which 10 mol% of the synthesized FSS catalyst was added. The reaction mixture was then agitated by ultra-sonication for 30 minutes. To our pleasure, TLC monitoring showed that reaction started to progress within 15 mins with the formation of single spot in TLC which was assumed to be of solketal. The completion of the reaction was achieved within half an hour. Further $^1$H NMR analysis verified the product as 4-hydroxymethyl-2,2-dimethyl-1,3-dioxolane i.e. solketal. This observation motivated to explore the optimized conditions for the reaction.

## Optimization of different parameters:

To obtain the maximum yield of product, reactions were carried out by varying different parameters. Initially the amount of catalyst was optimized, followed by optimization of

glycerol: acetone ratio used in the synthetic process and the results are shown in Table 3.5 and Table 3.6, respectively.

**TABLE 3.5** Optimization of catalyst amount[a]

| Entry | Catalyst amount (mol%) | Time (min) | Yield (%)[b] |
|---|---|---|---|
| 1 | No catalyst | 120 | 15 |
| 2 | 2 | 40 | 60 |
| 3 | 3.33 | 30 | 88 |
| 4 | 5 | 15 | 95 |
| 5 | 10 | 15 | 95 |

[a]Reaction conditions: Glycerol (1 mmol), Acetone (5 mmol), Ultrasonication, SolFc; [b]Isolated yield

The final product yield increases with gradual increase in catalyst amount used in the protocol, however after 5 mol% catalyst, no change in the yield was observed even after increasing the catalyst amount to 10 mol% (Table 3.5, Entry 5). The optimal amount of catalyst was obtained as 5 mol%. Similar trend was observed in optimization of glycerol: acetone ratio. (Table 3.6) The optimal ratio of glycerol to acetone was noted as 1:5.

**TABLE 3.6** Optimization of glycerol:acetone molar ratio[a]

| Entry | Glycerol:Acetone molar ratio | Time (min) | Yield (%)[b] |
|---|---|---|---|
| 1 | 1:1 | 15 | 67 |
| 2 | 1:2 | 15 | 83 |
| 3 | 1:5 | 15 | 95 |
| 4 | 1:8 | 15 | 95 |

[a]Reaction conditions: Glycerol (1 mmol), Catalyst 5 mol%, Ultrasonication., SolFc; [b]Isolated yield

A comparative study of different reaction conditions preferable for the protocol was also investigated by carrying out the reaction under room temperature, conventional heating and ultra-sonication. Different agitation speeds were employed to check the effect of mass transfer on the kinetics of the reaction. Literature shows that varied conclusions have been drawn by studies engrossed in investigation of agitation speed on reaction kinetics.[61] This indicates that mass transfer may influence the progress of reaction depending upon the catalytic system, reactant mixing operation, reactant molar ratio, equipment used, product properties and many other such parametres.[62] The results of our studies are depicted in Table 3.7.

**TABLE 3.7** Effect of reaction condition and mass transfer on reaction progress[a]

| Entry | Reaction condition | Temperature (°C) | Agitation speed (rpm) | Time (min) | % Yield[b] |
|---|---|---|---|---|---|
| 1 | Conventional | RT | 400 | 360 | 65 |
| 2 | Conventional | RT | 600 | 360 | 72 |
| 3 | Conventional | RT | 800 | 120 | 75 |
| 4 | Conventional | RT | 1000 | 60 | 84 |
| 5 | Conventional | RT | 1200 | 60 | 87 |
| 6 | Conventional | 60[c] | 1000 | 45 | 90 |
| 7 | Conventional | 70[c] | 1000 | 45 | 90 |
| 8 | Conventional | 80[c] | 1000 | 45 | 86 |
| 9 | Ultrasonication | RT | - | 15 | 95 |

[a]Reaction conditions: Glycerol (1 mmol), Acetone (5 mmol), Catalyst 5 mol%, SolFc; [b]Isolated yield, [c]in pyrex glass pressure tube.

The inferences suggest that by increasing the stirring speed, reaction proceeds in forward direction resulting in an increase in product yield (Table 3.7, Entry 1-5). After introducing higher temperature to reaction system, it took less time for glycerol conversion, however, not much enhancement in the product yield was noted (Table 3.7, Entry 6-8). In contrast, at 80°C the product yield noticeably decreased (Table 3.7, Entry 8) which might be

due to the evaporation of acetone and reduced interaction of gaseous acetone and liquid glycerol.[63]

Finally, when mechanical stirring was replaced by ultra-sonication of the reaction mixture, it was observed that maximum conversion and better isolated yield was resulted within minimum duration of time (Table 3.7, Entry 9). This observation probably can be explained by the assumption that under conventional reaction condition and at low stirring speed, the water molecule generated as by-product in the reaction accumulates on the surface of catalyst and this hampers further progress of the acetalization process. However when reaction mixture is sonicated, the vigorous agitation of the reactant molecules gives no time to accumulate the water molecules and consequently the reaction proceeds in forward direction giving rise to higher yields of desired solketal product.

After establishing the optimization conditions for the reaction, synthesis of solketal was carried out using glycerol and acetone (1:5 molar ratio) and 5 mol% of FSS catalyst under ultra-sonication which took only 15 minutes to achieve nearly full conversion of glyceol. (Scheme 1). Interestingly, no side-product was observed in the TLC, which indicated that there is no formation of six-membered ring as side-product. GC-analysis provided the glycerol conversion as 97% and further confirmed the selectivity of the acetalization reaction as 100%. After separating the catalysts from the reaction mixture using external magnet and evaporating the excess acetone in rotary evaporator, the reaction finally resulted 95% isolated yield of solketal as product.

## Analysis of synthesized product by NMR and GC-MS:

The synthesized product after isolation was first analyzed by NMR spectroscopy to verify its formation and purity. The $^1H$ and $^{13}C$ NMR spectra of the isolated product are displayed in Fig. 3.9(a)-(b) respectively. In the $^1H$ NMR spectra (Fig. 3.8 (a)), the two distinct singlets at δ1.38 and δ1.45 refers to the six methyl (-CH₃) protons of 1,3-dioxolane product while the broad singlet peak for hydroxyl proton appears at δ 1.75. Peaks in the slightly deshielded region near δ 3.58-4.28 having total integration of five protons stand for the –CH₂ and –CH protons present in the product structure.



SCHEME 3.9 Acetalization of glycerol using FSS MNP catalyst
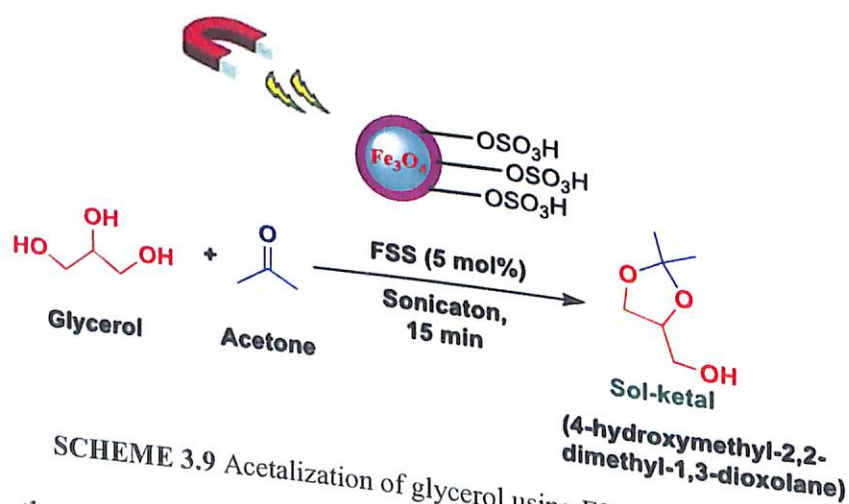
On the other hand, $^{13}C$ NMR spectra of the sol-ketal product is shown in Fig.3.8 (b) where the most shielded peaks at δ 25.25 and δ 26.70 arise due to the methyl carbons. The peak at δ 76.09 may be due to the –CH carbon and the other two peaks at δ 65.60 and 62.96 refers to the two –CH₂ carbons. The most deshielded peak at δ 109.41 must appear due to the carbon atom attached to the methyl carbons. These two spectra clearly provide evidences for the formation of sol-ketal as acetalization product of glycerol.
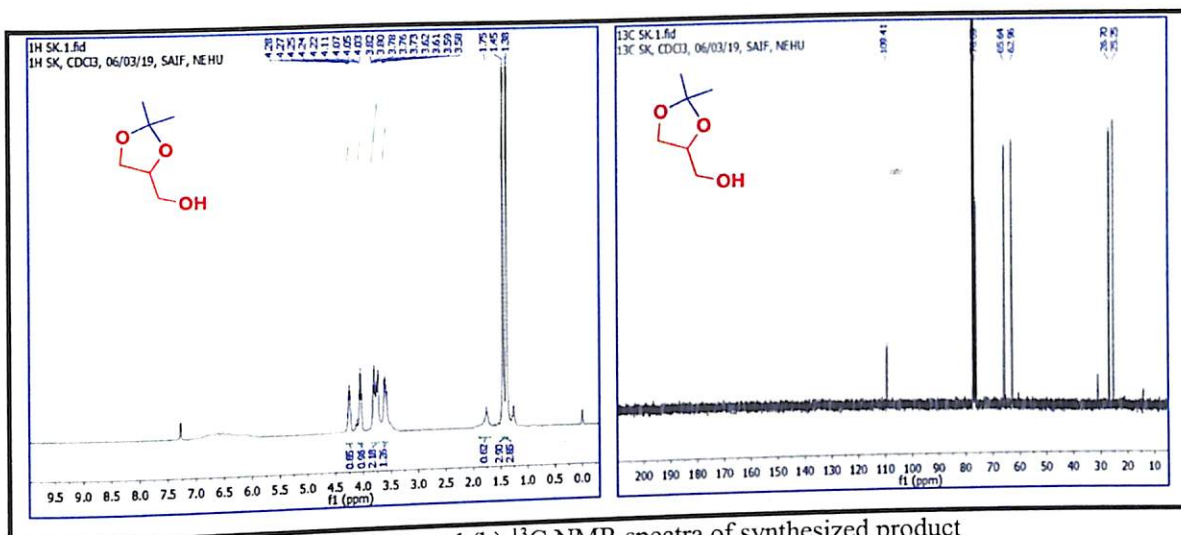
FIGURE 3.8 (a) $^1$H NMR and (b) $^{13}$C NMR spectra of synthesized product

The formation of sol-ketal or 1,3-dioxolane product was further verified by GC-MS analysis and the GC-HRMS chromatogram is shown in Fig. 3.9. The chromatogram suggests exclusive formation of sol-ketal with five-membered ring structure and discards development of any six-membered ring acetal structure in the product.
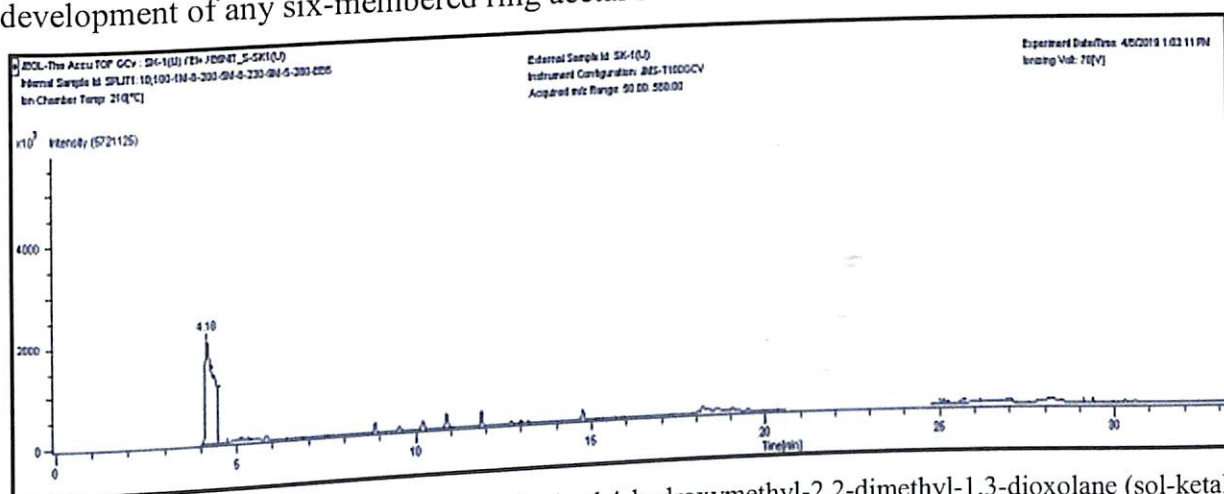


FIGURE 3.9 GC-MS chromatogram of synthesized 4-hydroxymethyl-2,2-dimethyl-1,3-dioxolane (sol-ketal) product

## Mechanism of acetalization of glycerol:
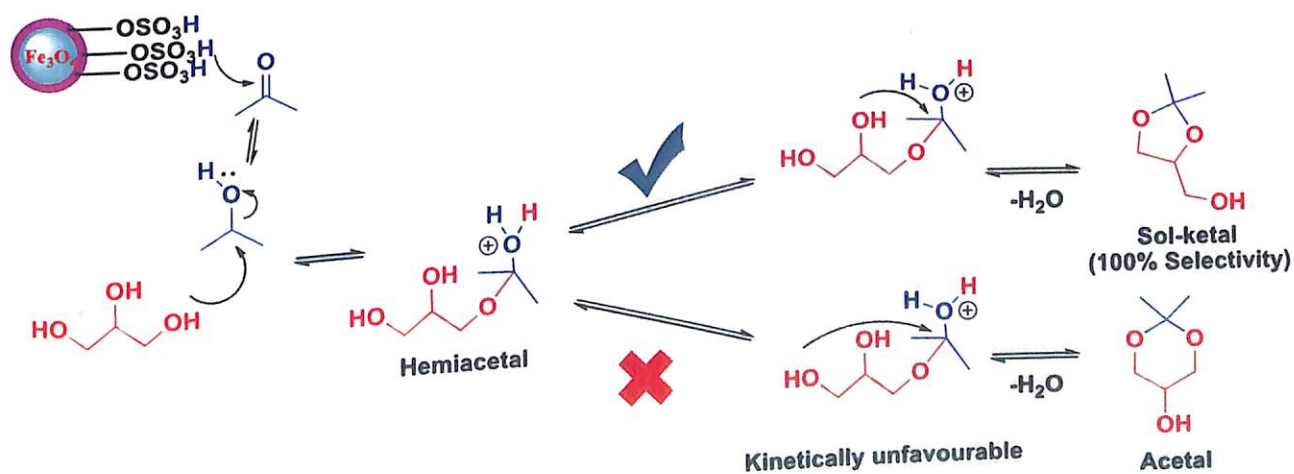


SCHEME 3.10 Mechanism of acetalization of glycerol using FSS MNP catalyst

To elucidate the high-selectivity of sol-ketal over the six-membered acetal ring, various theoretical and experimental explanations have been put forwarded. Ketal mechanism is the mostly discussed mechanism to explain sol-ketal formation.[64,65]

It is proposed here that in the first step, the carbonyl group of acetone was activated by the acid-sites of the catalyst. Then the hydroxyl group of glycerol attacks the carbonyl carbon and forms an intermediate called hemiacetal. This intermediate then undergoes cyclization by the attack of lone pair electron of either by the adjacent –OH or by the terminal –OH to form 5-membered sol-ketal or 6-membered cyclic acetal by the removal of $H_2O$ molecule. However it is established that formation of 6- membered acetal ring is not favorable kinetically. Consequently the reaction leads to exclusive formation of 5-membered 1,3-dioxolane ring suggesting 100% selectivity of the protocol.

## Comparative studies of various catalytic systems for glycerol acetalization:

The efficiency of the present catalyst was compared with several other reported catalytic methodologies in literature. The result is displayed in Table 3.8.

TABLE 3.8 Comparative analysis of present protocol with reported catalytic methods

| Sl no | Catalyst | Reaction condition: Glycerol: acetone, Temperature, Time | Glycerol Conversion (%) | Reference |
|---|---|---|---|---|
| 1 | PTSA | 1:6, 60°C, 12 h | 60-82.7 | 66 |
| 2 | H$_2$SO$_4$ | 1:1.5, 100°C, 4 h | 69-89 | 62 |
| 3 | H beta zeolite | 1:3, RT, 40 min | 62-86 | 28 |
| 4 | Zeolite beta | 1:1.2, 70°C, 40 min | 90 | 67 |
| 5 | K10 montmorillonite | 1:20, 60°C, 2 h | 82 | 49 |
| 6 | Amberlyst-36 | 1:1.5, 38-40°C, 8 h | 88 | 68 |
| 7 | Amberlyst-35* | 1:2.5, 25°C, 60 min | 74 | 34 |
| 8 | Phenolsulfonic acid-formaldehyde resin | 1:5, 40°C, 4 h | 97 | 69 |
| 9 | Mo$^{6+}$-doped SnO$_2$ | 1:1, RT, 1.5 h | 61 | 65 |
| 10 | TiO$_2$-SiO$_2$ | 1:4, 40°C, 1 h | 72-98 | 50 |
| 11 | Nb$_2$O$_5$ | 1:3, 70°C, 6 h | 80 | 70 |
| 12 | FSS** | 1:5, RT, 15 min | 97 | Present work |

* Ethanol used as additional solvent, **Ultrasonic reaction

However, most of the methods seems to involve some serious disadvantages including high temperature conditions, need for additional solvent, long reaction time and less yield. The present protocol outperforms most of the catalytic methods in literature especially in terms of ease of isolation, reaction time and yield.

## Recyclability test:

The recyclability of FSS catalyst after acetalization of glycerol was investigated by carrying out successive reactions utilizing the reused catalyst. The results are displayed in Fig. 3.10 which states that even after 5$^{th}$ catalytic runs, any depreciation in its activity was observed to be minimal. After 5$^{th}$ cycle, 95% conversion of glycerol was recorded while isolated yield was 90%. Interestingly, in each case, selectivity remained 100% and only 5-membered sol-ketal ring was obtained as product.

Additionally, no difference in FT-IR spectrum of the catalyst was observed after these repeated cycles (Figure 3.1(d)). The EDX spectra of the recovered FSS catalyst (after 5 consecutive cycles) also showed similar elemental composition with fresh catalyst (Figure 3.5 (d)). The spectra recorded wt% of S in the recovered catalyst as 1.20%, which is only 0.18% less than that of the fresh catalyst. The VSM magnetization curve of the recovered FSS (Figure 3.6 (d)) confirms the retention of the magnetic behavior of the catalyst even after repeated use in five catalytic runs. The saturation magnetization value of the recovered

64

catalyst was obtained as 16.55 emu/g, which is slightly less than the fresh catalyst (16.91 emu/g) and it is sufficient for operating magnetic separation. The morphology of the recycled catalyst was also found to be similar as revealed by its TEM image in Figure 3.11.
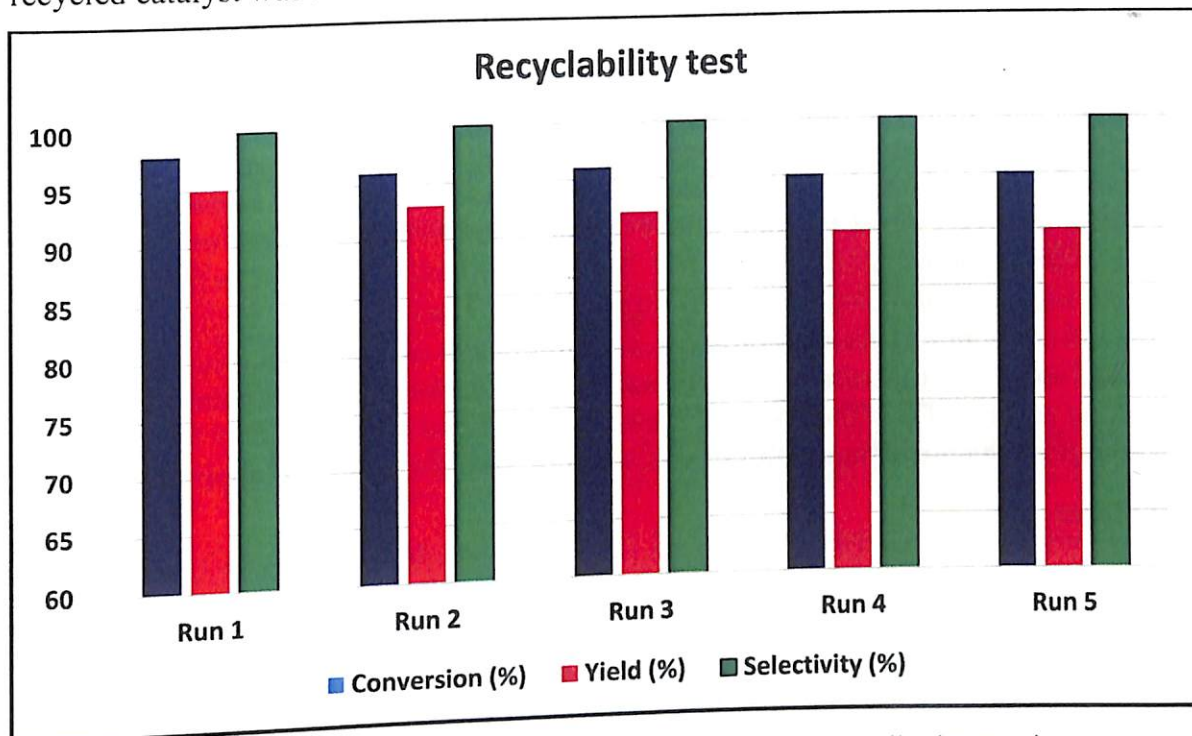


FIGURE 3.10 Recyclability test of FSS catalyst after glycerol acetalization reaction
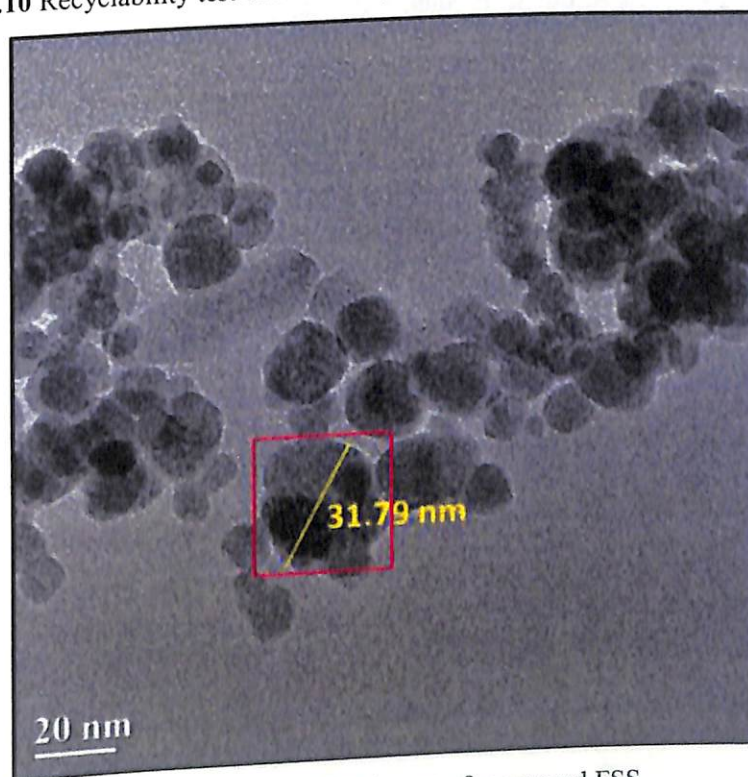


FIGURE 3.11 TEM image of recovered FSS

## 3.4 Conclusion

Protection/deprotection is one of the most frequently applied synthetic strategies by organic chemists; discovery of more green and efficient heterogeneous catalysts for these reactions has been a fundamental necessity. The tetrahydropyranylation of alcohols using our reported magnetic $Fe_3O_4$@silica sulfonic acid nanocatalyst offers a green, mild, less toxic, stable, and

solvent-free process of protection/deprotection reaction with easy recoverability of the catalyst. In short, protection deprotection using FSS catalyst is highly economical and environmentally benign method.

In similar way, glycerol based acetals are finding immense importance in recent times as fuel additives due to which designing simple, eco-friendly and efficient methodology for their synthesis is a need of the hour. Introduction of magnetically retrievable catalyst to the solketal synthesis can be a highly strategic way for hurdle-free separation of catalyst from the reaction mass. The protocol involves an ultrasonic pathway and operates in a very short reaction time (15 mins) and offers excellent conversion rate (97%), isolated product yield (95%) and most importantly 100% selectivity of five-membered solketal ring. Easy magnetic separation of catalyst, good recyclability, cost-effective and environment-friendly protocol, no requirement of additional solvent, ultrasonic reaction and ambient temperature con .tion are the key factors of the FSS-catalyzed glycerol acetalization process. Thus, the protocol presents a click chemistry pathway for production of solketal using magnetic nanocatalyst which can be vital for industrial application.

# References

1. R. A. Sheldon and R. S. Downing, *Appl. Catal. A.* 1999, **189**, 163.
2. B. F. G Johnson, Top. *Catal.* 2003, **24**, 147.
3. D. Astruc, F. Lu and J. R. Aranzaes, *Angew. Chem. Int. Ed.* 2005, **44**, 7852 – 7872.
4. M.-C. Daniel and D. Astruc, *Chem. Rev.* 2004, **104**, 293.
5. D. I. Gittins and F. Caruso, *Angew. Chem.* 2001, **113**, 3089.
6. Y. Zhu, L. P. Stubbs, F. Ho, R. Liu, C. P. Ship, J. A. Maguire and N. S. Hosmane, *ChemCatChem* 2010, **2**, 365 – 374.
7. S. Ko and J. Jang, *Angew. Chem.* 2006, **118**, 7726 –7729.
8. L. M. Rossi, N. J. S. Costa, F. P. Silva and R. V. Gonçalves, *Nanotechnol Rev.* 2013, **2**, 597–614.
9. Polshettiwar V. and Varma R. S., *Green Chem.* 2010, **12**, 743.
10. W. Wu, Q. He and C. Jiang, *Nanoscale Res. Lett.* 2008, **3**, 397–415.
11. L. M. Liz-Marzin and P. Mulvaney, *J. Phys. Chem. B* 2003, **107**, 7312.
12. O. B. Miguel, P. Tartaj, M. P. Morales, P. Bonville, U. G. Schindler, X. Q. Zhao and S. V. Verdaguer, *Small* 2006, **2**, 1476.
13. P. Sudarsanam, R. Zhong, S. V. d. Bosch, S. M. Coman, V. I. Parvulescu and B. F. Sels, *Chem. Soc. Rev.* 2018, **47**, 8349-8402.
14. S. Wang, Z. Zhang, B. Liu and J. Li, *Catal. Sci. Technol.* 2013, **3**, 2104–2112.
15. Y. Chiang, S. Dutta, C. Chen, Y. Huang, K. Lin, J. C. S. Wu, N. Suzuki, Y. Yamauchi and K. C. W. Wu, *ChemSusChem* 2015, **8**, 789–794.
16. N. Koukabi, E. Kolvari, M.A. Zolfigol, A. Khazaei, B.S. Shaghasemi and B. Fasahatib, *Adv. Synth. Catal.* 2012, **354**, 2001–2008.
17. B. Dam, A. Kumar Pal and A. Gupta, *Synth. Comm.* 2016, **46**, 275–286.
18. A. R. Kiasat, J. Davarpanah, *J. Mol. Catal. A: Chem.* 2013, **373**, 45-54.
19. M. A. Ghasemzadeh, M. H. Abdollahi-Basir and M. Babaei, *Green Chem. Lett. Rev.* 2015, **8**, 40–49.
20. B. Kumar, M. A. Aga, D. Mukherjee, S. S. Chimni and S. C. Taneja, *Tetrahedron Lett.* 2009, **50**, 6236.
21. T. W. Greene and P. G. M. Wuts, in *Protective Groups in Organic Synthesis*, John Wiley & Sons, New York, 2007.
22. D. B. G. Williams, S. B. Simelane, M. Lawton and H. H. Kinfe, *Tetrahedron* 2010, **66**, 4573.
23. M. Miyashita, A. Yoshikoshi and P. A. Grieco, *J. Org. Chem.* 1977, **42**, 3774.
24. T. Sato, J. Otera and H. Nozaki, *J. Org. Chem.* 1990, **55**, 4770.
25. H. Firouzabadi, N. Iranpoor and H. Hazarkhani, *Tetrahedron Lett.*, 2002, **43**, 7139.
26. S. Kim and W. J. Lee, *Synth. Commun.* 1986, **16**, 659.
27. B. Akhlaghinia, *Phosphorus, Sulfur Silicon Relat. Elem.* 2004, **179**, 1783.
28. P. Manjunathan, S. P. Maradur, A.B. Halgeri and G. V. Shanbhag, *J. Mol. Catal. A: Chem.* 2015, **396**, 47-54.
29. A. R. Trifoi, P. Ş. Agachi and T. Pap, *Renewable Sustainable Energy Rev.* 2016, **62**, 804-814.
30. P. Saxena, S. Jawale and M. H. Joshipura, *Proced. Eng.* 2013, **51**, 395-402.
31. L. Li, T. I. Korányi, B. F. Sels and P. P. Pescarmona, *Green Chem.* 2012, **14**, 1611-1619.

32. F. Ma and M. A. Hanna, *Bioresour. Technol.* 1999, **70**, 1-15.
33. B. Mallesham, P. Sudarsanam, and B. M. Reddy, *Ind. Eng. Chem. Res.* 2014, 53, 18775-18785.
34. M. R. Nanda, Z. Yuan, W. Qin, H. S. Ghaziaskar, M. A. Poirier and C. C. Xu, *Fuel* 2014, **117**, 470-477.
35. R. S. Karinen and A. O. I. Krause, *Appl. Catal. A.* 2006, **306**, 128-33.
36. N. Suriyaprapadiloka and B. Kitiyanan, *Energy Procedia* 2011, **9**, 63-69.
37. J. M. Clomburg and R. Gonzalez, *Trends Biotechnol.* 2013, **31**, 20-28.
38. S. H. Chai, H. P. Wang, Y. Liang and B. Q. Xu, J., *Catal.* 2007, **250**, 342–349.
39. M. A. Dasari, P. P. Kiatsimkul, W. R. Sutterlin and G. J. Suppes, *Appl. Catal. A* 2005, **281**, 225–231.
40. S. Zhu, Y. Zhu, Xiaoqing Gao, T. Mo, Y. Zhu, Y. Li., *Bioresour. Technol.* 2013, **130**, 45–51.
41. K. Klepáčová, D. Mravec and M. Bajus, *Appl. Catal. A* 2005, **294**, 141–147.
42. R. R. Soares, D. A. Simonetti and J. A. Dumesic, *Angew. Chem. Int. Ed.* 2006, **45**, 3982–3985.
43. E. Garcia, M. Laca, P. Pe´rez, A. Garrido and J. Peinado, *Energy Fuels* 2008, **22**, 4271-4280.
44. C. J. A. Mota, C. X. A. Silva, N. Rosenbach, J. Costa and F. Silva, *Energy Fuels* 2010, **24**, 2733-2736.
45. J. S. Clarkson, A. J. Walker and M. A. Wood, *Org. Process Res. Dev.* 2001, **5**, 630-635.
46. M. J. Climent, A. Corma and A. Velty, *Appl. Catal. A* 2004, **263**, 155–161.
47. M. J. Climent, A. Velty and A. Corma, *Green Chem.* 2002, **4**, 565–569.
48. A. Sokołowski, A. Piasecki and B. Burczyk, *J. Am. Oil Chem. Soc.* 1992, **69**, 633–638.
49. H. Serafim, I. M. Fonseca, A. M. Ramos, J. Vital, J. E. Castanheiro, *Chem. Eng. J.* 2011, 178, 291-296.
50. C. N. Fan, C. H. Xu, C. Q. Liu, Z. Y. Huang, J. Y. Liu, Z. X., *React Kinet. Mech. Cat. Lett.* 2012, **107**, 189-202.
51. P. Ferreira, I. M. Fonseca, A. M. Ramos, J. Vital, J. E. Castanheiro, *Appl. Catal. B: Environ.* 2010, **98**, 94-99.
52. B. Mallesham, P. Sudarsanam and B. M. Reddy, *Catal. Sci. Technol.* 2014, **4**, 803-813.
53. L. Pizzuti, P. L. G. Martins, B. A. Ribeiro, F. A. Quina, E. Pinto, A. F. C. Flores, D. Venzke and C. M. P. Pereira, *Ultrason. Sonochem.* 2010, **17**, 34-37.
54. M. A. P. Martins, C. M. P. Pereira, W. Cunico, S. Moura, F. Rosa, R. L. Peres, P. Machado, N. Zanatta and H. G. Bonacorso, *Ultrason. Sonochem.*, 2006, **13**, 364- 370.
55. P. Cintas, J. L. Luche, *Green Chem.* 1999, **1**, 115-125.
56. P. T. Anastas and J. C. Warner Green Chemistry: Theory and Practice, Oxford University Press, Oxford, 1998, pp. 11–54.
57. G. Chatel, *Ultrason. Sonochem.* 2018, **40**, 117-122.
58. H. Naeimi and S. Mohamadabadi, *Dalton Trans.*, 2014, **43**, 12967.
59. F. Nemati, M.M. Heravi and R. Saeedirad, *Chin. J. Catal.*, 2012, **33**, 1825.
60. N. Koukabi, E. Kolvari, M. Ali Zolfigol, A. Khazaei, B. S. Shaghasemi and B. Fasahati, *Adv. Synth. Catal.* 2012, **354**, 2001-2008.
61. C. S. Gill, B. A. Price and C. W. Jones, *J. Catal.* 2007, **251**, 145-152.
62. A. R. Trifoi, P. Ş. Agachi and T. Pap., *Renewable Sustainable Energy Rev.* 2016, **62**, 804-814.
63. E. A. Bratu, Operatii unitare in ingineria chimica, Ed.Tehnica, Bucuresti, 1984.
64. M. Shirani, H. S. Ghaziaskar and C. C. Xu, *Fuel Process. Technol.* 2014, **124**, 206-211.
65. B. Mallesham, P. Sudarsanam, G. Raju and B. M. Reddy, *Green Chem.*, 2013, **15**, 478-490.
66. N. Suriyaprapadilok and B. Kitiyanana, *Energy Procedia* 2011, **9**, 63-69.
67. J. Deutsch, A. Martin and H. Lieske, *J. Catal.* 2007, **245**, 428-435.
68. C. X. A. Da Silva and C. J. A. Mota, *Biomass Bioenergy* 2011, **35**, 3547-3551.
69. I. B. Laskar, K. Rajkumari, R. Gupta and Lalthazuala Rokhum, *Energy Fuels* 2018, *32*, 12567-12576.
70. G. S. Nair, E. Adrijanto, A. Alsalme, I. V. Kozhevnikov, D. J. Cooke, D. R. Brown and N. R. Shiju, *Catal. Sci. Technol.* 2012, **2**, 1173-1179.
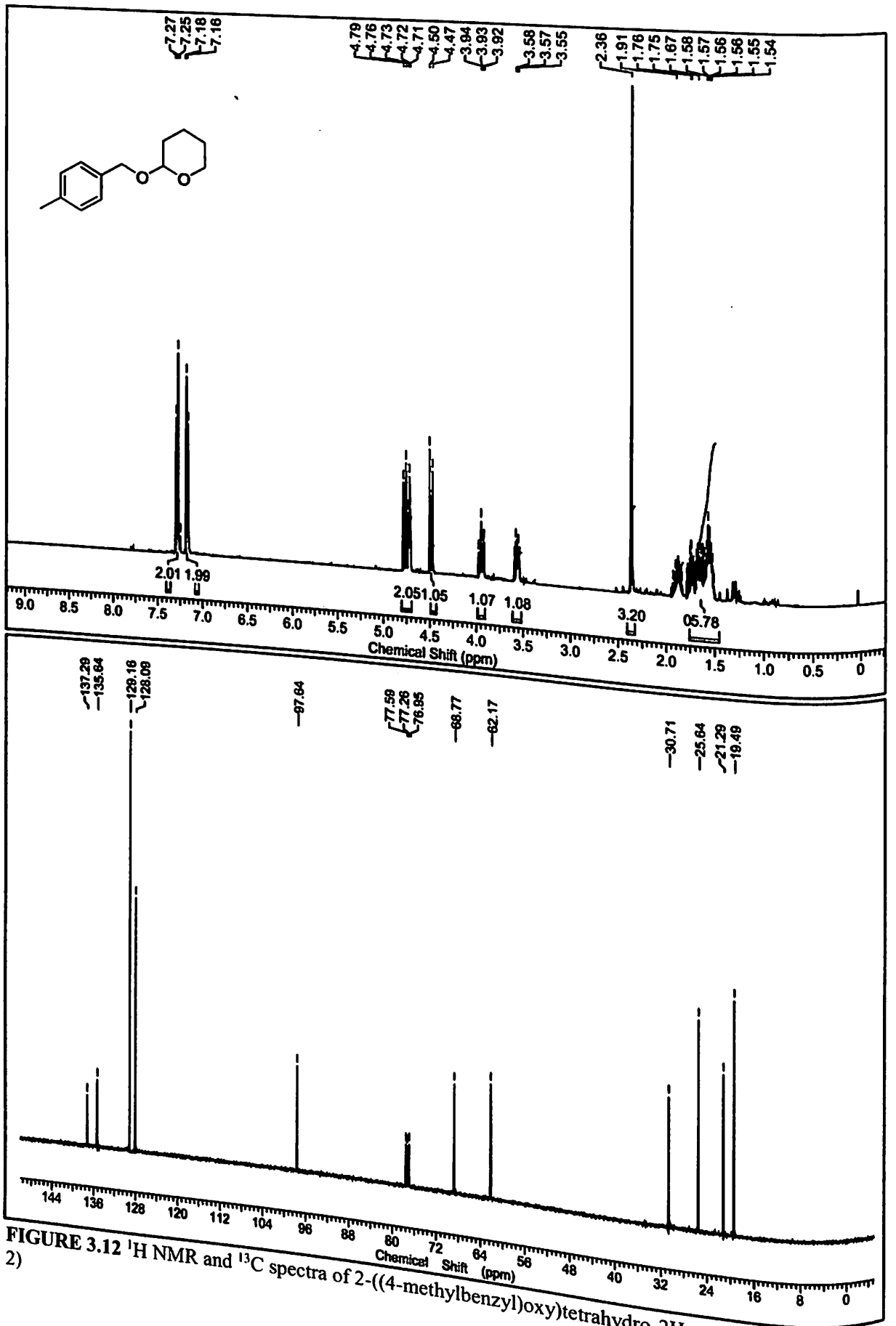
FIGURE 3.12 $^1$H NMR and $^{13}$C spectra of 2-(((4-methylbenzyl)oxy)tetrahydro-2H-pyran (Table 3.2, Entry 2)

68
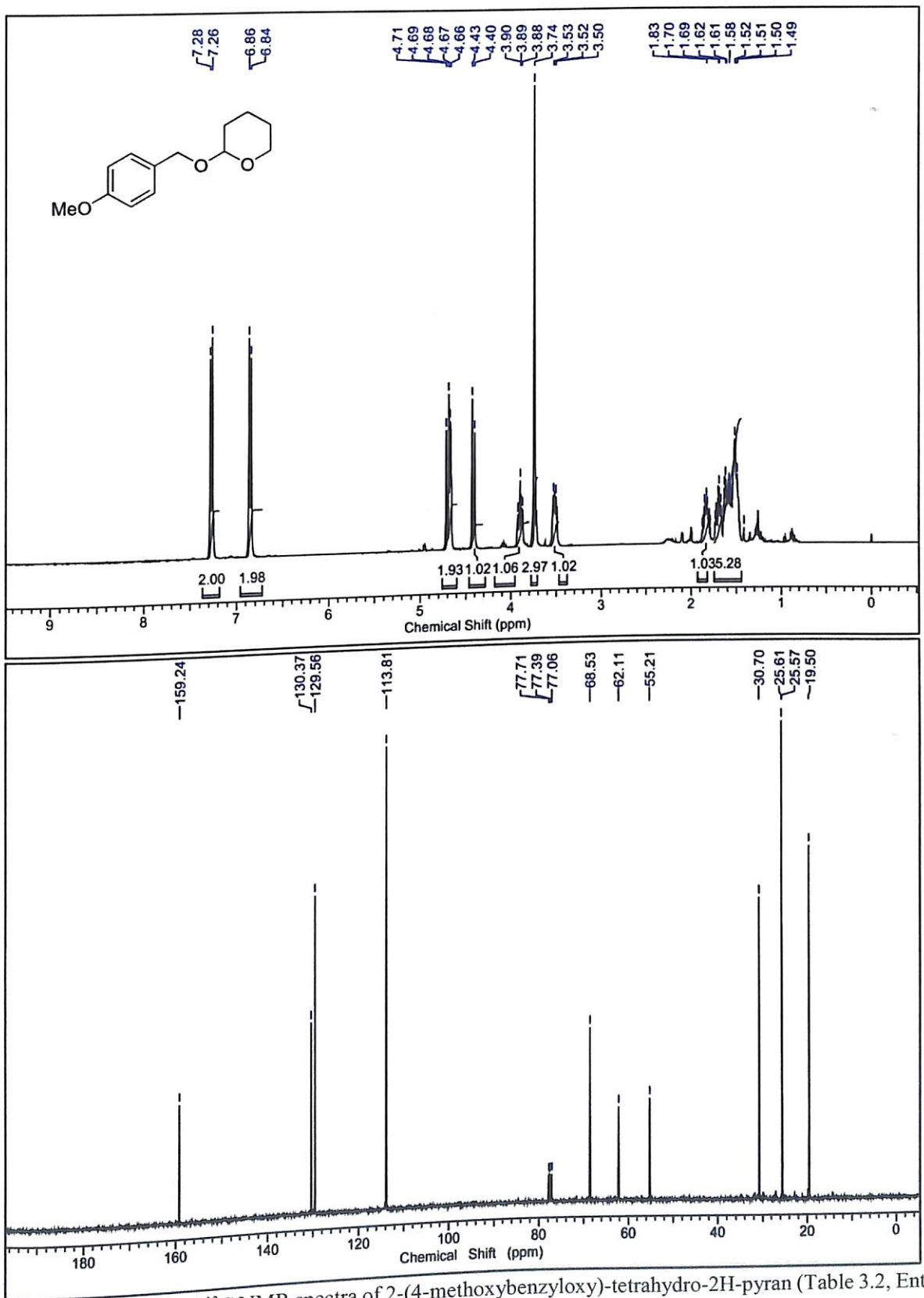
FIGURE 3.13 $^1$H and $^{13}$C NMR spectra of 2-(4-methoxybenzyloxy)-tetrahydro-2H-pyran (Table 3.2, Entry 3)

69
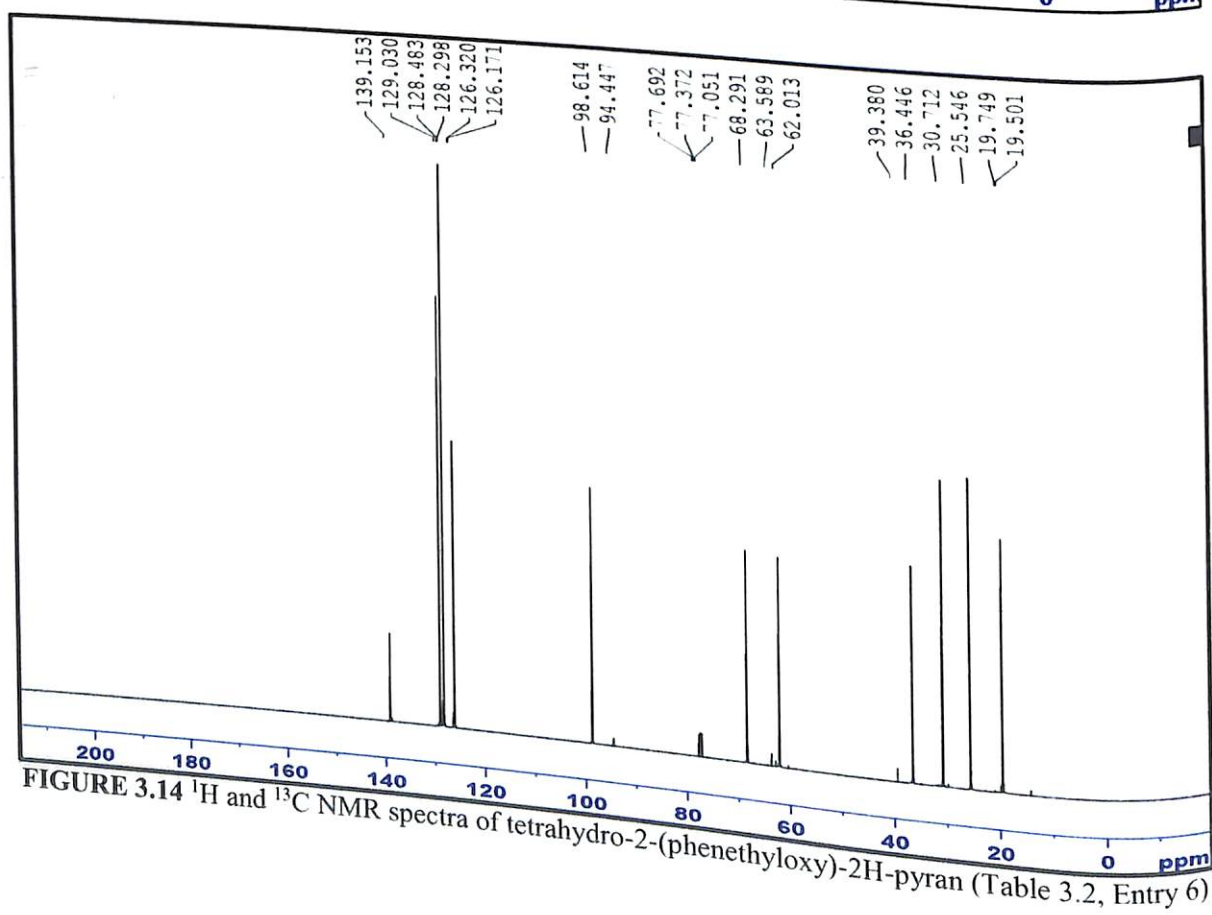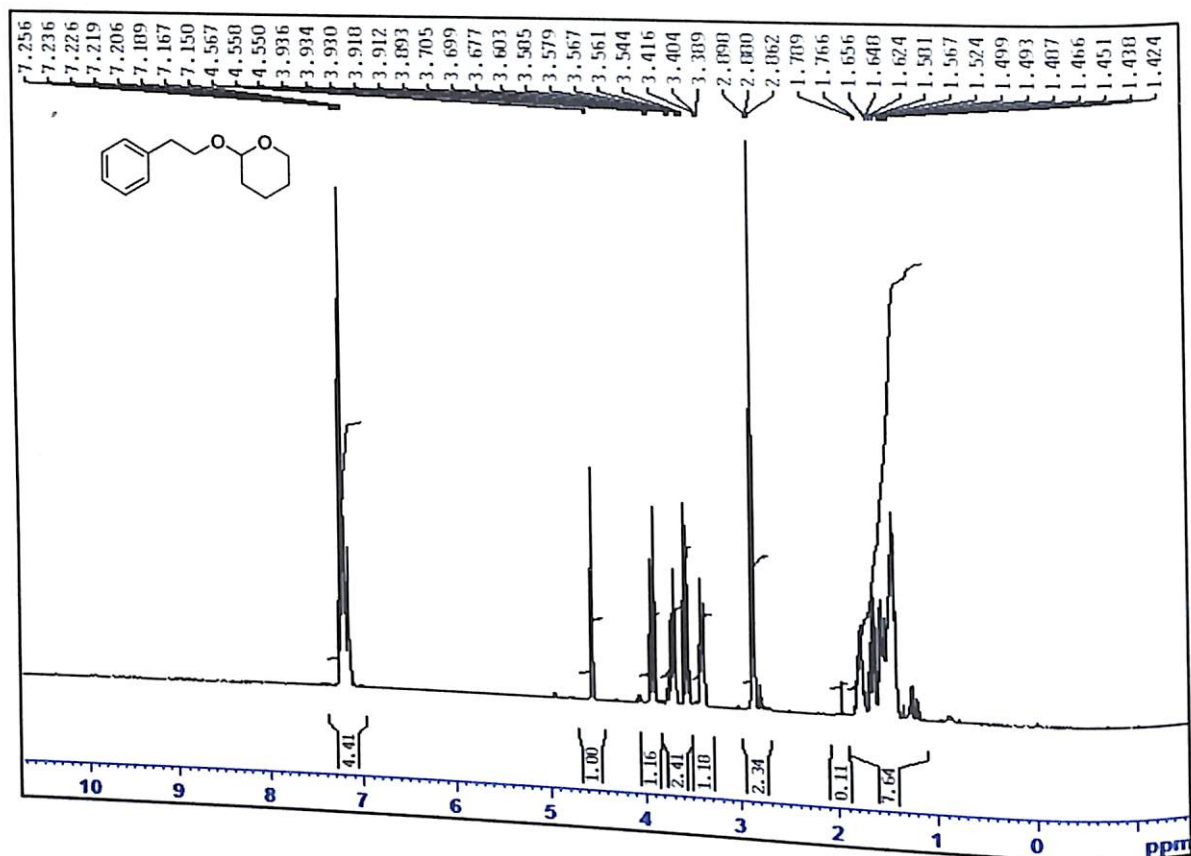
FIGURE 3.14 $^1$H and $^{13}$C NMR spectra of tetrahydro-2-(phenethyloxy)-2H-pyran (Table 3.2, Entry 6)

70
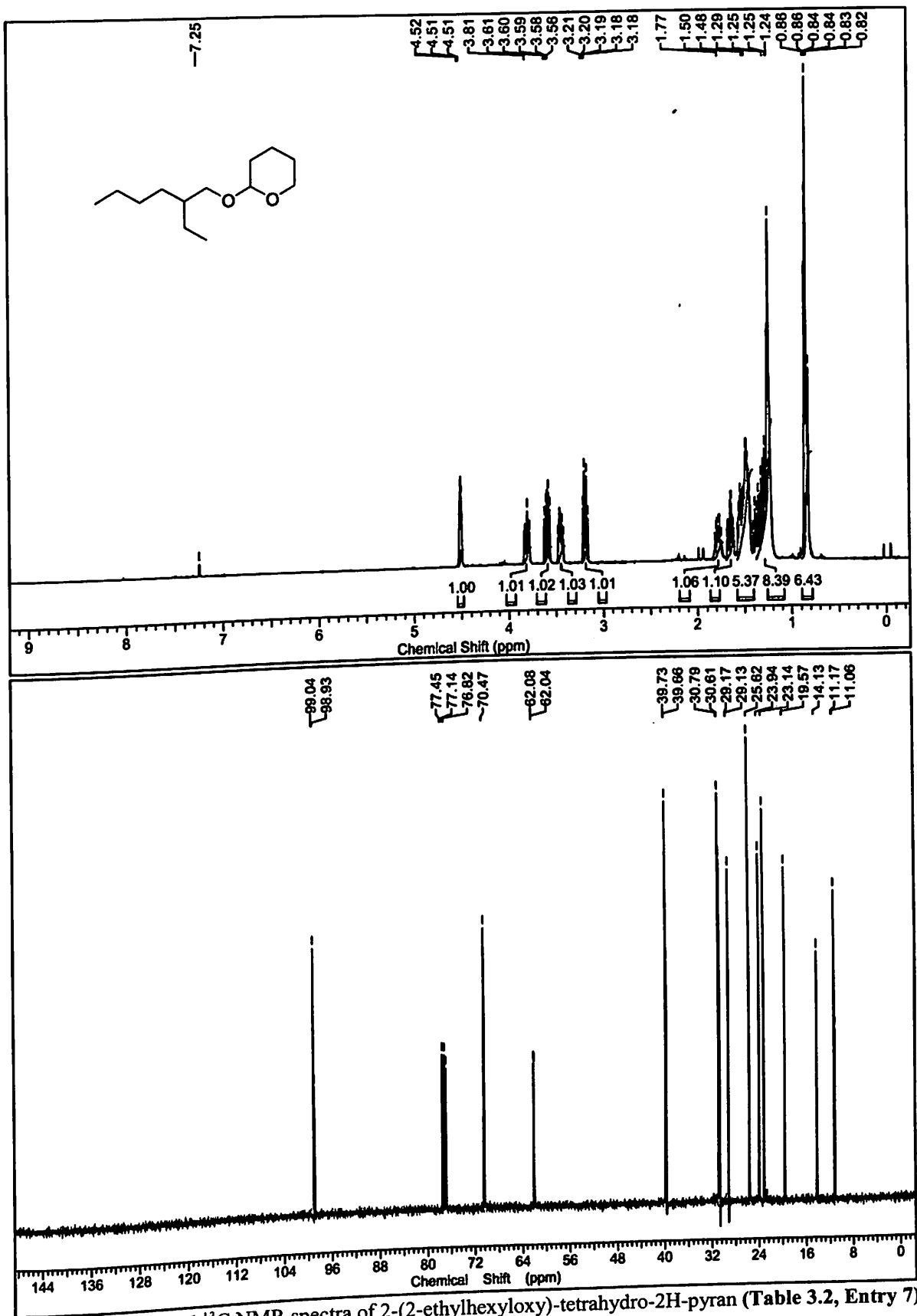
**FIGURE 3.15** $^1$H and $^{13}$C NMR spectra of 2-(2-ethylhexyloxy)-tetrahydro-2H-pyran (**Table 3.2, Entry 7**)

71
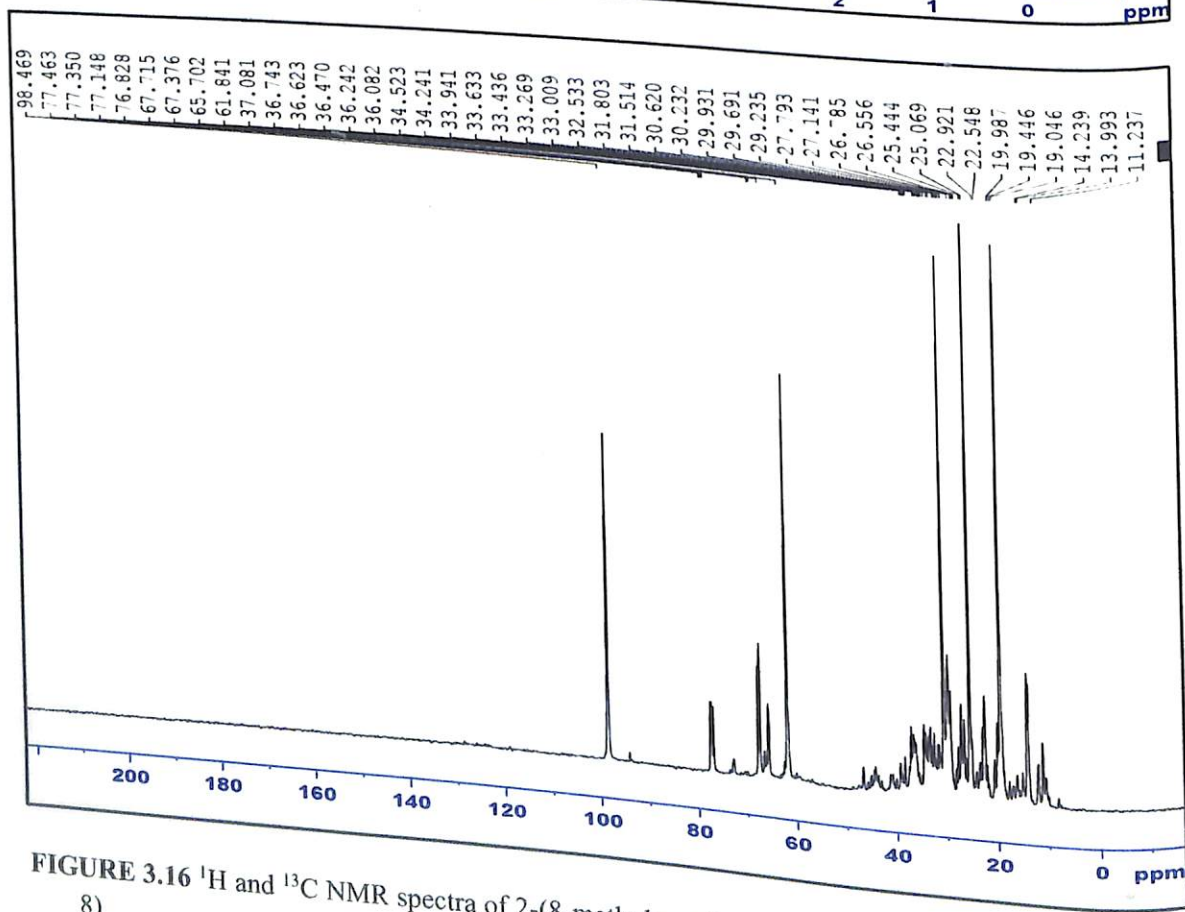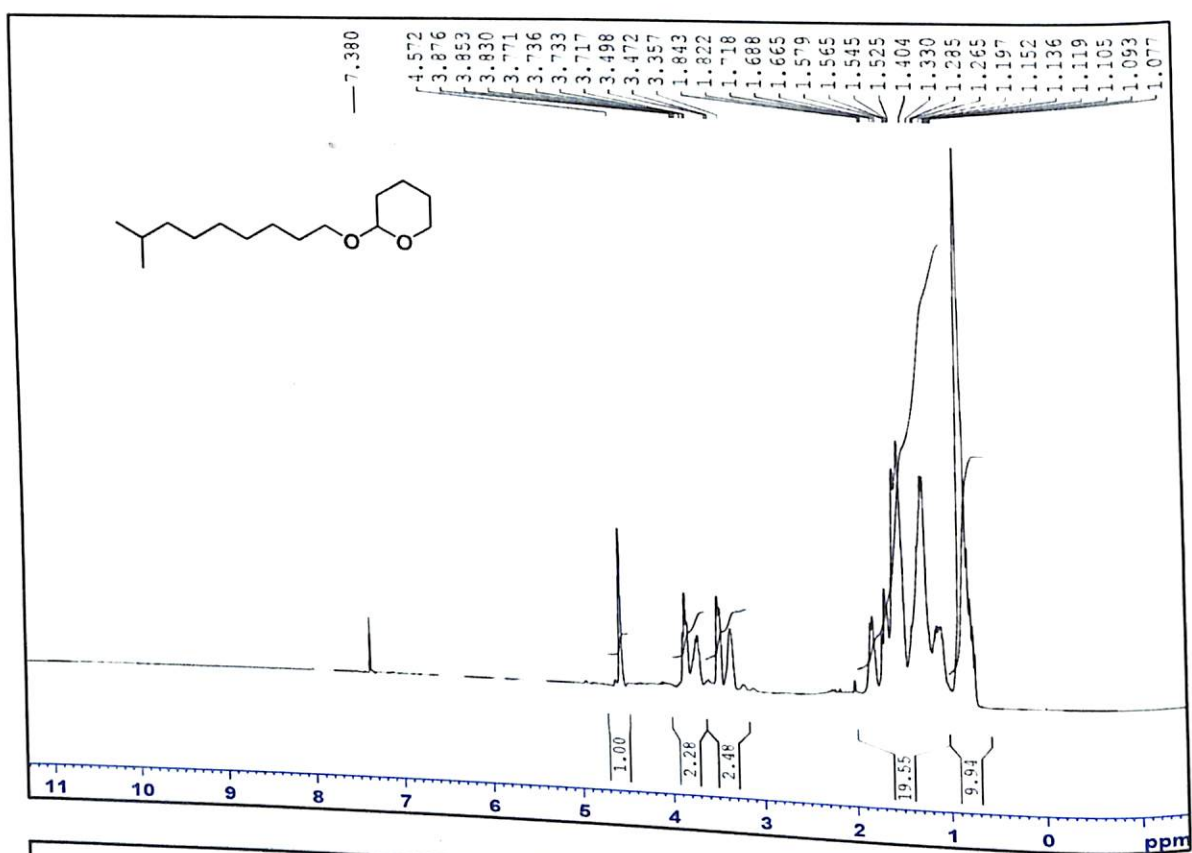
FIGURE 3.16 $^1$H and $^{13}$C NMR spectra of 2-(8-methylnonyloxy)-tetrahydro-2H-pyran (Table 3.2, Entry 8)
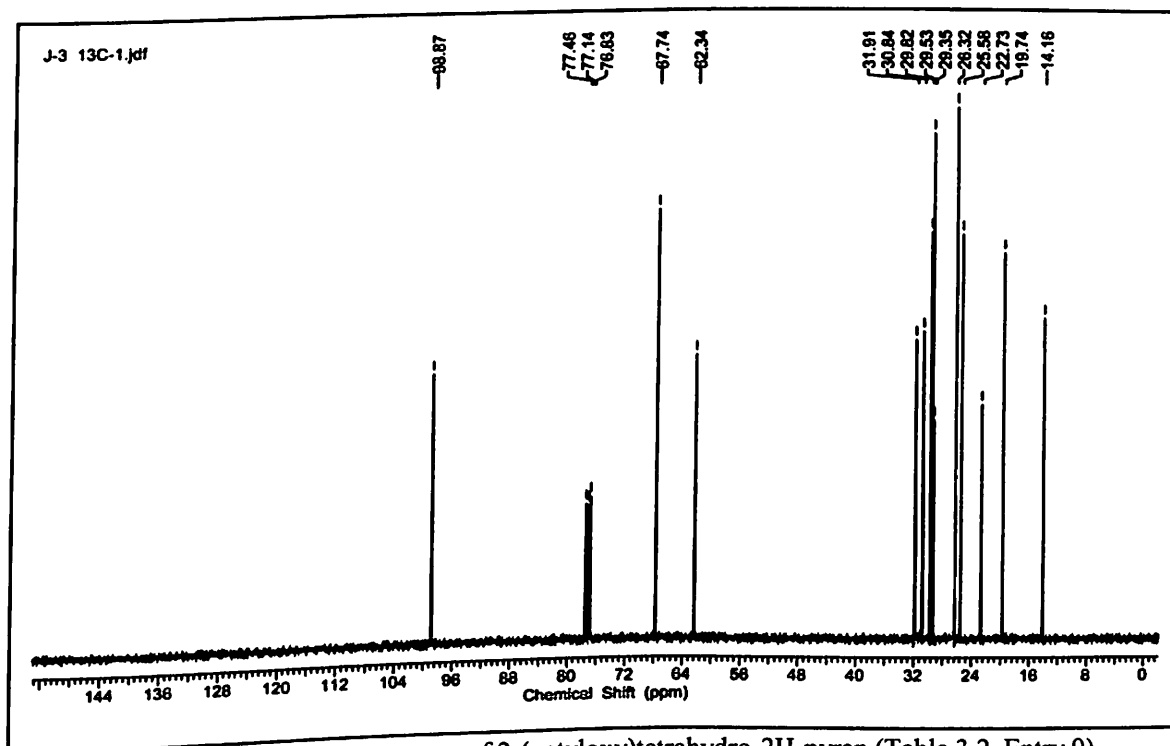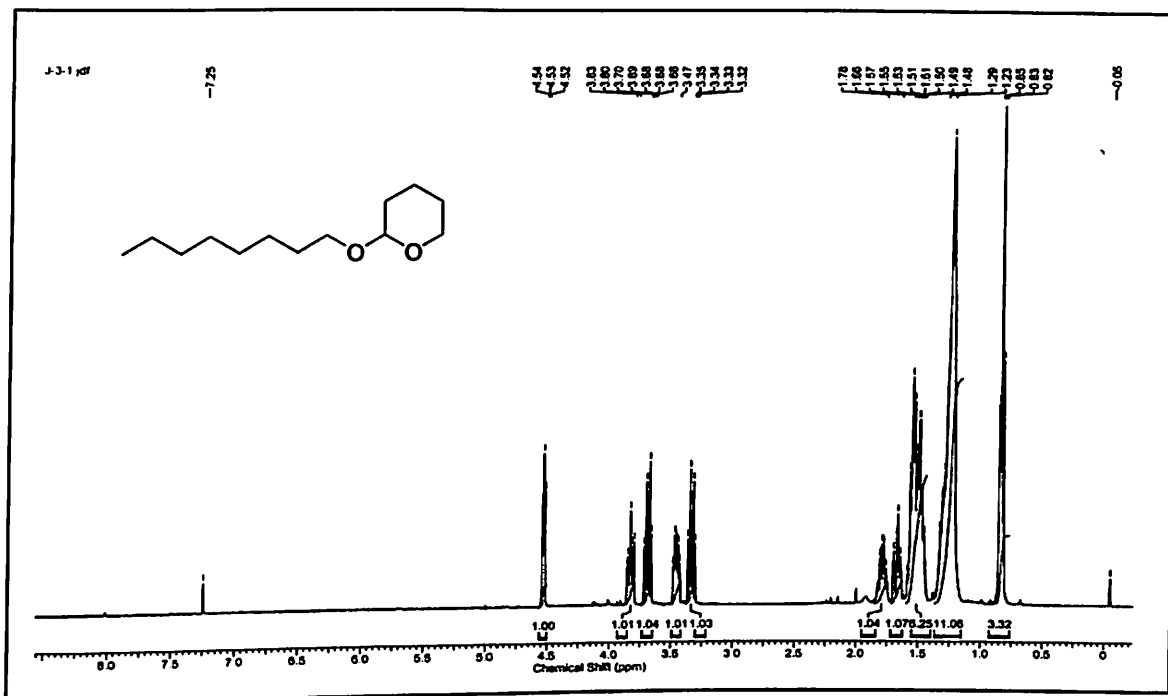
**FIGURE 3.17** $^1$H and $^{13}$C NMR spectra of 2-(octyloxy)tetrahydro-2H-pyran (Table 3.2, Entry 9)

73

# CHAPTER

# 4

# Highly selective Tetrahydropyranylation/ Dehydropyranylation of Alcohols and Phenols using Porous Phenolsulfonic Acid-Formaldehyde Resin Catalyst under Solvent-Free Condition

## 4.1 Introduction

The hunt for an alternative green and efficient catalyst with environment-friendly technologies has been a perceived attention in current scientific research. Heterogenization of homogeneous catalysts onto solid supports is undergoing well-investigation with an objective to enhance recyclability of catalyst and thereby minimize disposal problems.[1,2] Although polymer-supported catalysts and reagents are being utilized in organic synthesis for decades, but the high-cost issue involved in the post-immobilization process of such catalysts and low catalyst loading constrain their applicabilities.[3] As a powerful alternative to this, porous organic polymers synthesized via bottom-up approach has emerged to be simple, low-cost, easily separable and recoverable heterogeneous catalysts for organic transformations. Moreover, the bottom-up synthesis strategy offers prospects to design with different functionalities to be used as catalysts.[4-6] The framework of applications of carbon-based, metal-free polymeric resins are much wider and appreciable because they are mostly synthesized from renewable resources and therefore problems raised due to waste disposal, leaching, metal-contamination in desired products etc. can be avoided easily[7]

We report herein a mesoporous Phenolsulfonic Acid Formaldehyde Resin (PAFR) catalyst that exhibit efficient catalytic activity towards chemoselective protection and deprotection of alcohols and phenols. The history of resin based on phenol and formaldehyde

dates back to 1872 when it was discovered by A. Von. Bayer.[8] Since the introduction of ion-exchange property of phenol-formaldehyde resins by Adams and Holmes in 1935, they have been extensively studied and applied as ion exchangers both in academia and industries.[9] Functionalized ion exchange resins are regarded as a flag bearer of solid acid catalyst.[10-12]

Recently, Yamada et al.[13,14] reported an in-water direct dehydrative esterification process of alcohol and carboxylic acid utilizing Phenolsulfonic Acid Formaldehyde Resin as catalyst without removal of byproduct. In addition, our group reported the synthesis of solketal, a potent fuel additives[15] using PAFR resin as a recyclable solid catalyst. In the present study, PAFR was found to effectively catalyze the tetrahydropyranylation and depyranylation of alcohols and phenols. In a valuable multi-step organic synthetic route, protection/deprotection of reactive functional groups plays a fundamental yet immense useful step for chemoselective attack on certain specific reactive sites.[16,17] 3,4-dihydro-2H-pyran (DHP) is recognized as an ideal protecting group owing to its simple preparation, low cost, ease of handling, strong tolerability of the protected 2-tetrahydropyranyl (THP) ethers towards different reagents and . sy deprotection (Scheme 4.1).[18-21]

3,4-dihydro-2H-pyran (DHP)

R-OH        THPRN
Alcohol ⇌ DPRN

R\O\O

THP ether
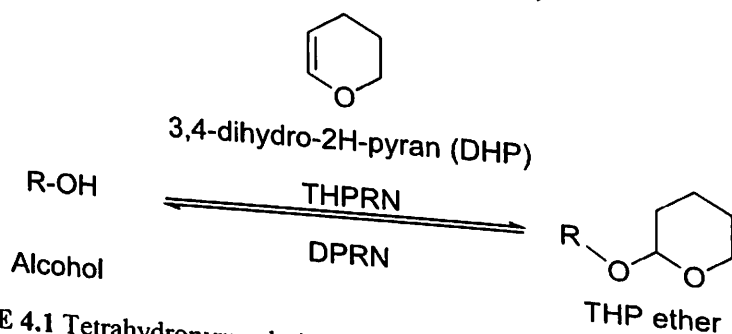
**SCHEME 4.1** Tetrahydropyranylation (THPRN)/depyranylation (DPRN)

Thesaurus of synthetic methodologies can be found in literature,[22-32] each method having their own pros and cons. Many of the protocols lack sustainability in their methods due to the use of corrosive acid catalysts like silica sulfuric acid, PTSA,[23,24] non- recoverable homogeneous catalysts,[25,26] hygroscopic, costly and non-recyclable catalysts like AlCl₃, molecular iodine etc.,[21,27] heterogeneous metal catalysts[28-30] which may create problems like waste- disposable, contamination of the metal to desired product etc. Moreover most of the reported protocol use of toxic chlorinated solvents,[15,31] high temperature[21,25] etc. and also need vigorous conditions to carry out protection of bulky substrates having secondary, tertiary carbons and phenols specifically.[31,32] A number of polymer-based heterogeneous catalytic systems comprising of commercially available ion-exchange resins and polymer-supported catalysts were reported previously to catalyze the tetrahydropyranylation (THPRN)/depyranylation (DPRN) processes of alcohols or phenols. Dowex[31], nafion[32], amberlyst[33] are some example of ion exchange resins found to effectively catalyze this transformation.

R-OH   +   DHP   →(Dowex 50WX4-100 / CH₂Cl₂, RT)→   R\O\O

Alcohol        DHP                                    THP ether
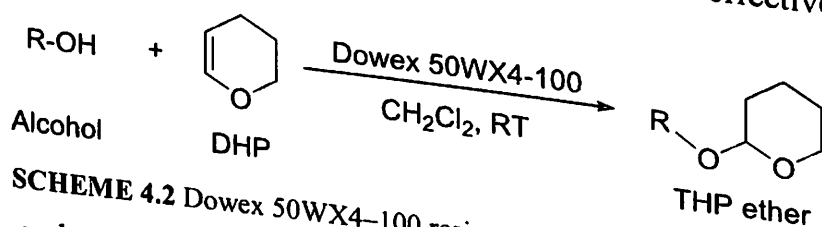
**SCHEME 4.2** Dowex 50WX4-100 resin catalyzed THPRN reaction.

Tamami and Borujeny[25] prepared polystyrene-supported AlCl₃ catalysts which performed chemoselective THPRN reaction to afford good to excellent yield of THP ethers from diverse range of alcohols and phenols. Also the protocol succeeded in monoprotection of symmetric diols.

76

$$R\text{-OH} \quad + \quad \text{DHP} \quad \xrightarrow[\text{CH}_2\text{Cl}_2,\ \text{RT}]{\text{Ps-AlCl}_3} \quad \text{THP ether}$$
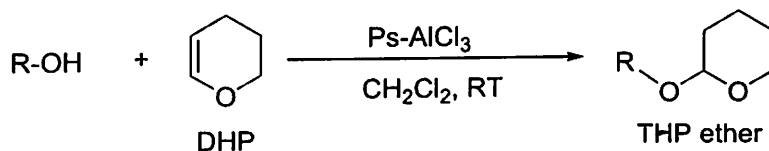
**SCHEME 4.3** Ps- AlCl₃ catalyzed THPRN reaction.

However almost all these processes are engrossed in the use of chlorinated solvents which restricts their applicability for environment-friendly synthesis.

Our continuous interest in the application of polymeric reagents and catalysts[35,36] and establishing a more general method for synthesis of THP ethers[37] prompted us to exploit the hydrophilic mesoporous PAFR catalyst for this conversion. This polymeric acid catalyst mimics the chemistry of enzymes through a phase separated reaction condition. The hydrophilic active site of the catalyst first attracts the fairly hydrophilic alcohol or phenol substrate and then after its conversion into the relatively hydrophobic ether product, it is apparently kicked out from the catalyst site. With this working hypothesis, we tried protection (deprotection) of alcohol and phenol substrate to their corresponding tetrahydropyranylated products. Since organic solvents are the major contributor of E-factors in the fine chemical and pharmaceutical industries, solvent-free reaction condition is a preferable solution to the waste problem.[38] Interestingly, our protocol showed excellent results in solvent-free condition and selectively protected a large variety of alcohol and phenol molecules affording high yield within a very short time at ambient temperature without any requirement to remove byproduct. The catalyst seems to be advantageous over several other industrially used catalyst for the tetrahydropyranylation and presents major benefits that comprises of easy recovery by filtration, high purity of products compared to homogeneous catalytic systems, metal-free catalyst, elimination of waste disposal problem, high selectivity, lack of side products and note worthily, environmentally benign solvent-free reaction condition. The reaction protocol developed is feasible at very mild reaction conditions viz., at room temperature, with very low catalyst loading and the catalyst employed is 'metal free' polymeric material.

# 4.2 Experimental section

## 4.2.1 Materials and methods

The chemicals required, different alcohols, 3,4-Dihydropyran (DHP), silica gel for thin layer chromatography (TLC) and column chromatography were of analytical grade and purchased from SpectroChem and were used without further purification. Formaldehyde and *p*-hydroxybenzenesulphonic acid used in preparation of the polymeric resin were purchased from Sigma Aldrich and used as such. Solvent used were of extra pure grade purchased from Merk India. Double distilled deionized water was used for the synthesis of the polymer catalyst.

High Resolution Transmission Electron Microscopy (HR-TEM) was recorded on an electron microscope JEM-2100, 200kV, JEOL. Scanning Electron Microscopy (SEM) and Energy dispersive X-ray spectrometry on SEM (SEM-EDX) were recorded on Zeiss Sigma 500VP FESEM instrument. Thermogravimetric (TG) and Differential Scanning Calorimetry (DSC) analysis were recorded for temperature range 0-500 °C at PERKIN ELMER, USA. Diamond TG/DTA model. Fourier Transform Infrared (FT-IR) Spectra were recorded on a Perkin-Elmer Spectrum One FTIR spectrometer. Inductively Coupled Plasma-Optical Emission Spectrometry (ICP-OES) was done on iCAP 7600 ICP-OES Duo model. Nuclear Magnetic

77

Resonance (NMR) spectra were recorded in Brukar Advance II, 400 MHz. The value of Chemical shifts were reported in ppm (δ-scale) relative to the internal standard TMS (0.00 ppm) using $CDCl_3$ as solvent.

## 4.2.2 Catalyst preparation

We prepared the PAFR solid acid polymer resin according to reported procedure in literature[12] where 4-hydroxybenzenesulphonic acid (phenolsulfonic acid) undergoes condensation polymerization with 5 mol equivalent of formaldehyde in $H_2O$ at 120 °C for 6-7 hours (Scheme 4.4).
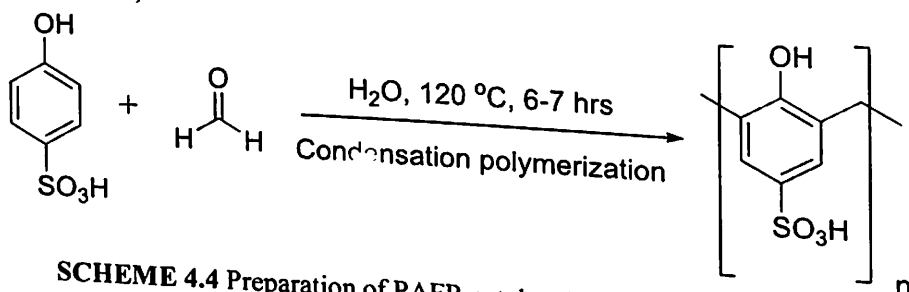


**SCHEME 4.4** Preparation of PAFR catalyst by condensative method.

The reaction mixture was then gradually cooled to 25 °C over 12 h which resulted a pale brownish gel. After being dried under reduced pressure in vacuum oven at 60 °C for 12 hrs, the gel became a reddish brown, hardly soluble solid giving 70% yield. The C to S ratio was obtained as 17.2:1 from EDX analysis which deduced that the phenolsulfonic acid moiety/ phenol moiety ratio is about 1:3.

## 4.2.3 Typical Procedure for Tetrahydropyranylation of alcohol using PAFR catalyst

As a pilot protocol, a mixture of 1-octanol (0.130 g, 1 mmol), DHP (0.084 g, 2 mmol) and PAFR catalyst (0.025 g, 7.48 mol%) was mechanically stirred in a small reaction vessel at room temperature (RT) under solvent-free (SolFc) condition. The progress of the reaction was monitored by thin layer chromatography (TLC). After completion of the reaction as indicated by TLC, the catalyst was separated by simple filtration and the reaction mixture was extracted with ethyl acetate, The extracted compound thus obtained was then charged into a short silica gel chromatography column using hexane/ethyl acetate (9:1 ratio) as eluent to afford 98% of isolated yield of desired product.
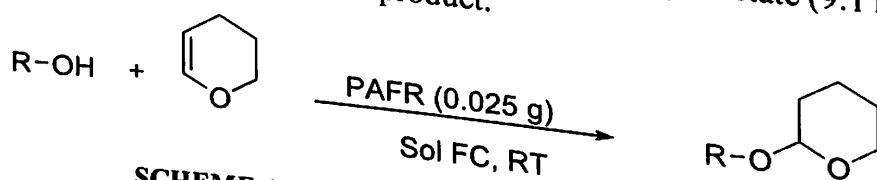


**SCHEME 4.5** THPRN reaction using PAFR catalyst

## 4.2.4 Depyranylation (deprotection) of alcohols using PAFR catalyst

2-(octyloxy)tetrahydro-2H-pyran, the THP ether of 1-Octanol, (0.198 g, 1 mmol) and PAFR catalyst (0.025 g, 7.48 mol%) were stirred in methanol (0.5 mL) in a mechanical stirrer for 1 hour. The cleavage of ether and regeneration of the corresponding alcohol was monitored by checking TLC. After complete generation of the alcohol, the catalyst was separated by filtration and the residue was eluted through a short column of silica gel to afford 97% of the isolated alcohol as product.



Byproduct

SCHEME 4.6 DPRN reaction using PAFR catalyst
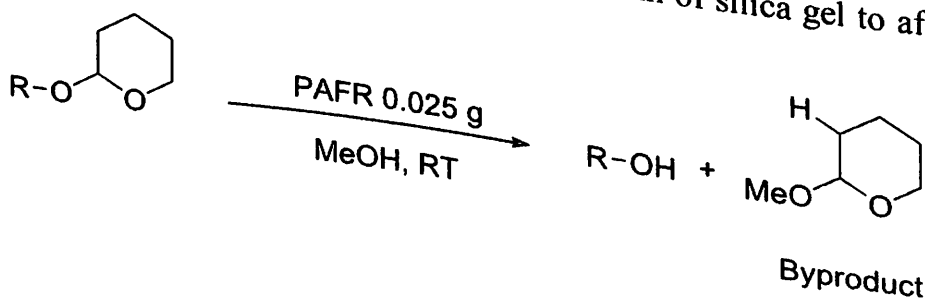
## 4.2.5 Catalyst recyclability test

The recyclability of mesoporous catalyst was investigated with consecutive tetrahydropyranylation reactions reusing the catalyst for multiple times. After each catalytic run, the catalyst was separated by simple filtration and washed it with methanol followed by hexane and finally with chloroform. The mentioned process was repeated twice or thrice followed by subsequent drying of the catalyst at 60 °C for 12 hour in oven and was then used for the next catalytic cycle. The recovered catalyst was further investigated by IR, SEM-EDX analysis.

## 4.2.6 Hot-filtration method

To verify the heterogeneity of the polymer catalyst, hot filtration method was employed. For this, after stirring the reaction mixture of protection of alcohol for 15 minutes (yield was 30% at that time), the catalyst was separated by centrifugation. The reaction mixture was then decanted and was continued to stir for another 6 hours. The further progress of the reaction was monitored with TLC and finally filtrate was analyzed by ICP-OES test.

# 4.3 Result and discussion

## 4.3.1 Catalyst characterization

At the onset, FT-IR spectroscopic analysis of the PAFR catalyst was carried out to identify the different functional groups present in the catalyst. The IR spectra in Fig. 4.1 shows distinguished peak at 1034 cm$^{-1}$ which is the characteristic absorption peak for symmetric S=O stretching due to the introduction of -SO$_3$H group in the polymer. The two peaks near 594 cm-1 and 3438 cm$^{-1}$ can be attributed to the bending and stretching vibrations of −OH group respectively while absorption at 1224 cm$^{-1}$ suggests aromatic −OH stretching. Another two absorption bands at 1474 cm$^{-1}$ and 1650 cm$^{-1}$ can be assigned to the C=C stretching of the benzene ring of the polymer.[39]
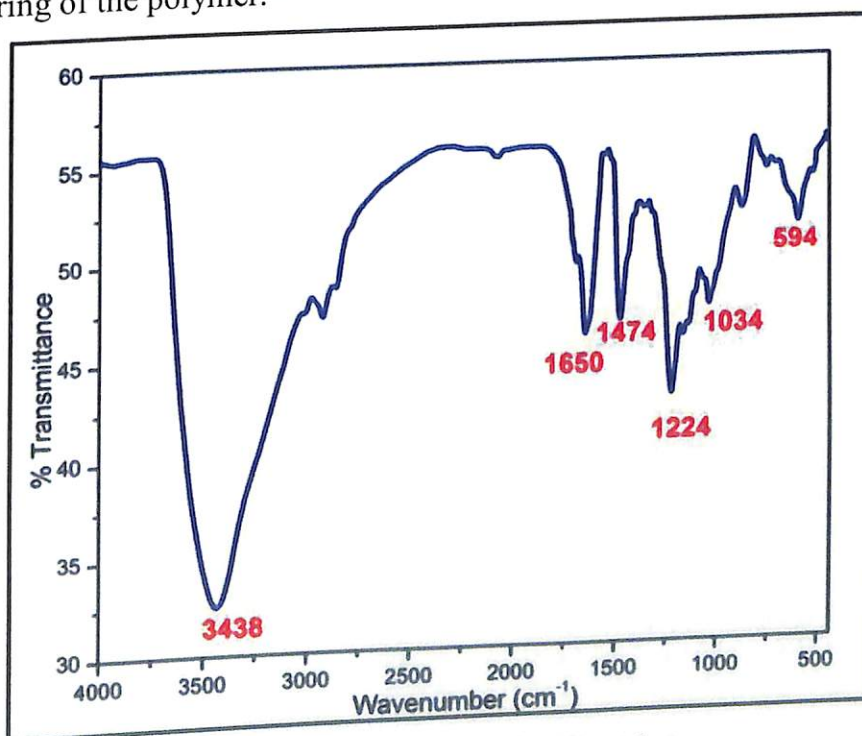


FIGURE 4.1 IR spectra of PAFR catalyst
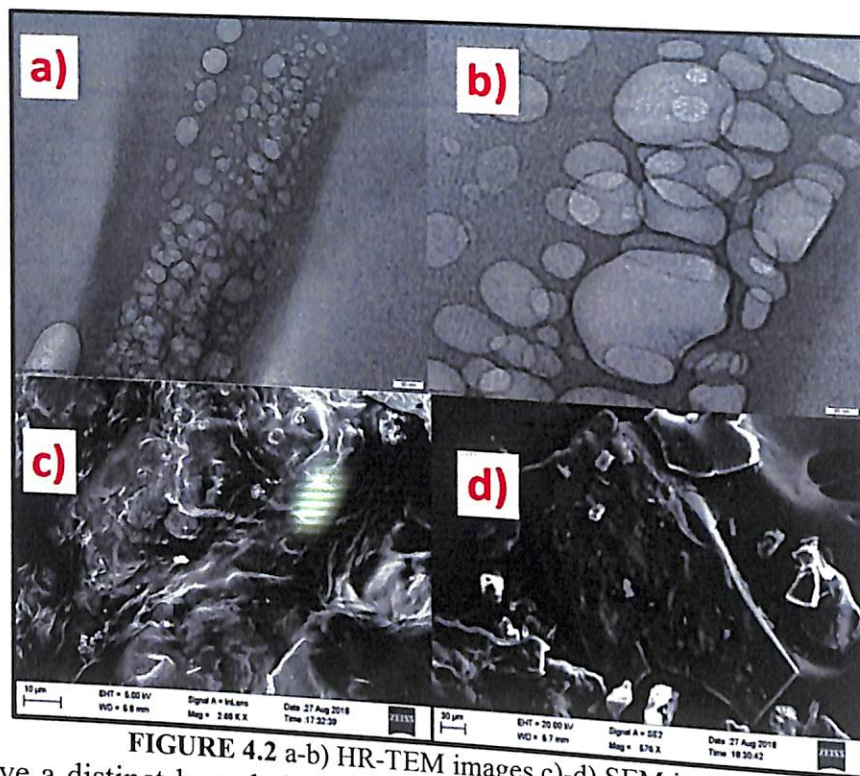
**FIGURE 4.2 a-b) HR-TEM images c)-d) SEM image**

To have a distinct knowledge about the morphology of the polymer catalyst, HR-TEM and SEM analysis were performed. HR-TEM images (Fig. 4.2a-b) revealed botryoidal structure of the catalyst and clearly showed its mesoporosity in the range 20-100 nm. SEM images (Fig. 4.2c-d) also exposed the mesoporous surface of the PAFR polymer catalyst. Results from SEM-EDX in Fig. 4.3 displayed the presence of sulfur in its structure confirming anchoring of $-SO_3H$ moiety to the polymer. The wt % of C, O and S were obtained as 68.98%, 27.01% and 4.01%.
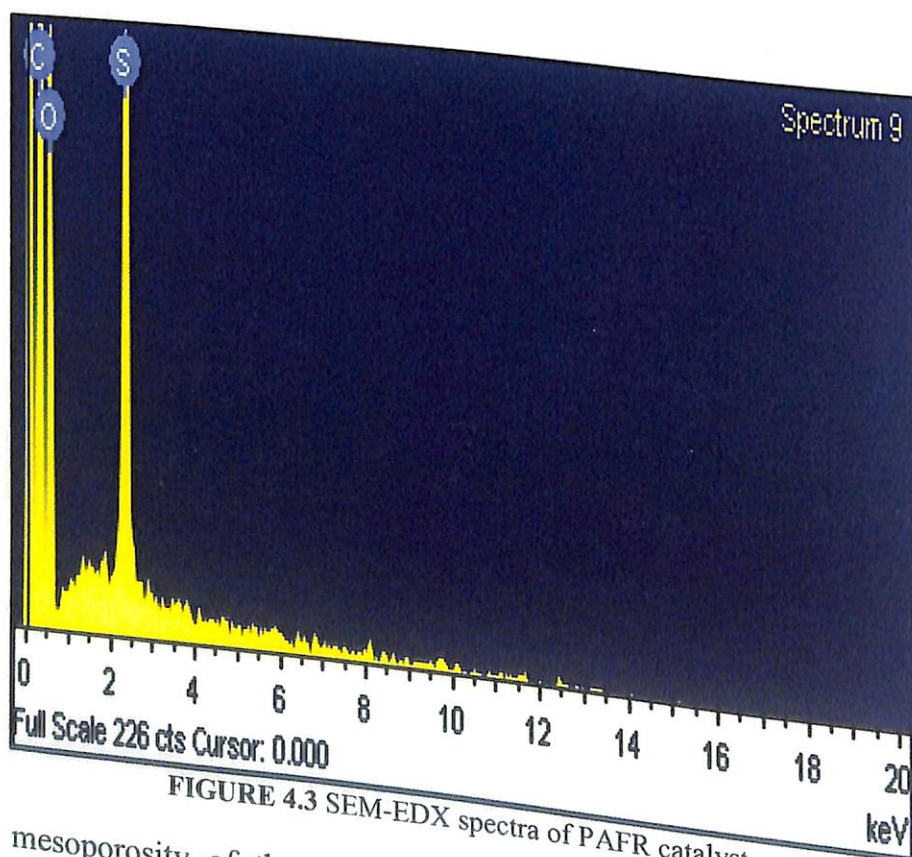


**FIGURE 4.3 SEM-EDX spectra of PAFR catalyst**

The mesoporosity of the catalyst was confirmed by $N_2$ adsorption-desorption analysis by BET model.[15] The adsorption-desorption isotherm (Fig. 4.4) showed

characteristic features of type IV hysteresis loop referring capillary condensation in mesopores. The surface area was obtained as 90.44 m²/g with average pore size of 5.23 nm. The pore-size distribution curve (Fig. 4.4 (inset)) shows uniform sizes of the porous structures.
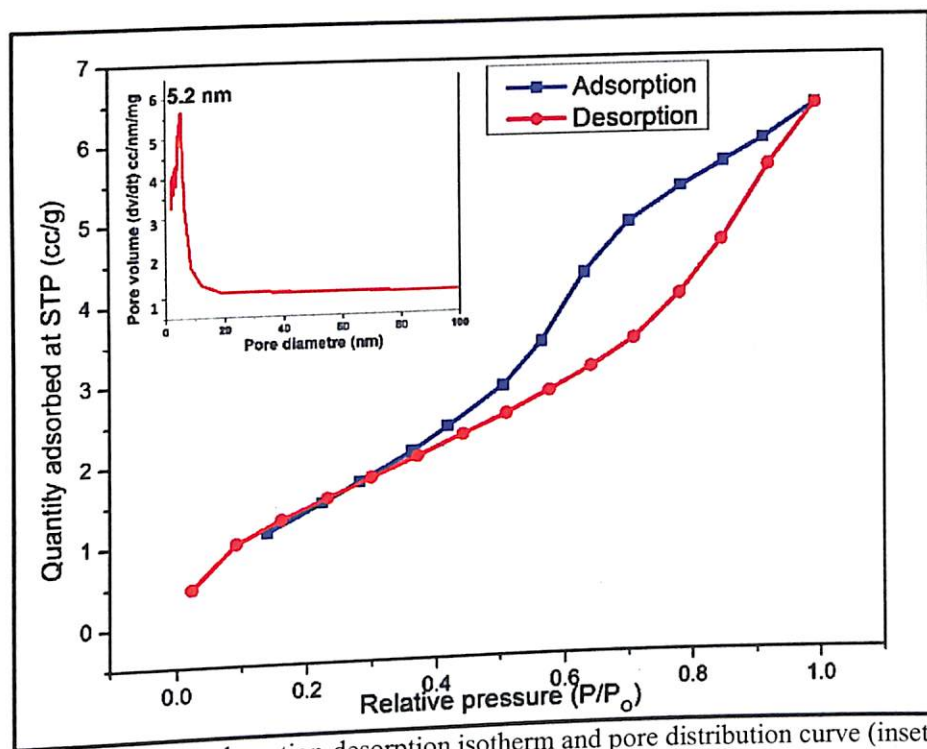


FIGURE 4.4 $N_2$ adsorption-desorption isotherm and pore distribution curve (inset)
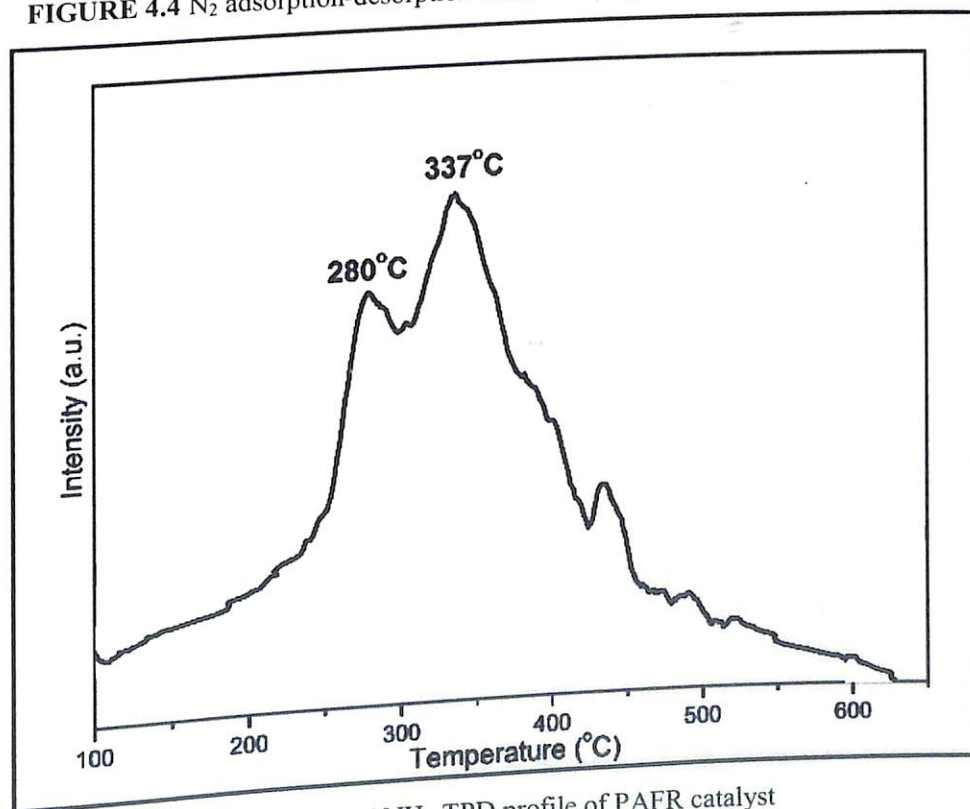


FIGURE 4.5 NH₃-TPD profile of PAFR catalyst

Results of NH₃-TPD (Temperature programmed desorption) test of PAFR catalyst exhibited ammonia desorption peaks at 280°C and 337°C suggesting Brønsted acid sites[40] in the catalyst surface offering moderate acidity having acid sites of 596 µmol g⁻¹ (Fig.4.5). Brønsted acid sites surrounded by hydrophobic organic moieties are found to be preferable condition for conducting in-water organic reactions in forward direction. It can be

anticipated that the hydrophobic 'tail' of the substrate alcohol lies parallel along the hydrophobic surface of the catalyst preventing adsorption of water over the active sites (which restricts its access with the substrate molecules) and thereby helps to retain its catalytic activity without interacting with by-product water.

The thermal stability of the catalyst was enquired by TGA and DSC analysis. The representative curve for TGA in Fig. 4.6 shows total three humps at 60-150°C, 200-300°C and 450-500°C. The weight loss near 100 °C can be associated with the release of physically adsorbed moisture on the surface of the polymer. The mass loss in the range 200- 300°C may be due to the decomposition of sulfonic acid group while in the third step, mass loss above 400°C is possibly attributable to the breakdown of polymeric backbone. The endothermic peaks appeared in the DSC plot also compliments the three steps of mass loss of the polymer as suggested by the TGA plot.[42]
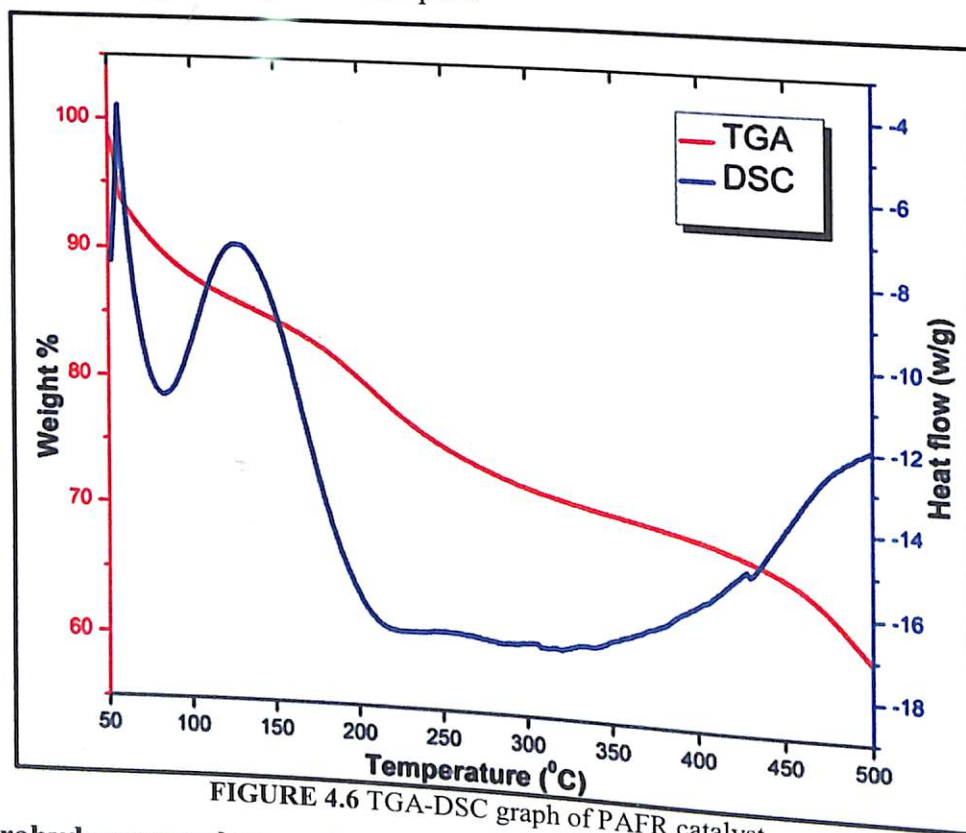


FIGURE 4.6 TGA-DSC graph of PAFR catalyst.

## 4.3.2 Tetrahydropyranylation of alcohols

After preparation and characterization of the catalyst, we proceeded for testing its catalytic activity against tetrahydropyranylation of alcohols and phenols as well. We, at the outset, took an equimolar mixture of 1-octanol and DHP and stirred it with 20 mg of PAFR catalyst in solvent-free condition at room temperature as a pilot protocol for the reaction. The activity and feasibility of the reaction was monitored by TLC. To our pleasure, the reaction was observed to progress indicating formation of tetrahydropyranylated ether in TLC and completion of the reaction was obtained after 3 hour of the reaction.
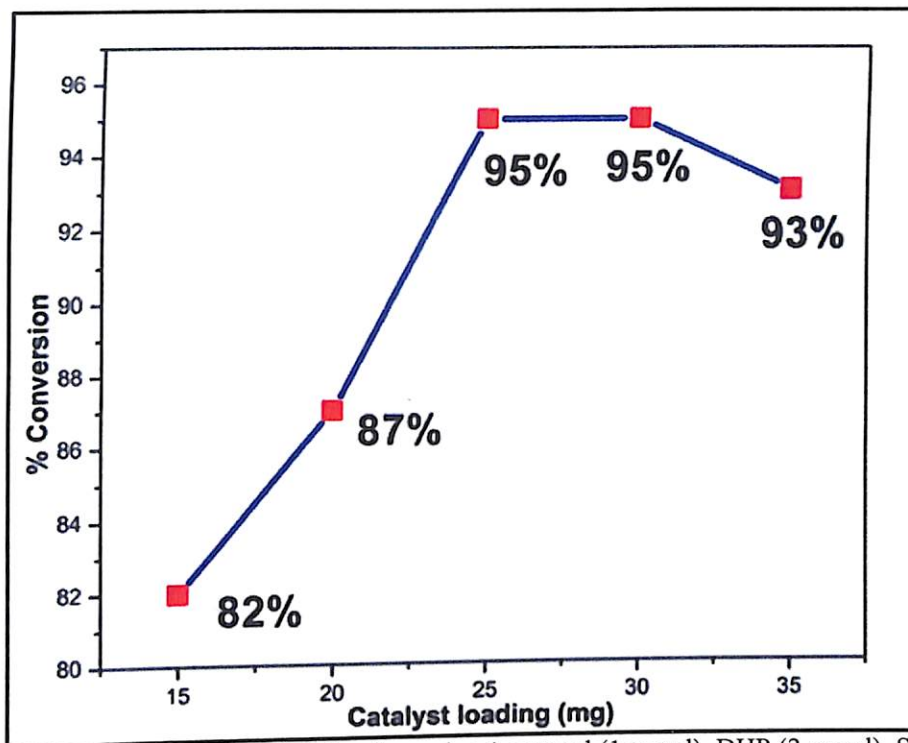
FIGURE 4.7 Optimization of catalyst loading using 1-octanol (1 mmol), DHP (2 mmol), SolFC, RT.
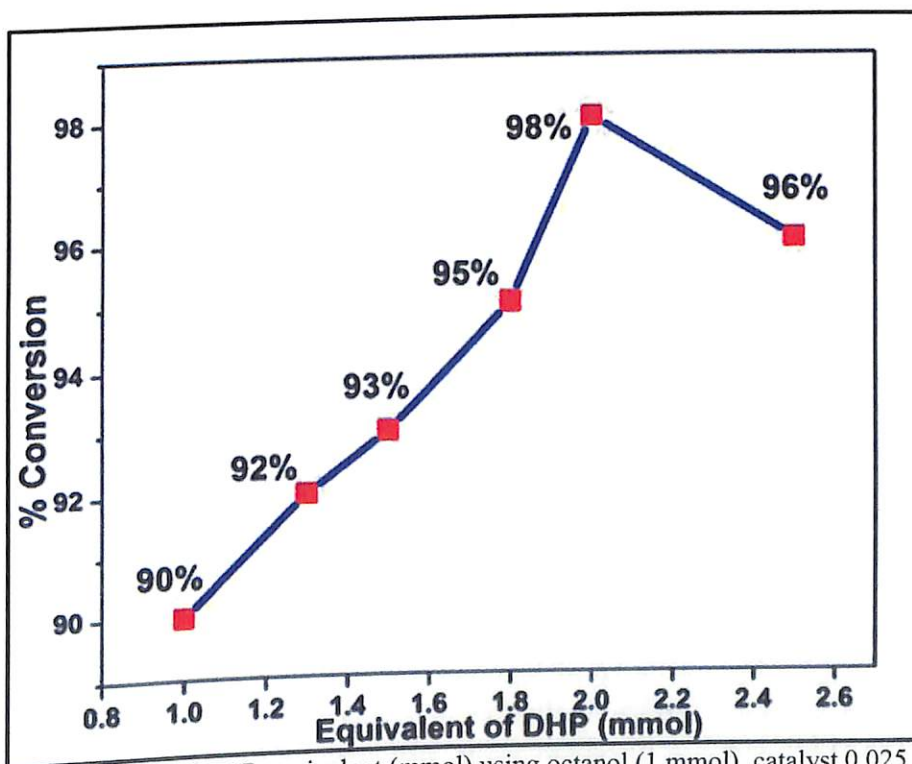


FIGURE 4.8 Optimization of DHP equivalent (mmol) using octanol (1 mmol), catalyst 0.025 g, SolFC, RT.

With this rough idea and in an attempt to find an optimum amount of catalyst for achieving maximum yield in minimum time, we checked feasibility of the reaction at the same conditions but with different amount of catalyst loading i.e. 0.015 g, 0.025 g, 0.030 and 0.035 g. It was found that the reaction resulted best yield in shortest time with 0.025 g (7.48 mol%) of catalyst (Fig. 4.7). Further increase in the catalyst amount had no any significant effect on the yield. The product yield and conversion time were developed by optimizing the appropriate amount of DHP which was obtained to be 2 equivalent of the alcohol (Fig. 4.8).
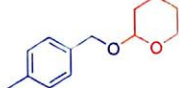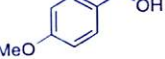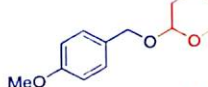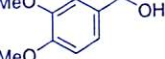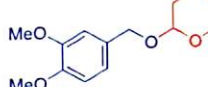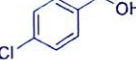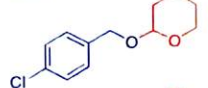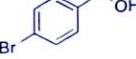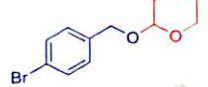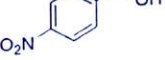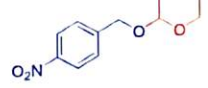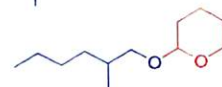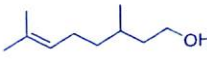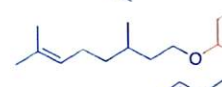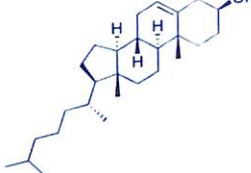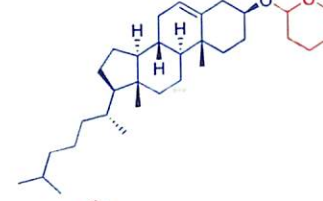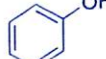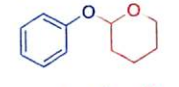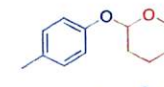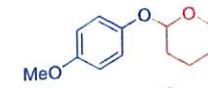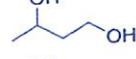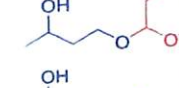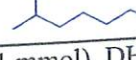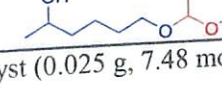
| Sl no | Catalyst | Conversion | Reaction condition | Reference |
|---|---|---|---|---|
| 1 | $Fe(ClO_4)_3$ | 75-98% | $Et_2O$, RT, 60-180 min | 28 |
| 2 | $SO_3H\text{-}SiO_2$ | 40-99% | $CH_2Cl_2$, RT, 15-100 mins | 24 |
| 3 | $AlCl_3.6H_2O$ | 74-98% | MeOH, 30-80°C, 30-180 mins | 21 |
| 4 | $Al(OTf)_3$ | 65-100% | $CH_2Cl_2$, RT, 45 min- 24 hr | 18 |
| 5 | Polyaniline salts | 38-75% | SolFc, 50 °C, 8 hr | 25 |
| 6 | Dowex 50WX4-100 | 75-98% | $CH_2Cl_2$, RT, 7 min- 24 hr | 31 |
| 7 | Polystyrene-supported $AlCl_3$ | 89-97% | $CH_2Cl_2$, RT, 7 min- 24 hr | 19 |
| 8 | Ersorb-4 (Zeolite) | 44-58% | Toluene, RT, 30-240 min | 34 |
| 9 | Brønsted–Lewis acidic Ionic Liquid | 70-97% (Phenol 0%) | SolFc, RT, 40-90 min | 43 |
| 10 | PAFR | 86-98% | SolFC, RT, 60-180 min | Present work |

We also compared the efficiency of the present catalyst with other reported methodologies for tet hydropyranylation of alcohols. The results are displayed in the Table 4.1. It was observed that most of the protocol uses some environmentally unfriendly solvents, while yield of the solvent-free protocols (Table 4.1, Entry 5 and 9) are not up to the mark, also need vigorous condition for the reaction (Table 4.1, Entry 5). Homogeneous catalysts (Table 4.1, Entry 1 and 5), on the other hand, finds difficulty in separating the catalyst from reaction mixture which needs tedious workup. Several heterogeneous polymer and zeolite catalyst were found to be employed in this protection reaction (Table 4.1, Entry 6-8) but use of dichloromethane ($CH_2Cl_2$) and toluene as solvents in their method contradict their benign nature. Imidazole-based Brønsted–Lewis acidic Ionic Liquid (Table 4.1, Entry 9) was also reported as a recyclable catalyst under solvent-free condition for this conversion but although the protocol selectively protected aliphatic and benzylic alcohols but remained ineffective in case of phenols. Apparently the present protocol for tetrahydropyranylation of alcohols and phenols using hydrophobic PAFR resin catalyst was appeared to be beneficial over most of the reported protocols in literature.

With the optimized conditions in hand, we investigated the scope of the polymeric PAFR acid catalyst for a large number of primary, secondary, tertiary, allylic and benzylic alcohols and phenols bearing various substituents ranging from electron-donating to electron-withdrawing groups at different position. The outcome is depicted in Table 4.2 where it can be observed that the alcohols were smoothly converted to the desired products in moderate to excellent yield. To our surprise, the catalytic system is equally effective in phenolic compounds (Table 4.2, Entry 14-16) also, which make the protocol extremely generalized. Some differences were encountered with different substrates in the time taken to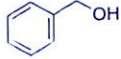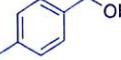 achieve completion of reaction. For instance, tetrahydropyranylation of aliphatic alcohol (Table 4.2, Entry 8-11) and those of benzylic alcohol with electron-donating substituent (Table 4.2, Entry 1-3) at one of its position in benzene ring was reported to be highly reactive giving corresponding ether in excellent yield. However, benzylic group with two electron-donating substituent at the same time (Table 4.2, Entry 4) was found to be quite slow as compared to aforementioned reactions. In contrast presence of electron-withdrawing substituent (Table 4.2, Entry 5-7) was observed to slow down the reaction. Further, the secondary hydroxyl group of Cholesterol (Table 4.2, Entry 12) and tertiary hydroxyl group of adamantanol (Table 4.2, Entry 13) were smoothly converted to corresponding desired products under the stated reaction condition without affecting the olefinic group of the substrate, which was observed in case of citronellol also (Table 4.2, Entry 11). This not only shows mild nature of the catalyst, but also exposes supreme chemoselectivity of the protocol.

**TABLE 4.2:** Scope of Tetrahydropyranylation of Alcohols and Phenol using PAFR catalyst[a]

R–OH  +  (DHP)  →[PSAF (0.025 g) / Sol FC, RT]→  R–O-(THP)

| Entry | Alcohol | Product | Time (hrs) | Yield[b] (%) |
|---|---|---|---|---|
| 1 | | | 1 | 95 |
| 2 | | | 1.10 | 97 |
| 3 | | | 1 | 98 |
| 4 | | | 2 | 94 |
| 5 | | | 1.15 | 97 |
| 6 | | | 1.15 | 97 |
| 7 | | | 2.5 | 95 |
| 8 | | | 1.30 | 98 |
| 9 | | | 1.10 | 96 |
| 10 | | | 1.20 | 97 |
| 11 | | | 1.30 | 97 |
| 12 | | | 3 | 97 |
| 13 | | | 1.45 | 96 |
| 14 | | | 1.45 | 95 |
| 15 | | | 1.35 | 98 |
| 16 | | | 1.30 | 98 |
| 17 | | | 1.30 | 86 |
| 18 | | | 1.35 | 87 |

[a]Alcohol (1 mmol), DHP (2 mmol), catalyst (0.025 g, 7.48 mol%), SolFC, room temperature; [b]Isolated yield

85
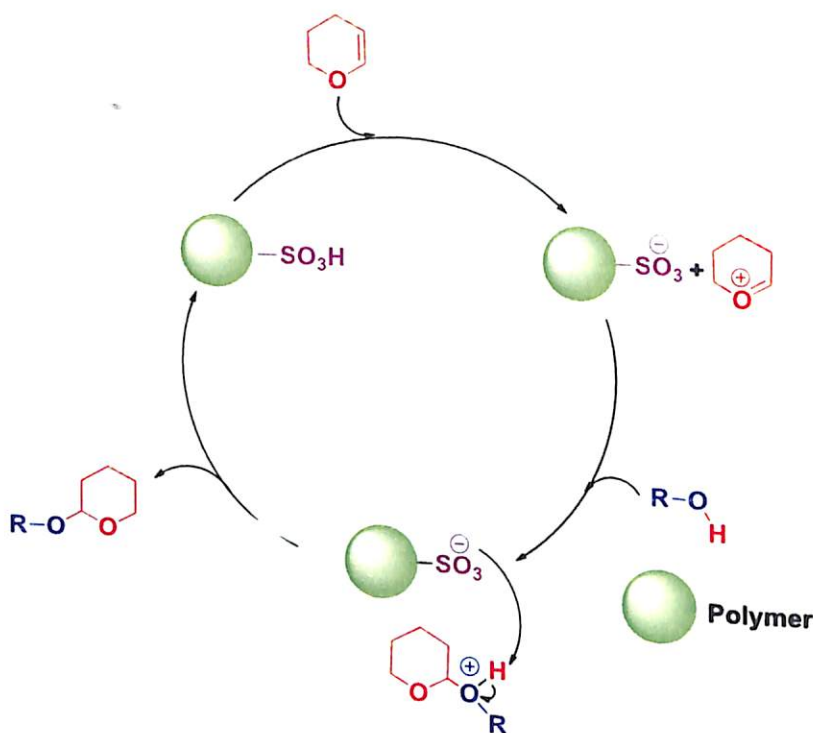
**SCHEME 4.7** Probable mechanism of tetrahydropyranylation using PAFR catalyst.

To study the selectivity between primary and secondary alcohols, we tried competitive reaction with 1,3-butandiol. Interestingly we observed that the terminal (primary) hydroxyl groups were protected selectively leading to exclusive formation of the corresponding ether (Table 4.2, entry 17). The structure of the product was confirmed by $^{13}C$ DEPT-135 NMR study (Fig. 4.26), wherein the presence of the tertiary carbon at δ 101.88 ppm and shifting of the adjacent methylene carbon to δ 66.56 ppm indicated the attachment of the DHP moiety to the primary hydroxyl group.

The probable mechanism of tetrahydropyranylation of alcohols using PAFR catalyst is depicted in Scheme 4.7.

## 4.3.3 Deprotection of THP ether using PAFR catalyst

In order to establish the regenerative potential of the protocol, the capability of PAFR catalyst to cleave the THP group was also investigated. For this, few drops of methanol was introduced to the reaction. We observed that addition of methanol served as a deprotecting agent to obtain the alcohols from THP ethers.

Interestingly variety of THP ethers were easily deprotected by stirring with 0.025 g (7.48 mol%) PAFR catalyst in 1 mL methanol within 40-60 minutes. The method afforded the respective free alcohol products with excellent yield. (Table 4.3) without the cleavage of functionalities present in the alcohol molecule other than the protected group. As selective cleavage under mild condition is one of the important criteria for an ideal protection methodology[44], therefore the present method shows great applicability in the protection of polyfunctional molecules.

The Mechanism proposed for deprotection of alcohols using PAFR catalyst is shown in Scheme 4.8.

**TABLE 4.3:** Deprotection of THP ethers using PAFR catalyst[a]
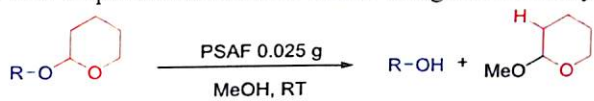


| Entry | THP ether | Deprotected product | Time (min) | Yield[b] (%) |
|-------|-----------|---------------------|------------|--------------|
| 1 | | | 55 | 97 |
| 2 | | | 60 | 95 |
| 3 | | | 50 | 96 |
| 4 | | | 45 | 97 |
| 5 | | | 55 | 94 |
| 6 | | | 40 | 92 |
| 7 | | | 40 | 96 |

[a]THP ether (1 mmol), catalyst (0.025 g, 7.48 mol%), methanol (1 mL), room temperature; [b]Isolated yield
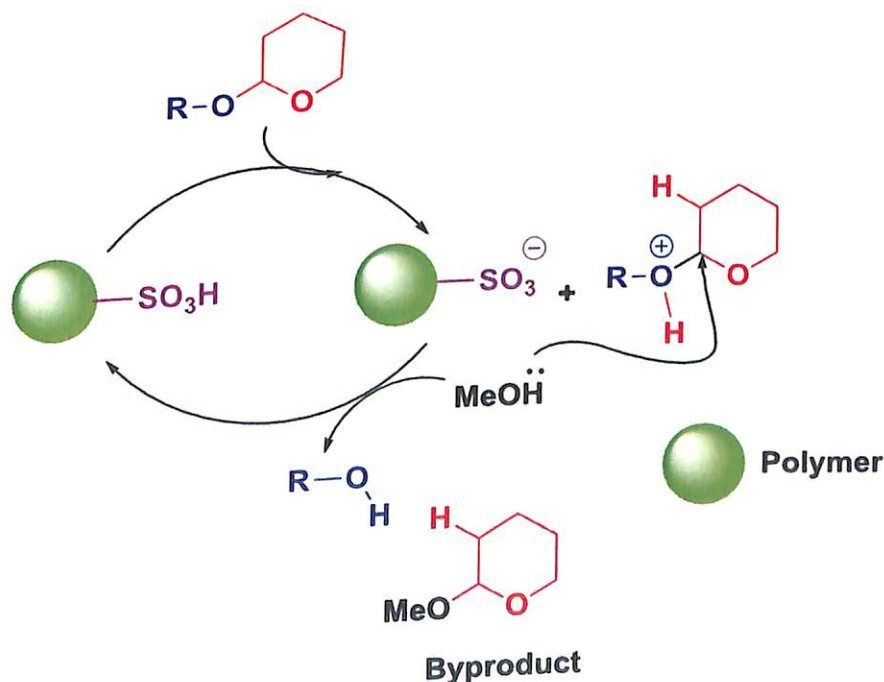


**SCHEME 4.8** Proposed mechanism for depyranylation of THP ethers using PAFR catalyst.

## 4.3.4 Recyclability test of catalyst

The reusability of the catalyst was also investigated by carrying out successive protection reaction of alcohol substrates. After each run, the catalyst was filtered and washed with hexane and chloroform and dried for the next catalytic run. The results of five catalytic

recycling runs are depicted in Figure 8. It clearly shows that the efficiency of the catalyst has not deteriorated much even after the tenth cycle which undoubtedly reveals the excellent recoverability of the catalyst.
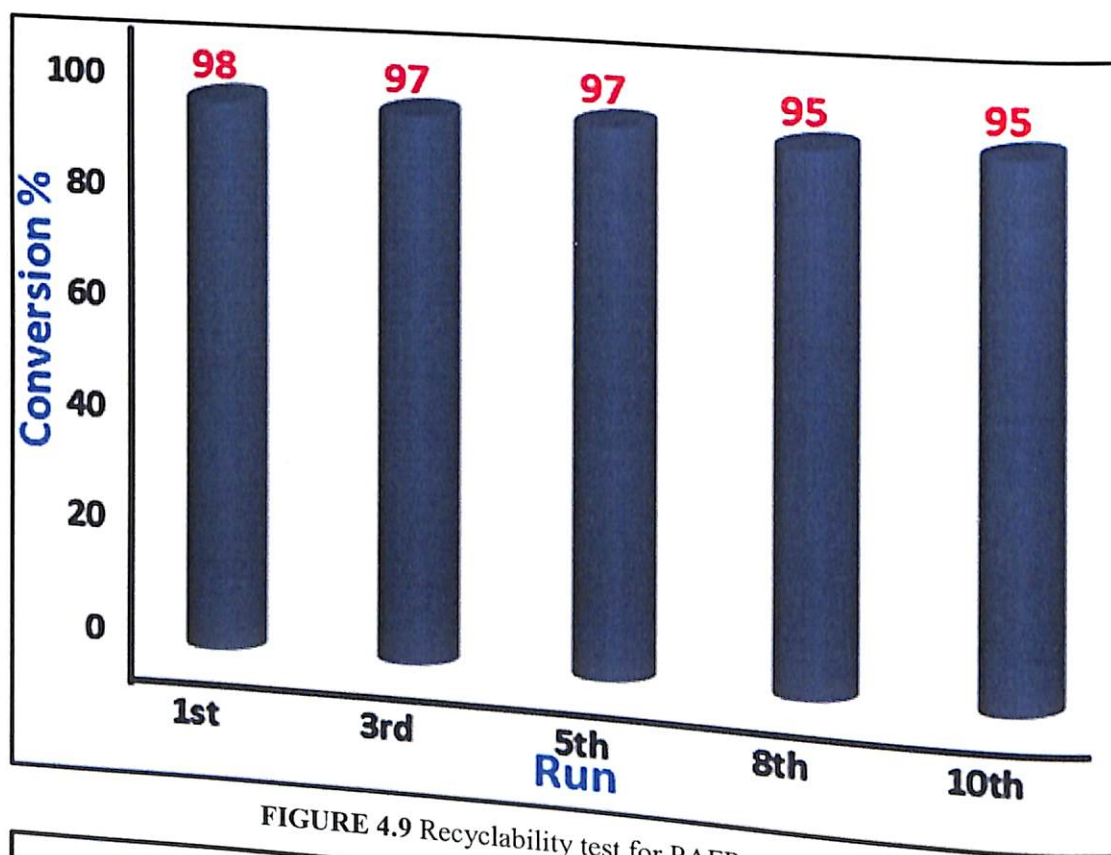


FIGURE 4.9 Recyclability test for PAFR catalyst
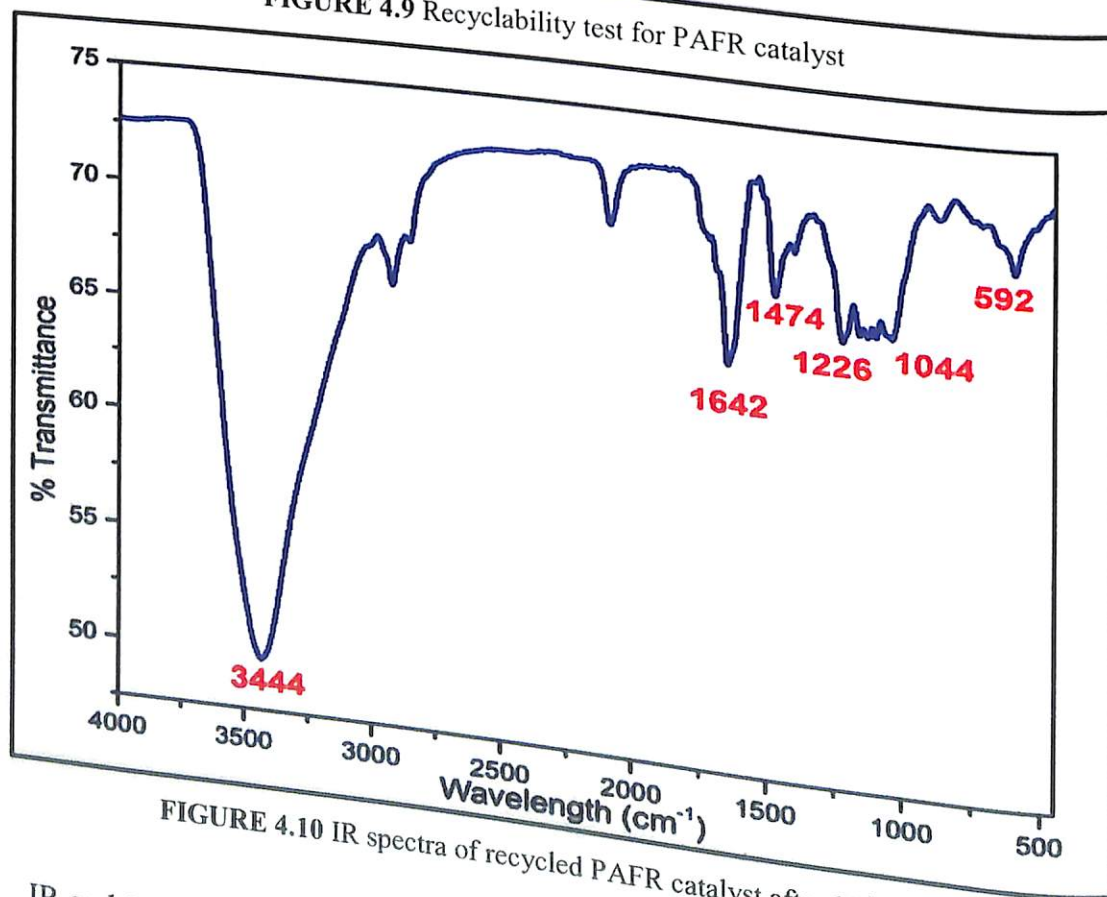


FIGURE 4.10 IR spectra of recycled PAFR catalyst after 10th cycle

IR and SEM-EDX analysis of the recovered catalyst after 10th catalytic cycles were also investigated to check any possible depreciation or change in its composition. To our

delight, the IR spectrum of the recovered catalyst gave similar peaks as in the spectrum of fresh catalyst (Fig. 4.10). Nevertheless, the morphology of the recovered catalyst as observed in its SEM image (Fig. Fig. 4.11a) is almost similar with the fresh one. The EDX analysis (Fig. 4.11b) revealed wt% of C, O and S as 67.71%, 28.70%, 3.59% respectively. A slight decrease in the weight % of S from 4.01% to 3.59% in the recycled catalyst can be attributed to its little leaching of $SO_3H$ group from the catalyst surface during washing.
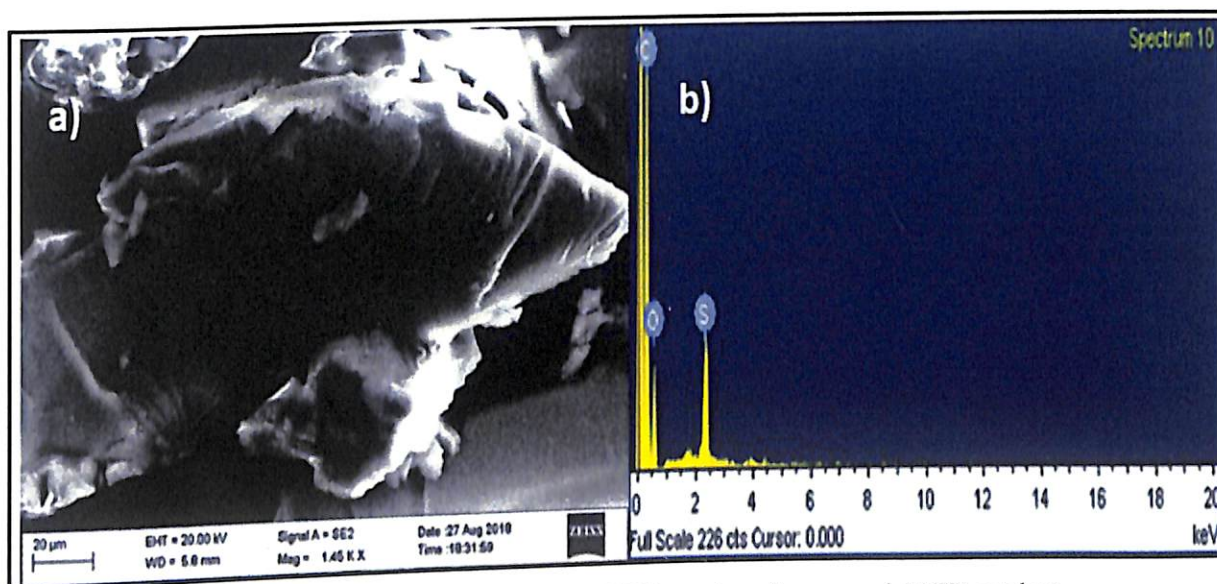


FIGURE 4.11 a) SEM image and b) EDX spectra of recovered PAFR catalyst

## 4.3.5 Hot filtration method

The heterogeneous nature of the PAFR catalyst was examined by Sheldon's Hot filtration method to investigate possible leaching of active species of the catalyst to the reaction mixture. For this, the catalyst was separated from the reaction mixture after 15 minutes of the reaction and then the decanted reaction mixture was continued to stir for another 6 hours. But it was observed that the reaction did not progress at all during this time and also no trace of S was obtained in ICP analysis of the filtrate. This confirmed that no leaching of acid sites from the catalyst surface took place to the reaction medium and established the excellent heterogeneity of PAFR catalyst as well.

## 4.3.6 Spectroscopic data of synthesized compounds

**2-(benzyloxy)tetrahydro-2H-pyran (Table 4.2, entry 1)**

$^1$H-NMR (400 MHz, CDCl$_3$, TMS): δ 7.27-7.38 (m, 5H), 4.70-4.82 (m, 2H), 4.51(t, J=15Hz), 3.87-4.02 (m, 1H), 3.51-3.57 (m, 1H), 1.88-1.51(m, 6H); $^{13}$C-NMR (100 MHz, CDCl$_3$, TMS): δ 157.08, 129.39, 121.60, 116.48, 96.35, 77.26, 62.09, 30.43, 25.25, 18.86; IR (cm$^{-1}$) 2970, 1653, 1542, 1027, 892, 776; Elem. Anal. Calcd. for C$_{12}$H$_{16}$O$_2$: C 74.97, H 8.39, O 16.64; Found: C 74.95, H 8.38, O 16.67.

**2-(3,4-dimethoxybenzyloxy) tetrahydro-2H-pyran (Table 4.2, entry 4)**

$^1$H-NMR (400 MHz, CDCl$_3$, TMS): δ 7.02 (s, 1H), 6.91 (d, J=8.4Hz, 2H), 6.83 (d, J= 10.5 Hz, 1H), 4.74-4.68 (m, 2H), 4.45 (d, J= 12 Hz, 1H), 3.95-3.91 (m,1H), 3.89 (s, 3H), 3.87 (s, 3H), 3.56-3.52 (m, 1H), 1.88-1.26 (m, 6H); $^{13}$C-NMR (100 MHz, CDCl$_3$, TMS): 148.9, 148.5, 130.7, 120.52, 110.99, 110.93, 97.50, 68.76, 62.28, 55.83, 30.64, 25.35, 19.53 ; IR (cm$^{-1}$) 3089, 2968, 1663, 1563, 1053, 951; Elem. Anal. Calcd. for C$_{14}$H$_{20}$O$_4$: C 66.65, H 7.99, O 25.36; Found: C 66.65, H 7.97, O 25.38.

**2-(4-Chlorobenzyloxy)tetrahydro-2H-pyran (Table 4.2, entry 5)**

$^1$H-NMR (400 MHz, CDCl$_3$, TMS): δ 7.46 (d, J=5 Hz, 2H), 7.29 (d, J= 5 Hz, 2H), 4.96 (s, 2H), 4.76-4.46 (m, 1H), 3.88 (s, 1H), 3.52 (t, J= 7.5 Hz, 1H), 1.87-1.14 (m, 6H); $^{13}$C-NMR (100 MHz, CDCl$_3$, TMS): 128.49,

128.32, 118.33, 110.70, 94.67, 71.08, 62.97, 30.68, 29.69, 25.43, 19.76; IR (cm⁻¹) 3023, 2893, 1612, 1597, 1032, 992, 815; Elem. Anal. Calcd. for $C_{12}H_{15}O_2Cl$: C 63.58, H 6.67, O 14.11, Cl 15.64; Found: C, H, O.

## 2-(4-Bromobenzyloxy)tetrahydro-2H-pyran (Table 4.2, entry 6)

¹H-NMR (400 MHz, CDCl3, TMS): δ 7.42 (d, J= 10 Hz, 2H), 7.19 (d, J= 9.5 Hz, 2H), 4.71-4.66 (m, 2H), 4.41 (d, J= 15.5 Hz, 1H), 3.85 (t, J= 12.5 Hz, 1H), 3.51 (t, J= 7.5Hz, 1H), 1.84-1.51 (m, 6H). ¹³C-NMR (100 MHz, CDCl3, TMS): 137.42, 131.38, 129.36, 121.26, 97.69, 67.93, 61.99, 30.52, 25.47, 19.31; IR (cm⁻¹) 2931, 1678, 1572, 1038, 813, 648; Elem. Anal. Calcd. for $C_{12}H_{15}O_2Br$: C 53.16, H 5.58, O 11.80, Br 29.46; Found: C, H, O.

## 2-(Octyloxy)-tetrahydro-2H-pyran (Table 4.2, entry 8)

¹H-NMR (400 MHz, CDCl₃, TMS): δ 4.51 (t, J=5 Hz, 1H), 3.84-3.77 (m, 1H), 3.67-3.66 (m, 1H), 3.44-3.37 (m, 1H), 3.32-3.28 (m, 1H), 1.85-1.43 (m, 6H), 1.34-0.19 (m ,12H), 0.81 (t, J=10 Hz, 3H); ¹³C-NMR (100 MHz, CDCl₃, TMS): δ 98.80, 66.86, 61.58, 30.84, 29.78, 28.87, 28.76, 25.25, 24.52, 23.78, 21.66, 18.74, 13.08; IR (cm⁻¹) 3017, 2986, 1654, 1534, 1 ⁓7, 992, 865; Elem. Anal. Calcd. for $C_{13}H_{16}O_2$: C 72.85, H 12.23, O 14.92; Found: C 73.02, H 12.26, O 14.6⁻.

## 2-(8-Methylnonyloxy)-tetrahydro-2H-pyran (Table 4.2, entry 9)

¹H-NMR (400 MHz, CDCl₃, TMS): δ 4.50 (s, 1H), 3.79 (t, J= 10Hz, 1H), 3.65 (t, J=8, 1H), 3.43 (d, J=13 Hz, 1H), 3.39 (t, 7.8, 1H), 1.51-1.02 (m, 18H), 0.80-0.67 (m, 6H); ¹³C-NMR (100 MHz, CDCl₃, TMS): δ 98.64, 67.47, 61.97, 38.39, 33.28, 31.83, 30.10, 29.68, 26.62, 26.52, 25.46, 22.52, 19.36; IR (cm⁻¹) 2934, 1449, 1363, 1127, 1051; ; Elem. Anal. Calcd. for $C_{15}H_{20}O_2$: C 74.32, H 12.48, O 13.20; Found: C 74.32, H 12.52, O 13.30.

## 2-(3,7-Dimethyloct-6-enyloxy) tetrahydro-2H-pyran (Table 4.2, entry 11)

¹H-NMR (400 MHz, CDCl₃, TMS): 5.02 (t, J= 5.6 Hz, 1H), 4.49 (d, J= 4 Hz, 1H), 3.82-3.68 (m, 2H), 3.44-3.30 (m, 2H), 1.93-1.89 (m, 2H), 1.77-1.05 (m, 17H), 0.84-0.78 (m, 3H); ¹³C-NMR (100 MHz, CDCl₃, TMS): 130.02, 123.84, 97.81, 64.94, 61.23, 36.25, 29.79, 23.69, 24.45, 24.35, 18.55, 16.60; IR (cm⁻¹) 2945, 1509, 1246, 1142, 1019; Elem. Anal. Calcd. for $C_{15}H_{28}O_2$: C 74.95, H 11.75, O 13.31; Found: C 74.32, H 11.82, O 13.86.

## 3-(((3S, 8S, 9S, 10S, 13R, 14S, 17R)-10, 13-Dimethyl-17-( (R)-6-methylheptan-2-yl)-2, 3, 4, 7, 8, 10, 11, 12, 13, 14, 15, 16, 17-tetradecahydro-1H-cyclopenta[a]phenanthren-3-yl)oxy)tetrahydro-2H-pyran (Table 4.2, entry 12)

¹H-NMR (400 MHz, CDCl₃, TMS): δ 5.28 (t, J=5.6 Hz, 1H), 4.65 (s, 1H), 3.86-3.82 (m, 1H), 3.49-3.39 (m, 2H), 2.29 (s, 2H), 2.29 (d, J= 9 Hz, 2H), 1.95-0.79 (m, 42H), 0.79 (s, 3H), 0.60 (s, 3H); ¹³C-NMR (100 MHz, CDCl₃, TMS): δ 139.94, 120.53, 95.87, 76.20, 74.97, 61.85, 55.72, 55.10, 49.13, 41.28, 39.21, 38.48, 37.74, 38.48, 36.29, 35.15, 34.77, 30.88, 30.25, 28.66, 27.22, 26.97, 24.46, 23.26, 22.79, 21.81, 21.54, 20.02, 19.05, 18.36, 17.68, 10.82; IR (cm⁻¹) 3023, 2348, 1698, 1476, 1008, 637; Elem. Anal. Calcd. for $C_{32}H_{54}O_2$: C 81.64, H 11.56, O 6.80; Found: C 82.24, H 11.39, O 6.37.

## 2-(((3s, 5s, 7s)-Adamantan-1-yl)oxy) tetrahydro-2H-pyran (Table 4.2, entry 13)

¹H-NMR (400 MHz, CDCl₃, TMS): δ 4.84 (s,1H), 3.97 (t, J= 10.8 Hz, 2H), 3.45 (s, 1H), 2.13-0.71 (m, 12H); ¹³C-NMR (100 MHz, CDCl₃, TMS): δ 92.78, 76.71, 63.61, 45.33, 42.67, 41.75, 36.37, 36.05, 35.98, 32.61, 31.62, 30.78, 29.65, 25.42, 21.13; IR (cm⁻¹) 2913, 2338, 1478, 1502, 1019, 633; Elem. Anal. Calcd. for $C_{15}H_{24}O_2$: C 76.23, H 10.24, O 13.54; Found: C 75.98, H 10.33, O 13.69.

## 2-phenoxytetrahydro-2H-pyran (Table 4.2, entry 14)

¹H-NMR (400 MHz, CDCl₃, TMS): δ 7.30-7.26 (m, 2H), 7.06 (d, J= 5 Hz, 2H), 6.98 (t, J= 10 Hz, 1H), 5.43 (t, J= 5 Hz, 1H), 3.96- 3.90 (m, 1H), 3.63- 3.58 (m, 1H), 2.07-1.60 (m, 6H); ¹³C-NMR (100 MHz, CDCl₃, TMS): δ 157.08, 129.39, 121.60, 116.48, 96.35, 62.09, 30.08, 25.25, 18.86; IR (cm⁻¹) 2954, 1467, 1232, 947, 846; Elem. Anal. Calcd. for $C_{11}H_{14}O_2$: C 74.13, H 7.92, O 17.95; Found: C 74.30, H 7.86, O 17.84.

## 2-(p-Tolyloxy) )tetrahydro-2H-pyran (Table 4.2, entry 15)

¹H-NMR (400 MHz, CDCl₃, TMS): δ 7.08 (d, J= 8.4 Hz, 2H), 6.95 (d, J=8.4 Hz, 2H), 5.37 (t, J= 4Hz, 1H), 3.95-3.89 (m, 1H), 3.61-3.56 (m, 1H), 2.28 (s, 3H), 2.27-2.01 (m, 1H), 1.99-1.41 (m, 5H); ¹³C-NMR (100 MHz, CDCl₃, TMS): δ 154.47, 129.83, 116.65, 115.05, 96.54, 62.03, 30.56, 25.29, 20.53, 18.87; IR (cm⁻¹) 2939, 1498, 1213, 950, 824; Elem. Anal. Calcd. for $C_{12}H_{12}O_2$: C 74.97, H 8.39, O 16.64; Found: C 74.71, H 8.45, O 16.84.

## 4-((Tetrahydro-2H-pyran-2-yl)oxy)butan-2-ol (Table 4.2, entry 17)

$^1$H-NMR (400 MHz, CDCl$_3$, TMS): δ 4.57-4.51 (m, 1H), 4.09-4.06 (m, 1H), 3.86- 3.69 (m, 2H), 3.50-3.35 (m, 2H), 1.84-1.41 (m, 8H), 1.24-1.22 (m, 3H), 0.87 (s, 1H, -OH); $^{13}$C-NMR (100 MHz, CDCl$_3$, TMS): δ 101.8, 67.33, 66.47, 62.19, 34.89, 30.67, 25.33, 20.53; IR (cm$^{-1}$) 3189, 2936, 2874, 1379, 1028, 885; Elem. Anal. Calcd. for C$_{10}$H$_{20}$O$_2$: C 69.72, H 11.70, O 18.57; Found: C 69.54, H 11.78, O 18.68.

## 4.4 Conclusion

Protection (and deprotection) of the free hydroxyl group in a multifunctional alcohol substrate is one of the most frequently confronted synthetic strategies, in which ecofriendly and efficient catalytic approaches are highly desirable. We reported here a facile protocol to synthesize THP ethers by protection of variety of alcohols and phenols using catalytic amount of mesoporous Phenolsulfonic Acid-Formaldehyde Resin catalyst which resulted moderate to excellent yield at room temperature. The same catalyst was also effective for cleavage of THP ethers to obtain the free alcohols by easy deprotection method. PAFR was found to be superior to many commercially available solid acid catalyst in terms of yield and rate of reaction. Excellent heterogeneity as verified by hot filtration method is another notable feature of the catalyst. Our protocols showed excellent chemoselectivity in favor of the primary alcohols. In addition, phenols were also successfully protected using our method, which otherwise are difficult to achieve. The reaction was carried out at room temperature under solvent-free condition and the spent catalyst was reused at least 10 times which are of great significant from green chemistry perspective.

## References

1. Y. Zhang and S. N. Riduan, *Chem. Soc. Rev.* 2012, **41**, 2083–2094.
2. M. X. Tan, L. Gu, N. Li, J. Y. Ying and Y. Zhang, *Green Chem.* 2013, **15**, 1127-1132.
3. K. C. Nicolaou and S. A. Snyder, Classics in Total Synthesis II, Wiley-VCH: Weinheim, 2003, pp 594.
4. P. Kaur, J. T. Hupp and S. B. T. Nguyen, *ACS Catal.* 2011, **1**, 819–835.
5. J. Lu, P. H. Toy, *Chem. Rev.* 2009, **109**, 815–838.
6. M. Benaglia, A. Puglisi and F. Cozzi, *Chem. Rev.* 2003, **103**, 3401-3427.
7. D. R. Dreyer and C. W. Bielawski, *Chem. Sci.*, 2011, **2**, 1233-1240.
8. A. Gardziella, L. Pilato and A. Knop, Phenolic Resins, Chemistry, Applications, Standardization, Safety and Ecology. Springer: Heidelberg, NY, 2000; pp 1–560.
9. R. S. Myers, J. W. Eastes and F. J. Myers, *Ind. Eng. Chem.* 1941, **33**, 697-706.
10. A. Chakrabarti and M. M. Sharma, *React. Polym.* 1993, **20**, 1-45.
11. G. Gelbard, *Ind. Eng. Chem. Res.* 2005, **44**, 8468-8498.
12. S. H. Ali, A. Tarakmah, S. Q. Merchant and T. Al-Sahhaf, *Chem. Eng. Sci.* 2007, **62**, 3197–3217.
13. M. Minakawa, H. Baek, Y. M. A. Yamada, J. W. Han and Y. Uozumi, *Org Lett.* 2013, **15**, 5798-5801.
14. H. Baek, M. Minakawa, Y. M. A. Yamada, J. W. Han and Y. Uozumi, *Sci Rep.* 2016, **6**, 25925-25934.
15. I. B. Laskar, K. Rajkumari, R. Gupta and L. Rokhum, *Energy Fuels* 2018, **32**, 12567-12576.
16. P. P. Bora, K. Vanlaldinpuia, L. Rokhum and G. Bez, *Synth. Comm.* 2011, **41**, 2674-2683.
17. K. Vanlaldinpuia, H. A. Sema, L. Rokhum and G. Bez, *Chem Lett.* 2010, **39**, 228-229.
18. D. B. G. Williams, S. B. Simelane, M. Lawton and H. Kinfe, *Tetrahedron* 2010, **66**, 4573-4576.
19. B. Tamami and K. P. Borujeny, *Tetrahedron Lett.* 2004, **45**, 715-718.
20. B. Kumar, M. A. Aga, D. Mukherjee, S. S. Chimni and S. C. Taneja, *Tetrahedron Lett.* 2009, **50**, 6236–6240.
21. V. V. Namboodiri and R. S. Varma, *Tetrahedron Lett.* 2002, **43**, 1143–1146.
22. B. Kumar, M. A. Aga, A. Rouf, B. A. Shah and S. C. Taneja, *RSC Adv.* 2014, **4**, 21121-21130.
23. J. H. V. Boom and J. D. M. Herscheid, *Synthesis* 1973, **3**, 169-170.
24. K. I. Shimizu, E. T. Hayashi, T. Hatamachi, T. Kodamab and Y. Kitayama, *Tetrahedron Lett.* 2004, **45**, 5135–5138.
25. S. Palaniappan, M. S. Ram and C. A. Amarnath, *Green Chem.*, 2002, **4**, 369–371.

26. C. E. Yeom, Y. J. Shin and B. M. Kim, *Bull. Korean Chem. Soc.* 2007, **28**, 103-107.
27. H. M. S. Kumar, B. V. S. Reddy, E. J. Reddy and J. S. Yadav, *Chem. Lett.* 1999, **28**, 857-858.
28. M. M. Heravi, F. K. Behbahani, H. A. Oskooie and R. H. Shoar, *Tetrahedron Lett.* 2005, **46**, 2543–2545.
29. S. A. Taghavi, M. Moghadam, I. M. Baltork, S. Tangestaninejad, V. Mirkhani and A. R. Khosropour, *C. R. Chimie* 2011, **14**, 1095–1102.
30. M. Moghadama, S. Tangestaninejada, V. Mirkhania, I. M. Baltorka and S. Gharaati, *J. Mol. Catal. A: Chem.* 2011, **337**, 95–101.
31. P. S. Poon, A. K. Banerjee, L. Bedoya, M. S. Laya, E. V. Cabrera and K. M. Albornoz, *Synth. Com.* 2009, **39**, 3369-3377.
32. A. Bongini, G. Cardillo, M. Orena and S. Sandri, *Synthesis* 1979, 618–620.
33. G. A. Olah, A. Husain and B. P. Sing, *Synthesis* 1983, 892–895.
34. A. Hegedüs, I. Vígh and   Hell, *Synth. Com.* 2004, **34**, 4145–4152.
35. G. Pathak and L. Rokhum, *ACS Comb. Sci.* 2015, **17**, 483-487.
36. D. Das, G. Pathak and L. Rokhum, *RSC Adv.* 2016, **6**, 104154-104163.
37. K. Rajkumari, J. Kalita, D. Das and L. Rokhum, *RSC Adv.* 2017, **7**, 56559-56565.
38. R. A. Sheldon, *Green Chem.* 2017, **19**, 18-43.
39. W. Zhou, M. Yoshino, H. Kita and K. I. Okamoto, *Ind. Eng. Chem. Res.* 2001, **40**, 4801-4807.
40. B. Mallesham, P. Sudarsanam, and B. M. Reddy, *Ind. Eng. Chem. Res.*, 2014, **53**, 18775-18785.
41. K. Stawicka, A. E. Díaz-Álvarez, V. C. Casilda, M. Trejda, M. A. Bañares and Maria Ziolek, *J. Phys. Chem. C* 2016, **120**, 16699-16711.
42. G. Fan, C. Liao, T. Fang, L. Shanshan and S. Guangsen, *Carbohydr. Polym.* 2014, **112**, 203-209.
43. N. Azizi, M. A. Senejani and F. Abbasi, *Tetrahedron Lett.* 2016, **57**, 5009–5011.
44. M. Schelhaas and H. Waldmann, *Angew. Chem. Int. Ed. Engl.* 1996, **35**, 2056-2083.
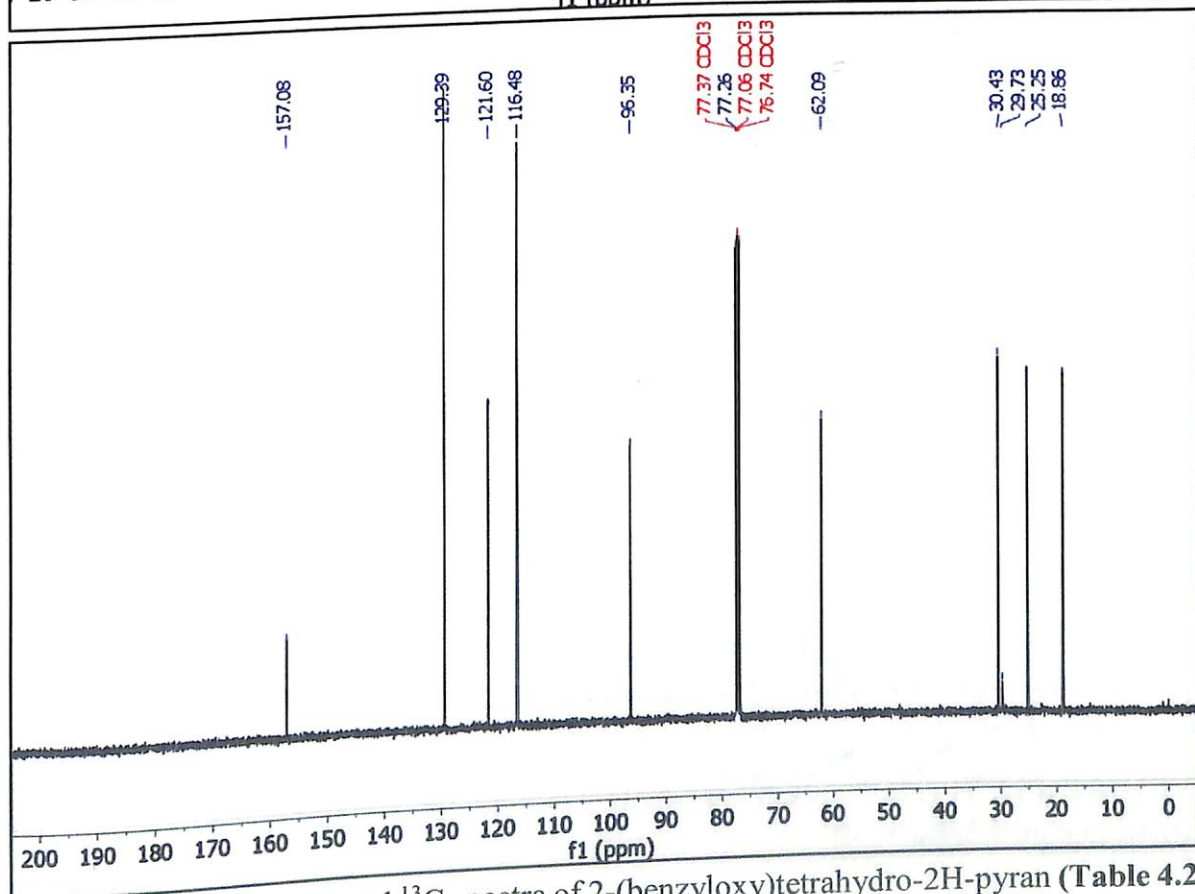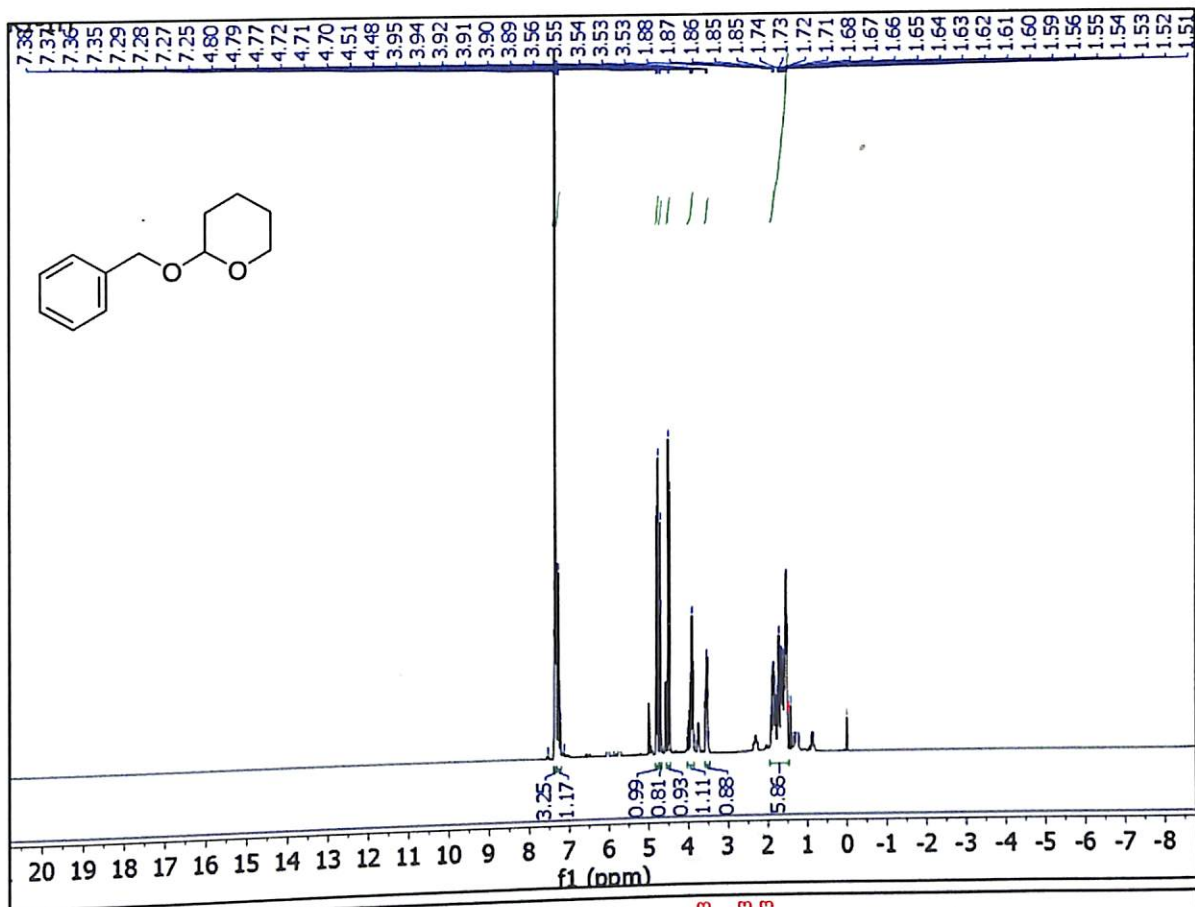
FIGURE 4.12 $^1$H NMR and $^{13}$C spectra of 2-(benzyloxy)tetrahydro-2H-pyran (Table 4.2, Entry 1)
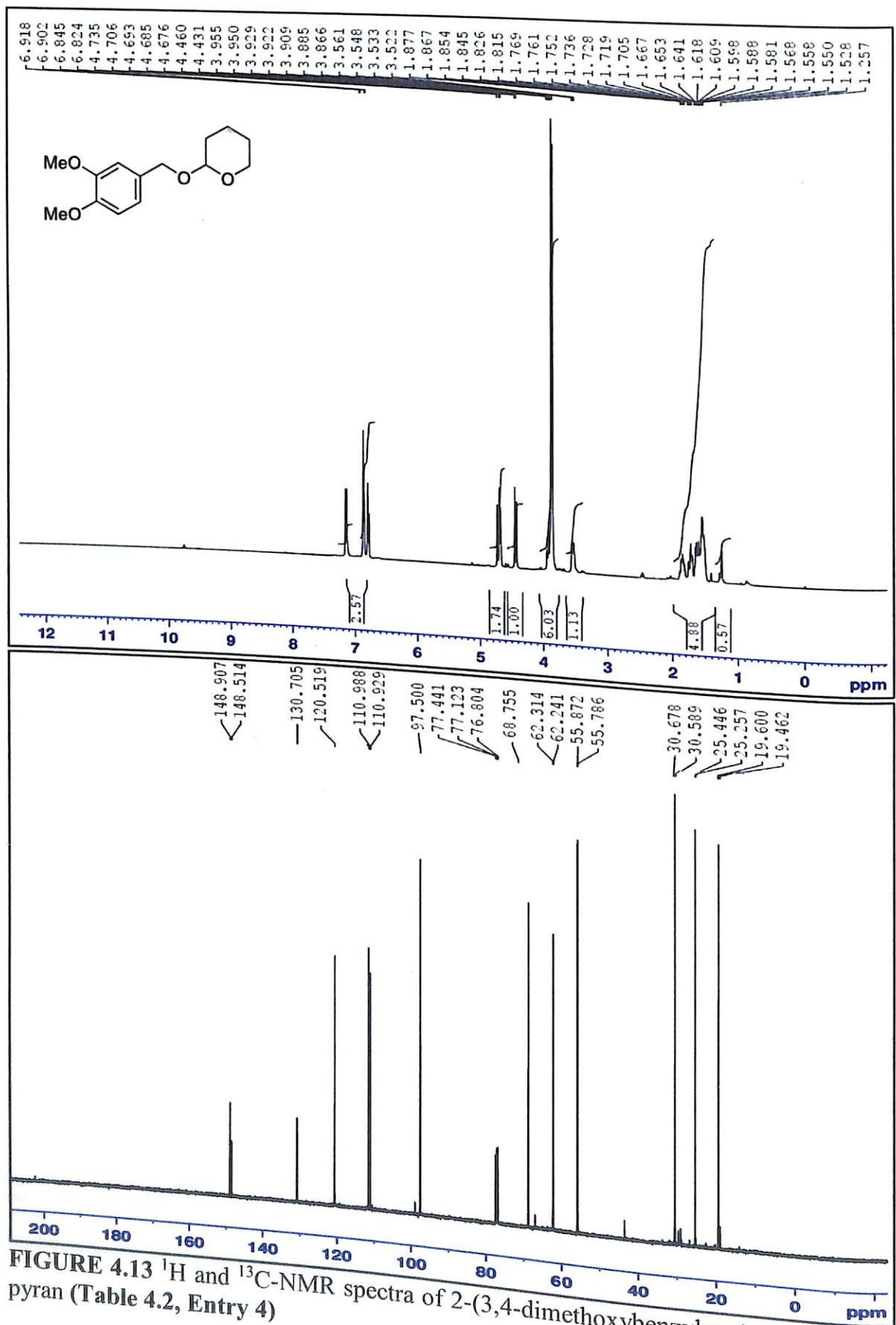
FIGURE 4.13 $^1$H and $^{13}$C-NMR spectra of 2-(3,4-dimethoxybenzyloxy) tetrahydro-2H-pyran (Table 4.2, Entry 4)

94
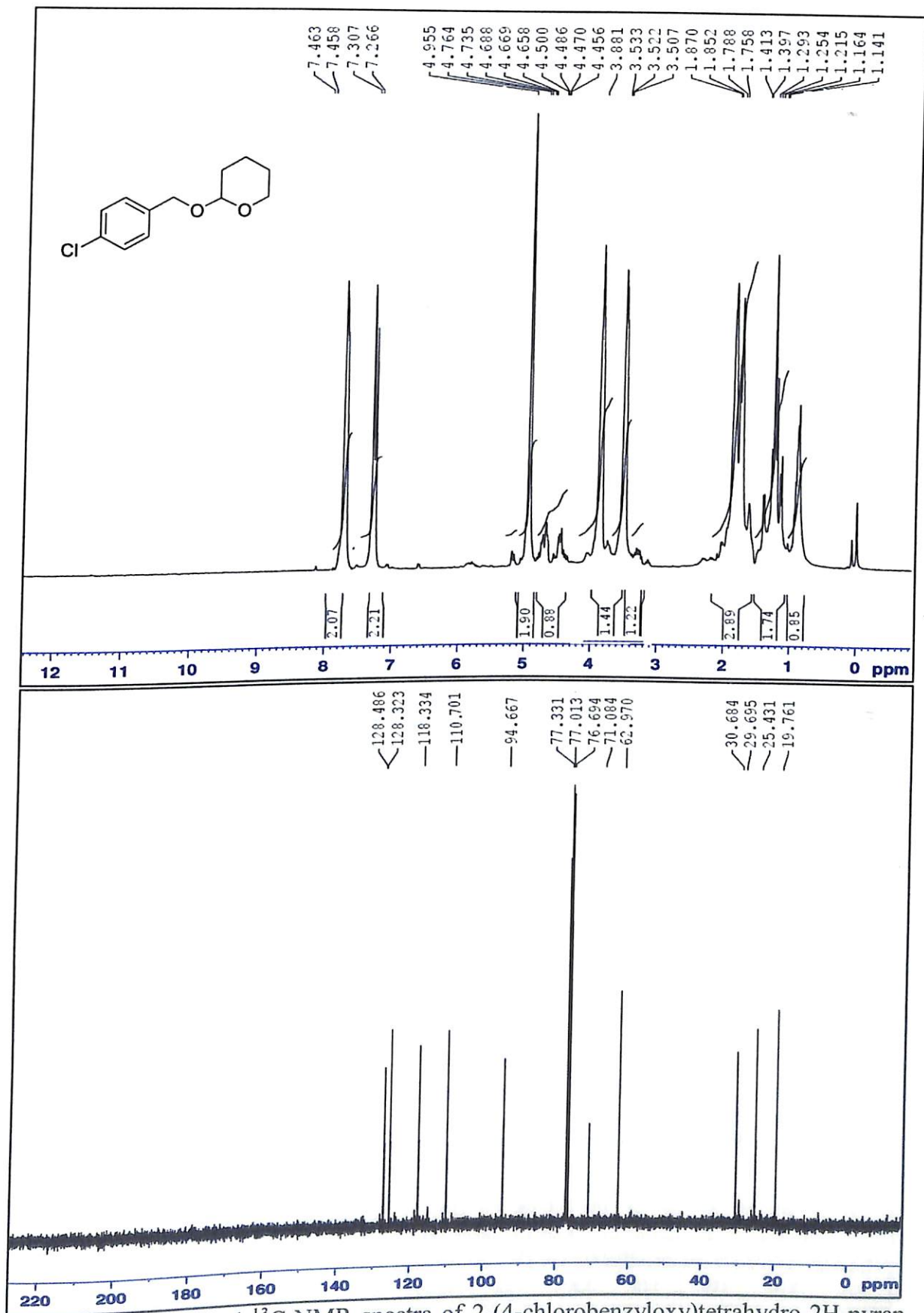
FIGURE 4.14 ¹H and ¹³C-NMR spectra of 2-(4-chlorobenzyloxy)tetrahydro-2H-pyran (Table 4.2, Entry 5)
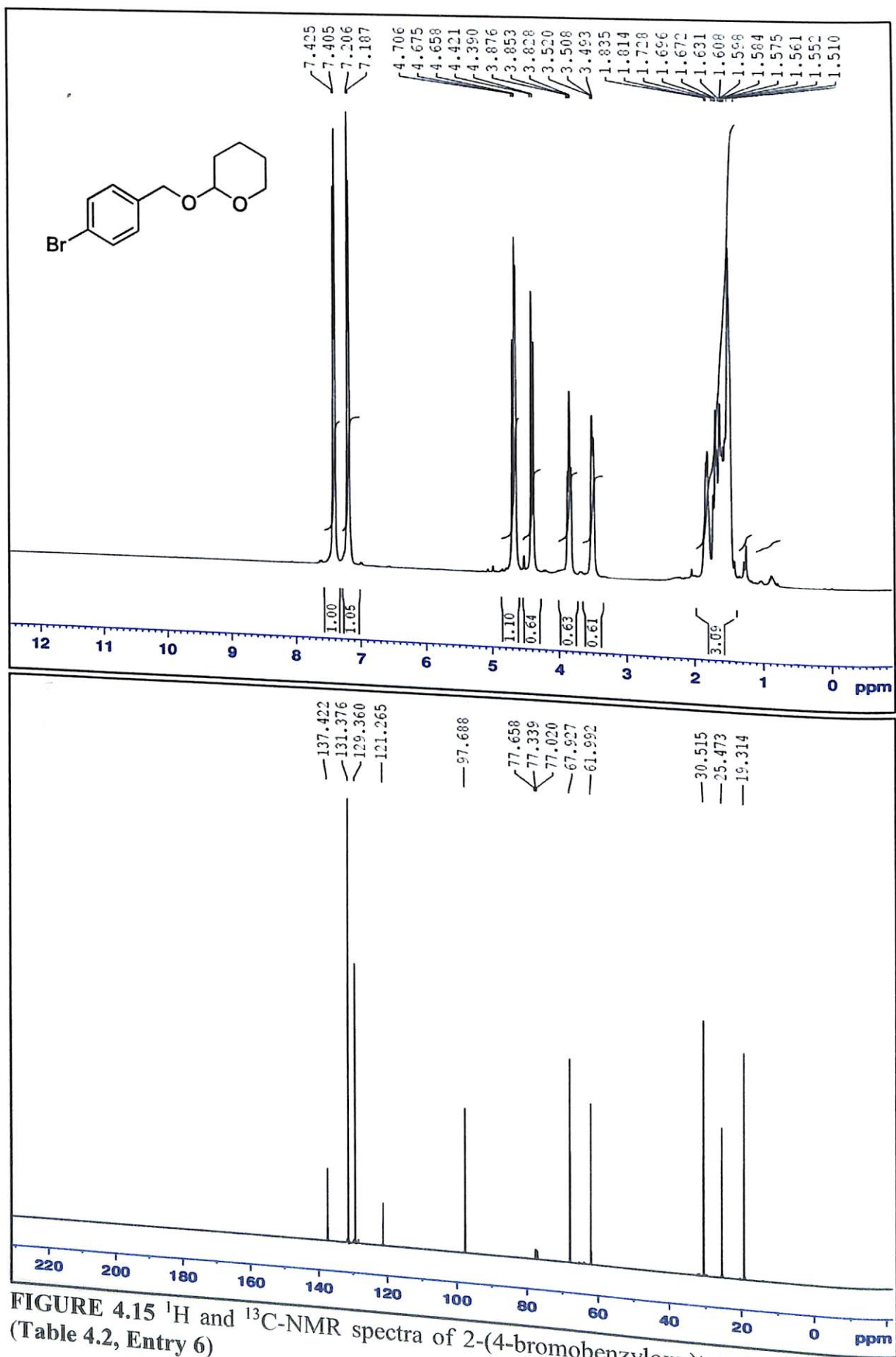
**FIGURE 4.15** $^1$H and $^{13}$C-NMR spectra of 2-(4-bromobenzyloxy)tetrahydro-2H-pyran (Table 4.2, Entry 6)

96
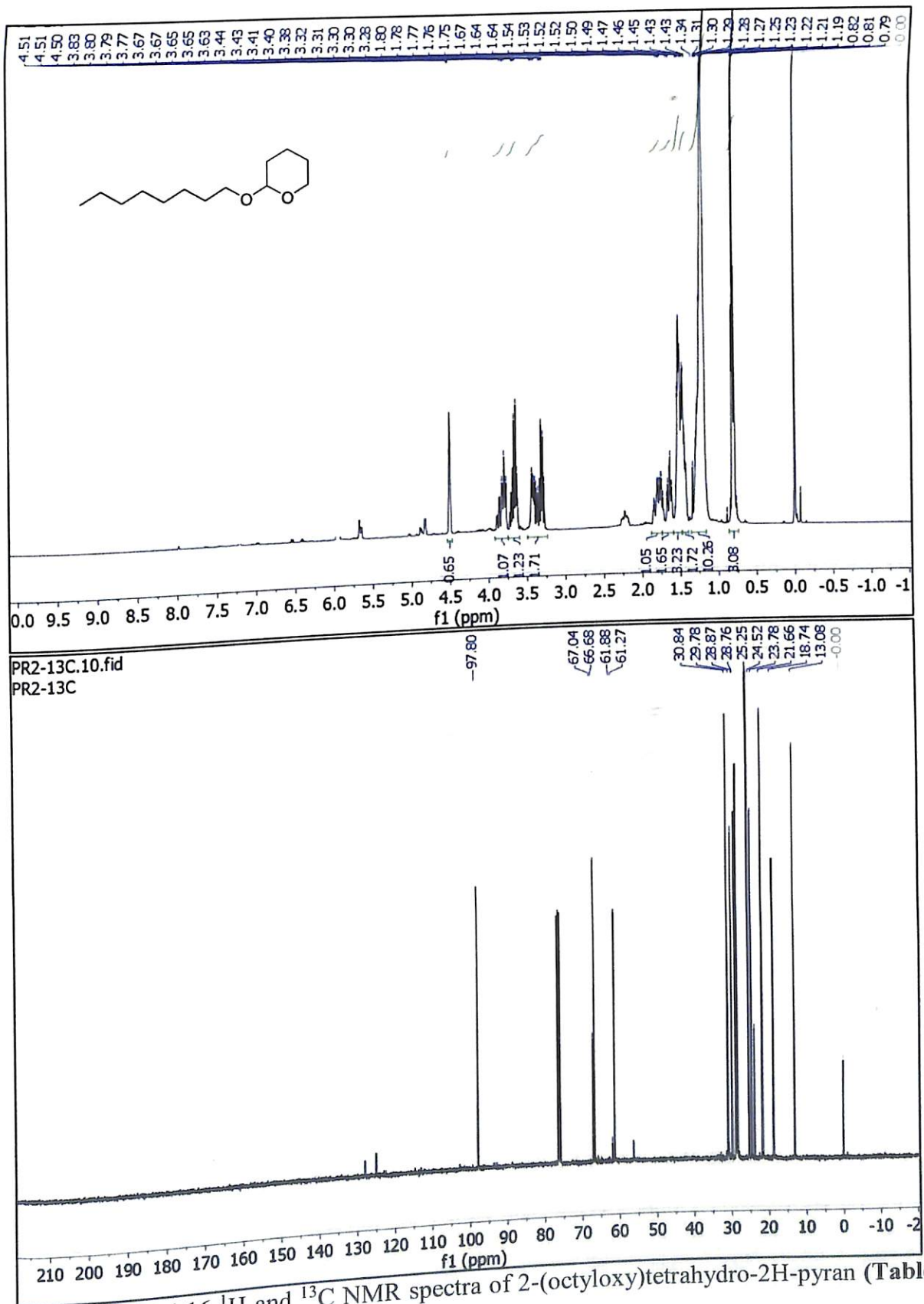
FIGURE 4.16 ¹H and ¹³C NMR spectra of 2-(octyloxy)tetrahydro-2H-pyran (Table 4.2, Entry 8)
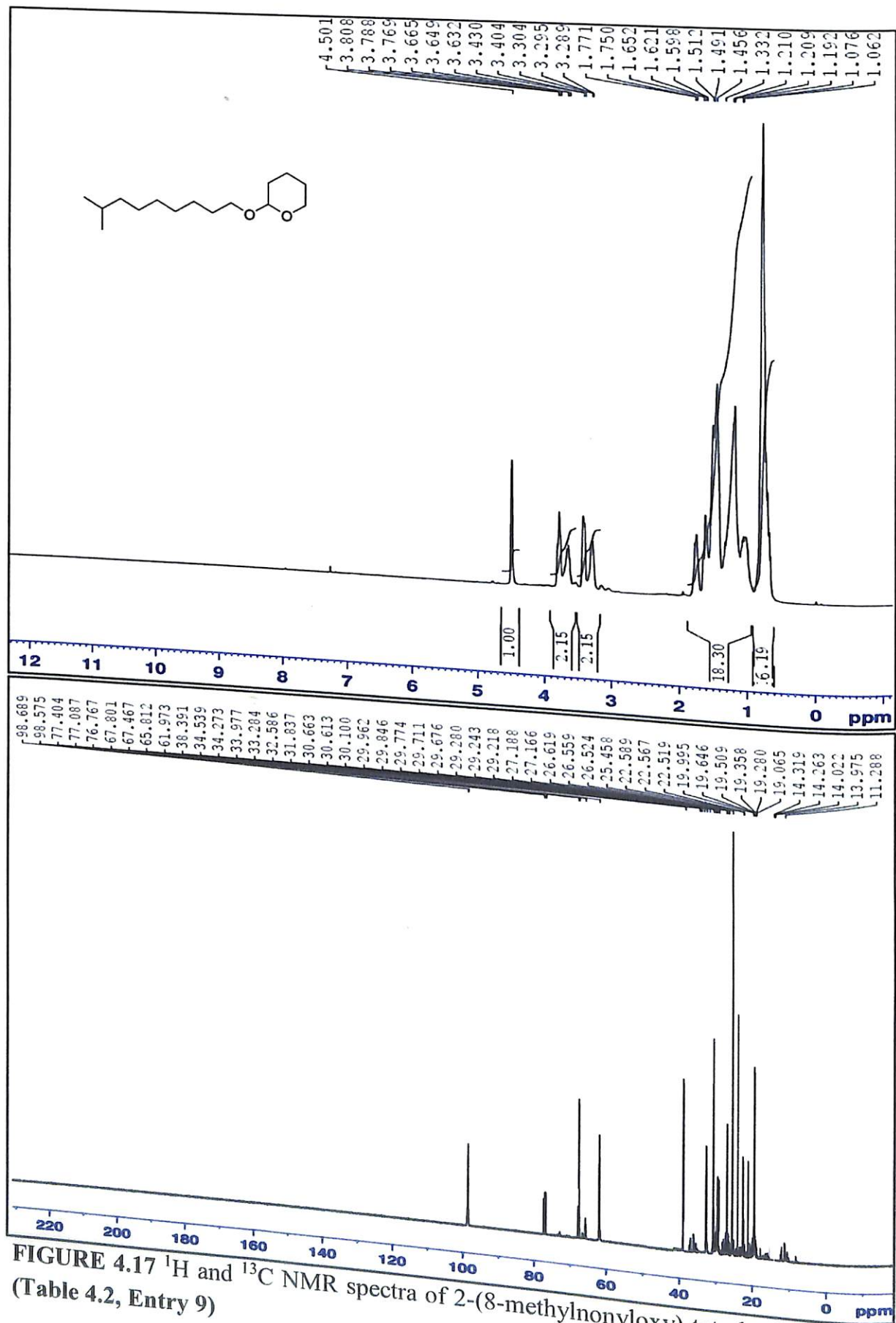
FIGURE 4.17 $^1$H and $^{13}$C NMR spectra of 2-(8-methylnonyloxy)-tetrahydro-2H-pyran (Table 4.2, Entry 9)

98
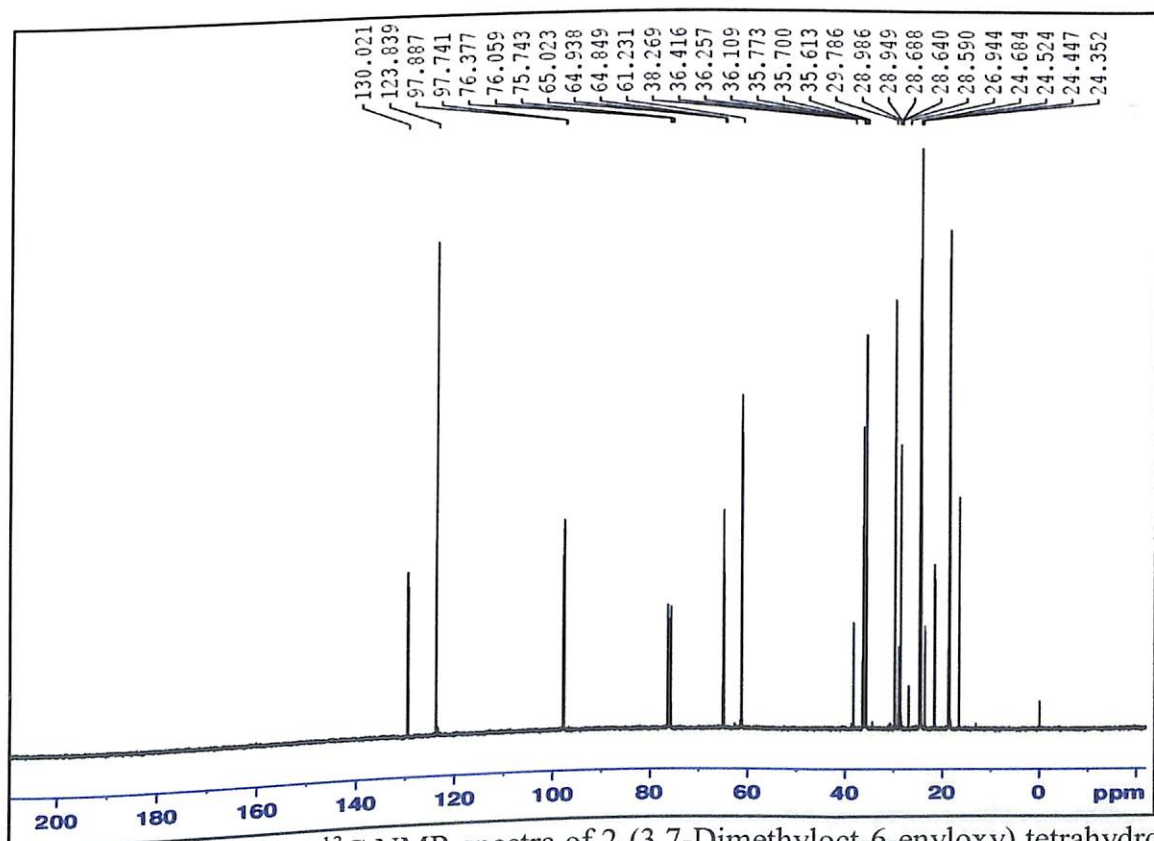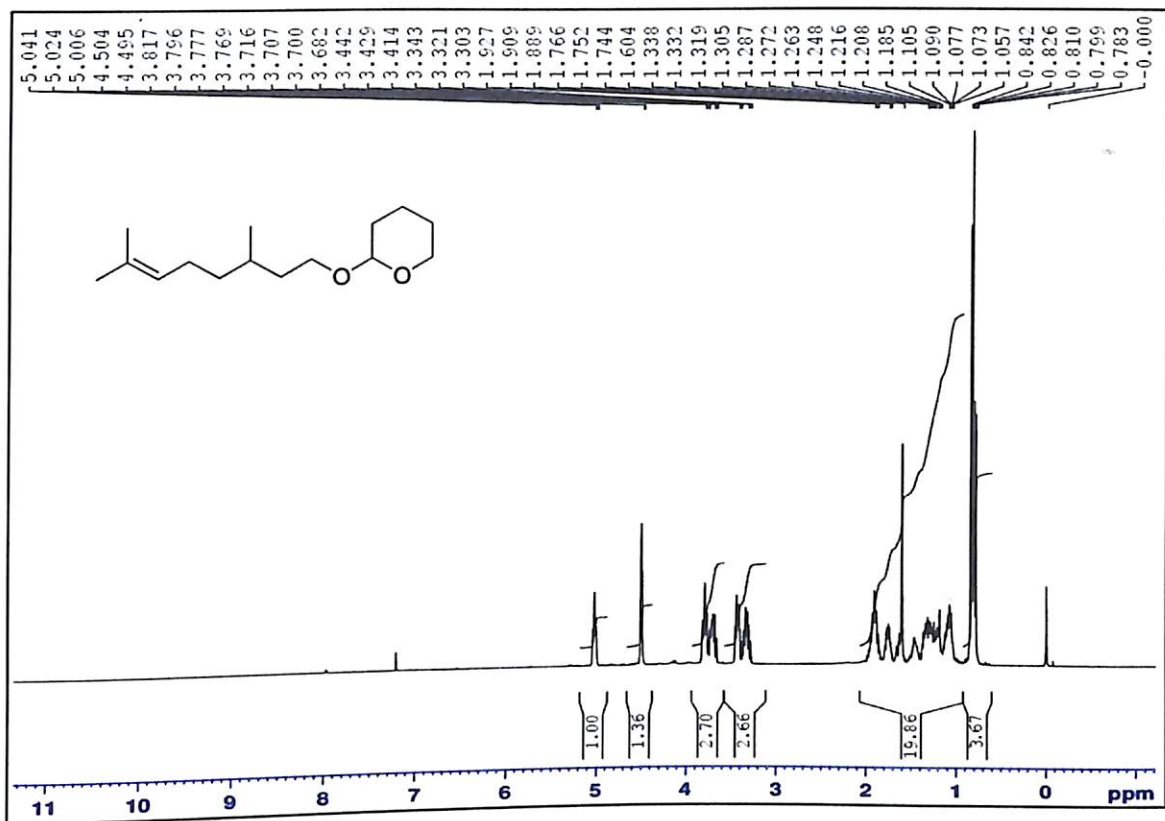
FIGURE 4.18 $^1$H and $^{13}$C NMR spectra of 2-(3,7-Dimethyloct-6-enyloxy) tetrahydro-2H-pyran (Table 4.2, entry 11)
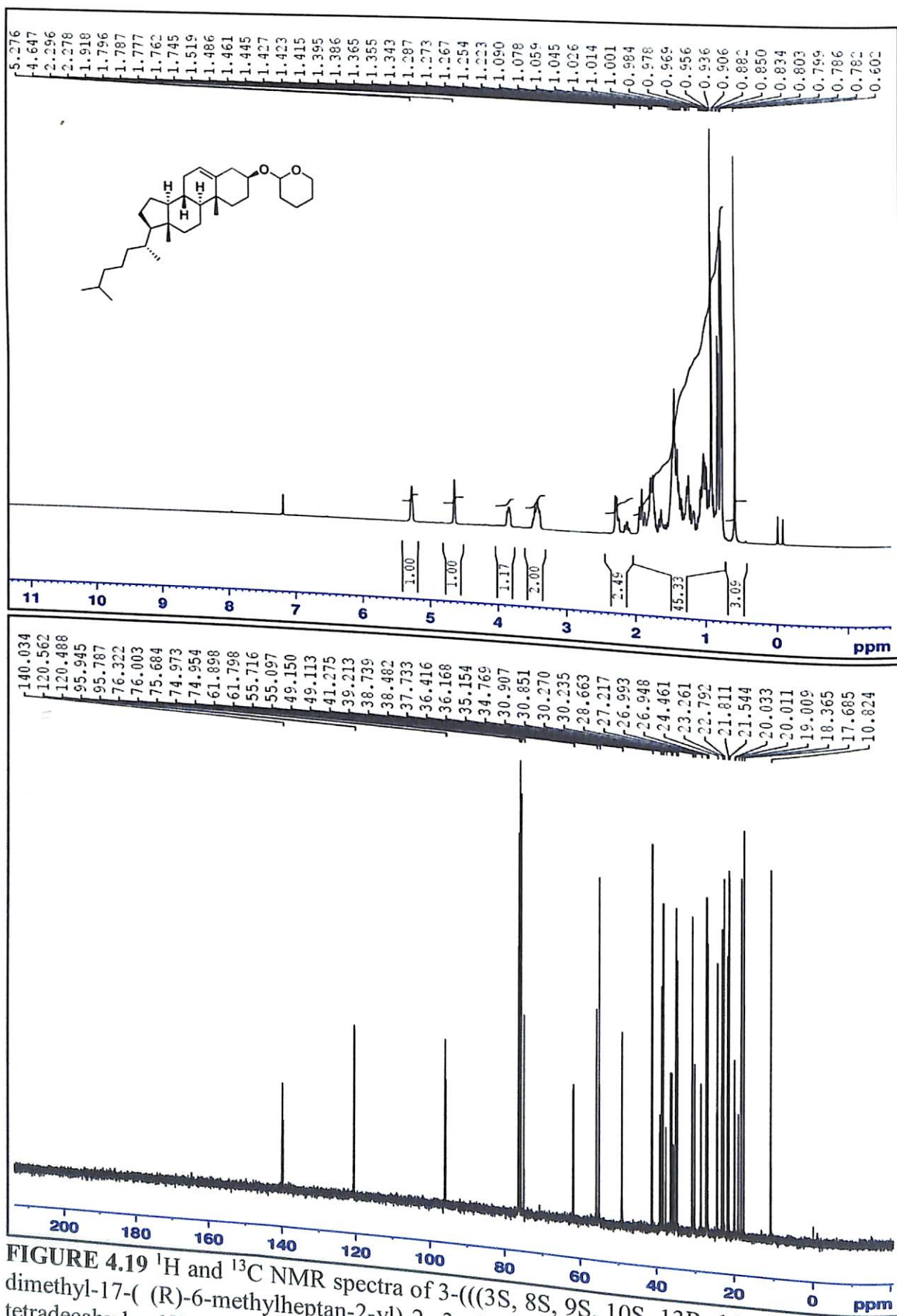
**FIGURE 4.19** ^{1}H and ^{13}C NMR spectra of 3-(((3S, 8S, 9S, 10S, 13R, 14S, 17R)-10, 13-dimethyl-17-( (R)-6-methylheptan-2-yl)-2, 3, 4, 7, 8, 10, 11, 12, 13, 14, 15, 16, 17-tetradecahydro-1H-cyclopenta[a]phenanthren-3-yl)oxy)tetrahydro-2H-pyran **(Table 4.2, Entry 12)**
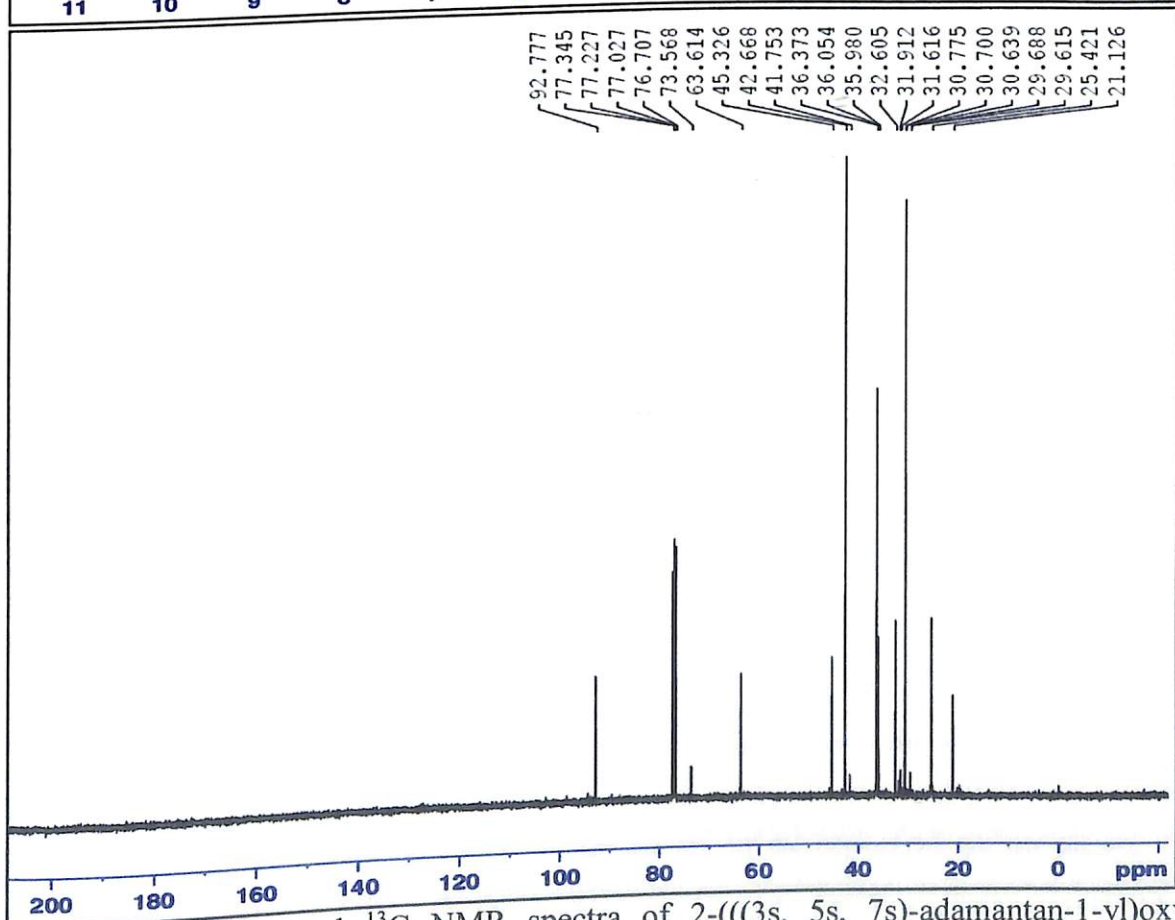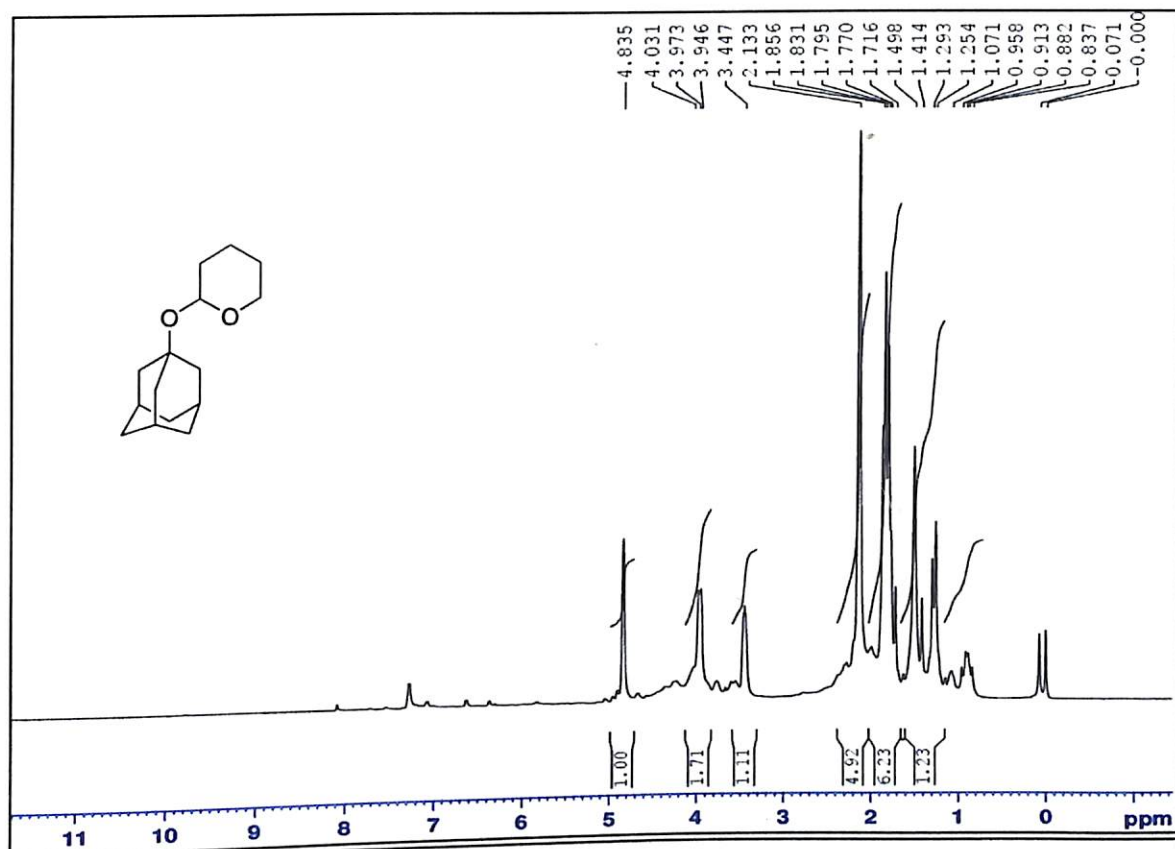
FIGURE 4.20 $^1$H and $^{13}$C NMR spectra of 2-(((3s, 5s, 7s)-adamantan-1-yl)oxy) tetrahydro-2H-pyran (Table 4.2, Entry 13)
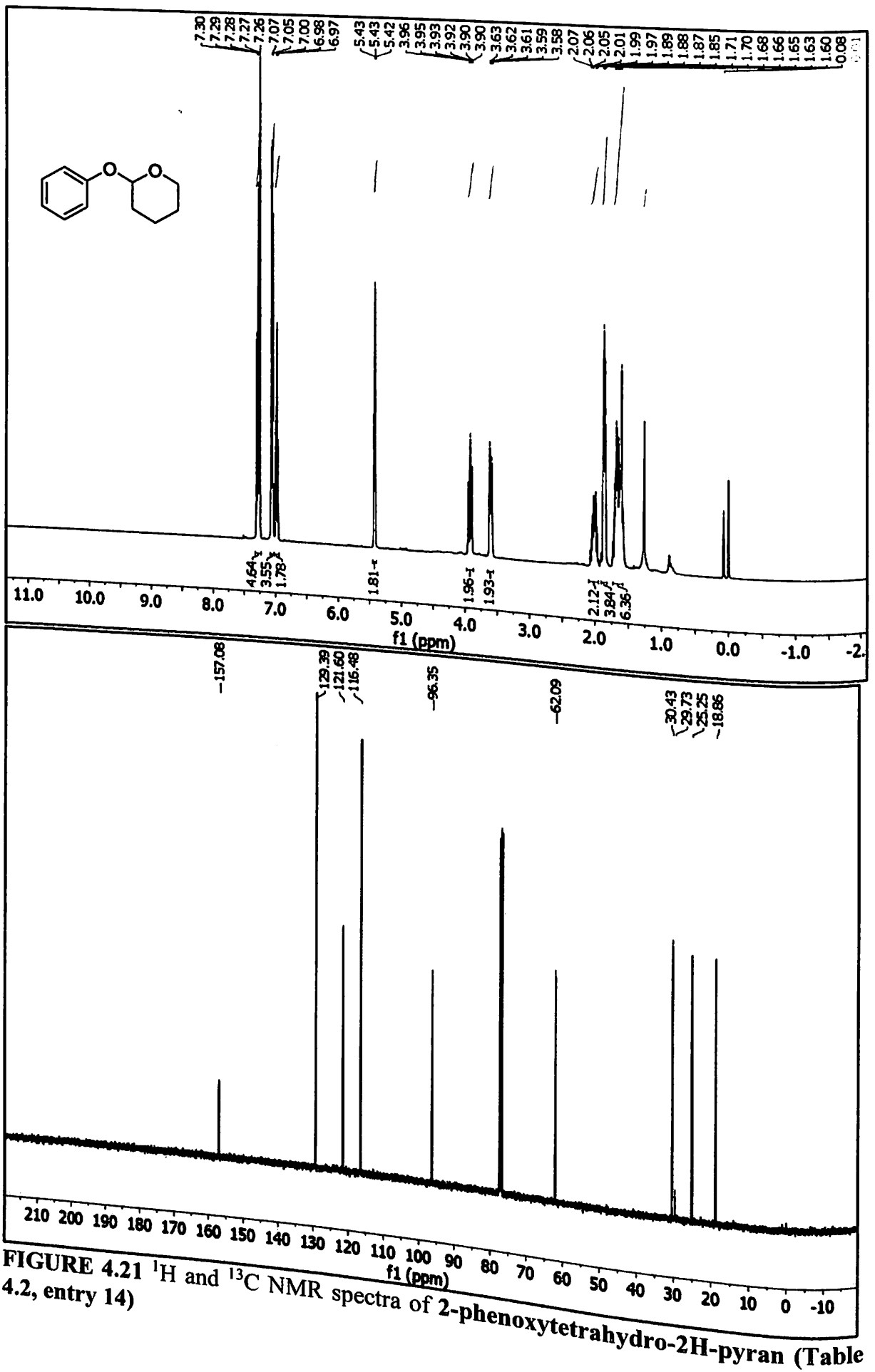
FIGURE 4.21 $^1$H and $^{13}$C NMR spectra of **2-phenoxytetrahydro-2H-pyran (Table 4.2, entry 14)**
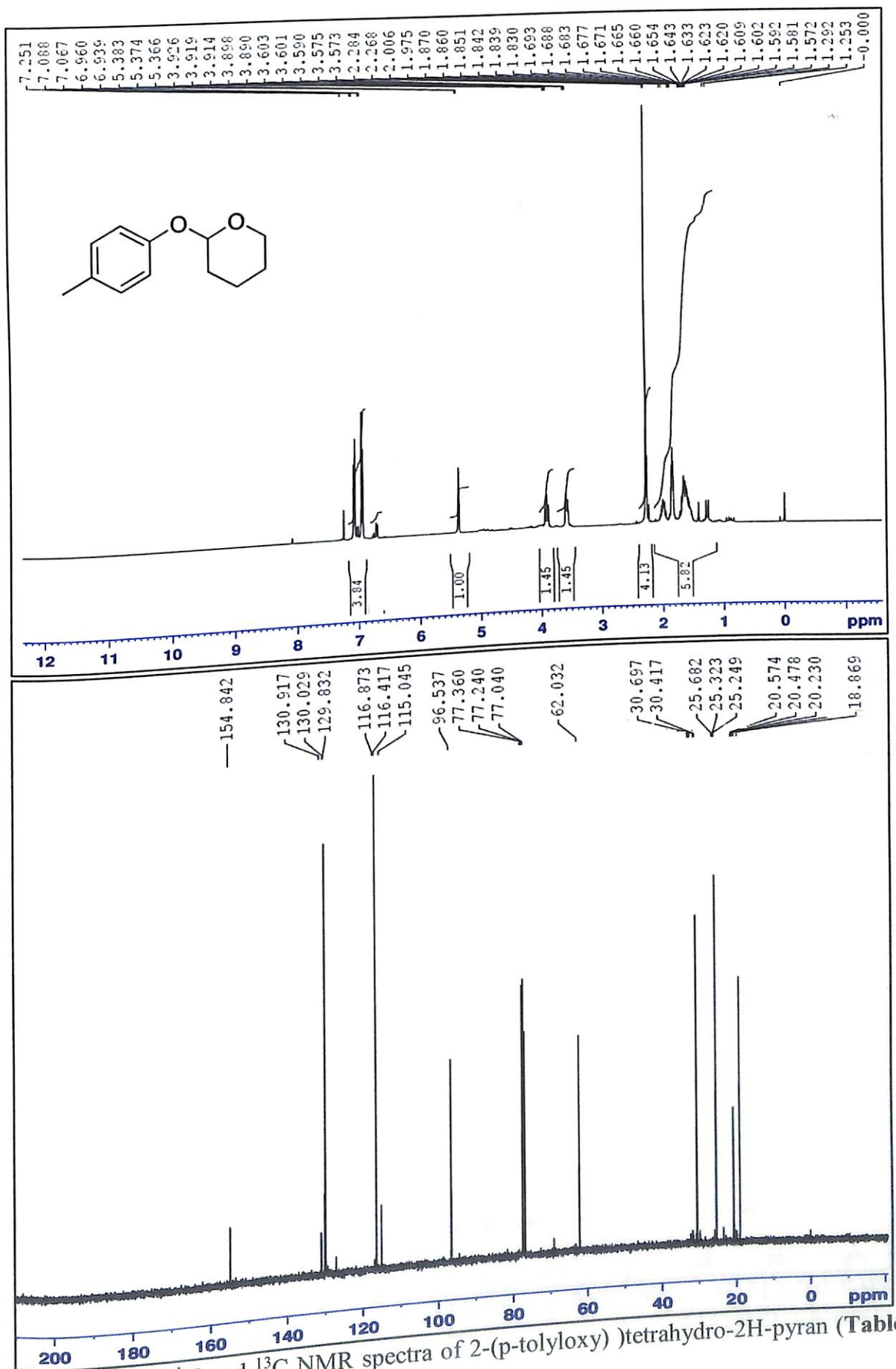
FIGURE 4.22 $^1$H and $^{13}$C NMR spectra of 2-(p-tolyloxy) )tetrahydro-2H-pyran (Table 4.2, Entry 15)
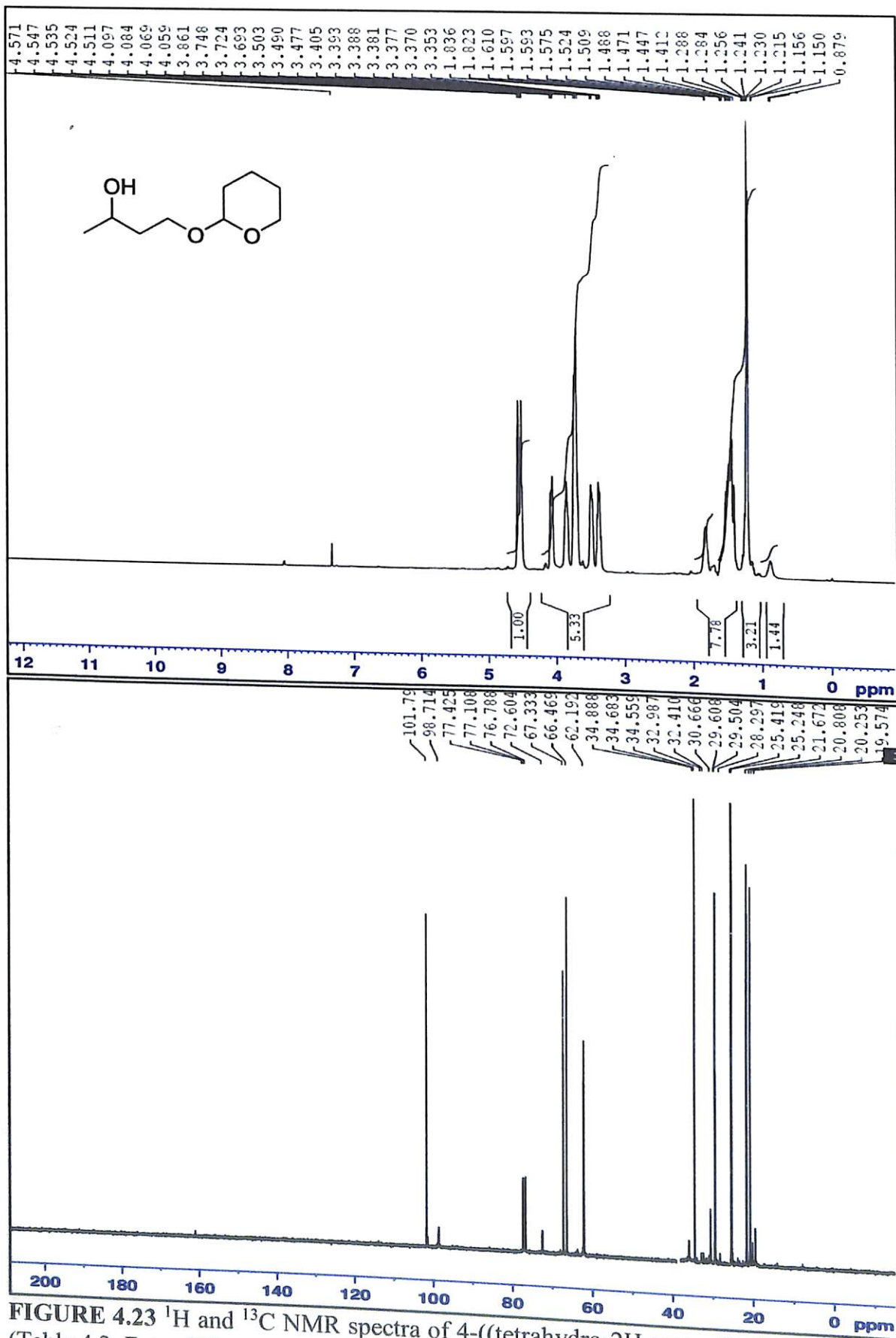
FIGURE 4.23 ${}^{1}$H and ${}^{13}$C NMR spectra of 4-((tetrahydro-2H-pyran-2-yl)oxy)butan-2-ol (Table 4.2, Entry 17)

104
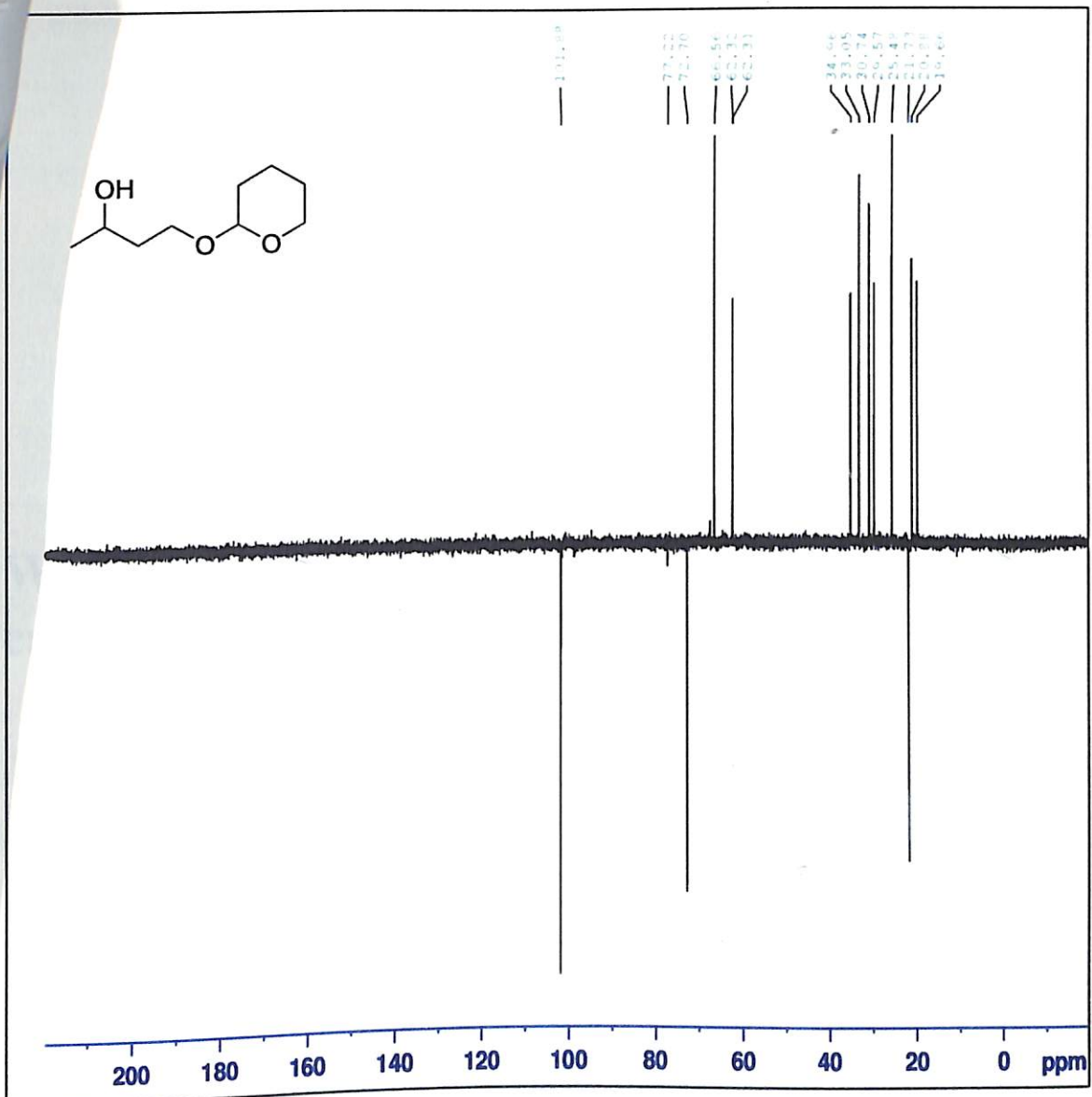
FIGURE 4.24 DEPT-NMR spectra of 4-((tetrahydro-2H-pyran-2-yl)oxy)butan-2-ol (Table 4.2, Entry 17)

# Waste-to-useful: Biowaste-derived heterogeneous catalyst for a green and sustainable Henry reaction

## 5.1 Introduction

The wastes from agricultural, food and chemical industries are produced several tones a day worldwide. Pilling up of wastes could be of great concern if not properly managed. On the other hand, "where there's muck there's money"- as they say, exploiting waste to useful materials is highly gainful both environmentally and economically and has received kindled attention in research.[1-4] Recently, waste biomass has been increasingly targeted as a sustainable feedstock for the production of fuels[5,6] and chemicals.[7,8]

As catalyst play a vital role in synthesis chemistry and offer major contribution towards the cost of a synthetic protocol, so maintaining sustainability of the catalytic substance is an essential part of production. However most of the catalyst traditionally used in synthetic chemistry are based on metals which have toxic effects towards environment and also expensive and scarce adding production cost to the proccess.[9] Exploitation of biomass waste for development of promising catalysts or catalyst-support or solvents can considerably alleviate the solid waste disposal problem and reduce possible environmental pollution. Also it make synthetic protocols eco-friendly, benign, biocompatible and economic due to the natural abundance of waste biomass.[10,11] These non-toxic, green catalysts can immensely contribute to minimize the hazards caused by chemical processes and thereby can give a new direction to the traditional thinking.

Recently extensive research works have appeared in academia utilizing biomass-based catalyst which include sulfonated biowaste-derived solid acid catalysts, waste shell derived solid base catalysts, bio char, several biomass ashes etc. Hara and his group[12] first established the synthesis of the sulfonated carbonaceous catalysts by incomplete carbonization of sulfoaromatic compounds[13] which paved the way to utilize biomass waste for preparing such sulfonated carbonaceous catalysts. A wide range of biomass waste are

being explored for carbonization such as rice husk[14], coffee residue[15], oil palm trunk[16], sugar cane bagasse[17], sweet potato[18] and many more. All these catalysts find attractive application in esterification reaction usefully in the field of biodiesel production. Similarly, a number of biowaste-derived solid base catalysts have been developed from waste shells that are rich in calcium.[19] Apart from these, several other bio-derived catalysts are being attempted to design by impregnating metal complexes or nanoparticles over biomass materials.[20,21]

However reported literature suffer from several demerits as most of the studies have engrossed in fabrication of biomass feedstock which need harsh, wasteful and expensive chemical processing like high temperature carbonization, complexation or doping with metals and acid functionalization etc.[22-24] Interestingly, in recent years, several raw waste biomass like biomass ashes are used as such (without any pre-chemical treatment) as a heterogeneous catalysts for biodiesel production by transesterification reaction.[25-27] Nevertheless, to the best of our knowledge, there are no reports in literature where raw biomass is exploited ; a solid catalyst for an all-important C-C bond formation reaction.

The Henry reaction, also known as the nitroaldol reaction, is one of the most important synthetic tools for C-C bond formation. The product β-nitroalcohol or β-nitroaldol can be potentially converted to many pharmaceutically significant organic compounds and thus it acts as a versatile intermediate in many organic transformations.[28,29] Literature suggests a good number of methodologies reported for synthesis of β-nitroalcohol products by Henry reaction, including both homogeneous and heterogeneous catalysts. The classical reaction, introduced by L. C. R. Henry[30] in 1896, involves coupling of a nucleophile produced from nitroalkane molecule with a carbonyl electrophile moiety to give rise to nitroaldol product. The reaction is routinely performed employing homogeneous basic catalysts like alkali metal hydroxides, alkoxides, amines etc. [31,32] However to tackle the difficulties involved in separation of homogeneous catalysis, recently various heterogeneous base catalysts are developed ranging from metal oxides to polymers or MOFs (Metal Organic Frameworks).[33-36]

Mélot et al.[37] in 1986 performed Henry reaction using Alumina-supported KF (KF/Al2O3) catalyst under room temperature (Scheme 5.1). Their method provided a simple procedure for the synthesis of nitroaldol using solid-supported catalyst under ambient condition which resulted 50-79% yield of the desired product.

$$R^1\text{-CHO} \ + \ R^2\text{-CH}_2\text{NO}_2 \ \xrightarrow[\text{R.T.}]{\text{KF/Al}_2\text{O}_3} \ R^1-\overset{H}{\underset{OH}{C}}-\overset{H}{\underset{NO_2}{C}}-R^2$$
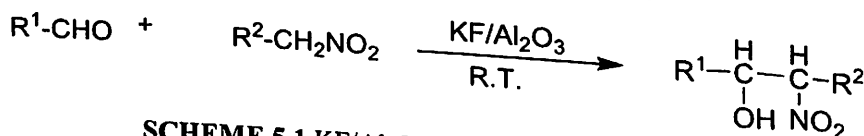
**SCHEME 5.1** KF/Al2O3 catalyzed Henry reaction.

Balini et al.[38] prepared a silica-supported N,N-diethylpropylamine (KG-60-NEt2) heterogeneous catalyst and employed it to carry out neat synthesis of nitroaldols (Scheme 5.2).
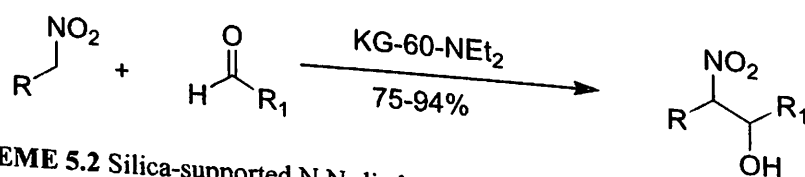


**SCHEME 5.2** Silica-supported N,N-diethylpropylamine catalyzed Henry reaction.

Gupta et al.[39] recently reported Henry reaction of different substituted aromatic aldehyde using a two dimensional Zn(II)-coordination polymer based catalytic system (Scheme 5.3). The reaction was performed at 70°C for 48 hours. The synthesized catalyst was found recyclable up to three times.
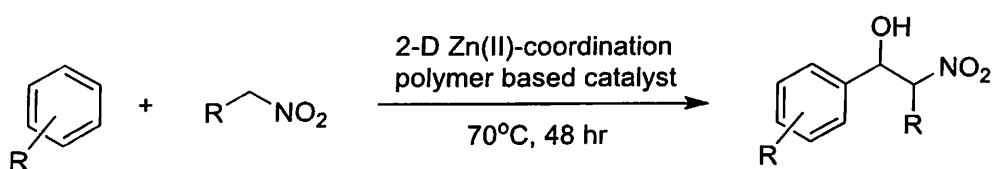
**SCHEME 5.3** Henry reaction using Zn(II)-coordination polymer based catalyst.

While varieties of synthetic heterogeneous catalyst from chemical industries are widely used for Henry reaction, only a few reports suit the '12 Principles of Green Chemistry' outlined by Anastas and Warner;[40] hence use of bio-waste catalysts are highly desirable from sustainability and green credential ethos. The significance of nitroalcohols in organic synthesis and our continued interest involving heterogeneous catalysts/reagents[41,42] prompted us to explore the Henry reaction further. Recently our group has reported a sustainable protocol for production of biodiesel using *Musa acuminata* peel ash as a heterogeneous catalyst.[43] Musa acuminata is a well-known and abundant species of banana found in all over south-east Asia. With our current interest in the application of waste biomass, we believed that basic *Musa acuminata* peel ash (MAPA) could be a promising catalyst for the Henry reaction.

# 5.2 Experimental

This section depicts the information regarding the chemicals and reagents used in the experiments, catalyst preparation methods, reaction procedure and different analytical and spectroscopic techniques used for catalyst characterization.

## 5.2.1 Materials and methods

Banana (*Musa acuminata*) peels were collected from Kolasib district of Mizoram, India and were dried in sunlight. All other chemicals and solvents used were of analytical grade, and they were procured from commercial sources and used as such without further purifications.

## 5.2.2 Catalyst preparation and characterization

Musa acuminata peels were collected and thoroughly washed with distilled water and sun-dried. The dried peels were then cut into small pieces and burnt in open air, and grinded to produce the ash catalyst. We also tried calcination of the dried peels in muffle furnace instead of open burning and observed almost same catalytic activity.

FT-IR, TEM-EDS, SEM, XRD, XRF, XPS, BET and TGA analysis were performed to evaluate the structure and morphology of the catalyst. IR spectra were recorded on a Perkin-Elmer Spectrum One FTIR spectrometer. XRD measurements were carried out on a Bruker AXS D8-Advance powder X-ray diffractometer with Cu-Kα radiation ($\lambda$=1.5418Å) with a scan speed of 2°/min. TEM-EDS images were obtained on a JEOL, JEM2100 equipment. $N_2$ adsorption-desorption isotherm was obtained with a Micromeritics ASAP 2010 surface area and porosity analyzer. XRF analysis of the powdered sample was performed on Bruker S4 Pioneer X-Ray fluorometre. XPS analysis was carried out in a Thermo Fischer Scientific, model no. ESCALAB Xi+ instrument under room temperature and 40% humidity. The thermogravimetric analysis was carried out in a Perkin Elmer, USAA, Diamond TG/DTA instrument. The weight loss of the catalyst was recorded within a temperature range 30 °C -800 °C, heating rate 0.1 °C -200 °C/min under constant flow of nitrogen gas. ^{1}H and ^{13}C NMR spectra of the synthesized compounds were recorded on a Bruker Avance II (400 MHz), Bruker Avance III (500 MHz) spectrometer using tetramethylsilane (TMS) as an internal reference.

### 5.2.3 Basic strength and basicity measurement of the catalyst

The basic strength of the solid base catalyst MAPA was investigated by Hammett indicator method. The Hammett indicators that were used in the experiments are bromothymol blue ($H\_ =7.2$), phenolphthalein ($H\_ =9.8$), alizarin yellow R ($H\_ = 11.0$), 2,4,6-trinitroaniline ($H\_ = 12.2$) and 2,4-dinitroaniline ($H\_ =15$). In each case, about 2 mL of Hammett indicator solution in benzene was added to 200 mg of the catalyst, was shaken, allowed to settle and was observed for any possible color change. If the solution shows any color change upon addition of an indicator, then this signals that basic strength of the catalyst is stronger than the indicator used and vice versa.

The basicity of the catalyst was determined by titrating with 0.1 N benzoic acid diluted by benzene and using bromothymol blue as indicator. The end-point was noted when the green color of the indicator disappeared completely.

### 5.2.4 Henry reactions and methods of analysis

The Henry reactions of aldehydes (1 mmol) with nitroalkanes (1 mmol) using MAPA catalyst were carried out in a 5 mL sample vial placed on a magnetic stirrer. The speed of mechanical stirrer was kept constant at 1000 rpm. Progress of the reaction was monitored by thin layer chromatography (TLC). Once the reaction was completed, the nitroaldol product was diluted by adding 3 mL ethyl acetate, isolated by centrifugation and decantation, and concentrated in rotary evaporator. The final nitroaldol product obtained was analyzed by FT-IR and NMR spectroscopy.

### 5.2.5 Catalyst recyclability test

The catalyst was tested also for its potential reusability. After each catalytic run, the catalyst were recovered by centrifugation and decantation, washed with ethyl acetate and then dried at 100 °C in hot air oven overnight before being used again in a new catalytic cycle. The recycled catalyst was characterized by XRF, XPS, XRD, EDS, TEM and SEM analysis to examine any possible change in elemental composition and morphology.



**SCHEME 5.4** Henry reaction of aldehyde using nitroalkane using MAPA catalyst

To verify the heterogeneity of the catalyst, hot filtration method was adopted which checked for possible leaching of active sites from the catalyst surface.[44] To carry out the test, Henry reaction with catalyst MAPA was set under optimized conditions and then after 5 minutes of the reaction, the catalyst was centrifuged and the reaction mixture was decanted to the reaction vessel again. The reaction was continued for another 6 hours with frequent checking of TLC.

## 5.3 Result and discussion

## 5.3.1 Catalyst characterization

FT-IR analysis, performed as a preliminary tool (Fig. 5.1) to investigate the functional group present in the catalyst, provided strong revelation about presence of metal oxides (O–K–O stretching at 702 cm⁻¹), metal carbonates (C-O stretching at 1655 and 1403 cm⁻¹), Si–O–Si (1006 cm⁻¹) bonds. The broad band at 3431 cm⁻¹ can be attributed to rapid hydration of the ash sample by absorption of moisture. [45,46]
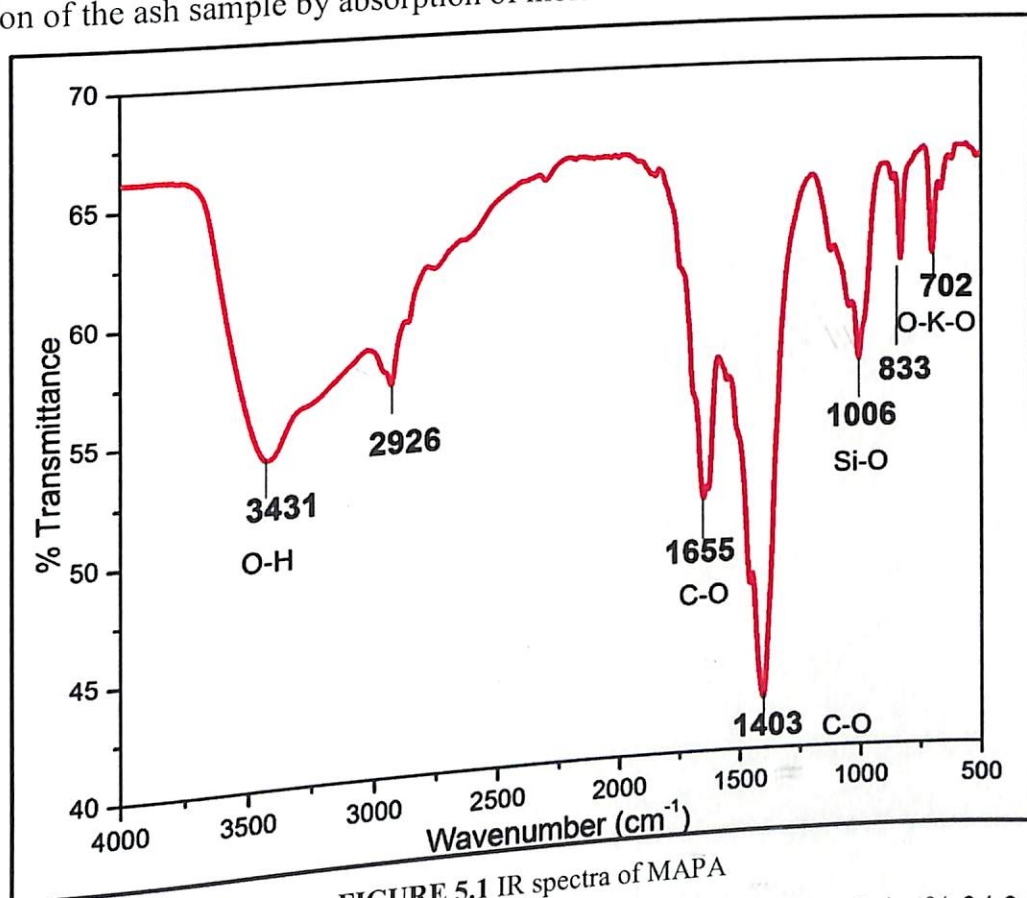


FIGURE 5.1 IR spectra of MAPA

The EDX analysis (Fig. 5.2) of the catalyst showed O (wt% 40.61), C (wt% 34.34) and K (wt% 20.77), as the major elements followed by Cl, Si, Ca, Mg, P and S as the other elements present in MAPA.
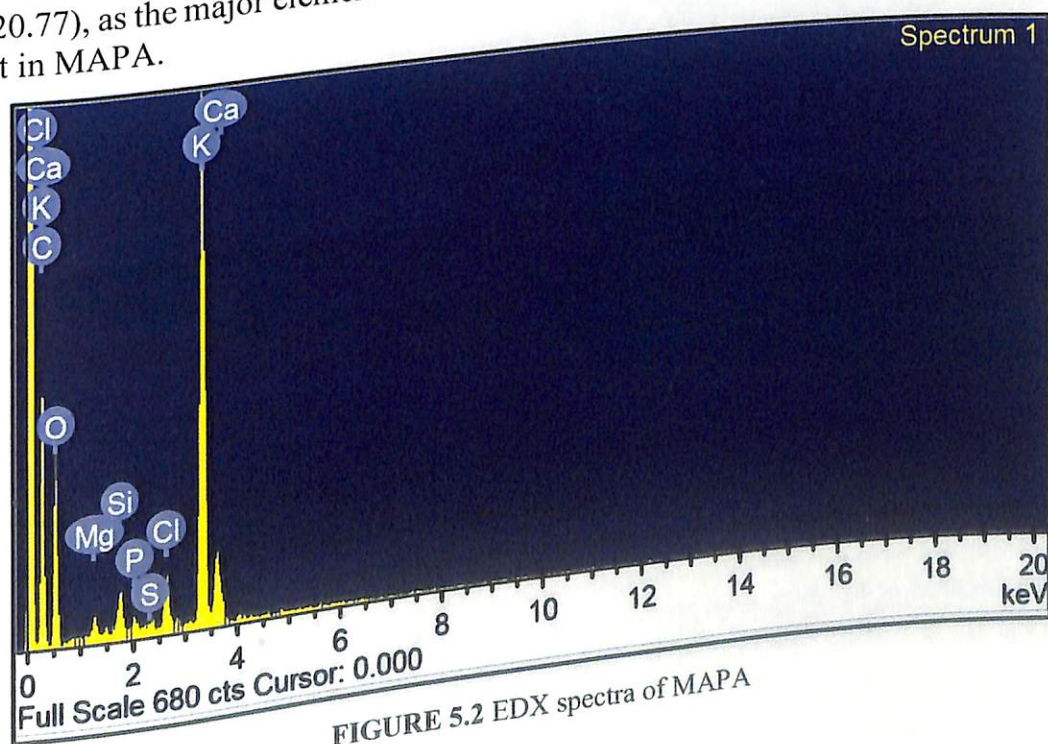


FIGURE 5.2 EDX spectra of MAPA

111
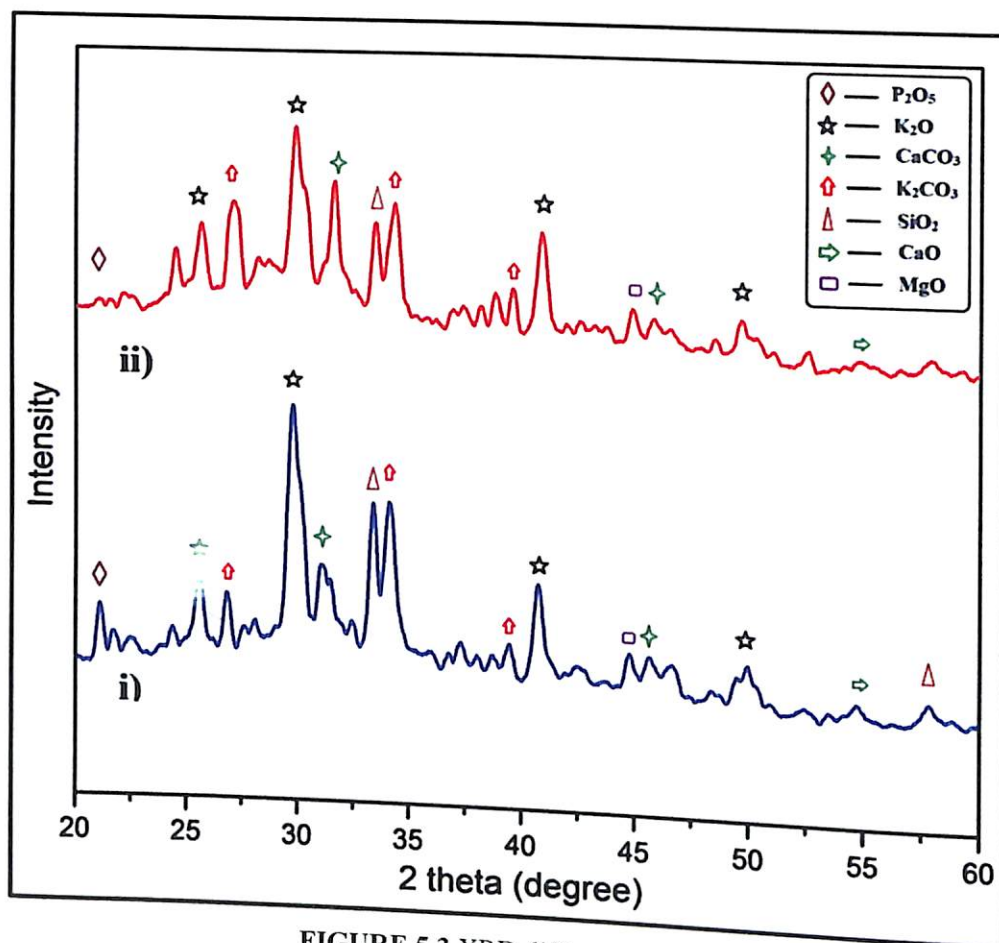
**FIGURE 5.3** XRD diffractogram of MAPA

The strong characteristic peaks of $K_2O$ were observed during XRD analysis (Fig. 5.3) of the ash sample at $2\theta$= 29.77, 25.59, 40.73, 49.91 which matched with the JCPDS reference file No- 77-2176. Presence of oxides and carbonates of Ca and Mg which have very strong basic sites were also evidenced by the XRD diffractogram.

SEM and TEM images revealed a number of aggregates with both mesoporous and microporous structure of the catalyst (Fig. 5.4a-d). Porous and spongy nature of the particles can be observed in the SEM images taken at 500 and 3000X resolution.

To investigate the particular chemical compositions of the inorganic phase of the fresh MAPA catalyst, XRF analysis was performed and it presented $K_2O$ as the predominant component (% mass fraction 65.11%) while $SiO_2$, CaO and $P_2O_5$ have mass fractions 10.86%, 7.78% and 6.07% respectively (Table 5.1).

To examine the greater detail of the species present in the ash sample, X-ray Photoelectron Spectroscopy (XPS) analysis was also performed. X-ray Photoelectron Spectroscopy (XPS) analysis enables to study the chemical composition near surface region of material which is of most importance in case of catalytic compound. Fig. 5.5 depicts the wide scan spectrum (Fig. 5.5a) of fresh ash catalyst along with deconvulated spectra (Fig. 5.5b-d) of major elements present in MAPA. It can also provide the information about oxidation state of an element by calculating the binding energies of particular components.

The XPS survey spectrum suggested exclusive presence of carbon (atomic wt% 45.59), oxygen (atomic wt% 36.54) and potassium (atomic wt% 12.18) near surface region. The overlapping peaks at binding energies 280-290 region is due to C1s and K2p states. The positions located at binding energies 284.1eV and 288.40 eV can be attributed to C-C and $CO_3^{2-}$ (e.g. metal carbonates) groups. Each K2p state was split into two sub-peaks: $2p_{3/2}$ and

$2p_{1/2}$, positioned at 292 eV and 294.4 eV. They both refer to the $K^+$ state bonded to smaller anions indicating oxides or carbonates. The O1s peak positioned at 530.5 eV corresponds to the presence of metal oxides.[47,48]
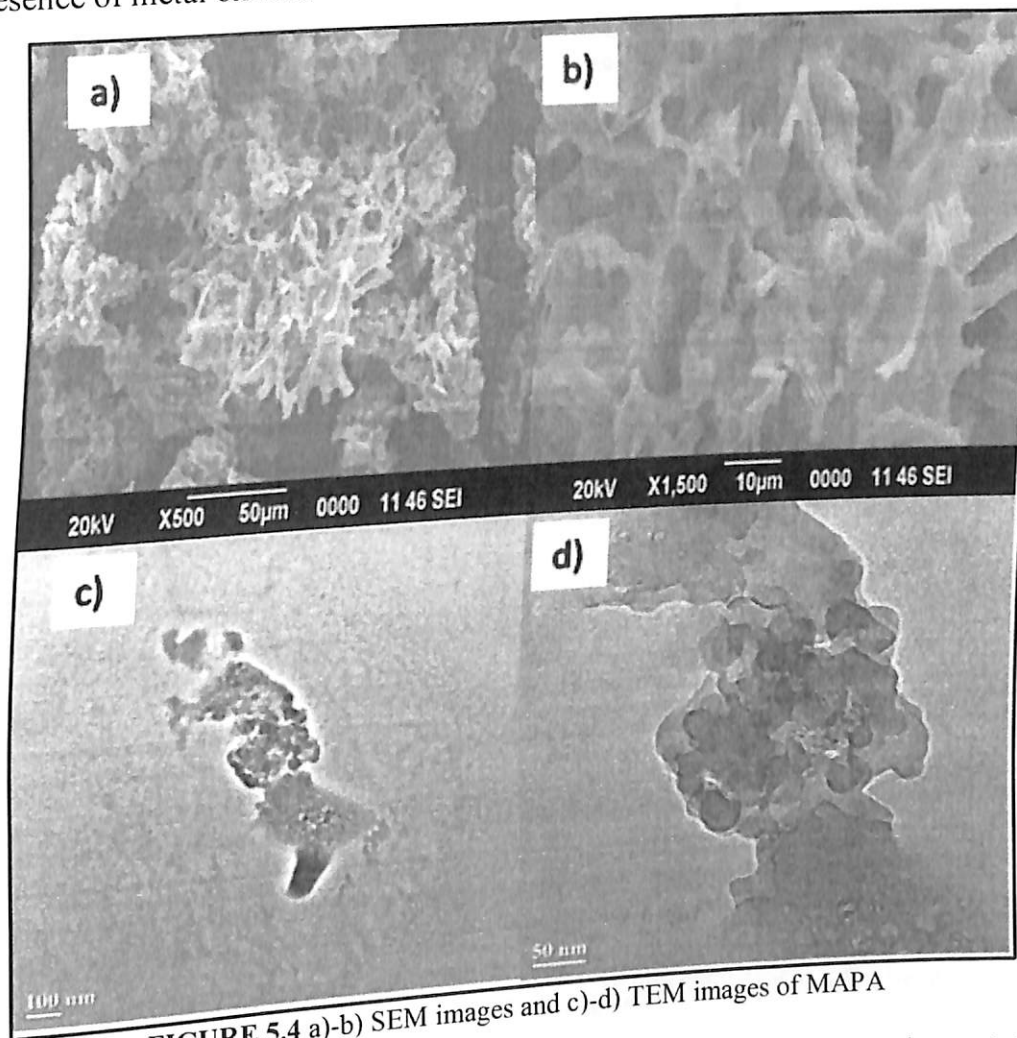


FIGURE 5.4 a)-b) SEM images and c)-d) TEM images of MAPA

TABLE 5.1 Metallic and non-metallic concentration in recovered MAPA after 10th recyclability test as given by XRF analysis.

| Sl No | Name of the component in the MAPA sample | % Mass fraction in fresh MAPA | % Mass fraction in recovered MAPA after 10th recycles. |
|---|---|---|---|
| 1. | $K_2O$ | 65.110 | 64.76 |
| 2. | $SiO_2$ | 10.864 | 2.38 |
| 3. | $CaO$ | 7.787 | 4.42 |
| 4. | $P_2O_5$ | 6.067 | 1.80 |
| 5. | $SO_3$ | 2.857 | 0.79 |
| 6. | $MgO$ | 2.427 | 0.69 |
| 7. | $Fe_2O_3$ | 1.152 | 1.29 |
| 8. | $Al_2O_3$ | 0.737 | 0.19 |
| 9. | $MnO$ | 0.227 | 0.40 |
| 10 | $CuO$ | 0.192 | 0.092 |

113
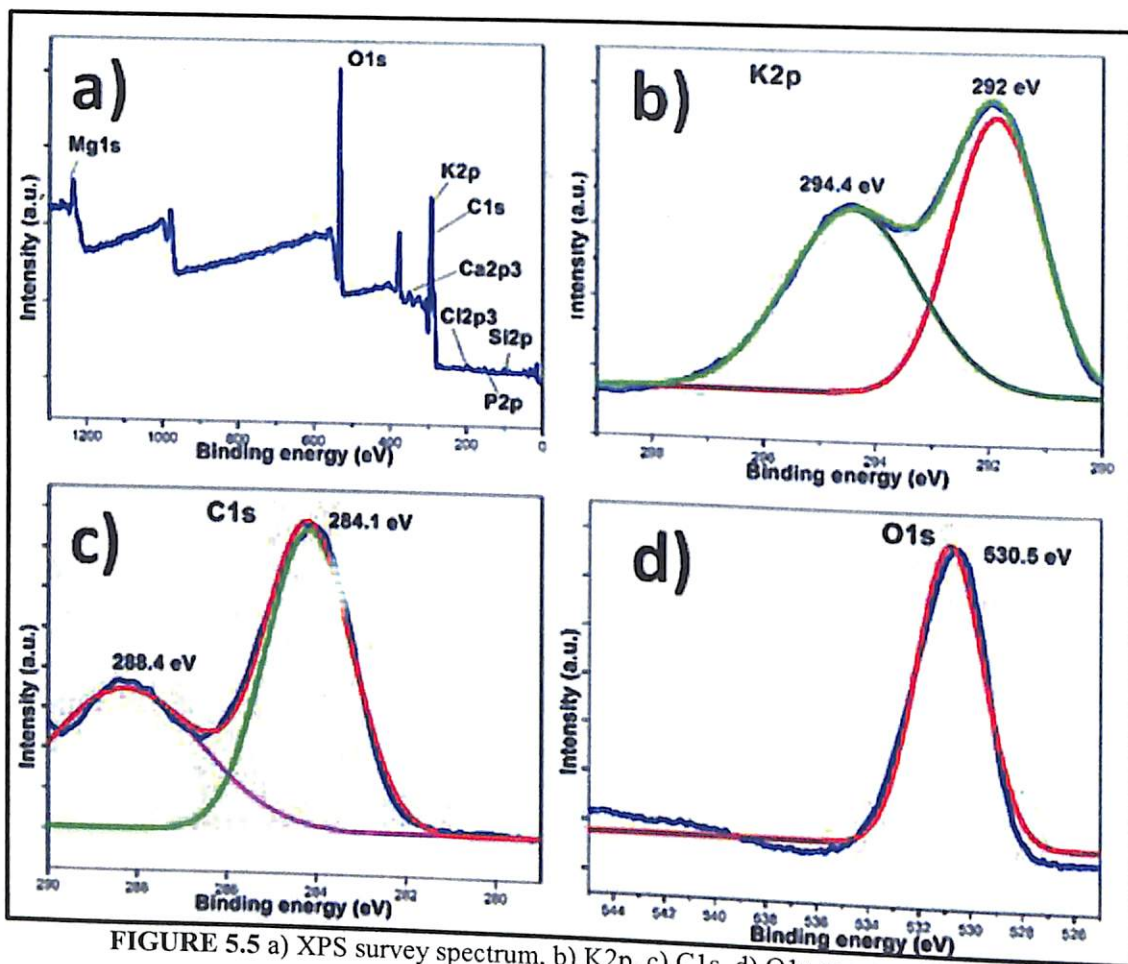
FIGURE 5.5 a) XPS survey spectrum, b) K2p, c) C1s, d) O1s spectra of MAPA

The TGA profile of the ash catalyst covering range of 0°-800 °C was presented in Fig. 5.6 which showed initial weight percent loss of 12% around 100-150 °C that can be attributed to evolution of moisture. The further decrease in mass of the catalyst around 400 °C may be mainly due to the oxidation of carbonaceous material present in the catalyst and release of $CO_2$.[48]

Results from $N_2$ adsorption-desorption analysis by BET model is presented in Fig. 5.7 which shows both $N_2$ adsorption-desorption isotherm and pore-size distribution curve (inset). The hysteresis loop can be clearly seen in the isotherm which is a characteristic feature of type-IV isotherm associated with capillary condensation in mesopores. The surface area of the catalyst was found to be 538.975 m²/g while pore volume and pore diameter are 0.522 cc/g and 3.379 nm respectively. The pore-size distribution curve (inset) depicts mesopores of very uniform sizes in the range 3-5 nm.

To investigate the surface basic strength of the catalyst, Hammett indicator method was employed using indicators like bromothymol blue, phenolphthalein, Alizarine Yellow R and 2,4,6-trinitroaniline.. It was noted from the experiment that when mixed with the catalyst, color of the first three indicators got changed but that of the 4th indicator did not change. This revealed that basic strength of the catalyst probably lie in the range of 11.0$\leq$ $H\_\leq$12.2. Also basicity of the catalyst was determined by benzoic acid titration method using bromothymol blue as indicator. The basicity was calculated to be 0.169 mmol/g which is moderate compared to many reported literature.[49,50]
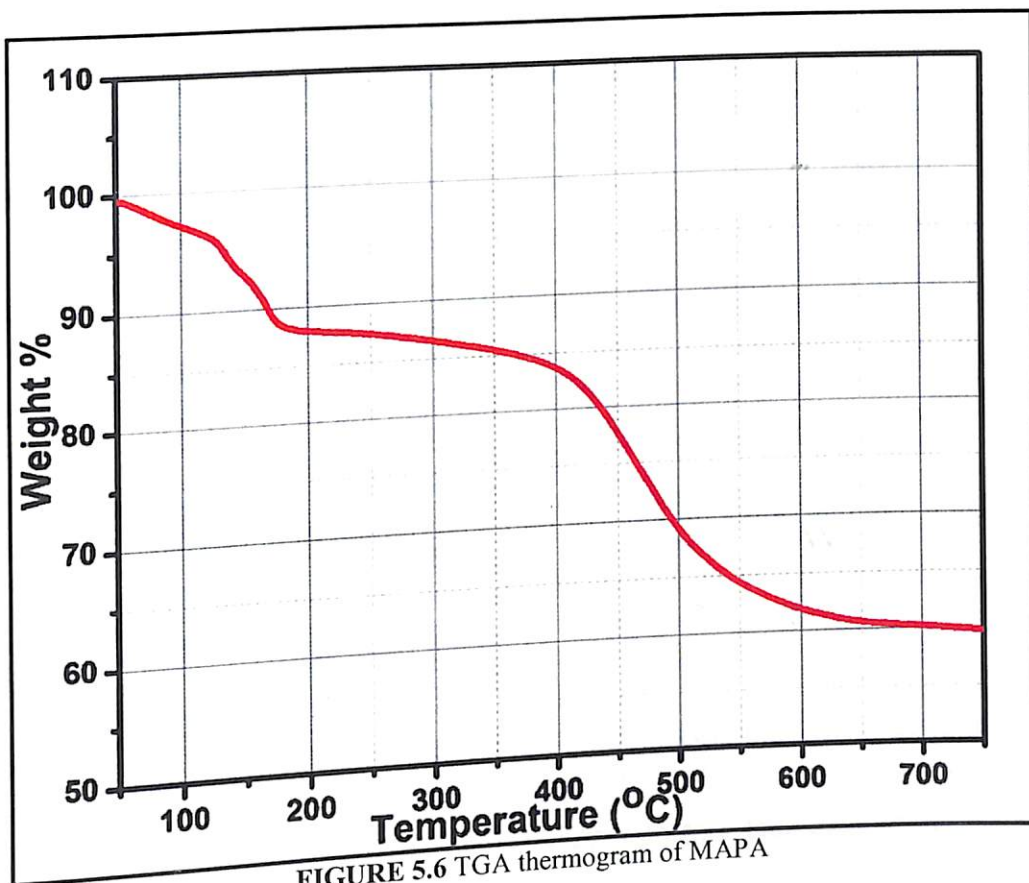
FIGURE 5.6 TGA thermogram of MAPA
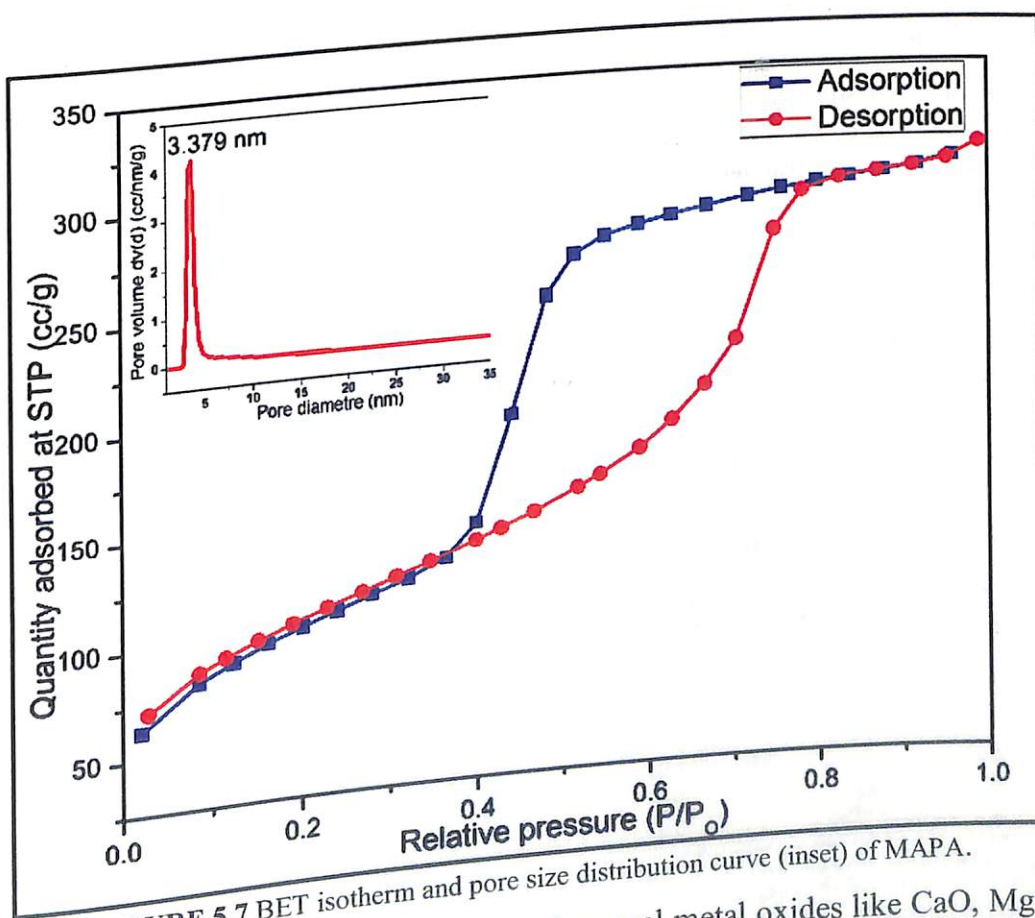


FIGURE 5.7 BET isotherm and pore size distribution curve (inset) of MAPA.

Recently, Akutu et al.[28] have examined several metal oxides like CaO, MgO, ZnO, SrO, BaO, ZrO$_2$ etc. as possible solid base catalysts and noticed that for alkaline earth metal oxides the trend for catalytic activity follows opposite the order of basicity but similar with the surface area of the oxides. So it was suggested that the abstraction of proton from

115

nitroalkane did not need strong basic strength, rather it is favorable with oxides having weak basic strength. Therefore the extremely high catalytic activity of MAPA can be justified with the high surface area (~539 m²/g) and its moderate basicity.

## 5.3.2 Henry reactions

We initially tried the Henry reaction by using the model reaction of 4-nitrobenzaldehyde and nitromethane under solvent-free condition at room temperature using *Musa acuminata* peel ash (MAPA). Formation of single, isolable β-nitroalcohol product was found to be completed within 15 minutes to generate 98% isolated yield. To our delight, no dehydrated product was observed as side product which ensured the selectivity of our method.

**TABLE 5.2** Study of the effect of nitromethane equivalence[a]

| Entry | Nitromethane (Equiv.) | Time (min) | Yield (%)[b] |
|-------|------------------------|------------|--------------|
| 1     | 0.5                    | 30         | 34           |
| 2     | 1                      | 15         | 98           |
| 3     | 2                      | 20         | 95           |
| 4     | 3                      | 20         | 92           |

[a] Aldehyde (1 mmol, 1 equiv.). [b] Isolated yield

Various solvents such as DCM, CHCl₃, THF, MeOH, EtOAc and diethyl ether were tested to examine the influence of the solvent on the model reaction. However, it was observed that solvent free reaction conditions gave best results in terms of chemical yields and reaction time.

Further, we studied the influence of nitroalkane equivalent on the reaction yield as well as the reaction time. No significant enhancement of the conversion of the reaction was observed by increasing the amount of nitroalkane to more than one equivalent (Table 5.2, entry 3 and entry 4).

The optimum catalyst loading was also investigated. Catalyst loadings of 10, 15, 20, 25 and 30 mg/mmol of substrate) were compared as shown in Table 5.3. Using 10 mg of the catalyst, the reaction took longer time (30 mins) to give low yield of the desired product (Table 5.3, entry 1). Interestingly, use of 20 mg of the catalyst gave very high yield of 98% within 15 mins (entry 4). However, the use of higher amount of the catalyst made the reaction mixture more viscous and probably due to that reason did not improve the yield (entries 5 and 6).

**TABLE 5.3** Optimization of catalyst loading[a]

| Entry | MAPA (mg) | Time (min) | Yield (%)[b] |
|-------|-----------|------------|--------------|
| 1     | 10        | 30         | 75           |
| 2     | 15        | 20         | 54           |
| 3     | 15        | 30         | 86           |
| 4     | 20        | 15         | 98           |
| 5     | 25        | 20         | 79           |
| 6     | 30        | 20         | 66           |

[a] Aldehyde (1mmol), nitromethane (1 mmol); [b] Isolated yield

After establishing the optimum condition for the Henry reaction with MAPA catalyst, we calculated the Atom economy and E-factor of the reaction. As the starting compound was taken in 1:1 molar ratio and there was no dehydrated side-product, so the

Atom economy was found to be 100% while E-factor was calculated as 0.115. These quantified results justified the sustainability and greenness of the protocol. The detailed calculation is shown below.

$$\text{Atom economy} = \frac{\text{Mass of atoms in desired product}}{\text{Mass of atoms in reactant}}$$

$$= \frac{0.212g}{(0.151+0.061)g} \times 100\% = 100\%$$

$$\text{E-factor} = \frac{\text{Total waste (g)}}{\text{Product (g)}}$$

Mass in the process = Aldehyde + Nitroalkane + Catalyst
$$= (0.151 + 0.061 + 0.020) \text{ g}$$
$$= 0.232 \text{ g}$$

Product = 0.208 g
Total waste = (0.232 - 0.208) g
$$= 0.024 \text{ g}$$

$$\text{E-factor} = \frac{0.024 \text{ g}}{0.208 \text{ g}} = 0.115$$

**TABLE 5.4:** Henry reactions of various aromatic and aliphatic aldehydes with nitromethane under solvent free conditions[a]



a, 20 m, 94%
b, 15 m, 98%
c, 20 m, 97%
d, 20 m, 97%
e, 20 m, 96%
f, 20 m, 98%
g, 25 m, 96%
h, 30 m, 90%
i, 30 m, 88%
j, 30 m, 87%
k, 30 m, 94%
l, 20 m, 92%
m, 20 m, 86%
n, 20 m, 85%
o, 15 m, 97%
p, 20 m, 97%
q, 20 m, 98%
r, 20 m, 98%
s, 25 m, 96%
t, 30 m, 93%
u, 25 m, 90%
v, 20 m, 84%
w, 25 m, 84%
x, 20 m, 90%
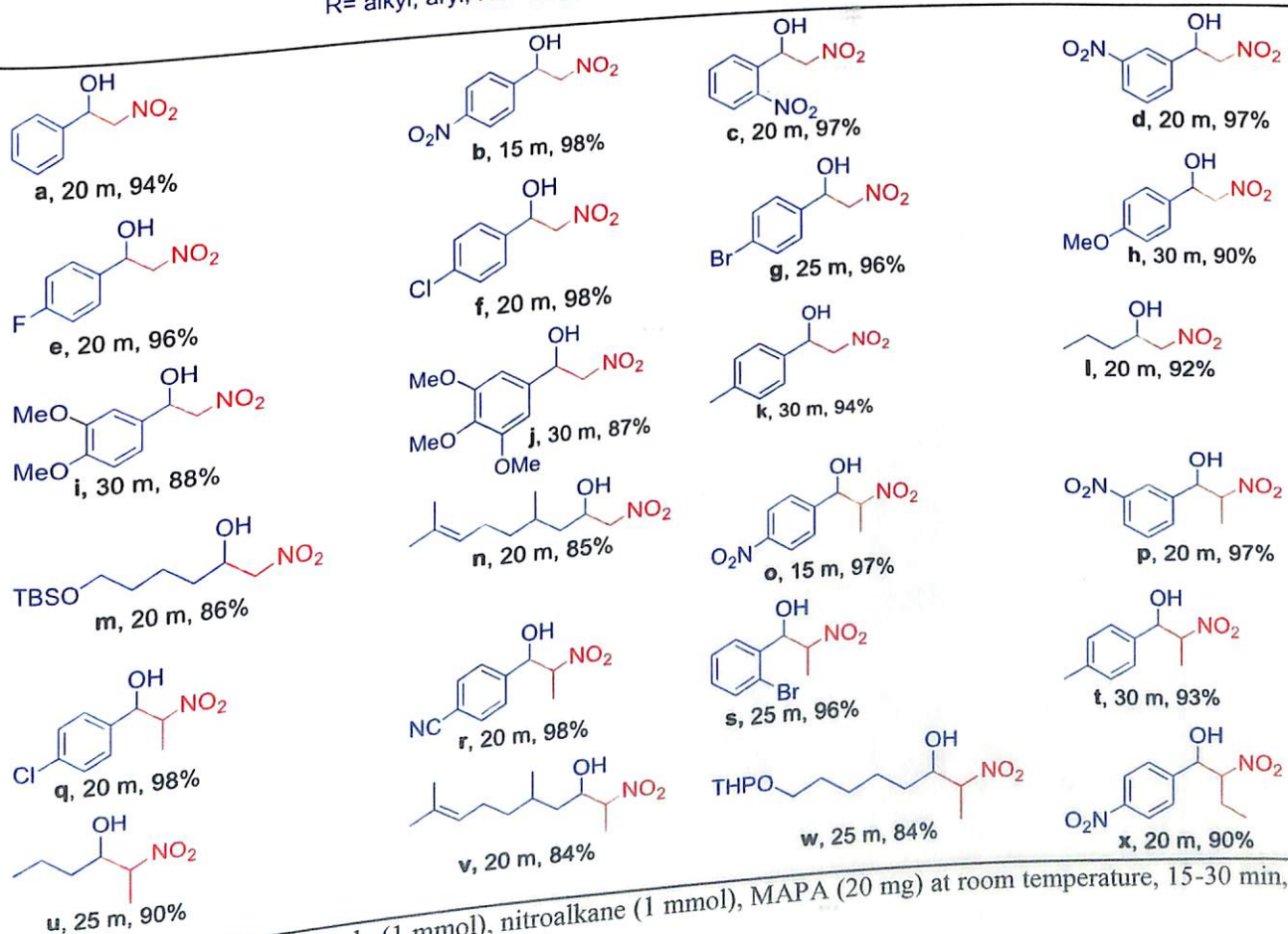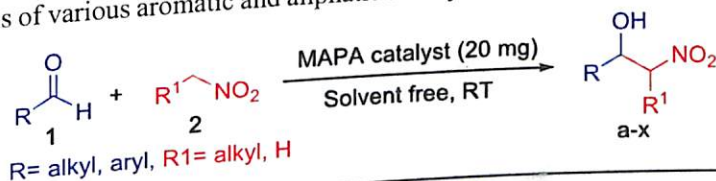
[a]Reaction conditions: Aldehyde (1 mmol), nitroalkane (1 mmol), MAPA (20 mg) at room temperature, 15-30 min, isolated yields.

117

We compared the catalytic ability of the MAPA catalyst with a variety of commercially available heterogeneous solid-base catalysts through Henry reaction of 4-Nitroaldehyde and nitromethane. MAPA exhibited excellent dominance in catalytic activity in terms of both yield and reaction time, when compared to Amberlyst-21, imidazole, L-proline and KF/ $Al_2O_3$.

To examine $K_2O$ to be the active site for Henry reaction, we opted for $K_2O$-$Al_2O_3$ catalyst system forwarded by Wang et al.[51] and compared the activity of that catalyst with MAPA keeping all reaction conditions same. Both sets of reactions were observed to give similar yield. However the reaction with catalyst MAPA took slightly less time for complete conversion than that with $K_2O$-$Al_2O_3$; which may be attributed to the synergic effect of other oxides and carbonates present in MAPA.

With the optimum reaction conditions in our hand, the reaction was generalized for diverse aldehydes to show the generality and scope of our method. The results were summarized in Table 5.4. We have found that the reaction of aldehydes with nitroalkane in the presence of MAPA catalyst gave good to excellent yields in all the cases within 15-30 minutes (Table 5.4, a-x). In general, aromatic aldehydes bearing an electron-withdrawing substituent like nitro group (-$NO_2$) (Table 5.4, b-g) undergo faster reactions while electron donating substituents such as methoxy group in the aromatic ring (Table 5.4, h-k) took longer time for complete conversion to their corresponding β-nitroalcohols. It was observed that our catalytic reaction system was tolerant to a broad functional groups such as -$NO_2$, -F, -Cl, -Br, -OMe, -CN, -$CH_3$ etc. as well as for aliphatic and olefinic aldehydes. In addition to these, common protecting groups such as -OTBS and -OTHP remained unaffected, which indicated the mild nature of our methods (Table 5.4, entry m and w).

Finally we also tried a 50 mmol scale-up of the proposed protocol of Henry reaction. 4-nitrobenzaldehyde (50 mmol) when treated with nitromethane (50 mmol) using 1g of catalyst gave the corresponding nitroalcohol product in almost quantitative yield (98%) after isolation.

### 5.3.3 Recyclability test of catalyst
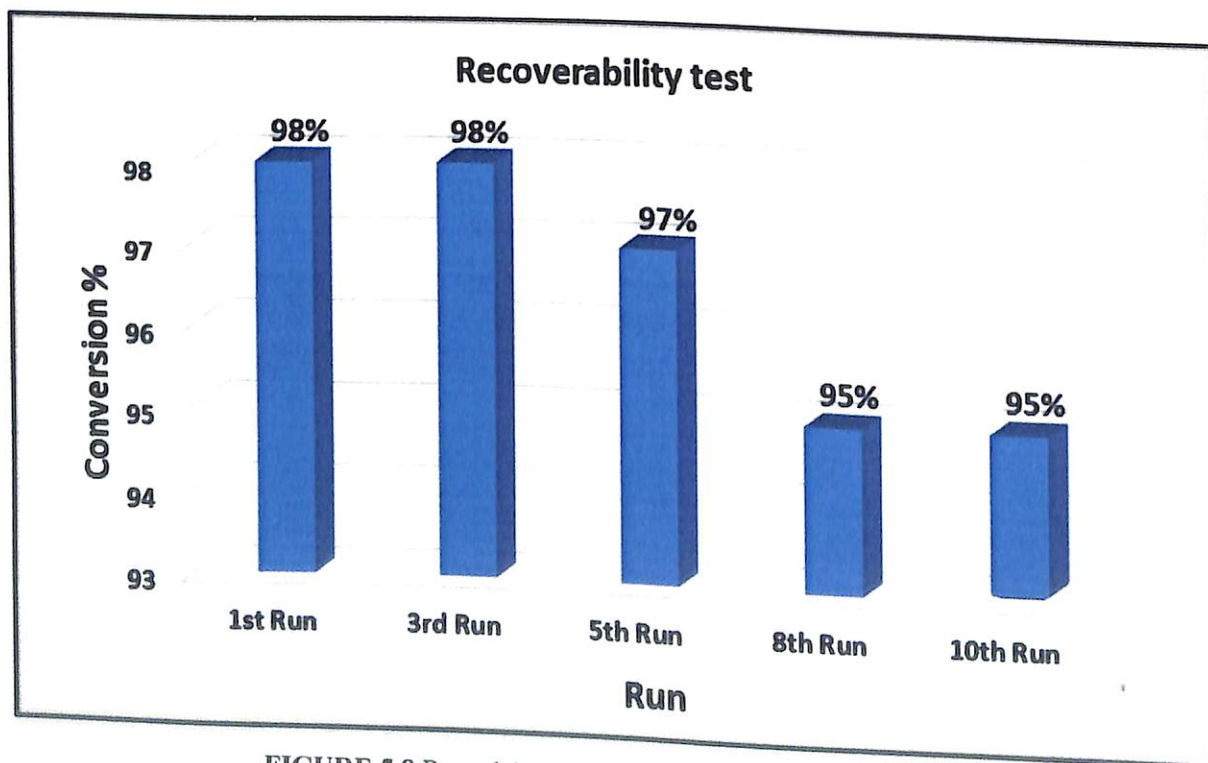


FIGURE 5.8 Recyclability test of MAPA in Henry reactions
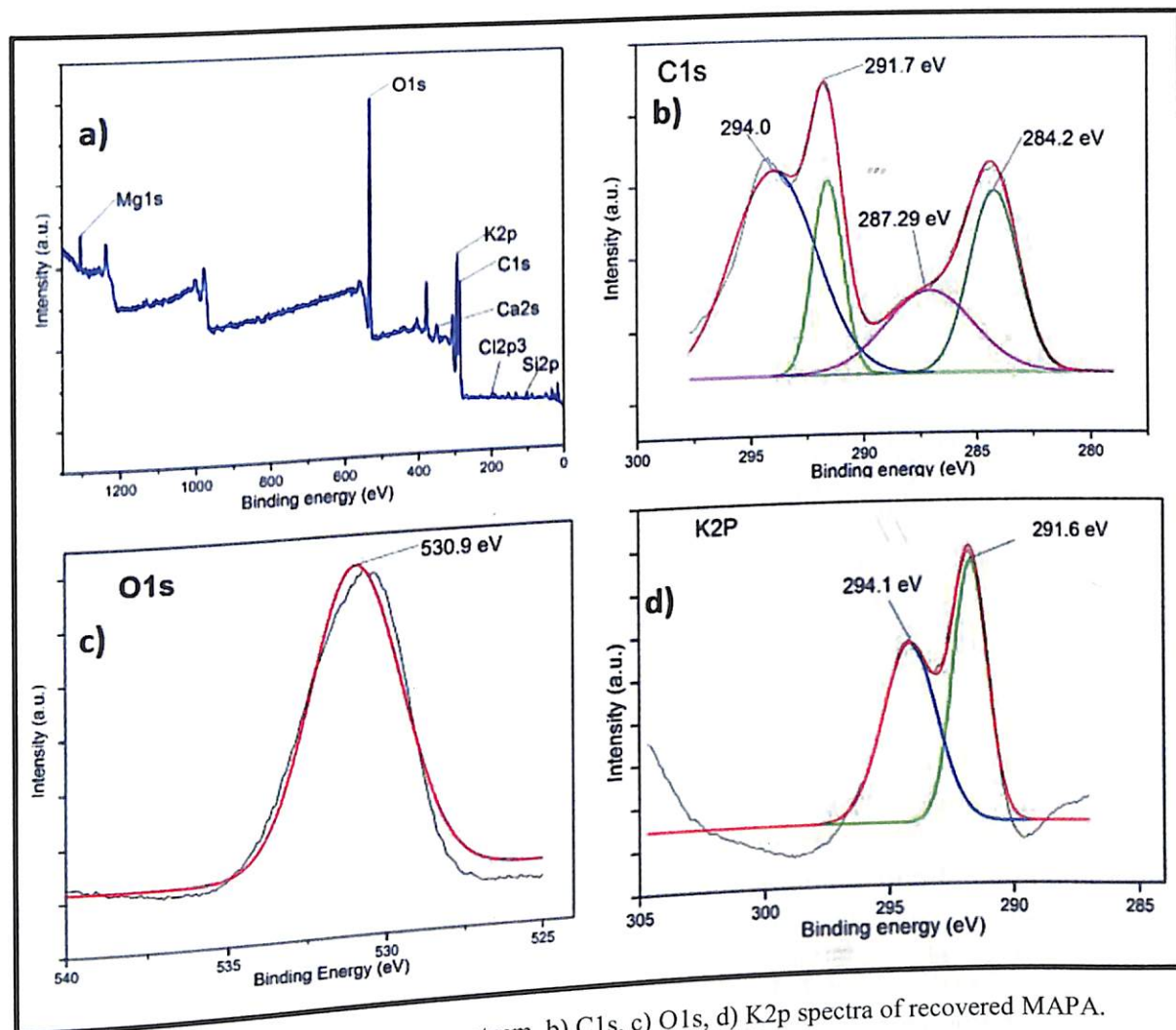
**FIGURE 5.9** a) XPS survey spectrum, b) C1s, c) O1s, d) K2p spectra of recovered MAPA.

The recyclability of MAPA was investigated with consecutive Henry reaction using different substrates. Fig. 5.8 depicted the results of consecutive runs performed by reusing the catalyst under our optimal reaction conditions. Negligible depreciations of catalytic performance were observed in all the test reactions even after ten catalytic cycles. XRF, XPS, XRD, EDS, TEM and SEM analysis of the recovered catalyst was also investigated which revealed no appreciable change in morphology and chemical composition of MAPA even after 10th cycle of reused.

The XRF study of the recycled catalyst displayed 64.76% of $K_2O$) which was only 0.35% less than that of the fresh catalyst. In XPS analysis of the recovered catalyst, the atomic wt% of K has slightly decreased from 12.18% to 10.88% only. The wide scan spectrum and deconvulated spectra of C1s, O1s and K2p were shown in Fig. 5.9 which are as similar as the fresh one. EDX study shows that the wt% of K and O of fresh catalyst was 20% and 40% respectively while in the recovered catalyst the wt% of the same are 13% and 27%, (Fig. 5.10).

All these results suggest very little leaching of the major catalytic active sites of MAPA even after the 10 successive cycles. The small declination of catalytic activity can be explained by this little leaching of $K_2O$ which also gives evidence for $K_2O$ to be major active site of the catalyst. The TEM, SEM images (Fig: 5.11) and XRD diagram (Fig. 5.3(ii)), of the recovered catalyst also provided evidence for retaining similar morphology and chemical composition to that of the fresh catalyst.
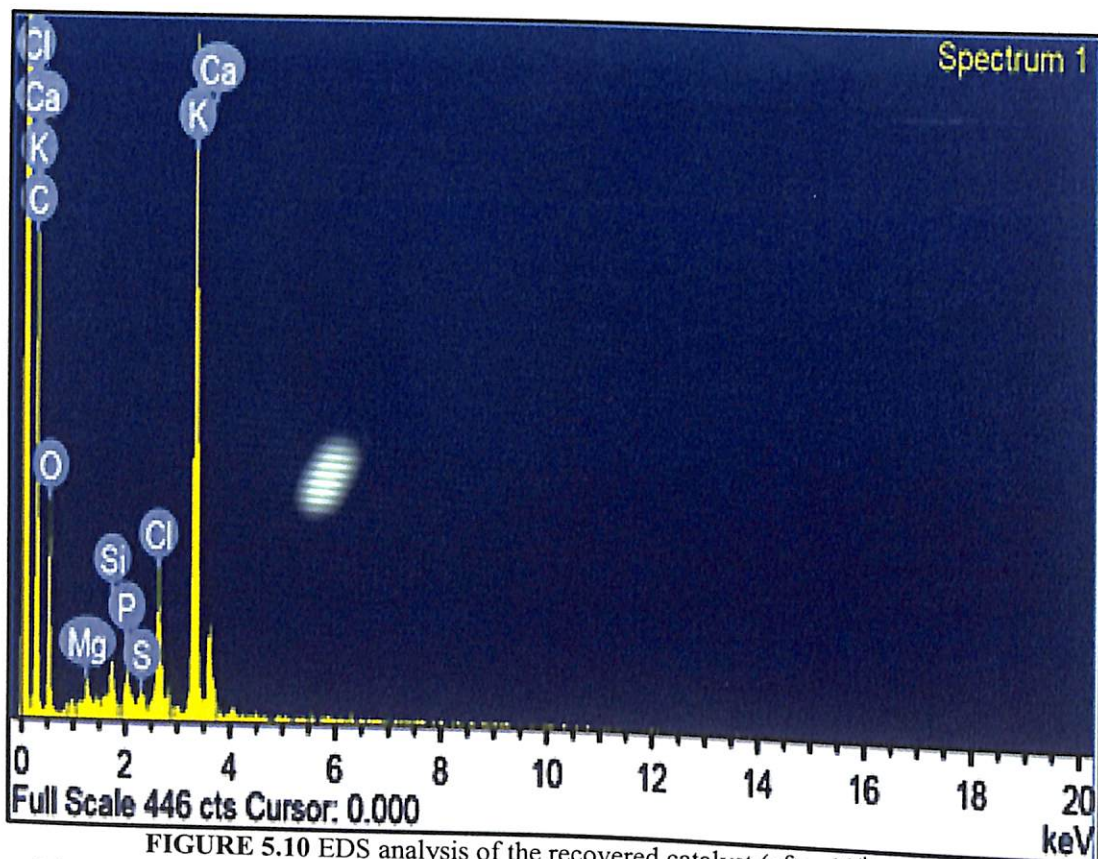
**FIGURE 5.10** EDS analysis of the recovered catalyst (after 10th cycle).

The heterogeneous nature of the catalyst was examined by hot filtration method where after 5 minutes of the reaction (yield was 40% at that time) the catalyst was separated by centrifugation. The decanted reaction mixture was then continued to stir for another 6 hours, but no progress of reaction and enhancement of yield was observed afterwards. Accordingly, it was concluded that no leaching of active metallic sites from catalyst surface took place into the reaction medium. This also confirms the heterogeneity of the catalyst.
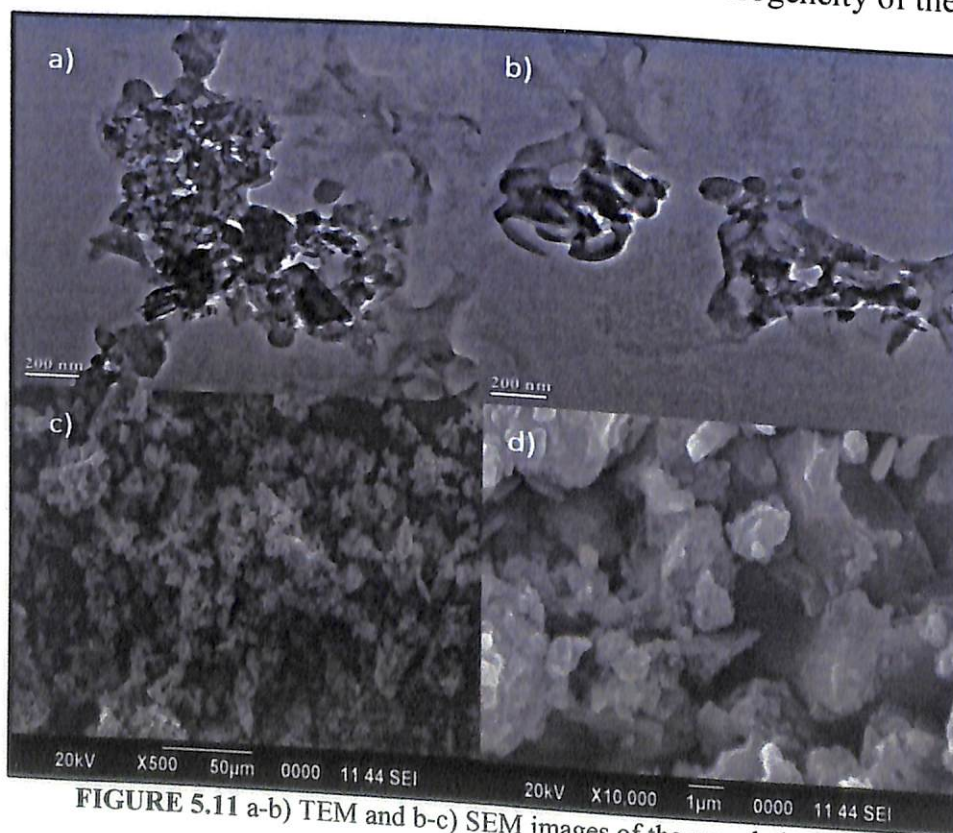


**FIGURE 5.11** a-b) TEM and b-c) SEM images of the recycled catalyst.

### 5.3.4 Spectroscopic data of synthesized compounds

**2-nitro-1-(4-nitrophenyl)ethan-1-ol (Table 5.4, entry b)**

Brown solid, $^1$H NMR (CDCl$_3$, 400 MHz): δ 3.60 (1H, s), δ 4.61 (2H, d, J= 20 Hz), δ 5.62(1H, m), δ 7.61 (2H,d, J=8Hz), δ 8.21 (2H, d, J=7.6 Hz); $^{13}$C NMR (CDCl$_3$, 125 MHz): δ 69.98, , 124.13, 127.01, 129.67, 145.31, 147.95; IR (KBr pellet, v$_{max}$/cm$^{-1}$): 3320, 3075, 2965, 2885, 1608,1532, 1508, 1430, 1358, 1320, 1112, 1058, 765, 654.

**2-nitro-1-(3-nitrophenyl)ethanol (Table 5.4, entry d)**

Yellow solid, $^1$H NMR (CDCl$_3$, 400 MHz): δ1.25 (1H, s), δ 4.49-4.71 (2H, m), δ5.61-5.64 (1H, m), δ7.61 (1H, t, J=8 Hz), δ7.79 (1H, d, J=8 Hz), δ8.19 (1H, d, J=8 Hz), δ8.31 (1H, s); $^{13}$C NMR (CDCl$_3$, 125 MHz): δ 69.84, 121.14, 123.77, 124.14 130.14, 132.15, 140.35, 148.45; IR (KBr pellet, v$_{max}$/cm$^{-1}$): v 33   04,   3075,   2956, 2870, 1612,1545, 1511, 1437, 1368, 1329, 1095, 1058, 775, 668.

**1-(4-methoxyphenyl)-2-nitroethan-1-ol (Table 5.4, entry h)**

Yellow liquid, $^1$H NMR (CDCl$_3$, 400 MHz): δ 2.92 (1H, s), δ 3.80 (3H, s), δ 4.46 (1H, d, J=12.4 Hz) ; δ 4.58 (1H, t, J=10 Hz), δ 5.382(1H,d, J=8 Hz), δ 6.90 (2H, d, J= 7.6 Hz), δ 7.30 (2H, d, J=7.2 Hz); $^{13}$C NMR (CDCl$_3$, 125 MHz): δ 55.35, 70.65, 114.35, 127.3, 128.55, 130.55, 159.96; IR (KBr pellet, v$_{max}$/cm$^{-1}$): 3378, 3083, 2943, 2896, 2780, 1612, 1536, 1425, 1182, 1050, 790, 663.

**2-nitro-1-(3,4,5-trimethoxyphenyl)ethan-1-ol  (Table 5.4, entry j)**

Brown solid, $^1$H NMR (CDCl$_3$, 400 MHz): δ 1.25 (1H, s), δ 3.82 (3H, s), δ 3.86 (6H, s), δ 4.482– 4.631 (2H, m), δ 5.38-5.41 (1H, m), δ 6.60 (2H, s); $^{13}$C NMR (CDCl$_3$, 125 MHz): δ 56.13, 60.85, 102.69, 133.97, 137. 93, 139.33, 153.58; IR (KBr pellet, v$_{max}$/cm$^{-1}$): 3308, 3025, 2960, 2856, 2775, 1608, 1556, 1423, 1110, 1043, 771.

**2-nitrohexan-3-ol (Table 5.4, entry u)**

Light yellow liquid, $^1$H NMR (CDCl$_3$, 400 MHz): δ 0.95- 0.98 (3H, m), δ 1.38-1.46 (4H, m), δ 2.047 (3H, d, J=4.4), δ 2.69 (1H, s), δ 3.90-3.94 (1H, m), δ 4.18-4.20 (1H, m); $^{13}$C NMR (CDCl$_3$, 125 MHz): δ 13.74, 16.12, 18.35, 34.91, 71.8, 86.41; IR (KBr pellet, v$_{max}$/cm$^{-1}$): 3306, 2946, 2830, 1608, 1536, 1206, 1148, 1035, 838, 755.

**2-nitro-7-((tetrahydro-2H-pyran-2-yl)oxy)heptan-3-ol (Table 5.4, entry w)**

Light yellow liquid, $^1$H NMR (CDCl$_3$, 400 MHz): δ 1.39-1.85 (17H, m) , δ 2.51 (1H, s), δ 3.37-3.43 (2H, m), δ 3.48-3.53 (1H, m), δ 3.63-3.78 (2H,m), δ 3.85-3.95 (1H, m), δ 4.48-4.56 (1H, m); $^{13}$C-NMR (100 MHz, CDCl$_3$, TMS): δ 10.1, 10.2, 17.6, 18.6, 18.7, 20.0, 20.3, 25.14, 25.19, 25.3, 25.7, 28.4, 25.7, 28.6, 28.8, 29.1, 35.7, 36.1, 37.6, 37.8, 40.1, 40.4, 69.8 70.1, 70.8, 71.1, 86.8, 87.9, 88.4, 124.3, 131.5, 131.6; IR (KBr pellet, v$_{max}$/cm$^{-1}$): 3310, 3016, 2940, 1656, 1530, 1403, 1350, 1180, 875, 761.

### 5.4 Conclusion

In conclusion, bio-waste *Musa acuminata* banana peel ash was used as a readily available, low-cost, renewable and non-toxic catalyst for the synthesis of β-nitroalcohols *via* Henry reaction at room temperature under solvent free conditions. The catalyst was well-

characterized by various spectroscopic and analytic techniques to obtain knowledge about its possible structure, composition and morphology. The catalyst can be easily recovered, and reused at least 10 times without any noticeable loss in its catalytic activities. Further, the ash catalyst is environmental friendly and eliminate any imminent disposal problem. The amenability to scale-up the protocol also makes it a convenient and competitive green heterogeneous catalyst for industrially important Henry reaction.

# References

1. C. O. Tuck, E. Pérez, I. T. Horváth, R. A. Sheldon and M. Poliakoff, *Science* 2012, **337**, 695-699.
2. C. S. K. Lin, L. A. Pfaltzgraff, L. Herrero-Davila, E. B. Mubofu, S. Abderrahim, J. H. Clark, A. A. Koutinas, N. Kopsahelis, K. Stamatelatou, F. Dickson, S. Thankappan, Z. Mohamed, R. Brocklesby and R. Luque, *Energy Environ. Sci.* 2013, **6**, 426-464.
3. J. A. Bennett, K. Wilson and A. F  ee, *J. Mater. Chem. A* 2016, **4**, 3617-3637.
4. R. A. Sheldon, *Green Chem.* 2014, **16**, 950-963.
5. A. V. Bridgwater, *Biomass and Bioenergy* 2012, **38**, 68-94.
6. S. H. Y. S. Abdullah, N. H. M. Hanapi, A. Azid, R. Umar, H. Juahir, H. Khatoon and A. Endut, *Renew. Sustain. Energy Rev.* 2017, **70**, 1040-1051.
7. L. A. Pfaltzgraff, M. De bruyn, E. C. Cooper, V. Budarin and J. H. Clark, *Green Chem.* 2013, **15**, 307.
8. C. G. S. Lima, J. L. Monteiro, T. de M. Lima, M. Weber Paixão, and A. G. Corrêa, *ChemSusChem* 2018, **11**, 25-47.
9. M. Poliakoff and P. Licence, *Nature* 2007, **450**, 810-813.
10. J. Song, B. Zhou, H. Zhou, L. Wu, Q. Meng, Z. Liu and B. Han, *Angew. Chem. Int. Ed.* 2015, **54**, 9399-9403.
11. Y. Gu and F. Jérôme, *Chem. Soc. Rev.* 2013, **42**, 9550-9570.
12. M. Hara, T. Yoshida, A. Takagaki, T. Takata, J. N. Kondo, S. Hayashi and K. Domen, *Angew. Chem. Int. Ed.* 2004, **43**, 2955 –2958.
13. H. Yu, S. Niu, C. Lu, J. Li and Y. Yang, *Fuel* 2017, **208**, 101–110.
14. D. Zeng, Q. Zhang, S. Chen, S. Liu and G. Wang, *Microporous Mesoporous Mater.* 2016, **219**, 54-58.
15. K. Ngaosuwan, J. G. Goodwin and P. Prasertdham, *Renewable Energy* 2016, **86**, 262–269.
16. F. Ezebor, M. Khairuddean, A. Z. Abdullah and P. L. Boey, *Energy* 2014, **70**, 493-503.
17. W. Y. Lou, Q. Guo, W. J. Chen, M. H. Zong, H. Wu and T. J. Smith, *ChemSusChem* 2012, **5**, 1533-1541.
18. H. Y. Chen and Z. W. Cui, *Catalysts* 2016, **6**, 211- 224.
19. J. Boroa, D. Dekaa and A. J. Thakur, *Renewable Sustainable Energy Rev.* 2012, **16**, 904– 910.
20. B. Sahoo, D. Formenti, C. Topf, S. Bachmann, M. Scalone, K. Junge and M. Beller, *ChemSusChem* 2017, **10**, 3035-3039.
21. Y. Morioka, A. Matsuoka, K. Binder, B. R. Knappett, A. E. H. Wheatley and H. Naka, *Catal. Sci. Technol.* 2016, **6**, 5801-5805.
22. J. Song, B. Zhou, H. Liu, C. Xie, Q. Meng, Z. Zhang and B. Han, *Green Chem.* 2016, **18**, 3956-3961.
23. M. Balakrisnan, V. S. Batra, J. S. J. Hargreaves, and I. D. Pulfordb, *Green Chem.* 2011, **13**, 16-24.
24. B. Sahoo, D. Formenti, C. Topf, S. Bachmann, M. Scalone, K. Junge and M. Beller, *ChemSusChem* 2017, **10**, 3035-3039.
25. D. C. Deka and S. Basumatary, *Biomass Bioenergy* 2011, **305**, 1797-803.
26. R. Chakraborty, S. Chatterjee, P. Mukhopadhyay and S. Barman, *Procedia Environ. Sci.* 2016, **35**, 546-554.
27. I. B. Laskar, K. Rajkumari, R. Gupta, S. Chatterjee, B. Paul and L. Rokhum, *RSC Adv.* 2018, **8**, 20131- 20142.
28. K. Akutu, H. Kabashima, T. Seki and H. Hattori, *Appl. Catal. A Gen.* 2003, **247**, 65–74.

29. V. J. Bulbule, V. H. Deshpande, S. Velu, A. Sudalai, S. Sivasankar and V. T. Sathe, *Tetrahedron* 1999, **55**, 9325.
30. L. C. R Henry, *Hebd. Seances. Acad. Sci.* 1895, **120**, 1265.
31. R. Ballini, G. Bosica and P. Forconi, *Tetrahedron* 1996, **52**, 1677-1684.
32. D. Seebach, A. K. Beck, T. Mukhopadhyay and E. Thomas, *Helv. Chim. Acta* 1982, **65**, 1102.
33. J. Boruwa, N. Gogoi, P. P. Saikia and N. C. Barua, *Tetrahedron: Asymmetry* 2006, **17**, 3315–3326.
34. A. Karmakar, S. Hazra, M. F. C. Guedes da Silva, A. Paul and A. J. L. Pombeiro, *CrystEngComm* 2016, **18**, 1337–1349.
35. L. X. Shi and C. D. Wu, *Chem. Commun.* 2011, **47**, 2928–2930.
36. F. A. Luzzio, *Tetrahedron* 2001, **57**, 915-945.
37. J. M. Mélot, F. T. Boullet and A. Foucaud, *Tetrahedron Lett.* 1986, **27**, 493-496.
38. R. Ballini, G. Bosica, D. Livi, A. Palmieri, R. Maggi and G. Sartori, *Tetrahedron Lett.*, 2003, **44**, 2271–2273.
39. M. Gupta, D. De, S. Pal, T. K. Pal and K. Tomar, *Dalton Trans.*, 2017, **46**, 7619-7627.
40. P. T. Anastas and J. C. Warner, *Green Chem. Theory Pract.* 1998, 30.
41. D. Das, G. Pathak and L. Rokhum, *RSC Adv.* 2016, **6**, 104154–104163.
42. L. Rokhum and G. Bez, *Can. J. Chem.* 2013, **91**, 300-306.
43. G. Pathak, D. Das, K. Rajkumari and L. Rokhum, *Green Chem.* 2018, **20**, 2365-2373.
44. R. Goyal, S. Sameer, B Sarkar, A. Bag, N. Singhal, and A. Bordoloi, *Chem. Eur. J.* 2017, **23**, 16555-16565.
45. M. Sharma, A. A. Khan, S. K. Puri and D. K. Tuli, *Biomass and Bioenergy* 2012, **41**, 94-106.
46. H. Li, S. Niu, C. Lu, M. Liu and M. Huo, *Energy Convers. Manag.* 2014, **86**, 1110-1117.
47. J. Zhang, R. Zhang and J. Bi, *Catal. Commun.* 2016, **79**, 1-5.
48. P. Knutsson, V. Cantatore, M. Seemann, P. L. Tam and I. Panas, *Appl. Catal. B.* 2018, **229**, 88-95.
49. W. Xie and H. Li, *J. Mol. Catal. A Chem.* 2006, **255**, 1-9.
50. G. E. G. Mucino, R. Romero, I. G. Orozcoa, A. R. Serranob, R. B. Jiméneza, R. Natividad, *Catal. Today* 2016, **271**, 220-226.
51. S. Wang, J. Li, W. Yang, Y. Yin and Zi-Hui Xie, *Synth. Commun.* 2004, **34**, 829-834.
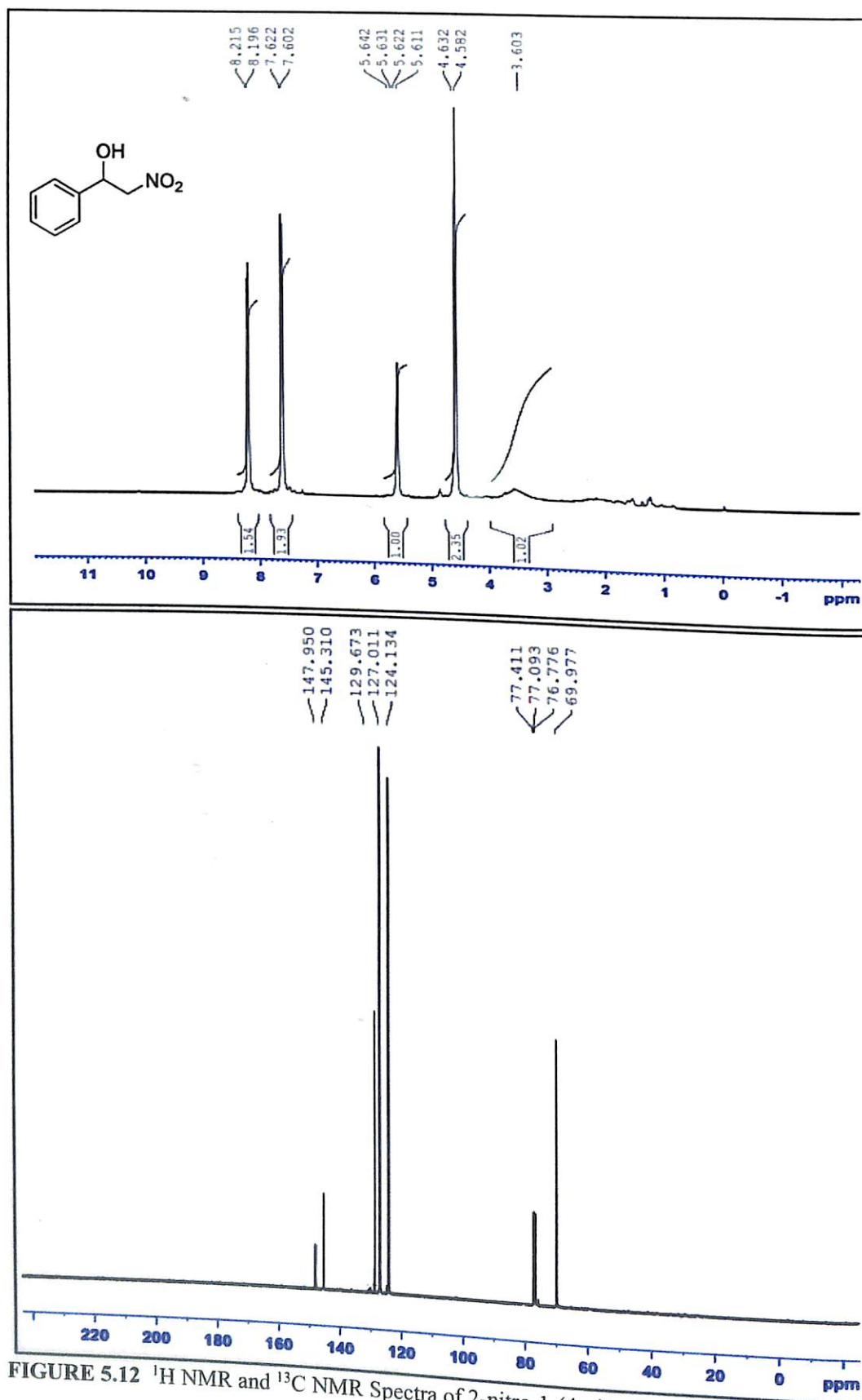
FIGURE 5.12 ¹H NMR and ¹³C NMR Spectra of 2-nitro-1-(4-nitrophenyl)ethanol (Table 5.4, Entry b)
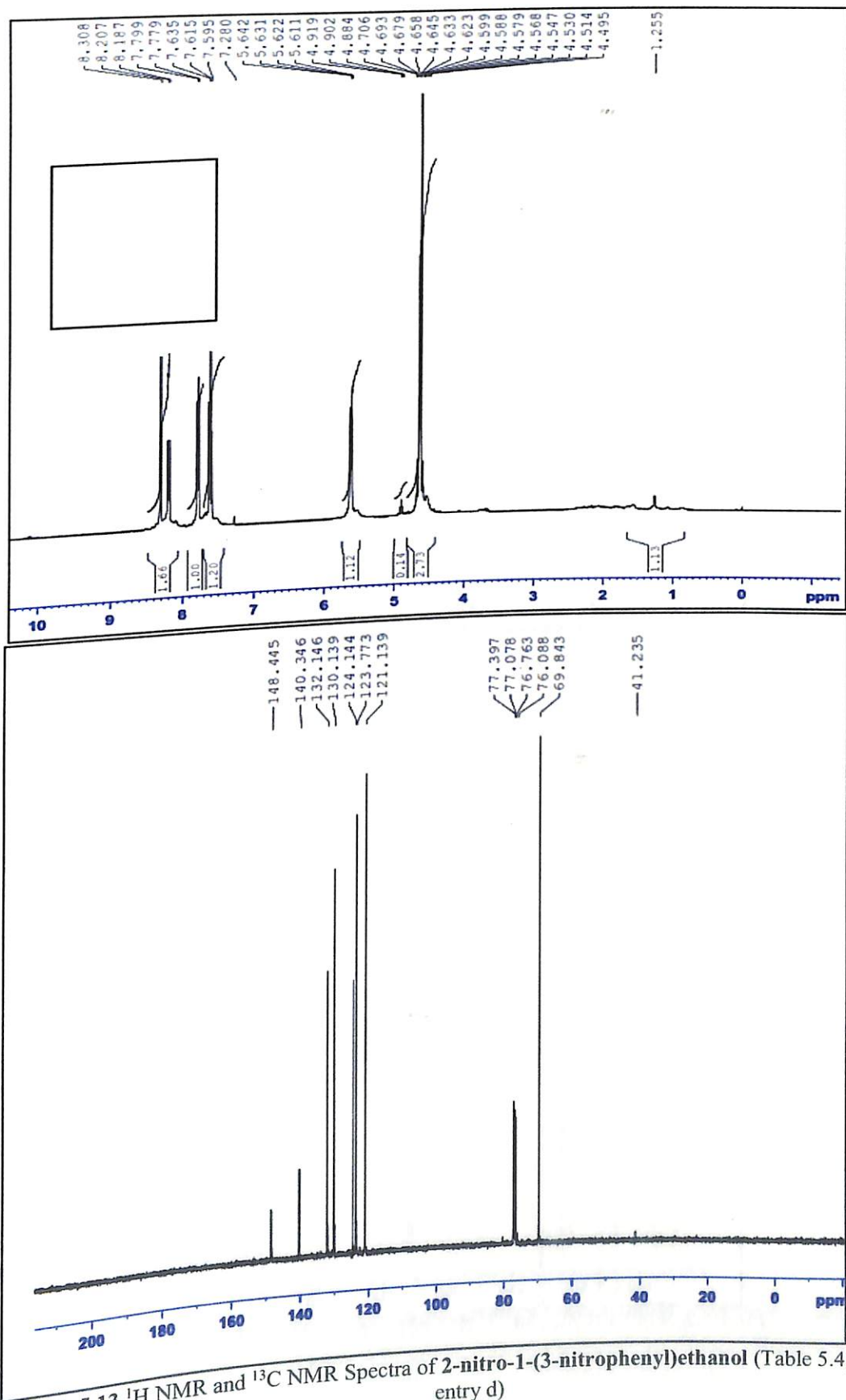
FIGURE 5.13 $^1$H NMR and $^{13}$C NMR Spectra of **2-nitro-1-(3-nitrophenyl)ethanol** (Table 5.4, entry d)
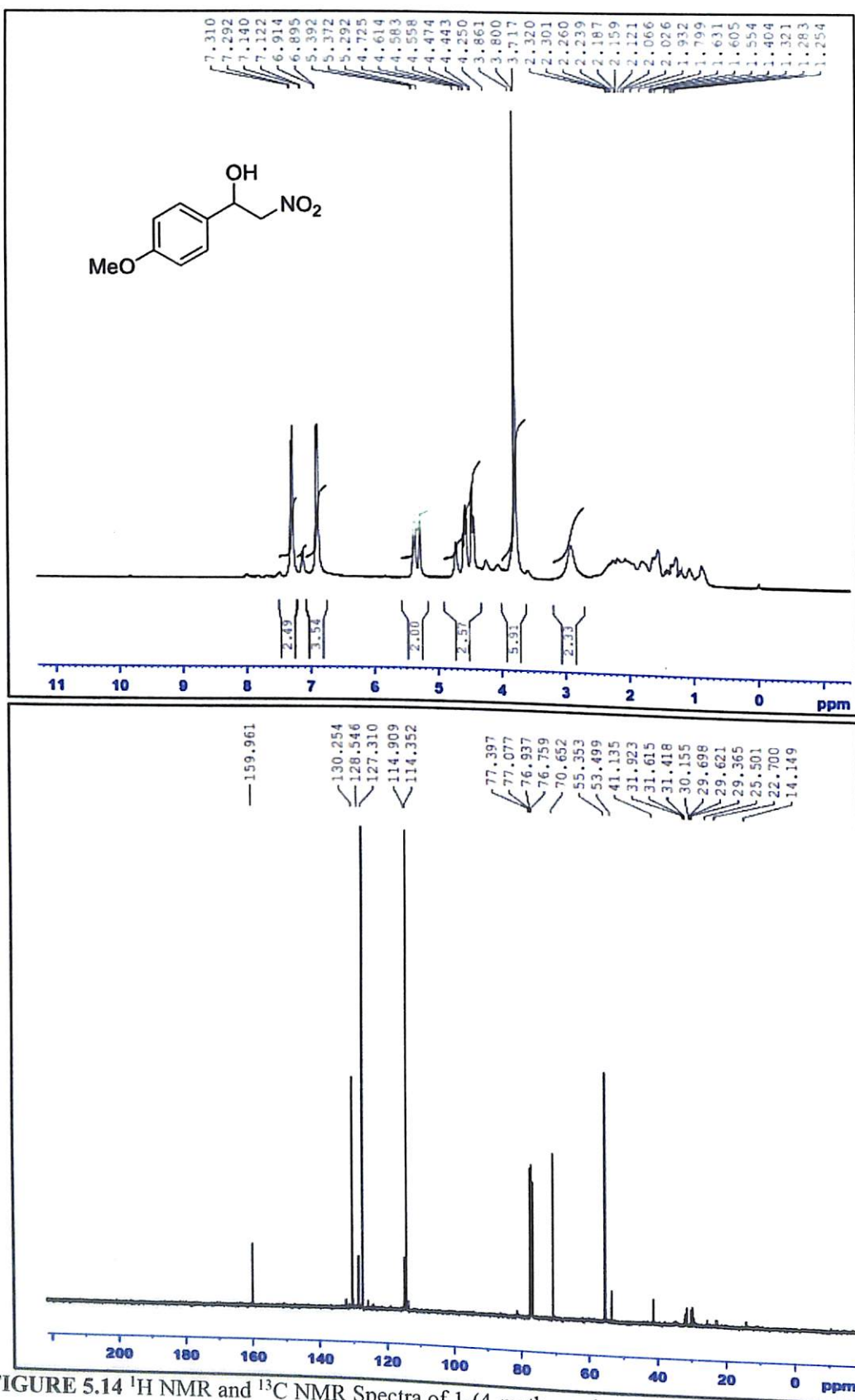
FIGURE 5.14 $^{1}$H NMR and $^{13}$C NMR Spectra of 1-(4-methoxyphenyl)-2-nitroethan-1-ol (Table 5.4, entry h)

126
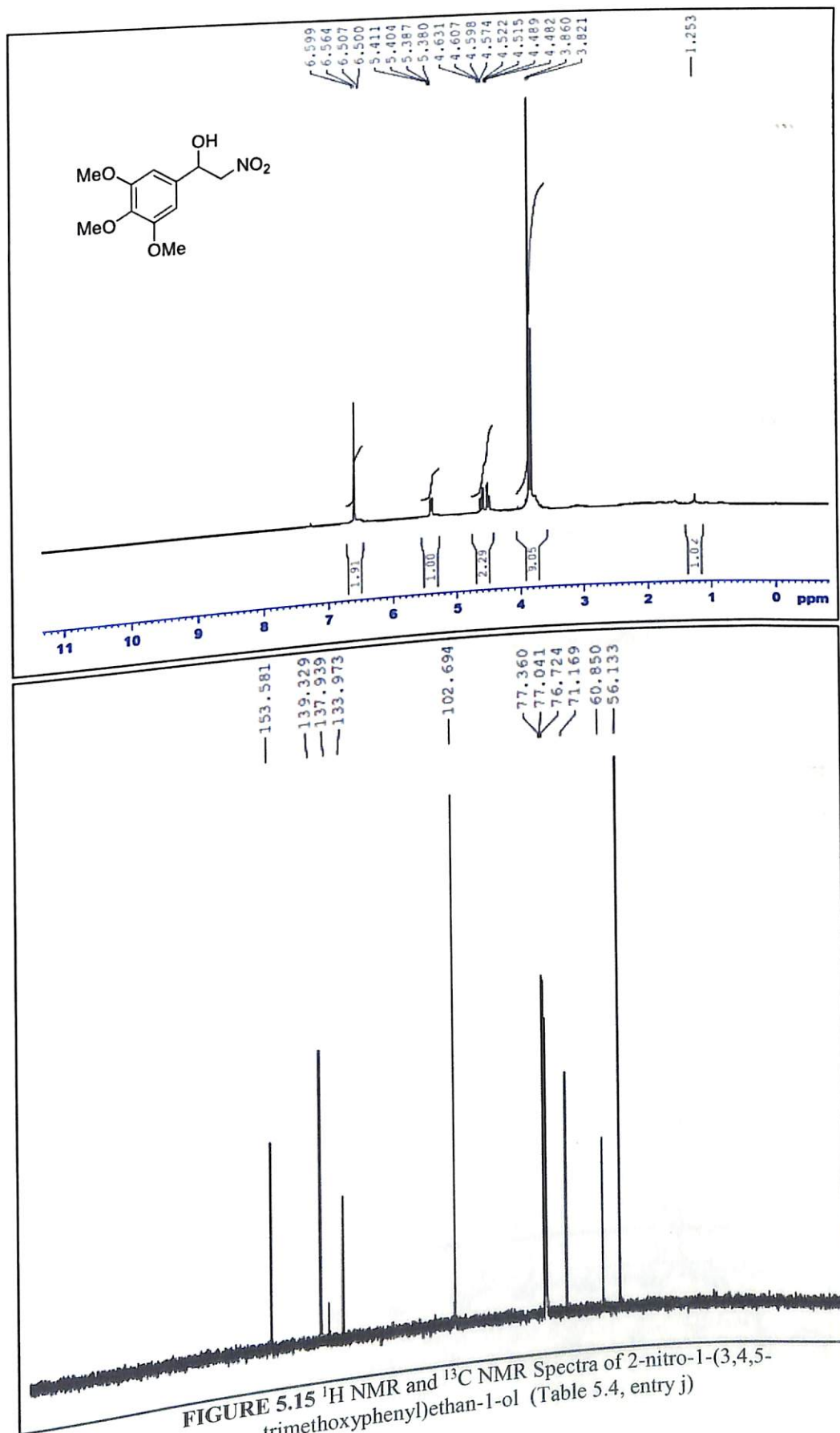
**FIGURE 5.15** $^1$H NMR and $^{13}$C NMR Spectra of 2-nitro-1-(3,4,5-trimethoxyphenyl)ethan-1-ol (Table 5.4, entry j)

127

FIGURE 5.16 ¹H NMR and ¹³C NMR Spectra of 2-nitrohexan-3-ol (Table 5.4, entry u)

128
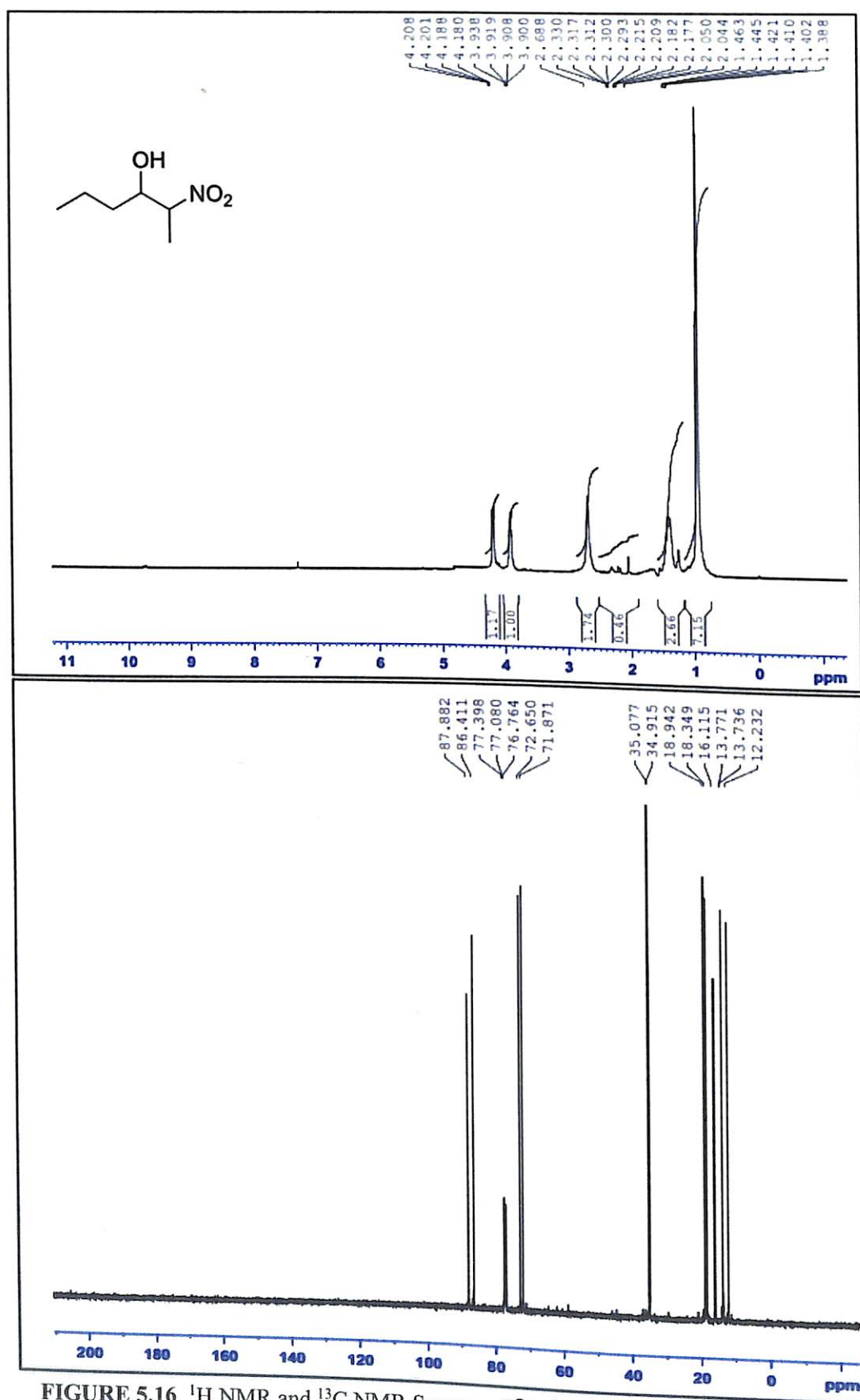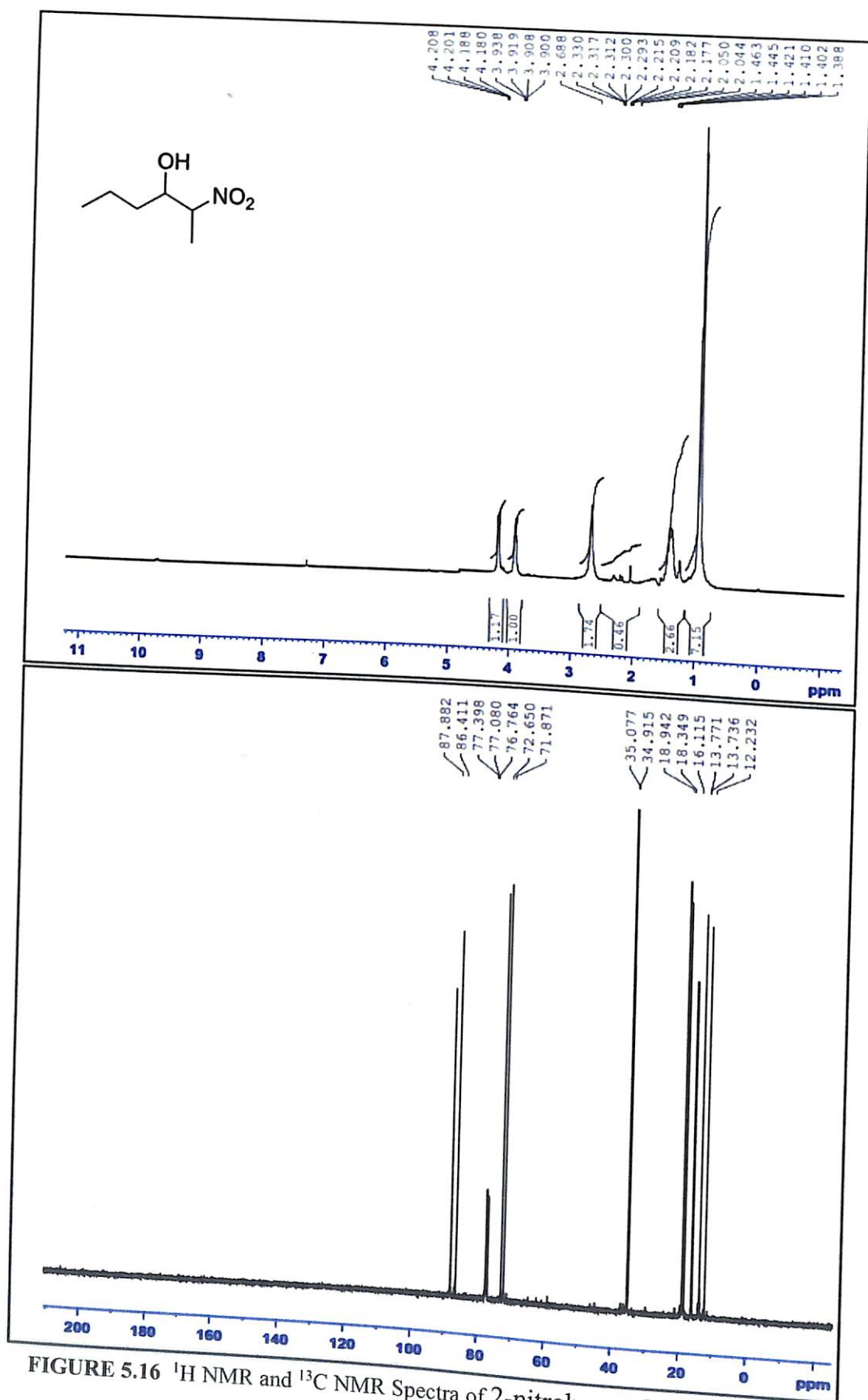
FIGURE 5.16 ¹H NMR and ¹³C NMR Spectra of 2-nitrohexan-3-ol (Table 5.4, entry u)
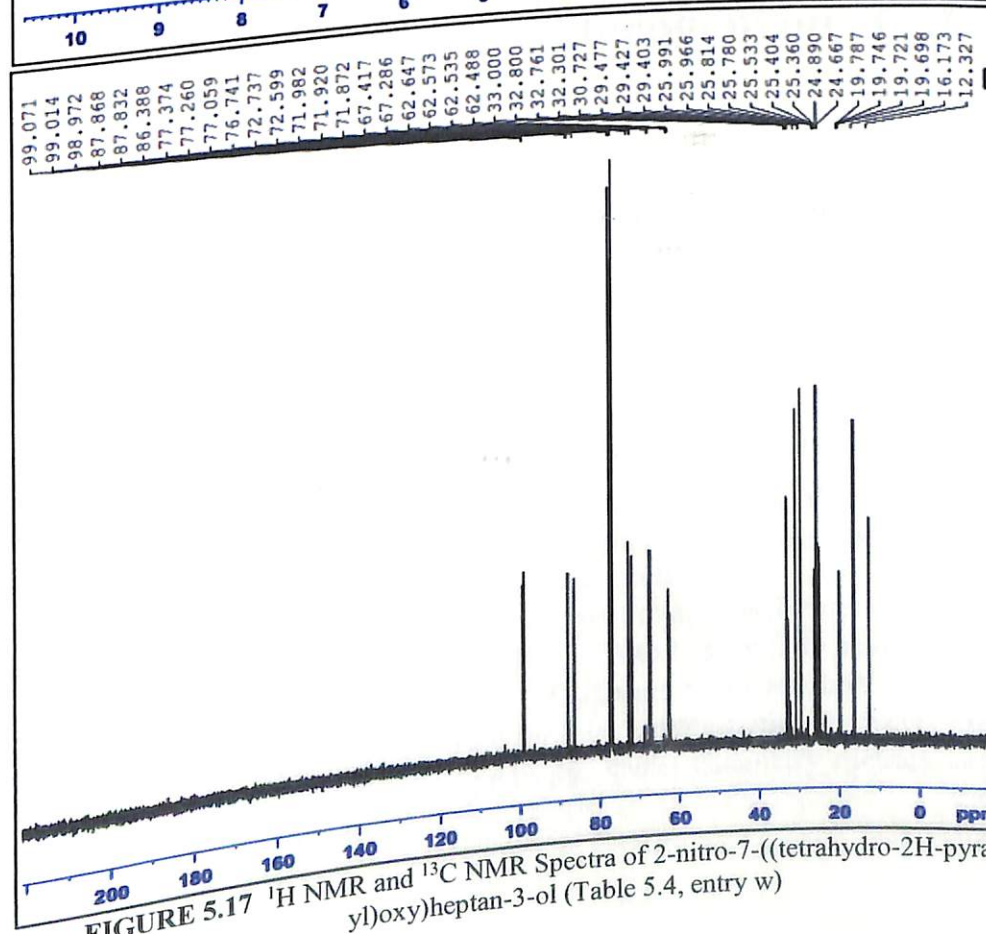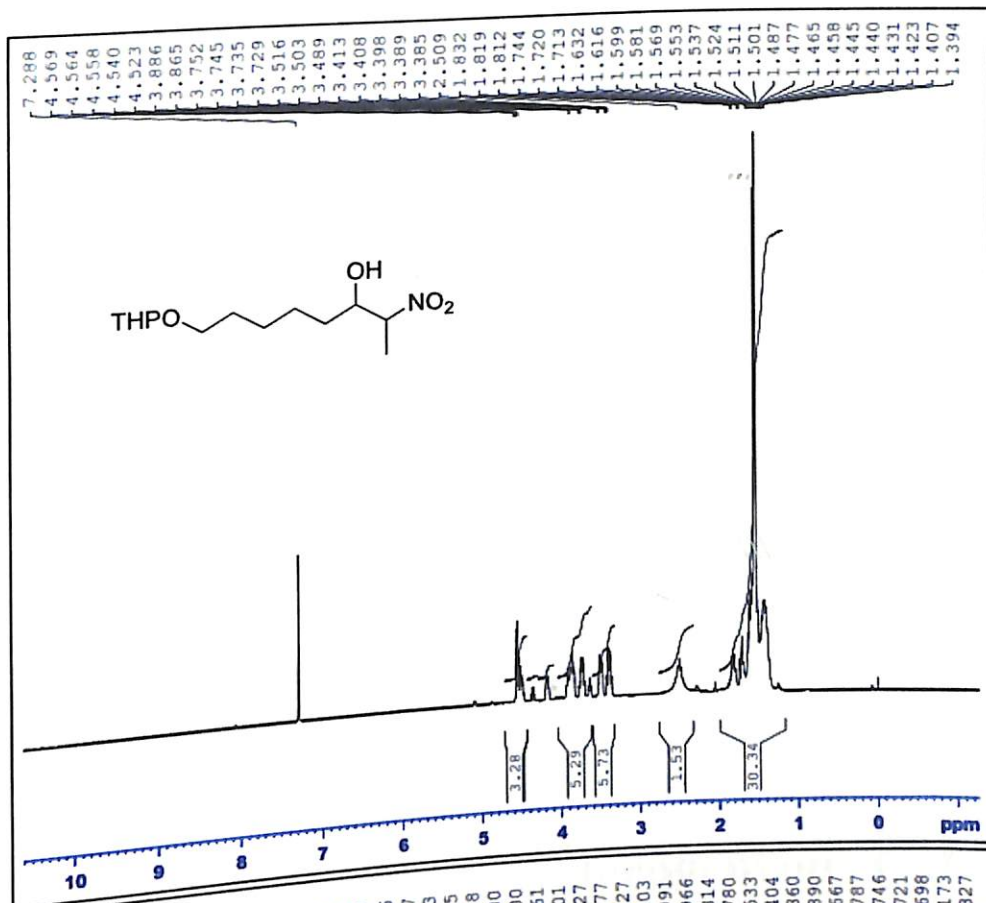
FIGURE 5.17 $^1$H NMR and $^{13}$C NMR Spectra of 2-nitro-7-((tetrahydro-2H-pyran-2-yl)oxy)heptan-3-ol (Table 5.4, entry w)

# CHAPTER

# 6

# A Sustainable Protocol for Production of Biodiesel by Transesterification of Soybean Oil Using Banana Trunk Ash as a Heterogeneous Catalyst

## 6.1 Introduction

Quest for new alternatives for energy instead of conventional fossil fuel has been a continuous effort in scientific community due to the growing demand of fuels associated with rapid urbanization and population growth.[1-4] The limiting supply of fossil fuel and their harmful effects towards environment, call an urgent need of powerful substitute to them. As a sustainable solution, biofuels such as biodiesel and bioethanol are emerging as green alternative sources of energy which results net reduction in $CO_2$ emission[5], no Sulphur content to provide better lubricity[6], high combustion efficiency and less emissions.[7]

Biodiesels, chemically termed as Fatty acid methyl esters (FAME), are produced from renewable biological sources like vegetable oils, animal fats etc. by chemical reactions like esterification, transesterification etc. The transesterification process reduces the viscosity of vegetable oils to make it usable in conventional diesel engines[8,9] where the triglyceride molecules of oil/fat react with alcohol molecules to give fatty acid methyl esters along with glycerol as by product (Scheme 6.1). Different small alcohol molecules like methanol, ethanol, amyl alcohol etc. can be used for this transformation; however methanol has been found more suitable in terms of reactivity, green chemistry metrics and cost-effectiveness.[10-12]
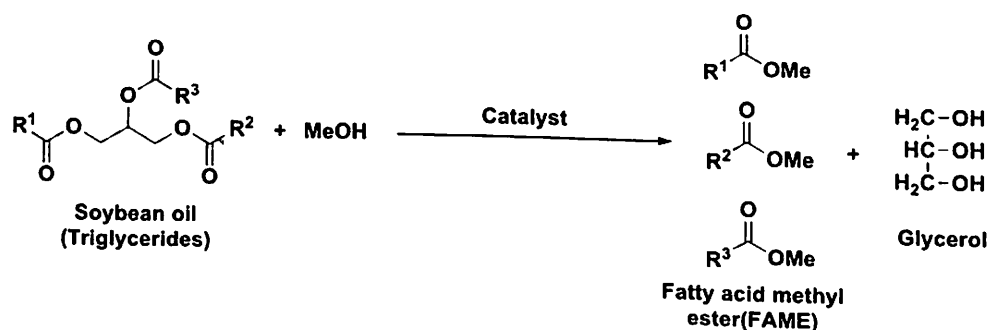
**SCHEME 6.1** Transesterification reaction

Bird's eye view of literature suggests plethora of both homogeneous and heterogeneous catalysts to catalyse transesterification reaction. Although several homogeneous base catalysts are being used for this reaction in industrial level due to their high reactivity[13], they have potential disadvantages which includes difficulty in product separation, sensitivity towards fatty acid content, formation of soap as side reaction product etc.[14-16] Heterogeneous catalysts can overcome these difficulties by easy separation and reusability of catalysts which also help to minimize the production cost. It is known that transesterification can be carried out by both acid and base catalysed procedure; but base catalysed reaction is reported to be 4000 times faster than the acid catalysed one.[17,18] Carbonates, alkali and alkaline earth metal oxides, zeolites, layered double hydroxides (LDH) etc. are some common solid base catalysts used for biodiesel production reaction.[19-22] However very few of these reported catalysts meet the required aspects of green chemistry. Owing to this, bio-derived or bio-based green catalysts for FAME production has emerged as a burgeoning field in sustainable catalysis. As catalysts play a key role in deciding the production cost of a synthetic method, valorization of waste materials into heterogeneous catalysts can be a highly lucrative concept. Use of bio-derived wastes as natural feedstock to prepare catalysts can potentially make a protocol cheaper, also impart greenness and benignity to the catalytic system. Recently natural biological resources are being targeted largely as heterogeneous catalysts by partial carbonization of the organic materials.23-27

However, most of these studies involve harsh fabrication of waste biomass, functionalization, metal impregnation or high temperature sulfonication of carbonaceous materials which lowers the sustainability of the method as well as limits its utilization in industrial scale.[28-31] So it is highly desirable to investigate simple, waste-derived, low-cost, eco-friendly yet efficient solid heterogeneous catalysts for biodiesel production to meet commercial viability.

Recently our group has reported an ecofriendly and efficient protocol for synthesis of biodiesel from soybean oil and even for C-C bond formation in production of nitroalcohols using *Musa acuminata* banana peel ash (MAPA) as a green heterogeneous catalyst.[32,33] The fact that, the amount of ash collected from the trunk of a banana plant is far more than that from its peels collected, aroused our interest to examine the catalytic properties of *Musa acuminata* banana trunk ash. Therefore in extension to our research interest in the development of green synthetic methods and catalytic techniques for production of biofuels[32-35], in this manuscript, we report herein the application of *Musa acuminata* banana trunk ash (MBTA) as waste biomass catalyst for synthesis of biodiesel from soybean oil under very mild reaction conditions.

# 6.2 Experimental section

## 6.2.1 Catalyst preparation and characterization techniques

*Musa acuminata* banana trunk was collected from Kolasib district of Mizoram and were washed properly with water and then sun-dried. They were cut into small pieces and then burnt. Finally it was grinded to fine powder to obtain the ash catalyst.

Infrared (IR), X-Ray Diffraction (XRD), X-Ray Fluorescence (XRF), Scanning Electron Microscope (SEM), High Resolution Transmission Electron Microscope (HR-TEM), Energy dispersive X-ray (EDX) and Thermogravimetry (TG) analysis were carried out to examine the structural composition and morphology of the catalyst. The FTIR spectra were noted on a Perkin-Elmer Spectrum One FTIR spectrometer. HR-TEM and EDX were experimented on JEM-2100, 200kV, JEOL Electron microscope. Powder XRD patterns were recorded on a X'Pert Pro, PAN analytical diffractometer with copper anode. A Perkin Elmer instrument with model no. TGA 4000 was used to carry out TGA analysis. $^1$H NMR spectra was obtained on a spectrometer of Bruker Avance II (400 MHz) using internal reference tetramethylsilane (TMS) and solvent CDCl$_3$.

## 6.2.2. Basicity measurement

The basic strength of a solid base catalyst is an extremely important information to measure its possible catalytic activity. To estimate the strength of basic sites of our proposed catalyst Hammett indicator method was employed. The following Hammett indicators were used in the experiments-bromothymol blue ($H\_=7.2$), phenolphthalein ($H\_=9.8$), alizarin yellow R ($H\_= 11.0$), 2,4,6-trinitroaniline ($H\_= 12.2$) and 2,4-dinitroaniline ($H\_=15$). About 0.2 g catalyst was shaken in 2 mL of Hammett indicator solution in benzene and left to equilibrate for some time. A change in color in the solution indicates higher basic strength of the catalyst than that of the indicator while no colour change refers lower basic strength than the indicator.

## 6.2.3. Transesterification of soybean oil

The Transesterification reaction was carried out by taking soybean oil (0.7 g), followed by addition of methanol (0.2 mL) and catalyst (0.050 g) taken in a round bottom flask and stirred magnetically for several hours. The development of reaction and formation of FAME was frequently checked by Thin Layer Chromatography (TLC). When TLC displays reaching completion of the transesterification reaction, the newly synthesized biodiesel was separated from the glycerol layer by centrifugation. Excess methanol present in the product mixture was then evaporated under rotary evaporator. The resulted Fatty acid methyl ester or biodiesel product was analysed by $^1$H NMR and GC-MS technique for confirmation about product formation and purity.

## 6.2.4. Catalyst reusability test

One of the most significant characteristic of a solid heterogeneous catalyst is its ability to be recycled for further application. To examine the probable reusability of the catalyst, transesterification of the soybean oil using recycled catalyst were performed under our optimized reaction conditions. After each catalytic run, the catalyst was centrifuged and decanted and then washed with ethyl acetate. The recovered catalyst was dried in vacuum oven at 80 °C for 5 h, and used for next cycles.

# 6.3 Result and discussion

## 6.3.1 Catalyst characterization

To have knowledge about the functional groups present in the catalyst, IR spectroscopic analysis was conducted. The spectra in Fig. 6.1 reveals the exclusive presence of metal

133

oxides and metal carbonates in the ash sample. The peak at 708 cm$^{-1}$ can be referred to the vibratory stretching of K–O bonds of potassium oxide while the peaks at 1636 cm$^{-1}$, 1400 cm$^{-1}$ can be accredited to the carbonyl vibration of metal carbonate entities. The broad peaks at 3416 cm$^{-1}$ appears due to the $\nu_{O-H}$ of moisture adsorbed on the surface whereas the characteristic vibration band for Si-O-Si bonds appears at 963 cm$^{-1}$.[32,36]
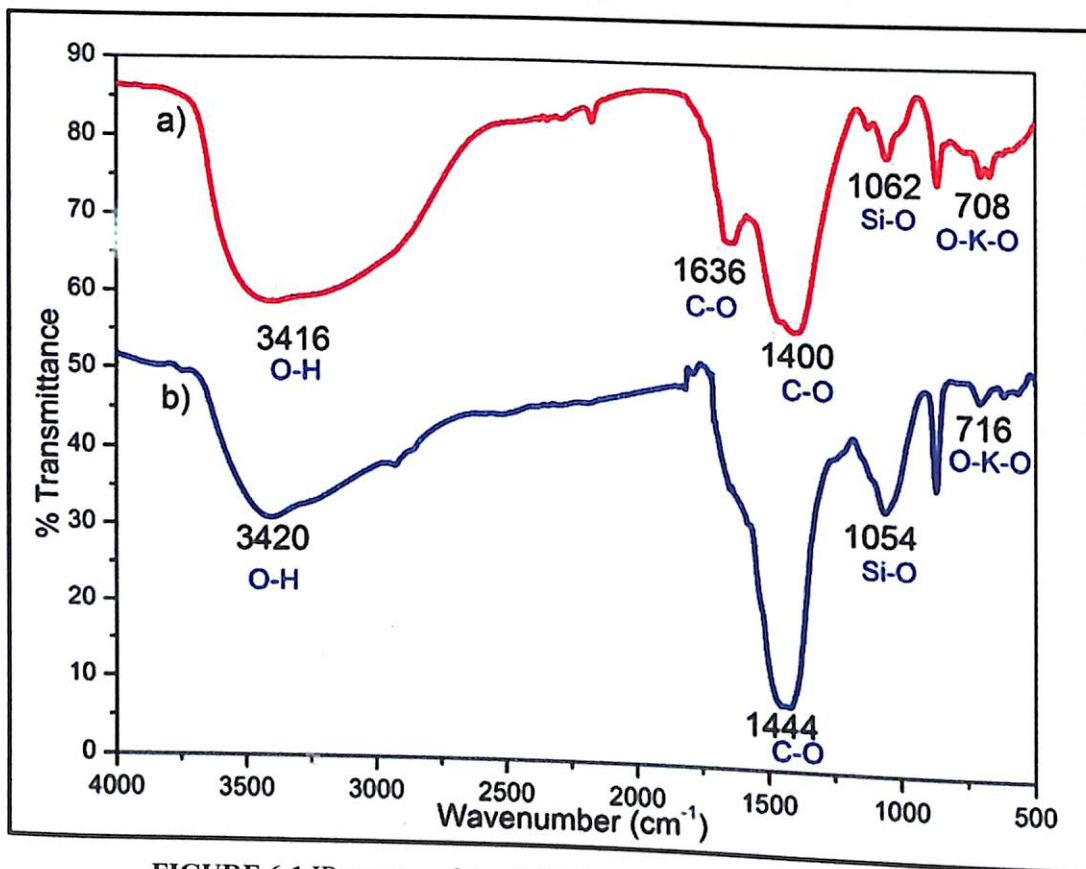


**FIGURE 6.1** IR spectra of the a) fresh catalyst, b) recovered catalyst



134
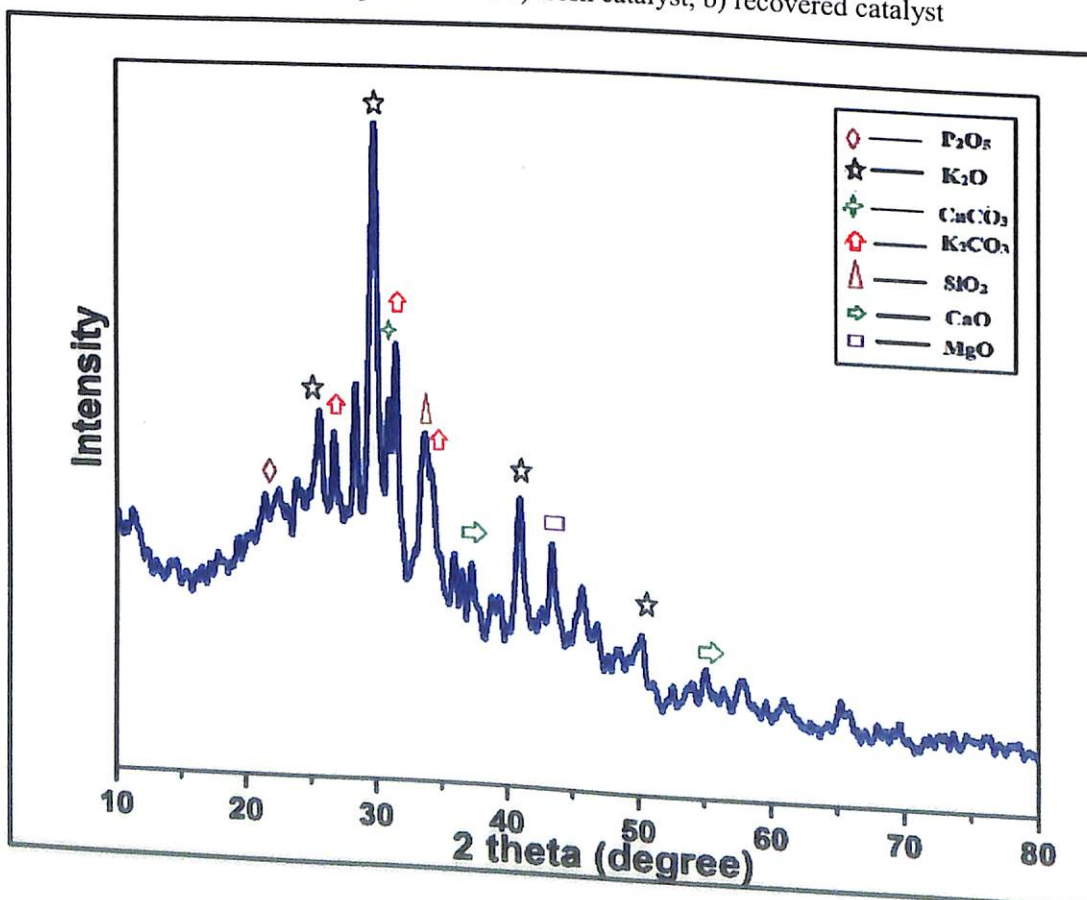
FIGURE 6.2 XRD diffractogram of the catalyst

XRD analysis of the catalyst was carried out in order to study the presence of possible crystalline entities in it. The occurrence of strong characteristic peaks of $K_2O$ can be observed in the diffractogram as shown in Fig. 6.2 at $2\theta= 29.81, 25.49, 40.99, 50.34$ (JCPDS reference file No- 77-2176). While strong diffraction peaks at $2\theta= 31.41, 26.74, 34.27$ can be assigned to $K_2CO_3$ (JCPDS reference file No- 87-0730), the peaks at $2\theta= 30.73$ and $2\theta= 37.23, 55.02$ are may be due to $CaCO_3$ and $CaO$ as according to JCPDS reference file No: 87-1863 and 82-1691. The existence of $SiO_2$ in the ash was confirmed by appearance of peaks at $2\theta=33.70$ (JCPDS reference file No: 89-3609). Apart from these, several low intense peaks were observed which may be attributed to the presence of $MgO$, $P_2O_5$ etc. in the solid ash catalyst.

The catalyst was also examined by XRF analysis which provides information about the inorganic components of the ash sample. The results strongly established $K_2O$ as the major component of the catalyst having % mass fraction 58.72% while $SiO_2$, $CaO$ and $MgO$ have mass fractions 17.45%, 6.8% and 4.6% respectively. Apart from these, various other elements and oxides were found to be present in the ash in trace amount. This results appropriately compliments the results obtained by IR and XRD analysis.
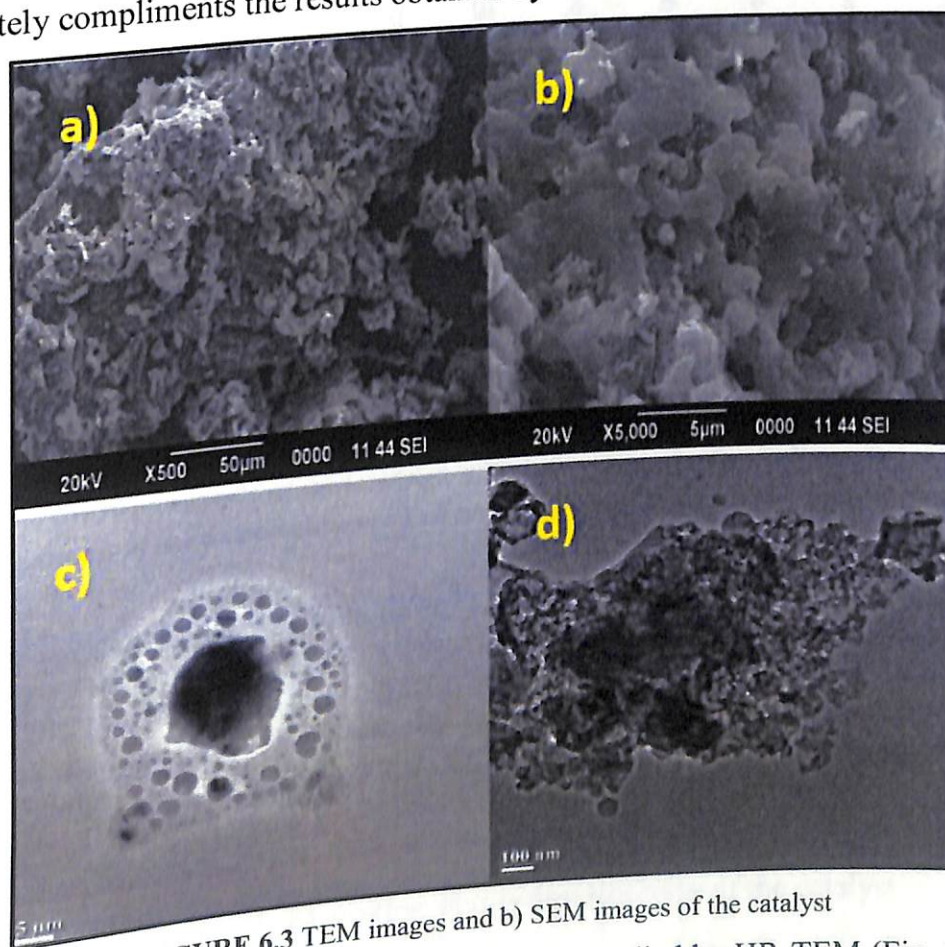


FIGURE 6.3 TEM images and b) SEM images of the catalyst

The external morphology of the catalyst was studied by HR-TEM (Fig. 6.3a-b) and SEM (Fig. 6.3b-c) analysis. The images in different magnification shows number of aggregates of porous and spongy structures of the catalyst.
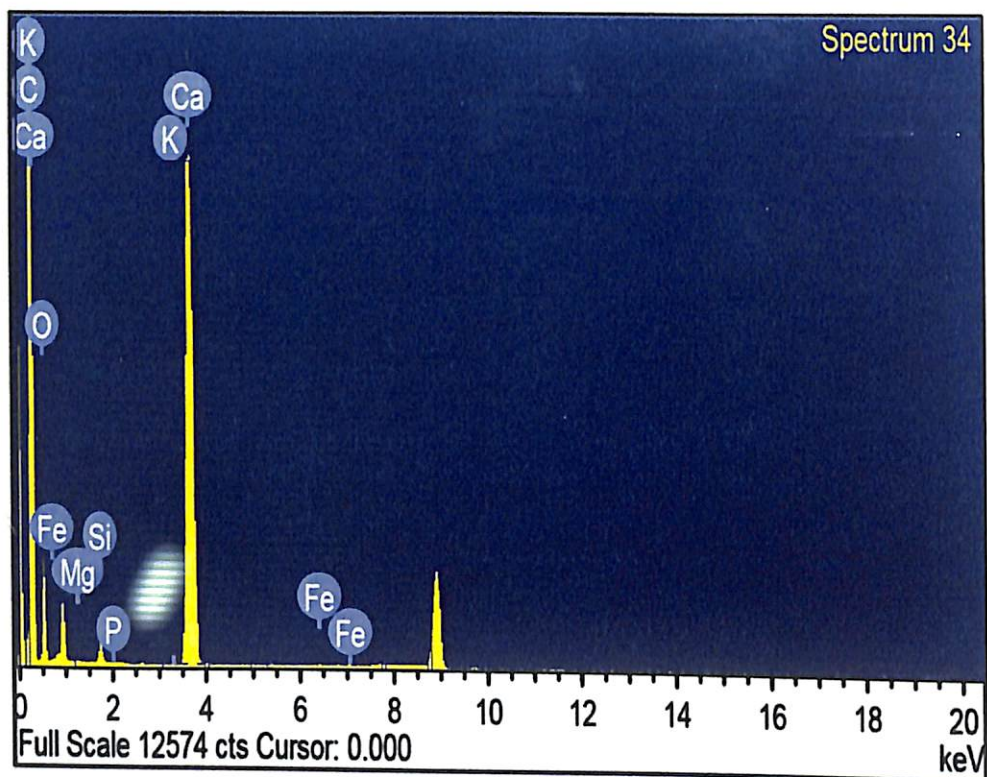
**FIGURE 6.4** EDX spectra of the catalyst

The EDX spectra (Fig. 6.4) showed K, O and C as the predominant elements present in the ash catalyst where wt % of O, C and K are 36.4%, 32.78% and 23.45% respectively. Some other major elements present are Si, Ca, Mg, Fe, P etc. This strongly supports the data given by XRD and XRF analysis and also establishes that $K_2O$ might be the major basic site present in the catalyst.

The thermal properties of the catalyst were also examined and Fig. 6.5 presents the TGA-DSC thermogram of the catalyst which presents the percentage weight loss of the catalyst with respect to temperature. Here the initial weight% loss near 150 °C can be attributed to evaporation of moisture, while the further loss in the range 700- 800 °C can be probably due to the release of CO and $CO_2$ due to the oxidation of carbonaceous matters in the catalyst.

Surface property of a catalyst plays an important role to analyse a catalyst's behaviour as the surface area and pore volume can be correlated with its activity. Therefore $N_2$ adsorption-desorption isotherm of the MBTA catalyst was elucidated by BET method as depicted in Fig. 6.6. The hysteresis loop in the isotherm clearly shows adsorption in mesoporous surface indicating type IV isotherm. The surface area of the catalyst was found to be 39.067 $m^2$/g while pore volume and pore radius are 0.21 cc/g and 2.77 nm. The porous structure of the catalyst gives major boost to the high catalytic activity of the catalyst accommodating the basic metallic sites.

136
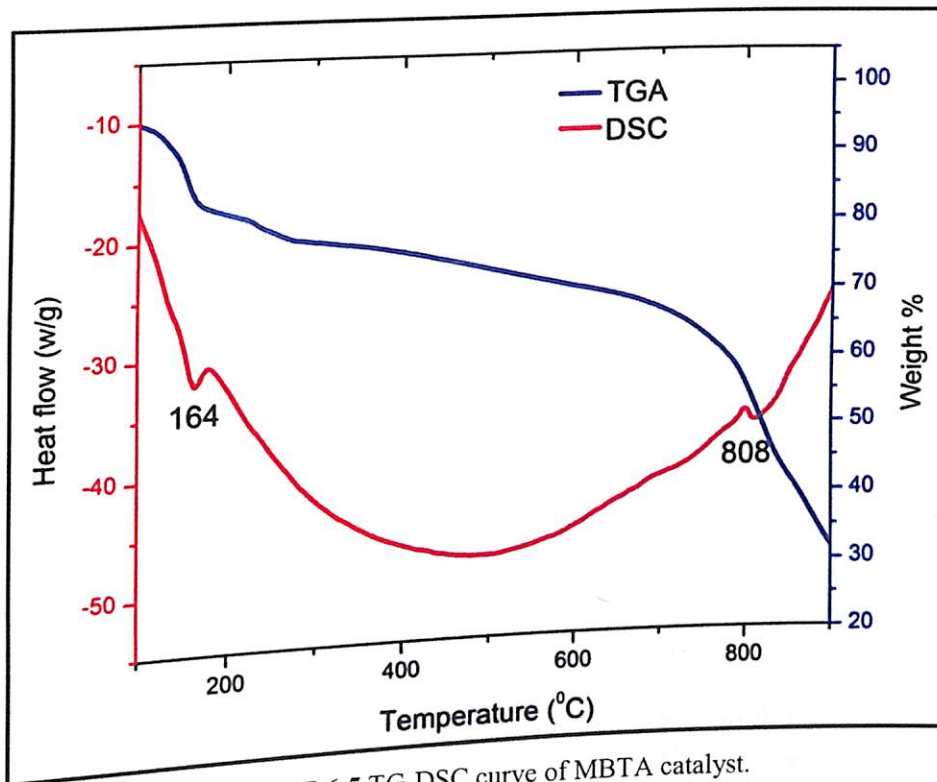
**FIGURE 6.5** TG-DSC curve of MBTA catalyst.
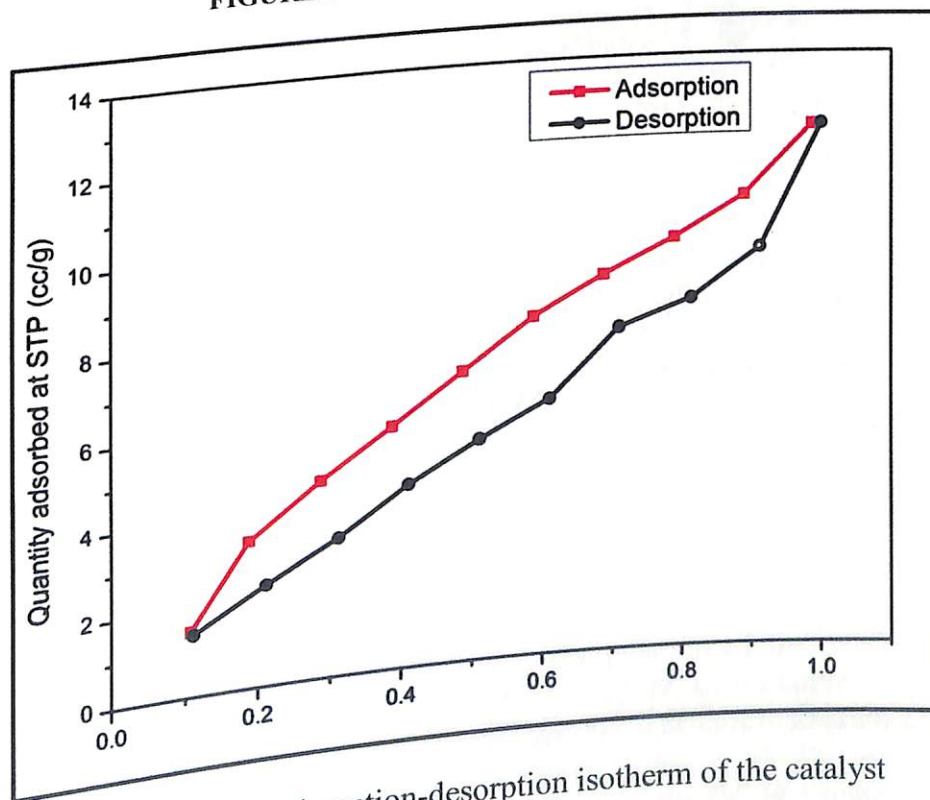


**FIGURE 6.6** $N_2$ adsorption-desorption isotherm of the catalyst

To study the surface basicity, the catalyst was also investigated by Hammett indicator method using different indicators like bromothymol blue, phenolphthalein and alizarin yellow R. It was noted from the experiment that when mixed with the catalyst, the first two indicators changed colour while colour of the third indicator did not change. This stated that basic strength of the catalyst may lie in the range of $9.8 \leq H \leq 11.0$.

**6.3.2 Synthesis of FAME from soybean oil using *Musa acuminata* banana trunk ash catalyst**

137

After characterising the *Musa acuminata* banana trunk ash catalyst it was checked for its potential application in synthesis of FAME by transesterification of soybean oil. As a pilot protocol, to 0.7 g of soybean oil, 0.2 mL of methanol was added with 0.05 g of the prepared catalyst and stirred the mixture in a 25 ml round bottom flask with constant stirring of 1000 rpm under room temperature. The reaction was regularly monitored by checking TLC and formation of FAME product was observed within 30 minutes of reaction. After 6 hrs of stirration, reaction was completed as indicated by TLC.
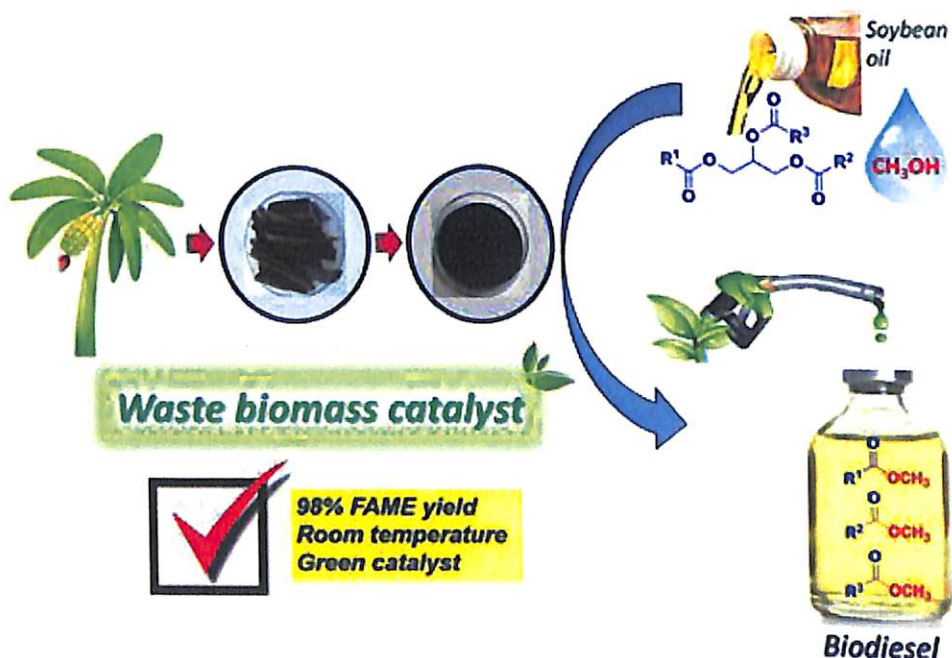


**FIGURE 6.7** Schematic diagram of production of biodiesel from soybean oil using MBTA catalyst

The reaction was then scaled up to gram scale and 7 g of soybean oil was allowed to stir with methanol (2 mL) and 0.5 g of catalyst under the same reaction condition. After completion of the reaction, the reaction mixture was centrifuged to separate the glycerol layer followed by evaporation of excess methanol in rotary evaporator.
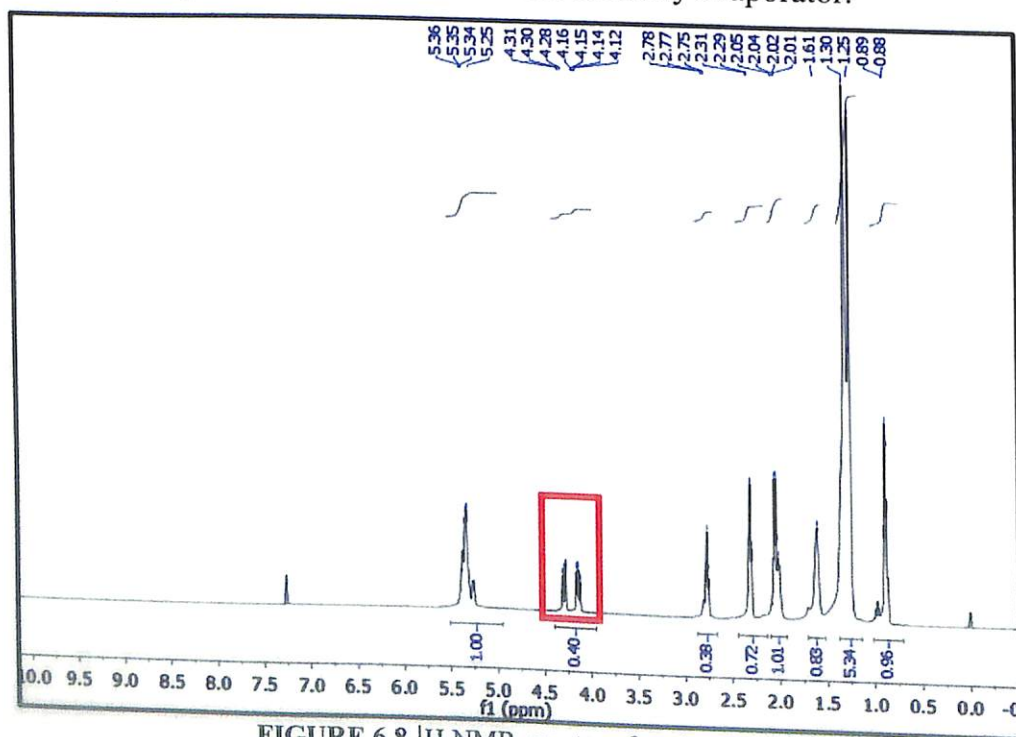


**FIGURE 6.8** $^1$H NMR spectra of soybean oil.
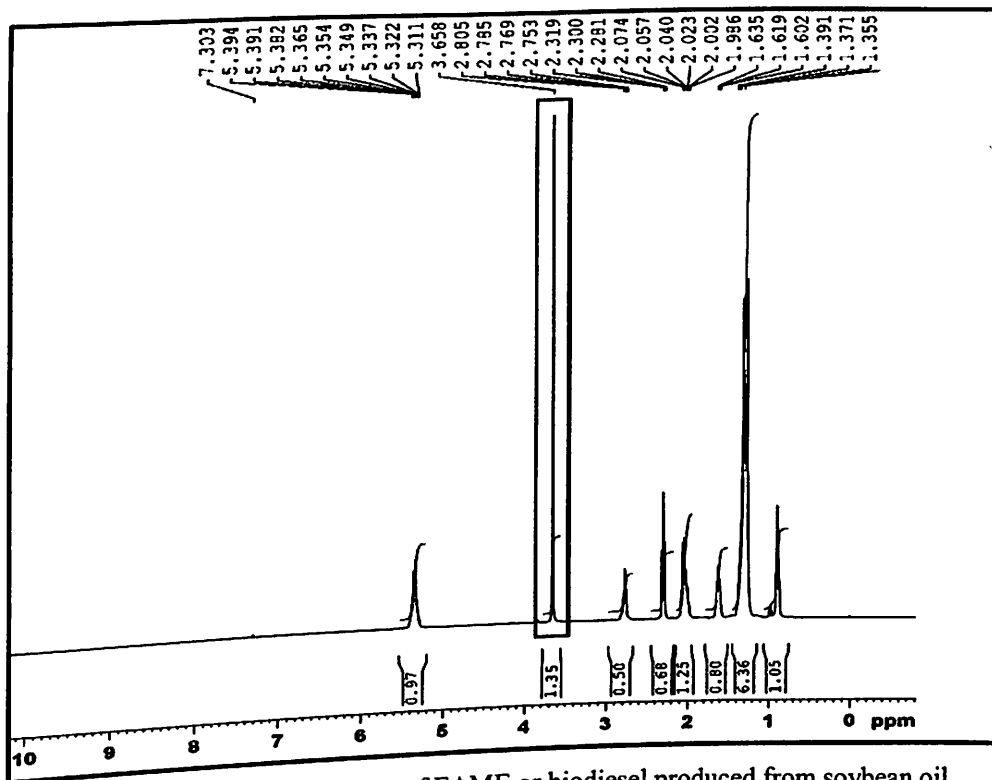
**FIGURE 6.9** $^1$H NMR spectra of FAME or biodiesel produced from soybean oil.

The $^1$H NMR study of the final product confirmed the formation of FAME as transesterification product of soybean oil. The $^1$H NMR spectra of soybean oil and synthesized biodiesel are presented in Fig. 6.8 and 6.9 respectively. In Fig. 6.9 it can be observed that the characteristic peak for methoxy proton appears as a singlet at 3.66 ppm and the peak of α-CH$_2$ protons is visible as a prominent triplet at 2.28 ppm. The appearance of these two peaks confirms the formation of corresponding methyl ester of soybean oil.

In Fig. 6.8, peaks due to glyceridic protons in soybean oil can be observed near 4-4.5 ppm, while in Fig. 6.9, the absence of peaks near this region supports the formation of FAME. To calculate the percentage conversion of soybean oil to the corresponding biodiesel (C) from $^1$H NMR spectra, the following equation is used where $A_{Me}$ and $A_{CH2}$ refers to the integration value of -OCH$_3$ (methoxy) proton and α- CH$_2$ (methylene) protons of methyl ester respectively which were observed to be 1.00 ppm and 0.68 ppm in the spectra. Apparently, the oil to FAME percentage conversion was calculated from the equation as 98.39%.

$$C = 100 \times (2A_{Me}/\ 3A_{CH2})$$

To have knowledge about the chemical composition of the synthesized FAME product, GC-MS study was carried out which enables quantitative analysis of the distinguished components present in the product sample. The chromatogram obtained from gas chromatography of the biodiesel sample is shown in Fig. 6.10. The identification and calculation of percentage composition of the FAME from the GC-chromatogram are listed in Table 6.1 also mentioning their retention time (R.T.). Quantification of composition of the soybean biodiesel product revealed that it consists of Methyl (14E)-14,17-octadecadienoate as major component (56.63%) followed by Methyl palmitate (20.68%), Methyl linoleate (20.55%), Methyl cis-11-eicosenoate (3.89%), Methyl Docosanoate (1.16%) etc.

139
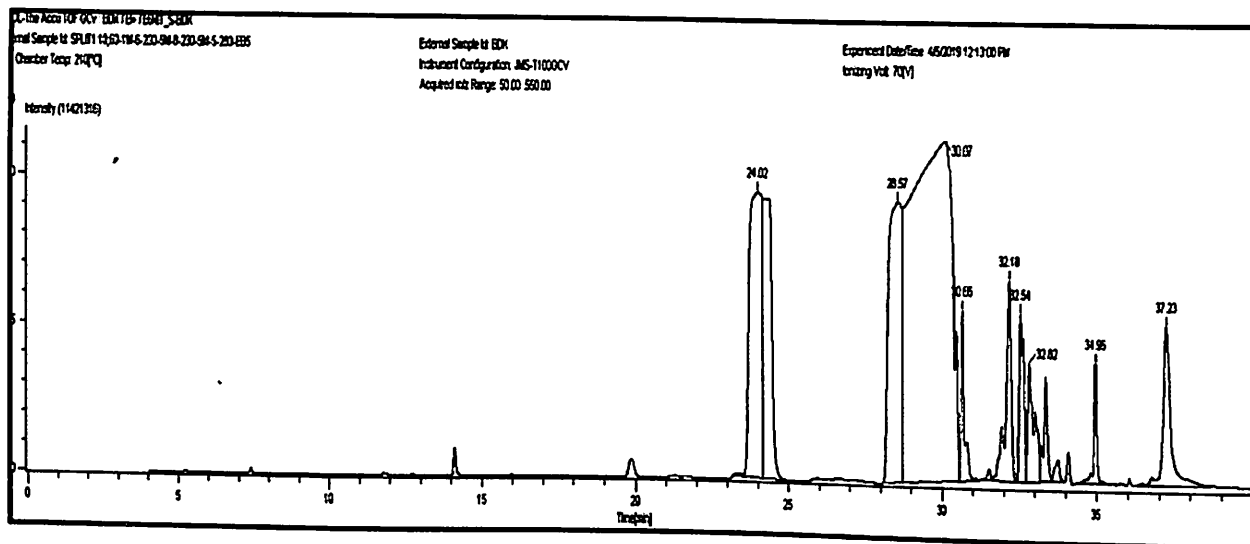
**FIGURE 6.10** GC-MS chromatogram of FAME

**TABLE 6.1** Chemical composition of the synthesized FAME derived from GC-MS studies

| Sl no | R.T. | Component identified | Corresponding acid | % composition |
|-------|------|---------------------|-------------------|---------------|
| 1 | 30.07 | Methyl (14E)-14,17-octadecadienoate | C19:2 | 56.63 |
| 2 | 24.02 | Methyl palmitate | C17:0 | 20.68 |
| 3 | 28.57 | Methyl linoleate | C19:2 | 14.55 |
| 4 | 32.18 | Methyl cis-11-eicosenoate | C21:1 | 3.89 |
| 5 | 34.96 | Methyl Docosanoate | C23:0 | 1.16 |
| 6 | 33.75 | Methyl 17-octadecynoate | C19:1 | 0.39 |

A biodiesel product is considered to be applicable in a diesel engine, only when it meets the standardized quality as specified by ASTM D6751 (American Society for Testing and Materials) and EN 14214 (European Committee for Standardization). Presence of impurities or contamination in biodiesel product may create several issues to the engine for which it is necessary to evaluate the product according to the standard measures. Viscosity, density, FFA acid value etc. are some important measures to examine the quality of a biodiesel sample. The physicochemical properties of the FAME synthesized from soybean oil using MBTA catalyst were analysed and Table 6.2 depicts the results along with the standard values. The values obtained were found to be within the range of international standard.

**TABLE 6.2** Physicochemical properties of the synthesized FAME

| Properties | Soybean oil biodiesel | ASTM standard value | EN standard value |
|-----------|----------------------|---------------------|-------------------|
| Density (g/cm³) | 0.872 | 0.870-0.890 | 0.860-0.900 |
| Kinematic Viscosity (mm²/s, at 40°C) | 5.42 | 1.9-6.0 | 3.5-5.0 |
| Acid value (mg of KOH/g of oil) | 0.48 | ≤0.5 | ≤0.5 |
| Flash point (°C) | 151 | >130 | >120 |
| Cloud point (°C) | -0.2 | - | - |

## 6.3.3 Reusability of the catalyst

The reusability or recyclability test for the *Musa acuminata* banana trunk ash catalyst was also investigated by carrying out repeated catalytic cycles under optimized condition. It was observed that after the 1st catalytic run, the oil to FAME conversion percentage was not depreciated much and was more or less same. However, after repeated cycles prominent

reduction in rate of the reaction as well as yield was observed and after the 4th cycle only 61% conversion could be obtained (Fig. 6.11).

This depreciation in catalytic activity may be attributed to the leaching of certain elements in the ash sample which can reduce the number of active sites of the catalyst. Possible accumulation of the by-product glycerol over the catalyst surface also may be another reason for this loss in activity which may lead to block the active sites resulting low biodiesel conversion compared to reaction with fresh catalyst. The IR spectra (Fig. 6.1b) and EDX spectra (Fig. 6.12) of recovered catalyst revealed no change in the morphology and composition of the catalyst after being recycled after 4th catalytic run.
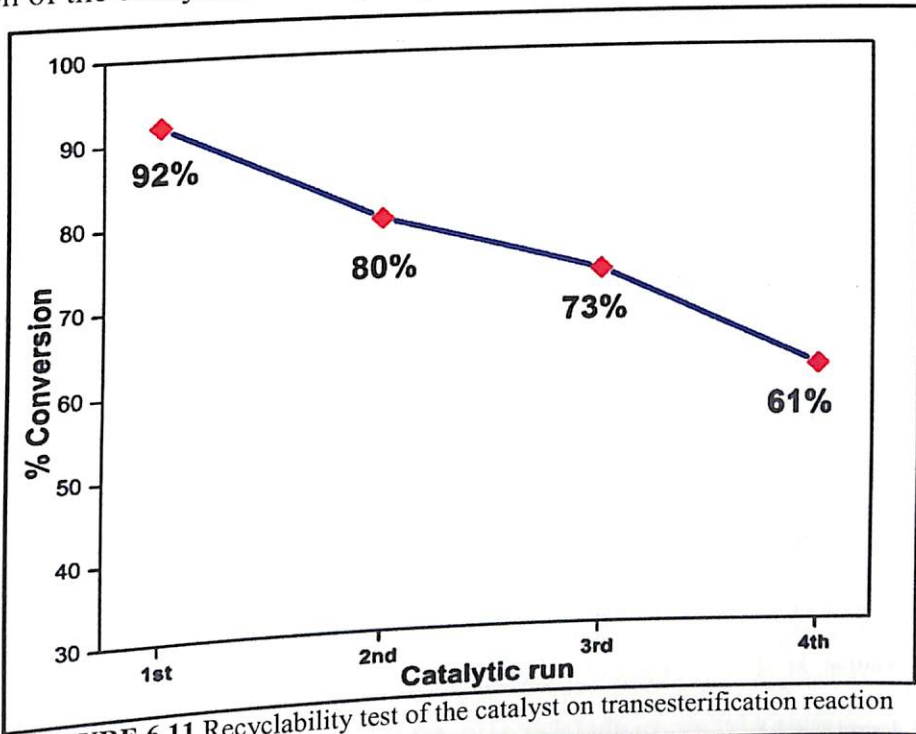


FIGURE 6.11 Recyclability test of the catalyst on transesterification reaction
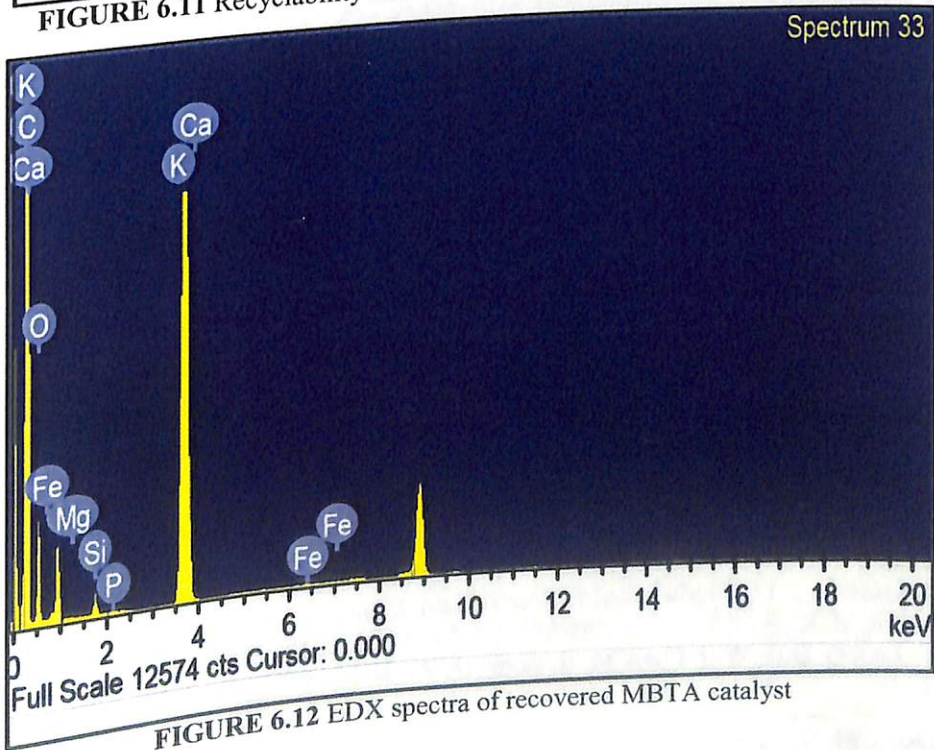


FIGURE 6.12 EDX spectra of recovered MBTA catalyst

## 6.4 Conclusion

141

Limiting fossil fuel reserves and the upward concerns regarding its detrimental environmental effects have made renewable fuels an extremely suitable alternative as a "fuel for the future". Biodiesel can be an attractive and technically feasible substitute to conventional diesel, however the commercialization of the product is still a matter of distress due to its high cost. As catalyst is an important contributing factor of the cost involved in production of biodiesel, introducing cheap and easily prepared benign catalysts can help in bringing down the cost of biodiesel synthesis, without negotiating the environmental factors.

In this work, we presented the application of banana trunk ash as a cost and labour effective green solid base catalyst for synthesis of biodiesel from soybean oil. The easy preparation method and its availability as natural waste material makes the catalyst exceptionally promising which do not require any chemical treatment. The reaction procedure also do not require elevated temperature and was carried out at room temperature. Due to the large economic viabi' y and environment-friendly nature, we believe that this protocol offers excellent industrial applicability for large-scale production of biodiesel in near future.

# References

1. S. H. Y. S. Abdullah, N. H. M. Hanapia, A. Azida, R. Umara, H. Juahira, H. Khatoon, and A. Endut, *Renewable Sustainable Energy Rev.* 2017, **70**, 1041-1051.
2. D. Y. C. Leung, X. Wu and M. K. H. Leung, *Appl. Energy*, 2010, **87**, 1083-1095.
3. M. D Serio, M. Ledda, M. Cozzolino, G. Minutillo, R. Tesser and E. Santacesaria, *Ind. Eng. Chem. Res.* 2006, **45**, 3009-3014.
4. B. Singh, A. Gulde, I. Rawat, F. Bux, *Renew Sustain Energy Rev.* 2014, **29**, 216-245.
5. F. Ezebor, M. Khairuddean, A. Z. Abdullah and P. L. Boey, *Bioresour. Technol.* 2014, **157**, 252-262.
6. A. M. Dekhoda, A. H. West and N. Ellis, *Appl. Catal. A. Gen.* 2014, **382**, 157-204.
7. F. Ma and M. A. Hanna, *Bioresour. Technol.* 1999, **70**, 1-15.
8. A. Dermibas, *Energy Convers. Manage.* 2008, **49**, 125-130.
9. A. L. Ahmad, N. H. M. Yasin, C. J. C. Derek and J. K. Lim, *Renew Sustain Energy Rev.* 2011, **15**, 584-593.
10. E. M. Guerra and V. G. Gude, *Appl. Sci.* 2017, **7**, 869-883.
11. M. E. Borges and L. Díaz, *Renew Sustain Energy Rev.* 2012, **16**, 2839-2849.
12. M. D. Serio, R. Tesse, L. Pengmei, E. Santacesaria, *Energy & Fuels* 2008, **22**, 207-217.
13. S. Semwal, A. K. Arora, R. P. Badoni and D. K. Tuli, *Bioresour. Technol.* 2011, **102**, 2151-2161.
14. G. E. G. Muciño, R. Romero, I. G. Orozco, A. R. Serrano, R. B. Jiménez and R. Natividad, *Catal. Today* 2016, **271**, 220-226.
15. A. T. Kiakalaieh, N. A. S. Amin and H. Mazaheri, *Appl. Energy*, 2013, **104**, 683-710.
16. K. Wilson, C. Hardacre, A. F. Lee, J. M. Monteroa and L. Shellard, *Green Chem.* 2008, **10**, 654-659.
17. L. J. Konwar, J. Boro and D. Deka, *Renew. Sustain. Energy Rev.* 2014, **29**, 546-564.
18. N. Kondamudi, S. K. Mohapatra and M. Misra, *Appl. Catal. A. Gen.* 2011, **393**, 36-43.
19. A. Refaat, *Int. J. Environ. Sci. Technol.* 2011, **8**, 203-221.
20. W. Xie and M. Fan, *Chem. Eng. J.* 2014, **239**, 60-67.
21. Z. Wen, X. Yu, S. Tu, J. Yan and E. Dahlquist, *Appl. Energy* 2010, **87**, 743-748.
22. A. Navajas, I. Campo, G. Arzamendi, W. Y. Hernández, L. F. Bobadilla and M. A. Centeno, *App. Catal. B: Env.* 2010, **100**, 299-309.
23. D. Zeng, Q. Zhang, S. Chen, S. Liu and G. Wang, *Microporous Mesoporous Mater.* 2016, **219**, 54-58.
24. Y. Zhou, S. Niu and J. Li, *Energy Convers.Manage.* 2016, **144**, 188-196.
25. K. Ngaosuwan, J. G. Goodwin and P. Prasertdham, *Renewable Energy* 2016, **86**, 262-269.
26. F. Ezebor, M. Khairuddean, A. Z. Abdullah and P. L. Boey, *Energy* 2014, **70**, 493-503.
27. W. Y. Lou, Q. Guo, W. J. Chen, M. H. Zong, H. Wu and T. J. Smith, *ChemSusChem* 2012, **5**, 1533-1541.
28. I. F. Nata, M. D. Putra, C. Irawan and C. K. Lee, *J. Environ. Chem. Eng.* 2017, **5**, 2171-2175.
29. J. R. Kastne, J. Miller, D. P. Geller, J. Locklin, L. H. Keith and T. Johnson, *Catal. Today* 2012, **190**, 122-132.

30. S. Kang, J. Ye and J. Chang, *Int. Rev. Chem. Eng.* 2013, **5**, 133-144.
31. P. Sudarsanam, R. Zhong, S. V. D. Bosch, S. M. C. Coman, V. I. Parvulescu and B. F. Sels, *Chem. Soc. Rev.* 2018, **47**, 8349-8402
32. G. Pathak, D. Das, K. Rajkumari and L. Rokhum, *Green Chem.*2018, **20**, 2365-2373.
33. K. Rajkumari, D. Das, G. Pathak and L. Rokhum, *New J. Chem.* 2019, **43**, 2134-2140.
34. I. B. Laskar, K. Rajkumari, R. Gupta, S. Chatterjee, B. Paul and L. Rokhum, *RSC Adv.* 2018, **8**, 20131- 20143.
35. I. B. Laskar, K. Rajkumari, R. Gupta and L. Rokhum, *Energy Fuels* 2018, **32**, 12567–12576.
36. H. Li, S. Niu, C. Lu, M. Liu and M. Huo, *Energy Convers. Manag.* 2014, **86**, 1110-1117.

# A microwave-assisted highly stereo-selective one-pot Wittig reaction under solvent-free conditions

## 7.1 Introduction

Olefination of carbonyl groups is one of the most fundamental yet fascinating synthetic transformations in organic chemistry due to the 'essential and ubiquitous' role of C-C double bond functionalization.[1] The Nobel prize-winning Wittig Olefination[2] reaction is regarded as the most applicable method for the exact placement of the C-C double bond to perform chemo- and regioselective preparation of alkenes even on the industrial scale.[3-5] The classical Wittig reaction allows the formation of alkene by the reaction of an aldehyde or ketone with triphenylphosphine ylide (Wittig reagent) eliminating triphenylphosphine oxide as a side product (Scheme 7.1).

$$Ph_3P \ + \ R'CH_2X \longrightarrow \overset{\oplus}{Ph_3}P\text{-}CH_2\text{-}R'X^{\ominus} \xrightarrow{\text{Base}} \overset{\oplus}{Ph_3}P\text{-}CH_2\text{-}R'^{\ominus}$$

Organic Halide          Phosphonium salt          Phosphorous Ylide

$$\overset{\oplus}{Ph_3}P\text{-}CH_2\text{-}R'^{\ominus} \ + \ O{=}C\overset{R_1}{\underset{R_2}{\big\langle}} \xrightarrow{\text{Wittig reaction}} \overset{R_1}{\underset{R_2}{\big\rangle}}C{=}CHR' \ + \ Ph_3P{=}O$$

Aldehyde /Ketone          Alkene          Triphenyl phosphine oxide
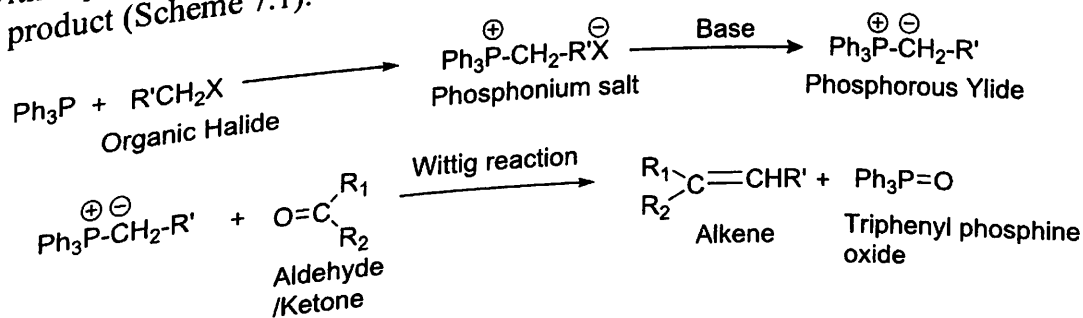
**SCHEME 7.1** Classical Wittig reaction

Despite the widespread prominence and recognition, it suffers from various difficulties like selectivity, separation, multistep protocol, less atom economy etc.[6,7] The main difficulty of this reaction is the removal of the side product triphenylphosphine oxide

in solution-phase reactions.[3] Another drawback of the Wittig reaction is the need for multistep synthesis that involves preparation of the precursor phosphonium ylide using alkyl halides and an external base (which leads to the formation of halide salts that require separation and disposal) and successive reaction of ylide with carbonyl to produce alkene.[8] In recent years, there are several successful attempts to overcome these drawbacks and to enhance green aspects of the Wittig reaction, which includes ball-milling,[9] one-pot synthesis,[10] microwave irradiation[3,7] and reaction in aqueous media,[6,11] etc.

From the first implementation of microwave technology in organic synthesis by Giguere and Gedye[12] in 1986, microwave-assisted organic chemistry experienced revolutionizing growth. This unconventional energy source eliminated the difficulties related to conventional heating th includes slow and time-consuming heating, unexpected decomposition of components, overheating of substrate or product, loss of energy etc., thereby, reducing reaction times from hours to minutes, increasing yields and selectivity.[10,11] This also enhanced the production purities by lowering the unwanted side-reactions as compared with the conventional heating methods. The conventional Wittig reaction, which is often tedious due to long reaction time, can be upgraded by employing microwave heating technique to make it time and energy-efficient.[3,14-16] Microwave irradiation in solvent-free condition is always preferable because it provides chances to work with open vessels avoiding the risk of high-pressure development and increasing the potential of such reactions to upscale.[17]

In 1968, Buddrus[18] demonstrated, for the first time, a one-pot Wittig olefination reaction which replaced the more energy and raw material consuming classical multiple step reaction, coupling three or more substrate components in a single efficient operation. This attempt commendably ameliorated the long, tiresome multiple-step process by reducing no only the operational time but also consumption of huge amount of solvent used in the overall procedure.[6,8] As for example, M. L. Kantam et al.[19] reported a protocol for one pot Wittig reaction among aldehyde, $\alpha$-halo esters and $PPh_3$ to afford quantitative yield of $\alpha,\beta$-unsaturated esters with subtantial $E$-selectivity using Mg/La mixed oxide as an efficient heterogeneous base.

$$R-CHO \ + \ \underset{R'}{\overset{X}{<}} \quad \xrightarrow[\text{DMF, RT}]{\text{Mg/La mixed oxide, } PPh_3} \quad \underset{R}{\overset{R'}{=}} \ + \ Ph_3P=O$$

**SCHEME 7.2** One-pot Wittig reaction using Mg/La mixed oxide
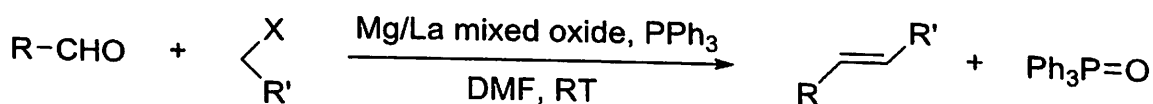
While the same transformation was carried out by B. M. Choudary et al.[8] using nanocrystalline magnesium oxide as an effective catalyst in one pot synthetic method. Liu and Tan[20], on the other hand, reported to perform one pot Wittig reaction for the synthesis of macrolides.

$$R-CHO \ + \ \underset{R'}{\overset{X}{<}} \quad \xrightarrow[\text{DMF, RT}]{\text{NAP-MgO, } PPh_3} \quad \underset{R}{\overset{R'}{=}} \ + \ Ph_3P=O$$
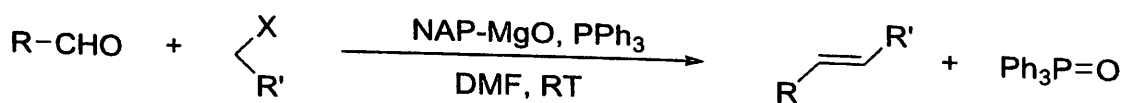
**SCHEME 7.3** One-pot Wittig reaction using nanocrystalline MgO

Balema et al.[9] in 2002 published a unique synthesis method of phosphrous ylides by ballmilling phosphonium salt with $K_2CO_3$. This result inspired them to design a mechanochemical, one-pot, solid-state synthetic method of Wittig Olefination starting with triphenyl phosphine, aldehyde/ketone and organic halides by ball milling together with $K_2CO_3$.

However, only limited reports have been published to compete with the demand for green and environmentally benign protocols.[4,21] In continuation of our interest in the application of soluble[22] and polymer-supported triphenylphosphine[23] for diverse organic transformation, we investigated a novel triphenylphosphine-mediated, solvent-free Wittig reaction under microwave irradiation.

**The reaction was first attempted with** α-halo esters which led to *in situ* formations of stabilized ylides and further extended to semi-stabilized ylides like (benzyl)triphenylphosphonium. Semi-stabilized or moderately reactive phosphorous ylides often show less stereocontrol of the olefination process which has been a recognized problem for a long time.[24,25] However to our delight, both the halides resulted in the predominant formation of the E- isomers of olefin products over Z- isomers indicating excellent stereoselectivity of the reaction. Thus our protocol offers an energy-efficient, atom-economical and neat synthetic route for Wittig olefination with high E- selectivity and excellent yield.

## 7.2 Experimental section

### 7.2.1 Materials and methods

All the chemicals were used without further purification. The alcohols and aldehydes were of analytical grade. The solvent used were of extra pure grade purchased from Merck India and were dried by the reported procedure. **Milestones' Start SYNTH microwave was used** for carrying out all the reactions. $^1H$ and $^{13}C$ NMR spectra were recorded on a BRUKER AV III (400 MHz) spectrometer using tetramethylsilane (TMS) as an internal reference. $^{13}C$ NMR spectra were recorded at 100 MHz. Chemical shifts for $^1H$ and $^{13}C$ NMR spectra are reported (in parts per million (ppm) relative to internal tetramethylsilane (TMS) (Me$_4$Si=0.0ppm) with CDCl$_3$ as a solvent. $^1H$ NMR data are reported in the order of chemical shift, multiplicity(s= singlet, d=doublet, t=triplet, dd= doublet of doublet, and m= multiplet), the number of protons, and coupling constant in hertz (Hz). TLC plates were visualized by exposing either in iodine chamber, UV-lamp or spraying with H$_2$SO$_4$ and heating.

### 7.2.2 General procedure for one-pot preparation of olefins (alkene) *via* Wittig reaction

A mixture of aldehyde (1 mmol), alkyl halide (1.6 mmol) and triphenylphosphine (1.3 mmol) were mixed and ground with 28.3 eqv (3 g) basic alumina) in a mortar. The ground mixture was then transferred to a 50 mL round bottom flask and irradiated in the microwave oven with temperature 90 °C, heat of 700 W for 30-60 minutes. After completion of the reaction (as detected by TLC), the crude product was directly charged into the silica gel chromatography column to afford the desired product using hexane/ethyl acetate (1:9 ratio) as eluent. The isolated product was then weighed to calculate the percentage yield and sent for NMR for confirmation of structure and purity. Structural isomer determination (E/Z ratio) was determined by $^1H$ NMR of the isolated product.
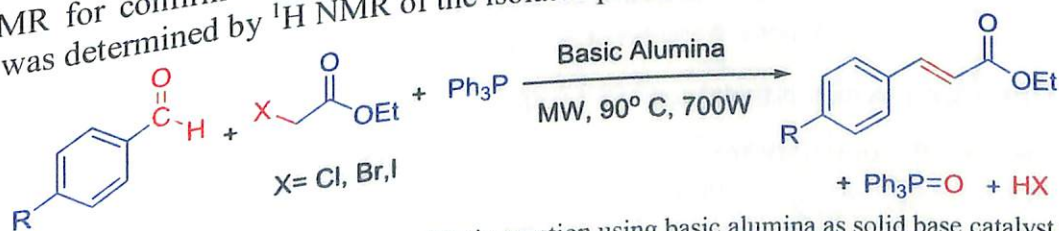


**SCHEME 7.4** Microwave-assisted one-pot Wittig reaction using basic alumina as solid base catalyst support

## 7.3 Result and discussion

Here we report a solid-state solvent-free one pot method for Wittig reaction of aldehyde, **triphenylphosphine and** α-halo esters or benzyl halides using basic alumina as a heterogeneous base catalyst-support. The reaction was conducted under microwave irradiation which affords corresponding alkenes in good to excellent yields with attractive *E*- selectivity. At the outset, to optimize the reaction condition giving best results, we investigated the Wittig reaction of benzaldehyde, ethyl chloroacetate (ECA) and triphenylphosphine (TPP) as a pilot protocol. The optimization of the stoichiometric ratio, catalyst loading, temperature and reaction time were performed in Figure 7.1-7.3. The overall results are illustrated in Table 7.1. After varying different parameters, an optimized condition of the reaction was achieved which resulted maximum isolated yield (93%) of desired olefin product within only 3 minutes.

### 7.3.1 Optimizations of catalyst-support loading

The catalyst loading was also optimized to reach the best possible yield (Table 7.1, Entry 10-15). For this, several reactions sets having various catalyst loadings were compared against the optimized ratio of reactants assisted by microwave heating at 90 °C. This investigation showed that 3 g (28.3 eqv) of basic alumina was the optimum amount of catalyst-support which gave 93% yield of the synthesized olefin (Table 7.1, Entry 14). When the amount of alumina exceeded this limit the reaction was observed to be slowed down slightly (Table 7.1, Entry 15). This might be attributed to the more distant active sites due to the high amount of catalysts which made it difficult to interact with substrates.
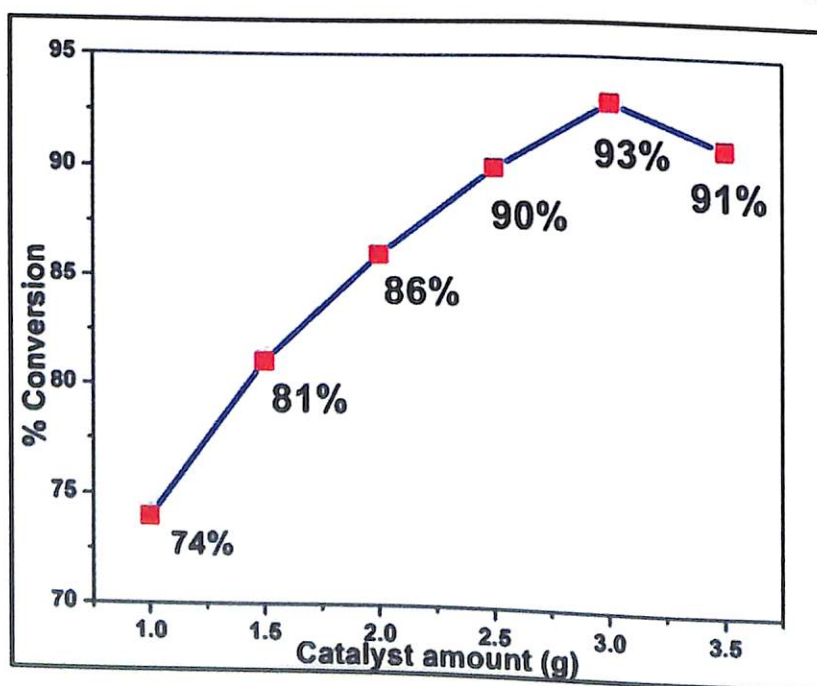


FIGURE 7.1 Effect of catalyst loading on % conversion

### 7.3.2 Optimization of temperature

To investigate the optimum temperature condition for the reaction, we allowed to stir the reaction for 60 minutes by varying the temperature of the reaction system and keeping the microwave heating 700 W. The result of the observation is shown in Table 7.1 (Entry 16-19). We observed that when the reaction was carried out at low temperature, the yield was

148

less. But when the temperature was increased to 90 °C, the reaction resulted better yield as shown in Table 7.1, Entry 18.
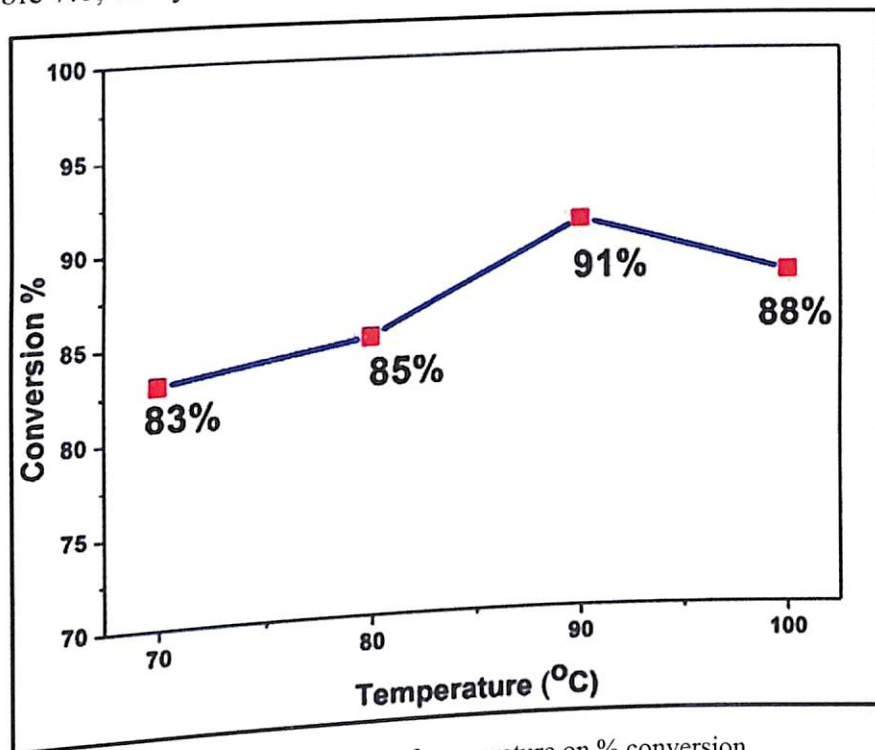


**FIGURE 7.2** Effect of temperature on % conversion

## 7.3.3 Optimization of reaction time
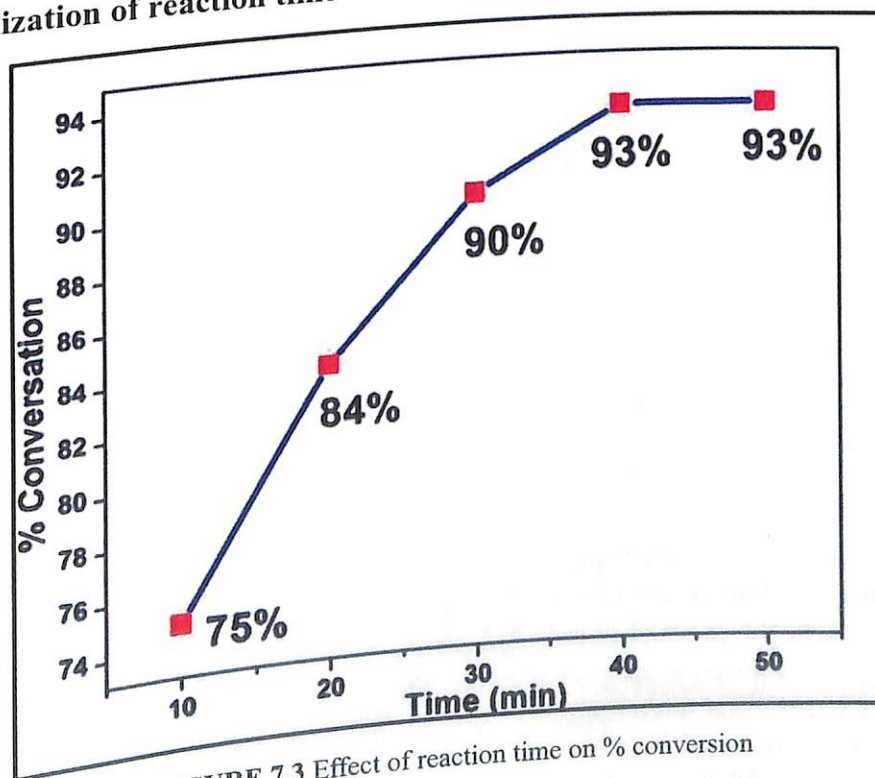


**FIGURE 7.3** Effect of reaction time on % conversion

Employing the optimum reaction conditions, the effect of reaction time on the Wittig reaction was also investigated (Table 7.1, Entry 20-23). The reaction was allowed to stir for 60 minutes and conversion of the reaction was monitored at an interval of 10 minutes. The

149

maximum conversion attained at 30 minutes after which no appreciable change in yield was noticed.

**TABLE 7.1 Optimisation of stoichiometric ratio of reactants**[a]

| Entry | Benzaldehyde: ECA: TPP | Catalyst loading (g) | Temperature (°C) | Time (min) | Yield (%) (Isolated) |
|---|---|---|---|---|---|
| 1 | 1: 1: 1 | 3g | 90 °C | 30 | 65 |
| 2 | 1: 1.2: 1 | 3g | 90 °C | 30 | 70 |
| 3 | 1: 1.2: 1.2 | 3 g | 90 °C | 30 | 83 |
| 4 | 1: 1.5: 1.2 | 3 g | 90 °C | 30 | 88 |
| 6 | 1: 1.6: 1.2 | 3 g | 90 °C | 30 | 90 |
| 7 | **1: 1.6: 1.3** | 3 g | 90 °C | 30 | 93 |
| 8 | 1: 2: 1.3 | 3 g | 90 °C | 30 | 89 |
| 9 | 1l: 1.6: 1.6 | 3 g | 90 °C | 30 | 89 |
| 10 | 1: 1.6: 1.3 | 1 g | 90 °C | 30 | 74 |
| 11 | 1: 1.6: 1.3 | 1.5 g | 90 °C | 30 | 81 |
| 12 | 1: 1.6: 1.3 | 2 g | 90 °C | 30 | 86 |
| 13 | 1: 1.6: 1.3 | 2.5 g | 90 °C | 30 | 90 |
| 14 | 1: 1.6: 1.3 | 3 g | 90 °C | 30 | 93 |
| 15 | 1: 1.6: 1.3 | 3.5 g | 90 °C | 30 | 91 |
| 16 | 1: 1.6: 1.3 | 3 g | 70 °C | 30 | 83 |
| 17 | 1: 1.6: 1.3 | 3 g | 80 °C | 30 | 85 |
| 18 | 1: 1.6: 1.3 | 3 g | **90 °C** | 30 | 93 |
| 19 | 1: 1.6: 1.3 | 3 g | 100 °C | 30 | 88 |
| 20 | 1: 1.6: 1.3 | 3 g | 90 °C | 10 | 75 |
| 21 | 1: 1.6: 1.3 | 3 g | 90 °C | 20 | 84 |
| 22 | **1: 1.6: 1.3** | 3 g | **90 °C** | **30** | **93** |
| 23 | 1: 1.6: 1.3 | 3 g | 90 °C | 40 | 93 |

Finally, after optimization of the reaction conditions, we extended the protocol for the Wittig reaction of various substituents of aldehyde assisted by microwave-irradiation using different halides to understand the scope and limitations of the reaction and to synthesize a good amount of olefin products. It was observed that the nature of the reactant i.e. carbonyl group in the substrate, influences the reaction time required to complete the reaction process. Aldehyde containing the electron-withdrawing group required nearly 45-55 minutes to form the product (Table 7.2, Entry 4-7). But when the reaction were carried out with the aldehydes containing the electron-donating group or neutral aromatic aldehyde, comparatively lesser time were required for complete conversion to olefin (Table 7.2, Entry 1-3). It was also observed that the selectivity of the product was high in case of para substituted aromatic aldehydes (Table 7.2, Entry 2, 4, 6, and 9), while it is less in ortho- and meta- substituents (Table 7.2, Entry 3, 5, 7 and 10).

The halide we commonly used in the reaction (ethyl 2-chloroacetate) led to the formation of stabilized ylide *in-situ* and thereby resulting *E*-isomers of olefin product formed

150

predominantly. The scope of semi-stabilized ylide was also investigated by using 1-bromo-4-(bromomethyl)benzene as a halide source in the reaction (Table 7.2, Entries 9 and 10). This also resulted in the excellent predominance of the E-isomer over Z- isomer confirming attractive stereo-selectivity of this protocol.

**TABLE 7.2** Wittig reaction of various aromatic aldehydes with halides and triphenylphosphine under solvent-free microwave heating conditions[a]

| Entry | Aldehyde | Halides | Product | Time (min) | E/Z ratio[b] | Yield[c] |
|-------|----------|---------|---------|-----------|--------------|----------|
| 1. | CHO | Cl–OEt | OEt | 40 | 91:9 | 93 |
| 2. | HO–CHO | Cl–OEt | HO–OEt | 30 | 94:6 | 94 |
| 3. | CHO, OH | Br–OEt | OEt, OH | 35 | 91:90 | 91 |
| 4. | Cl–CHO | Cl–OEt | Cl–OEt | 45 | 92: 8 | 85 |
| 5. | CHO, Cl | Br–OEt | Cl, OEt | 45 | 91:9 | 86 |
| 6. | Br–CHO | Cl–OEt | Br–OEt | 50 | 100 | 83 |
| 7. | Br–CHO | Cl–OEt | Br–OEt | 55 | 92:8 | 80 |
| 8. | CHO | Cl–OEt | OEt | 50 | 89:11 | 88 |
| 9. | Cl–CHO | Br–Br | Cl–Br | 45 | 88:12 | 86 |
| 10. | CHO, Br | Br–Br | Br, Br | 60 | 89:11 | 82 |

[a]Reaction conditions: Aldehyde (1.5 mmol), halide (2.5 mmol), PPh₃ (2 mmol), alumina (3 g or 28.30 eqv) at 90 °C, 700W; [b]Calculated from ¹H NMR spectra; [c]Isolated yield.

## 7.3.4 Probable Mechanism

151

The mechanism proposed for the one-pot Wittig reaction protocol is shown in Scheme 7.5. It is postulated that the basic sites of alumina abstracts the $-CH_2$ proton of phosphonium salt which then activates the aldehyde to form the cyclic oxaphosphetane ring. This cyclic intermediate then cleaves to yield the desired Wittig olefinic product and triphenylphosphine oxide as by-product. The halide ion of phosphonium salt regenerates the catalyst by abstracting the proton in its basic site to form hydrochloric acid.
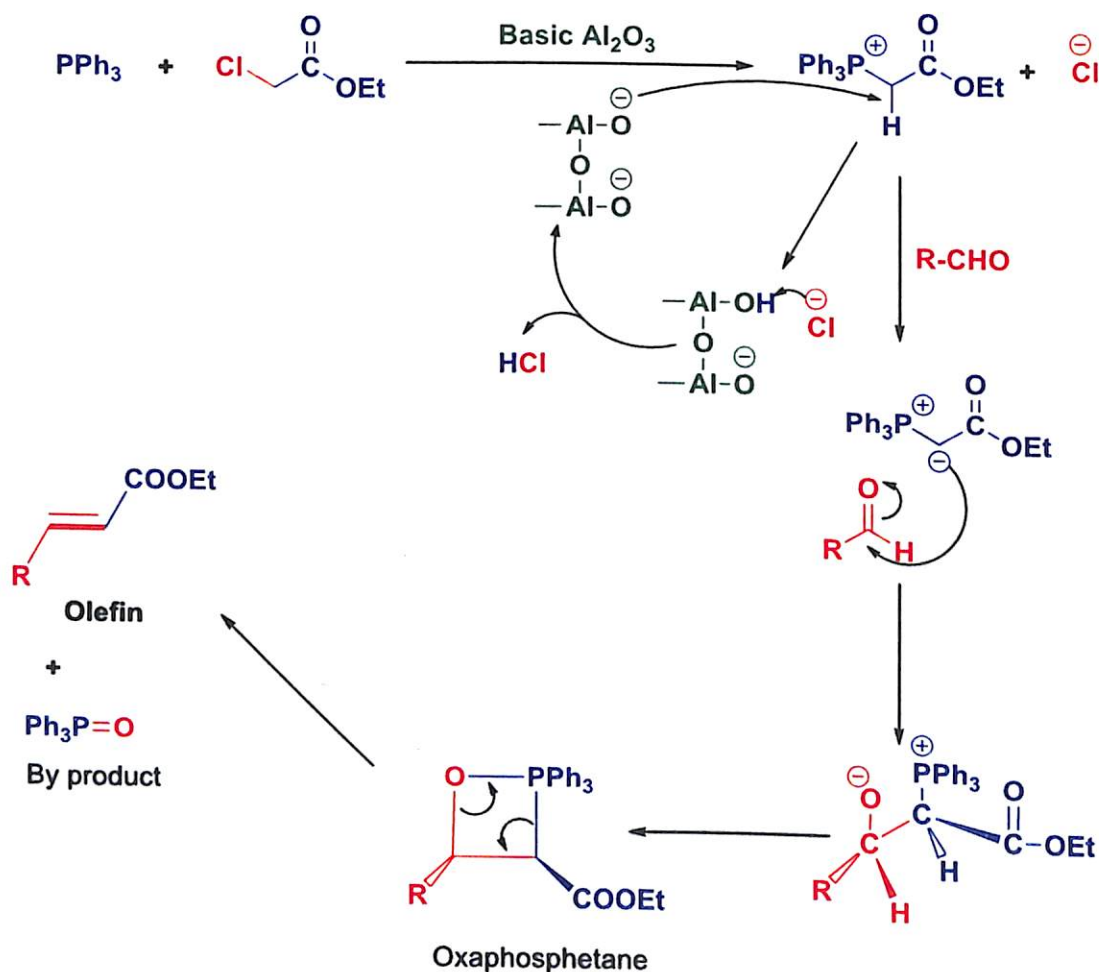


**SCHEME 7.5** Proposed mechanism for the solid-state one-pot Wittig reaction

## 7.3.5 Spectroscopic data of synthesized compounds

**(E)-Ethyl 3-(2-hydroxyphenyl)acrylate (Table 7.2, Entry 3)**

$^1$H NMR (400 MHz, CDCl$_3$, TMS):  δ 1.34 (3H, t, J=2.8Hz), 4.14 (2H, m), 6.66 (1H, d, J=12.8Hz), 6.89 (2H, m), 7.21 (1H, t, J=5.2Hz), 7.43 (1H, d, J=5.2Hz), 7.82 (1H, s), 8.08 (1H, d, J=12.8Hz); $^{13}$C NMR: δ 14.26, 60.80, 116.41, 117.59, 120.38, 121.66, 129.18, 131.5, , 141.13, 155.99, 168.8.

**(E)-Ethyl 3-(2-chlorophenyl)acrylate (Table 7.2, Entry 5)**

$^1$H NMR(400 MHz, CDCl$_3$, TMS): δ1.28 (3H, t, J=7.2Hz), 4.21(2H, m),, 6.36 (1H, d, 16Hz), 7.22 (1H, m), 7.36 (2H, m), 7.51 (1H, d, J=12 Hz), 8.02(1H, d, J=16Hz); $^{13}$C NMR: δ 14.26, 60.80, 120.38, 127.06, 127.62, , 129.45, 130.16, 130.76, 130.97, 140.37, 166.52.

**(E)-Ethyl 3-(4-bromophenyl)acrylate (Table 7.2, Entry 6)**

152

<sup>1</sup>H NMR(400 MHz, CDCl₃, TMS): δ 1.3 (3H, t, J=7.2Hz), 4.2 (2H, m), 6.47 (1H, d, J=16Hz), 7.67 (1H, d, J=16Hz), 7.76 (2H, d, J=7.6Hz), 8.15 (1H, d, J=1.2Hz), 8.17 (1H, d, J=1.2Hz); ¹³C NMR: δ 14.31, 60.62, 118.97, 124.44, 129.41, 132.108, 133.36, 143.16, 166.68.       ...

**(E)-Ethyl 3-(3-bromophenyl)acrylate (Table 7.2, Entry 7)**

¹H NMR(400 MHz, CDCl₃, TMS): δ1.26 (3H, t, J=7.2Hz), 4.19 (2H,m), 5.91(1H, d, J=12.8Hz), 6.35 (1H, d, J=16Hz), 6.79 (1H, d, J=12.4 Hz), 7.17(1H, t, J=7.6Hz), 7.35(1H, t, J=7.6Hz), 7.42(1H, d, J=8), 7.58 (1H, s); ¹³C NMR: δ14.26, 60.94, 121.46, 122.40, 124.48, 129.96, 133.61, 135.42, 141.67, 148.68, 166.13.

**(E)-1-(4-Bromostyryl)-4-chlorobenzene (Table 7.2, Entry 9)**

¹H NMR (400 MHz, CDCl₃, TMS):  δ 7.00 (1H, d, J=4.4Hz), 7.064 (1H, d, J=4.8Hz), 7.328 (2H, d, J=1.6Hz), 7.344 (2H, d, J=1.6Hz), 7.405 ( 2H, d, J=2Hz), 7.410(1H, d, J=2Hz), 7.422 (1H, d, J=1.6Hz); ¹³C NMR: δ121.82, 127.92, 128.21, , 128.31, 128.78, , 129.85, 129.91,, 133.71, 135.45, 136.16.

**(E)-1-bromo-2-(4-bromostyryl)benzene (Table 7.2, Entry 10)**

¹H NMR (400 MHz, CDCl₃, TMS): δ 6.97 (1H, d, J=2.39Hz), 7.05 (1H, d, J=6.8Hz), 7.23 (1H,d, J=0.4Hz), 7.25 (1H, d, J=1.67Hz), 7.33 (1H, d, J=2.4Hz), 7.36 (7.36(2H, d, J=2Hz), 7.43 (2H, d, J=2.4Hz), 7.53 (1H, d, J=1.2Hz). ¹³C NMR: δ121.42, , 126.85, 127.30, 127.74, 128.16, 128.27, , 130.83, 131.28, 131.49, 131.66, 133.27, 135.36.


## 7.4 Conclusion

In conclusion, we reported an efficient method for the synthesis of olefins under very mild condition. The conventional Wittig reaction in most cases is very tedious due to the long reaction time. Microwave irradiation is found to be a valid response to such problems. To our delight, our method of microwave-assisted Wittig reaction took only 30-50 minutes to attain the maximum yield (94%) and *trans* (E)-isomers selectivity (100%) under optimized reaction conditions. Our method offers energy and step-efficient, a neat synthetic route for Wittig olefination which has the potential to be up-scaled for industrial purpose due to its solvent-free and mild nature. To the best of our knowledge, this is the first report of one-pot solvent-free Wittig reaction under microwave irradiation.

## References

1. M. L. Schirmer, S. Adomeit and T. Werner, *Org. Lett.* 2015, **17**, 3078-3081.
2. G. Wittig and G. Geissler, *Liebigs Ann. Chem.* 1953, **580**, 44-57.
3. T. Werner, M. Hoffmann and S. Deshmukh, *Eur. J. Org. Chem.* 2014, 6873-6876.
4. B. E. Maryanoff, A. B. Reitz, *Chem. Rev.* 1989, **89**, 863-927.
5. H. Ernst, *Pure Appl. Chem.* 2002, **74**, 2213–2226.
6. L. A. Morsch, L. Deak, D. Tiburzi, H. Schuster and B. J. Meyer, *Chem. Educ.* 2014, **91**, 611-614.
7. M. Hoffmann, S. Deshmukh and T. Werner, *Eur. J. Org. Chem.* 2015, 4532-4538.
8. B. M. Choudary, K. Mahendar, M.L. Kantam M L, K. V. S. Ranganath and T. Atharb, *Adv. Synth. Catal.* 2006, **348**, 1977-1985.
9. V. P. Balema, J. W. Wiench, M. Pruski and V. K. Pecharsky, *J. Am. Chem. Soc.* 2002, **124**, 6244-6245.
10. J. Westman, *Org. Lett.* 2001, **23**, 3745-3747.
11. J. McNulty and P. Das. *Tetrahedron Lett.* 2009, **50**, 5737-5740.

12. R. Gedye, F. Smith, K. Westaway, H. Ali, L. Baldisera, L. Laberge and J. Rousell, *Tetrahedron Lett.* 1986, **27**, 279-281.
13. P. Lidström, J. Tierney, B. Wathey and J. Westman, *Tetrahedron* 2001, **57**, 9225-9231.
14. J. McNulty, P. Das and D. McLeod, *Chem. Eur. J.* 2010, **16**, 6756-6760.
15. C. Xu, G. Chen, C. Fu and X. Huang, *Synth. Commun.* 1995, **25**, 2229-2233.
16. S. Frattini, M. Quai and E. Cereda, *Tetrahedron Lett.* 2001, **42**, 6827–6829.
17. D. E.Crawford, C. K. G. Miskimmin , A. B. Albadarin, W. Walkerb and S. L. James, *Green Chem.* 2017, **19**, 1507-1512.
18. V. J. Buddrus, *Angew. Chem.* 1968, **80**, 535-536.
19. M. L. Kantam, K.B. S. Kumar, V. Balasubramanyam, G.T. Venkanna and F. Figueras, *J. Mol. Catal. A: Chem.* 2010, **321**, 10-14.
20. D. N. Liu and S. K. Tian, *Chem. Eur. J.* 2009, **15**, 4538-4542.
21. J. Wu and C. Yue, *Synth. Commun.* 2006, **36**, 2939.
22. G. Pathak, D. Das and L. Rokhum, *RSC Adv.* 2016, **6**, 93729.
23. D. Das, J. M. H. Anal and L. Rokhum, *Chem. Sci.* 2016, **128**, 1695.
24. D. Habrant, B. Stengel, S. M unier and C. Mioskowski, *Chem. Eur. J.* 2007, **13**, 5433-5440.
25. E. Vedejs and H. W. Fang. *Org. Chem.* 1984, **49**, 211-213.
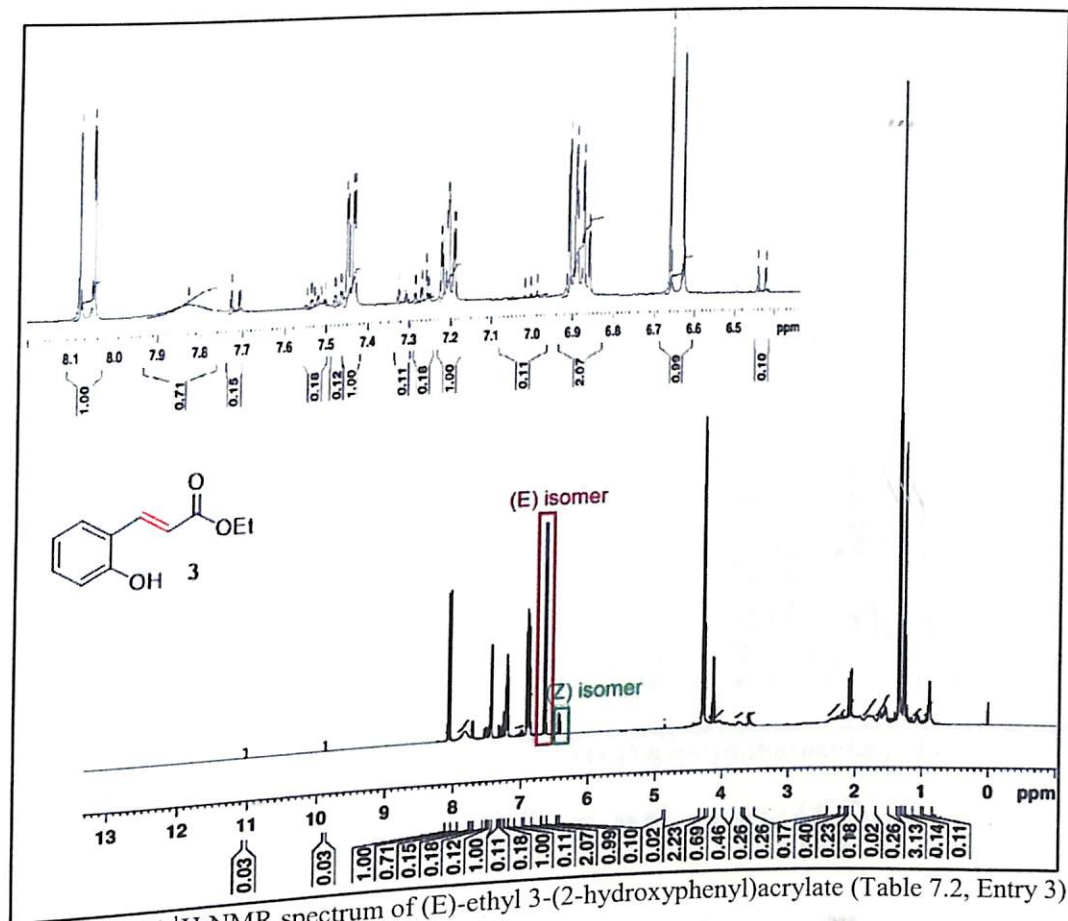
FIGURE 7.4 $^1$H NMR spectrum of (E)-ethyl 3-(2-hydroxyphenyl)acrylate (Table 7.2, Entry 3)

E/Z ratio calculation:

$$E=\left(\frac{0.99}{1.09}\right)\times100\%\approx91\%, \quad Z=\left(\frac{0.10}{1.09}\right)\times100\%\approx9\%$$
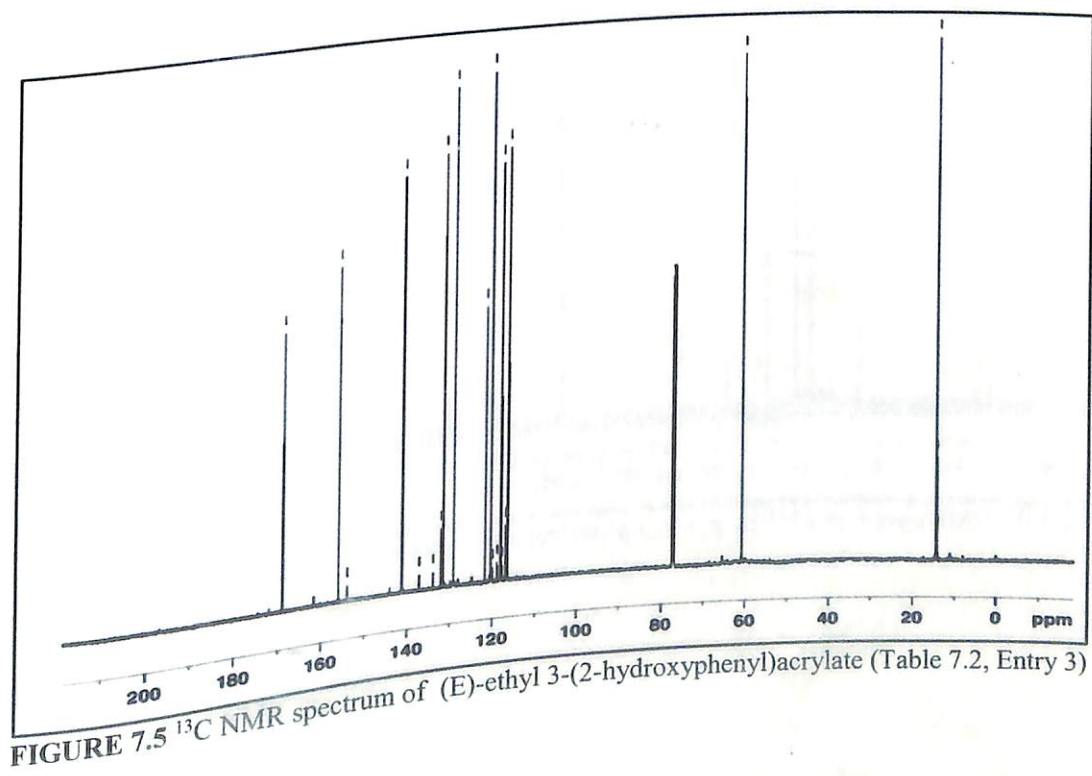


FIGURE 7.5 $^{13}$C NMR spectrum of (E)-ethyl 3-(2-hydroxyphenyl)acrylate (Table 7.2, Entry 3)

155
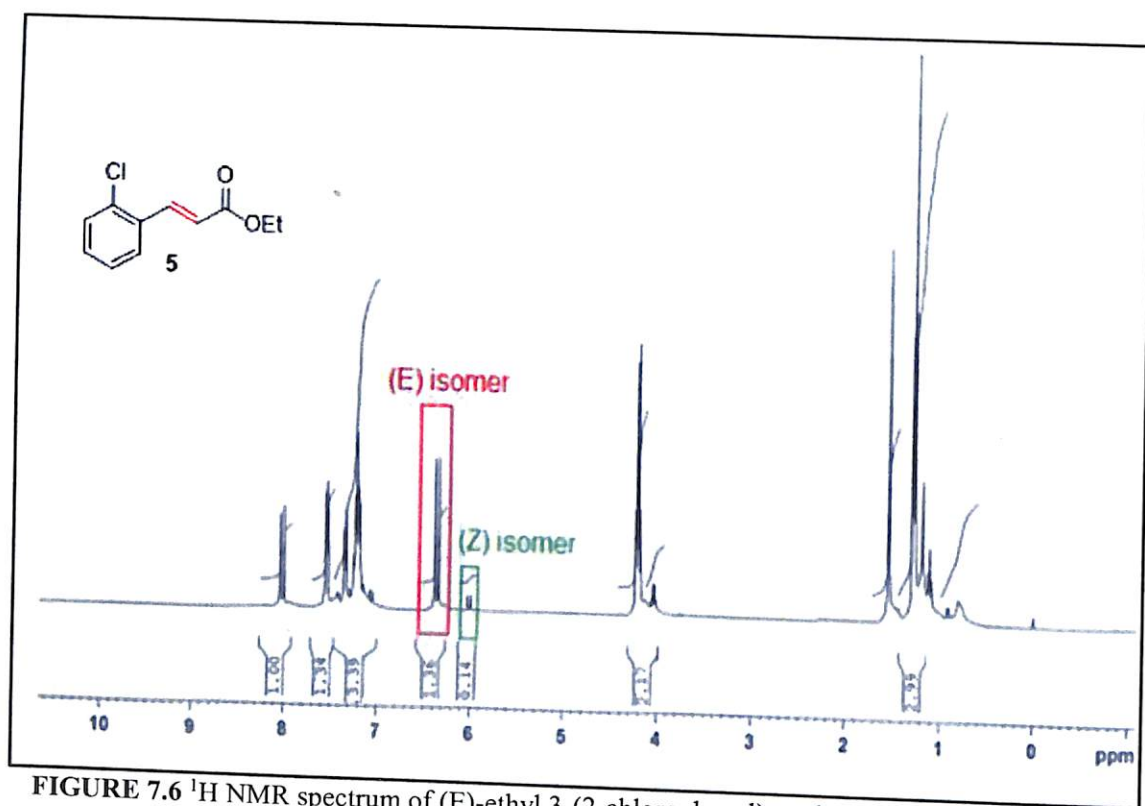
**FIGURE 7.6** $^1$H NMR spectrum of (E)-ethyl 3-(2-chlorophenyl)acrylate (Table 7.2, Entry 5).

E/Z ratio calculation: $E = \left(\frac{1.36}{1.50}\right) \times 100\% \simeq 91\%$, $Z = \left(\frac{0.14}{1.50}\right) \times 100\% \simeq 9\%$
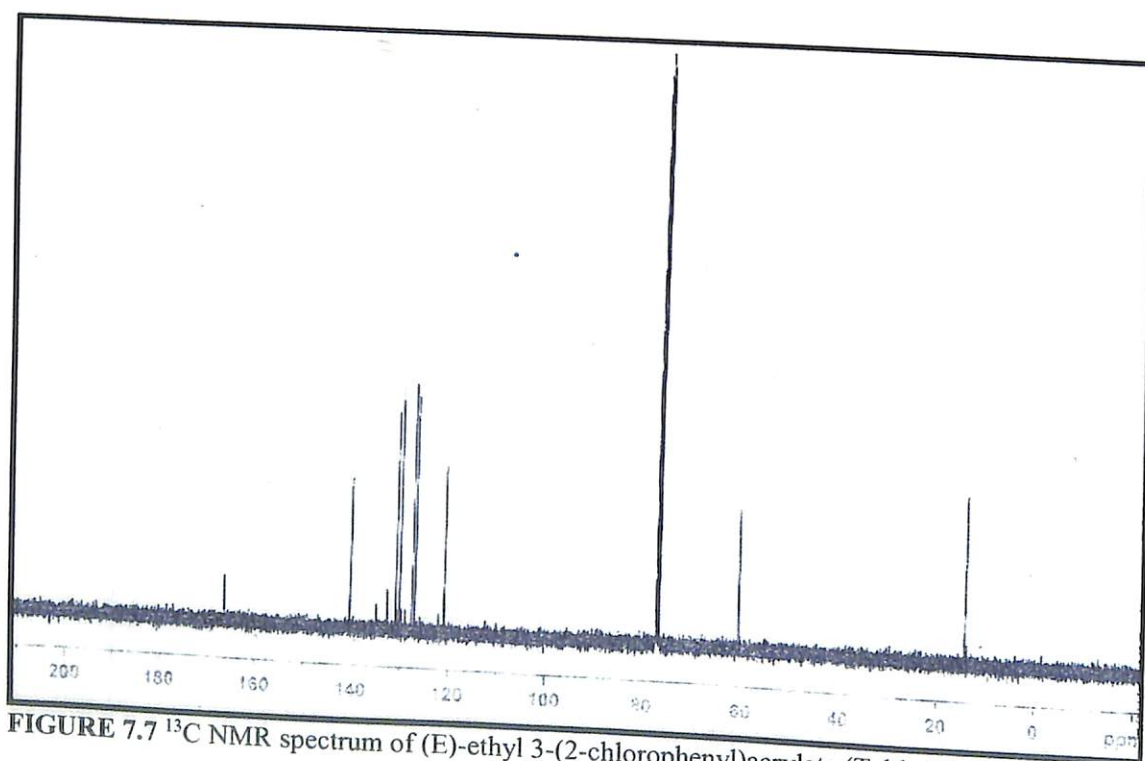


**FIGURE 7.7** $^{13}$C NMR spectrum of (E)-ethyl 3-(2-chlorophenyl)acrylate (Table 7.2, Entry 5)

156

FIGURE 7.8 $^1$H NMR spectrum of (E)-ethyl 3-(4-bromophenyl)acrylate (Table 7.2, Entry 6)

E/Z ratio calculation:
E= 100%, Z= 0%



FIGURE 7.9 $^{13}$C spectrum of (E)-ethyl 3-(4-bromophenyl)acrylate (Table 7.2, Entry 6)
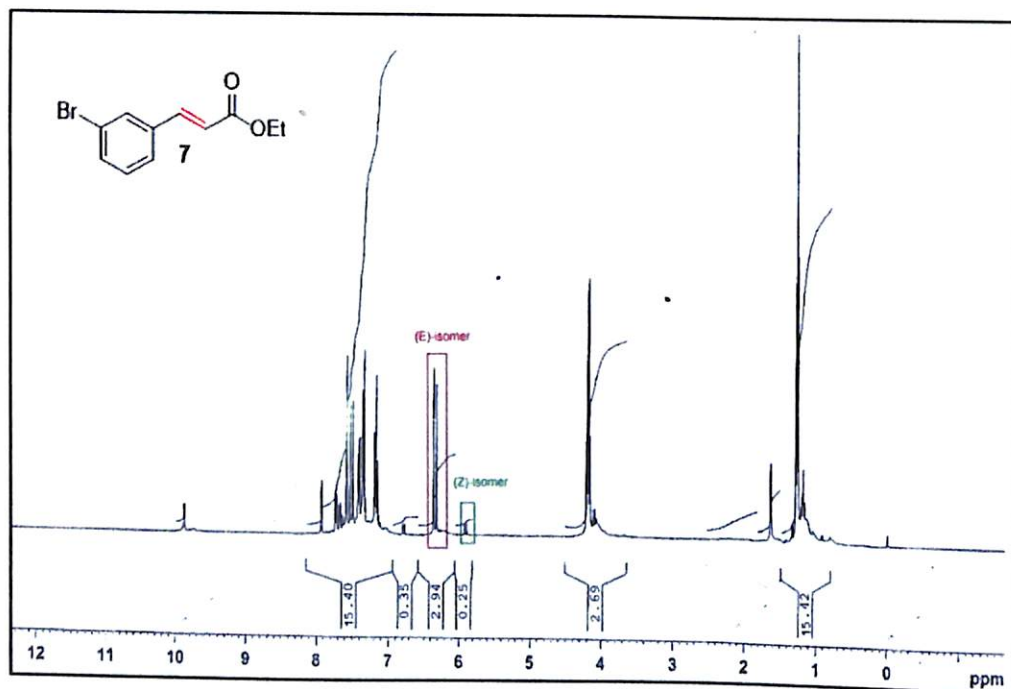
**FIGURE 7.10** $^1$H NMR of (E)-ethyl 3-(3-bromophenyl)acrylate (Table 7.2, Entry 7)

E/Z ratio calculation: E= $\left(\frac{2.94}{3.19}\right)$ ×100%≃92%, Z= $\left(\frac{0.25}{3.19}\right)$ ×100% ≃ 8%
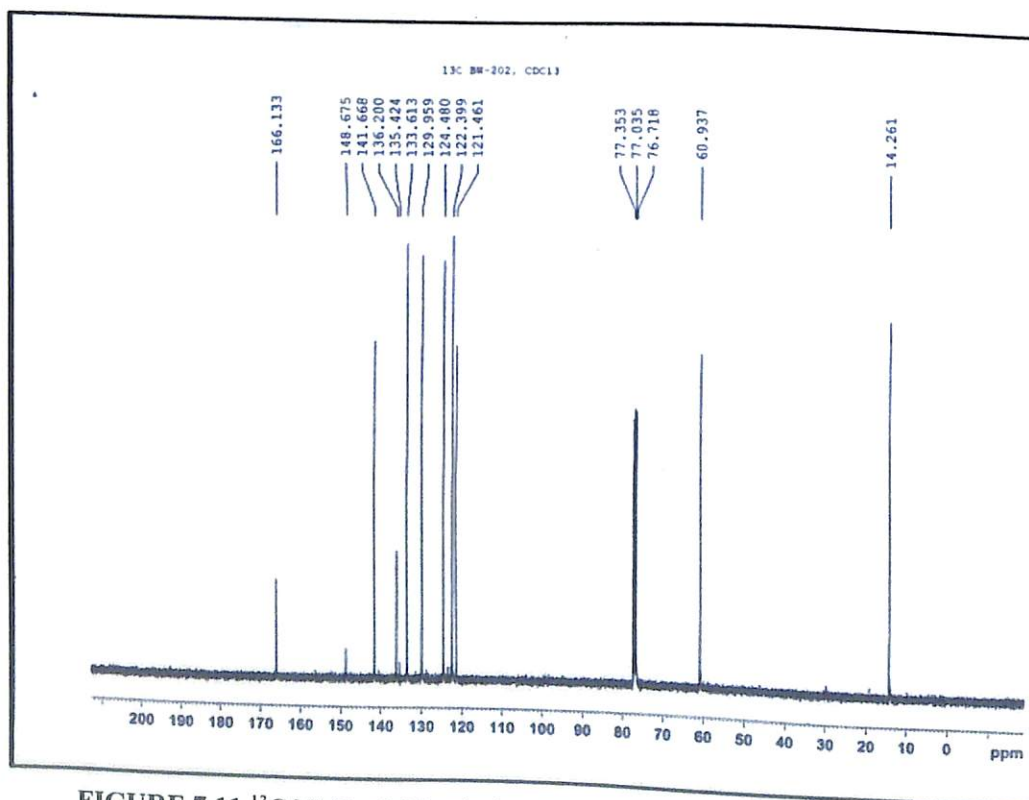


**FIGURE 7.11** $^{13}$C NMR of (E)-ethyl 3-(3-bromophenyl)acrylate (Table 7.2, Entry 7)

158
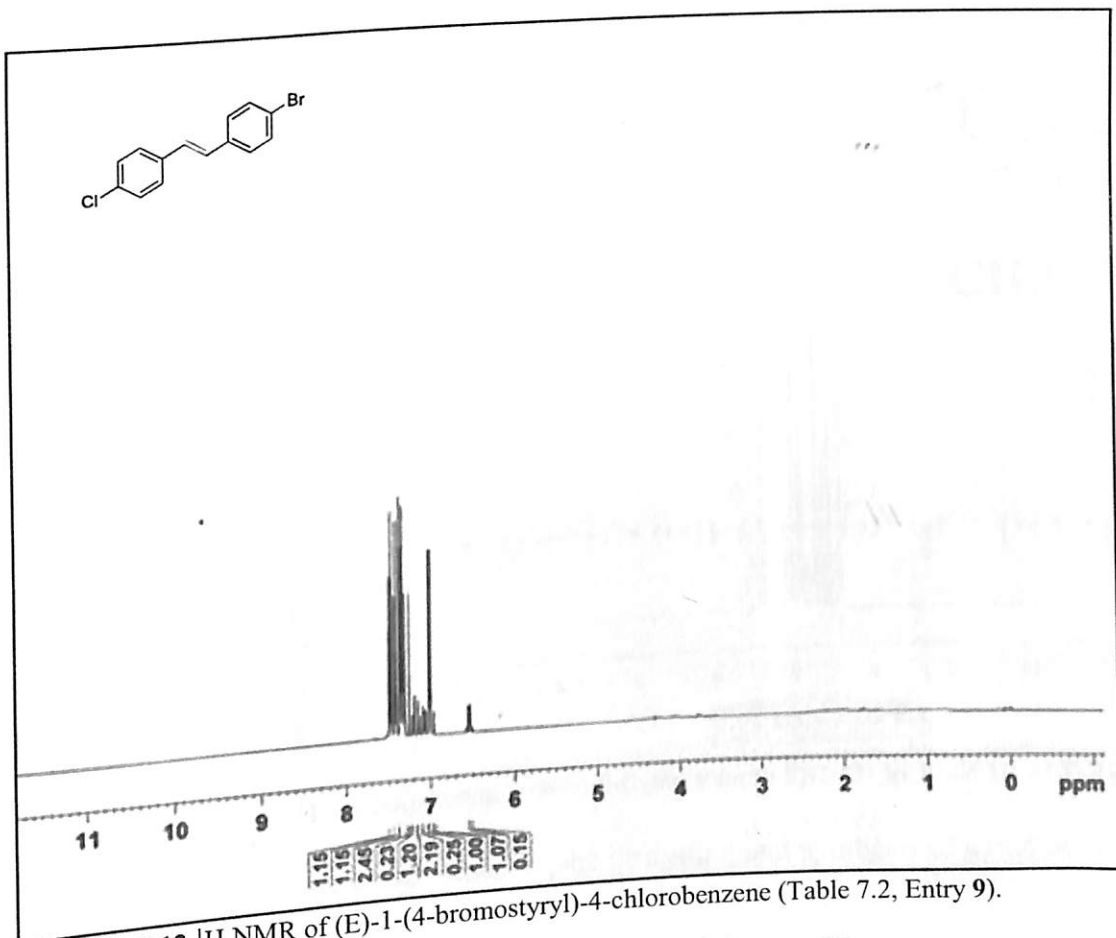
FIGURE 7.12 $^1$H NMR of (E)-1-(4-bromostyryl)-4-chlorobenzene (Table 7.2, Entry **9**).

E/Z ratio calculation: $E = \left(\frac{1.07}{1.22}\right) \times 100\% \simeq 88\%$, $Z = \left(\frac{0.15}{1.22}\right) \times 100\% \simeq 12\%$
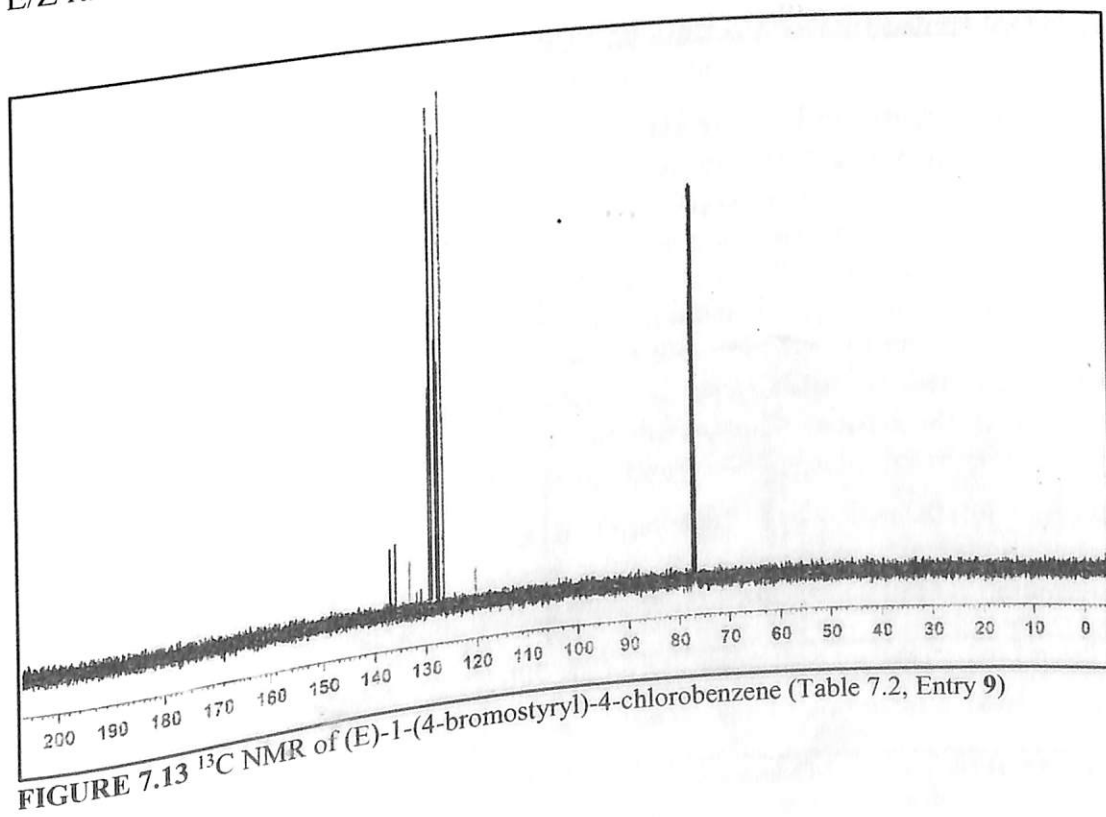


FIGURE 7.13 $^{13}$C NMR of (E)-1-(4-bromostyryl)-4-chlorobenzene (Table 7.2, Entry **9**)

159

**FIGURE 7.14** ${}^{1}$H NMR of (E)-1-(2-bromophenyl)-2-(4-bromophenyl)ethane (Table 7.2, Entry 10).

E/Z ratio calculation:

$$E = \left(\frac{1.46}{1.64}\right) \times 100\% \simeq 89\%, \ Z = \left(\frac{0.18}{1.64}\right) \times 100\% \simeq 11\%$$



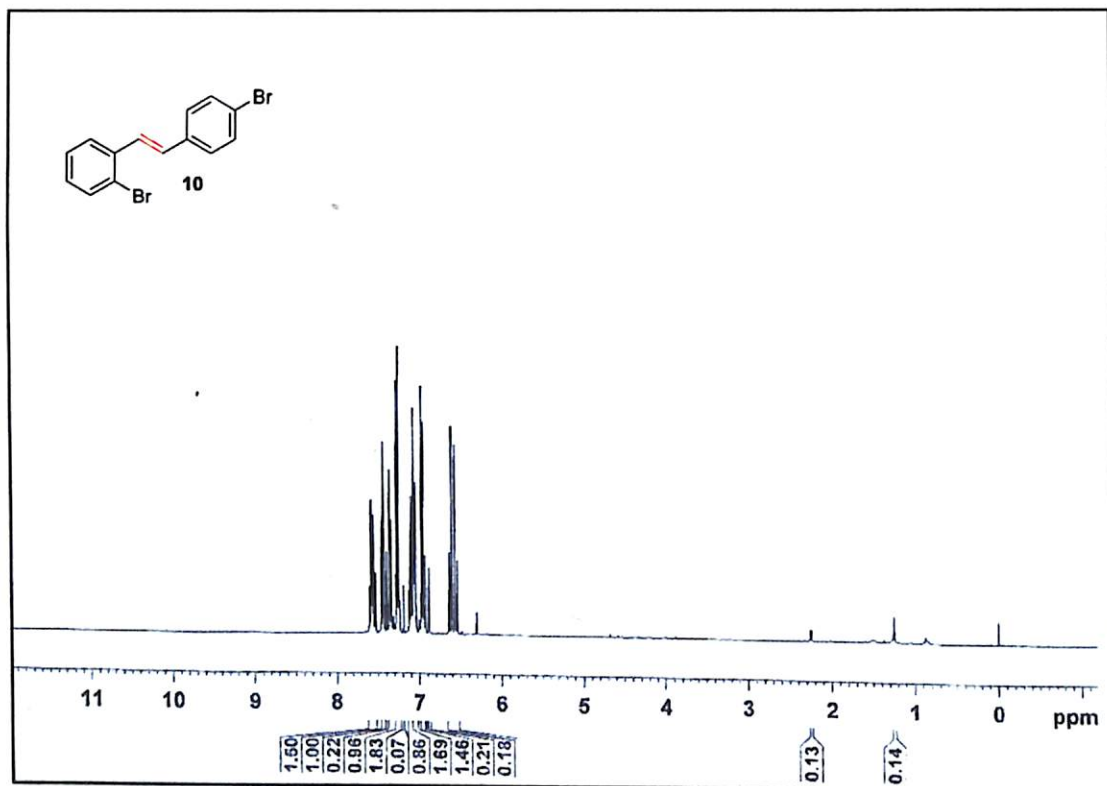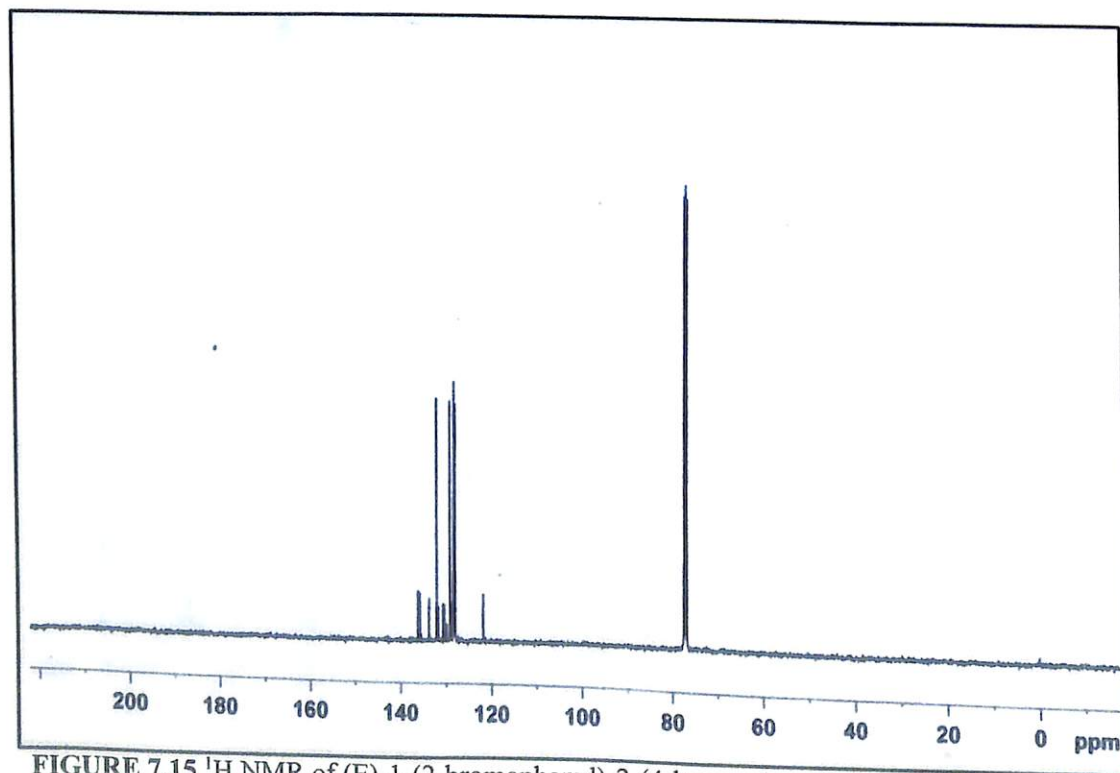**FIGURE 7.15** ${}^{1}$H NMR of (E)-1-(2-bromophenyl)-2-(4-bromophenyl)ethane (Table 7.2, Entry 10).

160

# Conclusion and future prospects

## 8.1 A brief summary of research work

The undertaken research work stands on the designing and synthesis of a number of chosen heterogeneous catalysts which find applications in several synthetically or industrially important chemical reactions. To validate the formation of a catalyst and investigate its physical and chemical properties, various characterization techniques were applied. The catalysts were then tested for possible catalytic ability and employed in valuable organic transformations. Synthesized chemical products were purified and analyzed by NMR, IR or GC-MS in several cases. The recyclability of catalysts is a coveted criteria for heterogeneous catalysts, so it was also studied for the catalytic systems.

In Chapter 1, a general introduction to catalysis and its historical background were mentioned in brief followed by the discussion in mechanistic principle of heterogeneous catalysis and its prominent advantages/disadvantages over homogeneous catalysis. The preface of different categories of heterogeneous catalysis and their scopes and various aspects were also conferred in the chapter. Based on the discussions and shortcomings related to already reported techniques, the motivation and scope of the present research work were presented. The chapter also comprises of the objectives of this research work which take account of synthesis, characterization and applications of different heterogeneous catalysts like nanocatalysts, polymer catalysts and biowaste based catalysts in useful organic transformations and designing green, solvent-free methodologies for organic synthesis.

In Chapter 2, systematic review of literature was presented for various organic transformations involved in this research work viz. tetrahydropyranylation/depyranylation of hydroxy group, Henry reaction, Wittig reaction, transesterification for biodiesel synthesis and glycerol valorization by solketal synthesis. The literature survey included study of varied range of heterogeneous catalysts used for these conversions with old to up to date examples. The assessment of the literature study furnished an idea about the present scenario of heterogeneous catalysis in the above reactions.

In Chapter 3, a sulfonated core shell magnetic nanocatalyst based on $Fe_3O_4$ MNPs $(Fe_3O_4@SiO_2@SO_3H$ or FSS) was presented which find applications in

tetrahydropyranylation/ depyranylation reactions of alcohols as well as ultrasonic-assisted solketal synthesis by acetalization of glycerol. Solvent free route for tetrahydropyranylation/ depyranylation of alcohols using magnetically retrievable FSS catalyst offers an easy, hurdle free protocol for protection/deprotection of alcohols. Also, as per our knowledge, magnetic MNP catalyst was employed for the first time to develop a green and cost-effective synthetic protocol for the production of sol-ketal which resulted excellent yield and selectivity within only 15 minutes.

Chapter 4 demonstrated chemoselective tetrahydropyranylation/ depyranylation of alcohols and phenols using mesoporous phenolsulfonic acid formaldehyde resins (PAFR) as catalyst under room temperature. The catalyst offered noticeable heterogeneity and recyclability. The protocol avoids the use of any hazardous solvent and successfully generalized for phenc , tertiary alcohols, large molecules like cholesterol which otherwise difficult to achieve.

In Chapter 5, a novel biowaste-derived, highly efficient solid-base catalyst was established from *Musa acuminata* (banana) peel ash (MAPA) and characterized its properties with various analytical techniques. The catalyst offered excellent activity in synthesis of nitroaldols *via* Henry reactions. It was recorded as the first report of exploitation of biowaste-derived heterogeneous catalyst in C-C bond formation reaction. Room temperature, solvent-free protocol, recyclability up to $10^{th}$ catalytic cycle and amenability to scale-up the protocol adds perk to the green synthetic method.

Chapter 6 established *Musa acuminata* banana trunk ash (MBTA) as a novel, cost and labour effective green solid base catalyst. The solid base catalyst MBTA was characterized by various analytical techniques to have knowledge about its composition, morphology and structure. The catalyst was tested for its catalytic activity in transesterification reaction of soybean oil which resulted a sustainable biodiesel production method in room temperature.

In Chapter 7, a one-pot, solvent-free protocol was presented for Wittig reaction under microwave irradiation. Commercially available basic alumina was used as a base catalyst-support in the reaction. It presented an energy and step-efficient, neat synthetic route for Wittig Olefination resulting *E*-selectivity up to 100%.

## 8.2 Future scope of research work

The major challenge of heterogeneous catalysis in present day scenario is to cope up with the high catalytic activity of homogeneous catalysis making best use of the recyclable nature of heterogeneous catalysts. Therefore designing new and advantageous heterogeneous catalyst is in high demand to design strategic catalytic paths for wide range of chemical reactions. Synthesis and applications of environment-friendly, benign, green heterogeneous catalysts should be encouraged to deal with the toxicity associated with chemical processes. In regard to the catalysts used in this research work, following points can be mentioned-

- Magnetic nanocatalysts can make any synthetic protocol much simple and time-efficient, for which more magnetic nano-catalyzed protocols are desirable in near future to avoid waste of hazardous solvents in purification processes. FSS has a wide scope to be employed in synthesis of organic compounds with or without further modifications.

- As an ion exchange resin, PAFR catalyst showed good activity towards protection/deprotection of wide range of hydroxy compounds. The heterogeneity and hydrophobicity of PAFR resin can be exploited for many in-water organic reactions.

- Witnessing the ongoing demand of biomass-derived catalysts and their confined applications in biofuel production area, it is comprehended that there is a vast scope to design efficient biowaste-based heterogeneous catalysts and elaborate their applications into synthetically all-important organic reactions for fine chemical production which has hardly been tried before. The bio-derived catalyst MAPA and MABTA can be excellent green catalysts for many base-catalyzed reactions owing to their natural sustainability, benign, abundant nature and most importantly very simple preparation method.
- Developing effective as well as green methodologies for catalytic synthesis needs much attention to maintain sustainability. Therefore minimizing or avoiding use of hazardous solvents during reactions should be one's prime motive. These efforts might encourage other researchers to extend the applications of the catalytic systems discussed here which will enhance the growth of the domain.

# LIST OF PUBLICATIONS

**A. Papers in Peer Reviewed International Journals:**

1. **K. Rajkumari**, J. Kalita, D. Das, L. Rokhum, Magnetic $Fe_3O_4$@silica sulfuric acid nanoparticles promoted regioselective protection/deprotection of alcohols with dihydropyran under solvent-free conditions, *RSC Adv.* 2017, **7**, 56559-56565. [Synfact highlighted: *Synfacts*, 2018, **14** (3), 0320]

2. **K. Rajkumari**, D. Das, G. Pathak and L. Rokhum, Waste-to-useful: a biowaste-derived heterogeneous catalyst for a green and sustainable Henry reaction, *New J. Chem.* 2019, **43**, 2134-2140.

3. **K. Rajkumari**, B. Lama, L. Rokhum, A microwave-assisted highly stereoselective one-pot Wittig reaction under solvent-free condition, *Turk. J. Chem.* 2019, **43**, 705-712.

4. **Kalyani Rajkumari**, Ikbal Bahar Laskar, Anupama Kumari, Bandita Kalita and Lalthazuala Rokhum*. Highly selective tetrahydropyranylation/dehydropyranylation of alcohols and phenols using porous phenolsulfonic acid-formaldehyde resin catalyst under solvent-free condition. *React. Funct. Polym.*, 2020, **149**, 104519-104527

5. **Kalyani Rajkumari** and Lalthazuala Rokhum. A sustainable protocol for production of biodiesel by transesterification of soybean oil using banana trunk ash as a heterogeneous catalyst. *Biomass Convers. Biorefin.*, 2020, https://doi.org/10.1007/s13399-020-00647-8.

**B. Papers under Review:**

1. **Kalyani Rajkumari**, Ananta Kr. Meher, Putla Sudarsanam and Lalthazuala Rokhum, Functionalized Magnetic Nanocomposite as an Efficient Reusable catalyst Catalyst for Bio-Fuel Additive Production from Glycerol: An Ultrasound-Assisted Solketal Synthesis.

**C. Papers in Peer Reviewed International Journals (Outside Ph.D work):**

1. G. Pathak, D. Das, **K. Rajkumari** and L. Rokhum, Exploiting waste: Towards a sustainable production of biodiesel using Musa acuminata peel ash as a heterogeneous catalyst, *Green Chem.* 2018 **20**, 2365-2373.

2. I. B. Laskar, **K. Rajkumari**, R. Gupta and L. Rokhum, Acid functionalized mesoporous polymer catalyzed acetalization of glycerol to solketal, a potential fuel additive under solvent-free conditions, *Energy Fuels* 2018, **32**, 12567–12576.

3. I. B. Laskar, **K. Rajkumari**, R. Gupta, S. Chatterjee, B. Paul and L. Rokhum, Waste snail shell derived heterogeneous catalyst for biodiesel production by transesterification of soybean oil, *RSC Adv.* 2018, **8**, 20131-20142.

4. G. Pathak, **K. Rajkumari** and L. Rokhum, Wealth from waste: M. acuminata peel waste-derived magnetic nanoparticles as a solid catalyst for the Henry reaction, *Nanoscale Adv.* 2019, **1**, 1013-1020.

5. C. Vanlalveni, **K. Rajkumari**, A. Biswas, P. P. Adhikari, R. Lalfakzuala, L. Rokhum, Green synthesis of silver nanoparticles using Nostoc linckia and its antimicrobial activity: a novel biological approach, *BioNanoscience* 2018, **8**, 1-8.

6. D. Das, **K. Rajkumari** and L. Rokhum, Polymer-bound Triphenylphosphine and 4,4'-Dinitroazobenzene as a Coupling Reagents for Chromatography-Free

Esterification Reaction, *Curr. Org. Synth.* 2019, Just accepted, DOI: 10.2174/1570179416666190919152424.

## D. Paper Presented at Conferences:

1. Presented poster in the 5th International Conference on Advanced Nanomaterials and Nanotechnology (ICANN 2017) organized by Centre of Nanotechnology, IIT, Guwahati, Guwahati-781039, Assam, India- held on18th -21st December, 2017.
(Title of paper- "Facile magnetic $Fe_3O_4$-$SiO_2$-$SO_3H$ nanoparticles catalyzed protection and deprotection of alcohols with 3,4-dihydro-2H pyran")
2. Presented poster and paper in the International Conference on Systems and Processes in Physics, Chemistry and Biology (ICSPPCB-2018) organized by Department of Physics, Assam University, Silchar- 788011, Assam, India- held on March 1st-3rd, 2018.
(Title of paper- "Magnetic $Fe_3O_4@SiO_2$-$NH_2$ nanoparticle catalyzed green synthesis of nitroalcohols via Henry reaction")
3. Oral presentation in the National Conference on Waste to Energy Conversion (NCWEC-2018) organized jointly by Department of Mechanical Engineering, National Institute of Technology, Mizoram, Aizawl, Mizoram, India and Indian Institute of Technology, Guwahati-781039, Assam, India- held on 28th -29th December, 2018.
(Title of paper-Waste to wealth: A sustainable protocol for production of biodisel by transesterification of soyabean oil using banana trunk ash as a heterogeneous catalyst)
4. Oral presentation in the National Seminar and Workshop on Applications of Nanotechnology and Biotechnology in Daily Life (NSW-ANBDL-2019) organized by IQAC, Sibsagar College, Joysagar in association with CPP-IPR, Sonapur, Assam, India- held in 26th to 28th September, 2019.
(Title of paper- A Magnetic Nano catalyzed Facile Route for Sol-ketal synthesis)